

US MINERALS MANAGEMENT SERVICE
1435-01-98-PO-16063
BEST PRACTICE FOR THE ASSESSMENT OF SPANS IN
EXISTING SUBMARINE PIPELINES
VOLUME 2 - APPENDICES

C811\01\007R REV 0 AUGUST 2002

Purpose of Issue	Rev	Date of Issue	Author	Checked	Approved
Final report	0	August 2002	JKS	HMB	HMB

Controlled Copy		Uncontrolled Copy	
-----------------	--	-------------------	--

BOMEL LIMITED

Ledger House
Forest Green Road, Fifield
Maidenhead, Berkshire
SL6 2NR, UK

Telephone +44 (0)1628 777707

Fax +44 (0)1628 777877

Email info@bomelconsult.com

CONTENTS

	Page No.
VOLUME 1	
EXECUTIVE SUMMARY	0.4
1. INTRODUCTION, BACKGROUND AND SCOPE OF WORK	1.1
1.1 INTRODUCTION	1.1
1.2 BACKGROUND	1.2
1.3 SCOPE OF WORK	1.3
2. APPROACHES TO SPAN ASSESSMENT	2.1
2.1 INTRODUCTION	2.1
2.2 PRINCIPAL CONSIDERATIONS	2.1
2.3 AVAILABLE APPROACHES	2.2
2.3.1 The Basic Approach	2.2
2.3.2 Screening Approach	2.4
2.3.3 The Tiered Approach	2.6
3. UNCERTAINTY	3.1
3.1 PREAMBLE	3.1
3.2 RISK AND RELIABILITY FUNDAMENTALS	3.4
3.2.1 Qualitative Indexing Systems	3.4
3.2.2 Quantitative Risk Systems	3.6
3.3 SPATIAL AND TEMPORAL VARIABILITY	3.10
4. DATA FOR SPAN ASSESSMENT	4.1
4.1 PREAMBLE	4.1
4.2 DATA CLASSES	4.1
4.3 DATA SOURCES	4.2
5. SURVEYS	5.1
5.1 PREAMBLE	5.1
5.2 SURVEY TECHNIQUES	5.1
6. ASSESSMENT BENCHMARKING	6.1

7.	DISCUSSION OF CURRENT PRACTICE	7.1
8.	WAY FORWARD	8.1
9.	REFERENCES	9.1

VOLUME 2

APPENDIX A -	PIPELINE DEFECT ASSESSMENT PROCESS: SPAN ANALYSIS FOR STATIC STRENGTH AT THE TIER 1 LEVEL
APPENDIX B -	PIPELINE DEFECT ASSESSMENT PROCESS: SPAN ANALYSIS FOR STATIC STRENGTH AT THE TIER 2 LEVEL
APPENDIX C -	PIPELINE DEFECT ASSESSMENT PROCESS: SPAN ANALYSIS FOR STATIC STRENGTH AT THE TIER 3 LEVEL
APPENDIX D -	PIPELINE DEFECT ASSESSMENT PROCESS: SPAN ANALYSIS FOR DYNAMIC OVERSTRESS AT THE TIER 1 LEVEL (VORTEX SHEDDING)
APPENDIX E -	DEVELOPMENT OF FATIGUE ASSESSMENT METHODOLOGY
APPENDIX F -	CRITERIA DETERMINING THE STATIC STRENGTH OF PIPELINE SPANS
APPENDIX G -	RECOMMENDED INSPECTION STRATEGY
APPENDIX H -	COPY OF REFERENCE: BOMEL, 1995

APPENDIX A

PIPELINE DEFECT ASSESSMENT PROCESS: SPAN ANALYSIS FOR STATIC STRENGTH AT THE TIER 1 LEVEL

TABLE OF CONTENTS

	Page No
A.1 INTRODUCTION	A.1.1
A.1.1 PURPOSE	A.1.1
A.1.2 SCOPE AND LIMITATIONS	A.1.1
A.1.3 REFERENCES	A.1.1
A.1.3.1 Codes And Standards	A.1.1
A.2 PROCESS	A.2.1
A.2.1 OBJECTIVE	A.2.1
A.2.2 ASSESSMENT STRATEGY AT THE TIER 1 LEVEL	A.2.1
A.2.2.1 Generic	A.2.1
A.2.2.2 Considerations In The Tier 1 Static Strength Analytical Method	A.2.1 A.2.2
A.2.3 DATA	A.2.2
A.2.3.1 Data Classes	A.2.2
A.2.3.2 Data Sources	A.2.3
A.2.4 LOADINGS AND LOAD COMBINATIONS IN GENERAL	A.2.3
A.2.4.1 General Points	A.2.3
A.2.4.2 Actions	A.2.3
A.2.4.3 Loadings	A.2.4
A.2.5 LOAD COMBINATION IN TIER 1 ANALYTICAL METHOD	A.2.4
A.2.5.1 Load Combination	A.2.4
A.2.5.2 Submerged Self-Weight	A.2.4
A.2.5.3 Environmental: Long-Term	A.2.5
A.2.5.4 Environmental: Short-Term	A.2.5
A.2.5.5 Operating	A.2.6
A.2.6 ANALYTICAL CRITERIA	A.2.6
A.2.6.1 General	A.2.6
A.2.6.2 Stress Criterion	A.2.6
A.2.6.3 Strain Criterion	A.2.7
A.2.6.4 Ovalisation Criterion	A.2.7
A.2.6.5 Local Buckling Criterion	A.2.7
A.2.7 TIER 1 STATIC STRENGTH ANALYTICAL METHOD	A.2.7
A.2.7.1 General	A.2.8
A.2.7.2 Loadings	A.2.8
A.2.7.3 Support Conditions	A.2.9
A.2.7.4 Material Characteristic	

TABLE OF CONTENTS/continued

	A.2.7.5	Cross-section Bending Resistance	A.2.9
	A.2.7.6	Span Mechanical Model	A.2.13
	A.2.7.7	Analysis Procedure	A.2.15
	A.2.7.8	Analytical Method Implementation	A.2.16
	A.2.8	ACCEPTANCE CRITERION	A.2.16
A.3		ATTACHMENTS	A.3

LIST OF TABLES

Table A.2.1	Data Classes
Table A.2.2	Relationship Between Actions, Loading And Load Combinations
Table A.2.2	Input And Response Parameters For Tier 1 Span Mechanical Model
Table A.3.1	Example Of Tier 1 Static Strength Analysis Proforma

LIST OF FIGURES

Figure A.2.1	Static Strength Assessment At The Tier 1 Level
--------------	--

A.1 INTRODUCTION

A.1.1 PURPOSE

The purpose of this process is to set down the methodology for the static strength analysis of pipeline spans at the Tier 1 level and to ensure that best practice is applied.

A.1.2 SCOPE AND LIMITATIONS

This process applies to pipelines laid directly onto the seabed. It applies to an individual span; that is, a single clear unsupported length of pipeline that is sufficiently isolated from other spans or features as to be judged to behave as a self-contained entity. It does not apply to pipelines that are trenched, trenched and backfilled, trenched and infilled due to natural soil migration, or pipelines that are piggybacked.

A.1.3 REFERENCES

A.1.3.1 Codes And Standards

- Rules For Submarine Pipeline Systems. Det Norske Veritas. **DNV, 1996.**
- Code Of Practice For Pipelines Subsea: Design, Construction And Installation. British Standards Institute (BSI). **BS 8010: Part 3: 1993.**
- American Petroleum Institute (API). Recommended Practice For Planning, Designing, And Constructing Fixed Offshore Platforms - Working Stress Design. **RP2A-WSD, 20th ed., July 1993.**

A.2 PROCESS

A.2.1 OBJECTIVE

The objective of this process is to ensure that the static strength analysis of pipeline spans at the Tier 1 level is conducted in a rigorous manner, with due regard to the mechanical characteristics of the problem, using appropriate analytical criteria, and that spans are determined to be acceptable or significant against acceptance criteria.

A.2.2 ASSESSMENT STRATEGY AT THE TIER 1 LEVEL

A.2.2.1 Generic

The recommended Pipeline Defect Assessment Procedure allows a tiered approach to analytical methods and span acceptance. Specifically, up to a three-tiered philosophy can be adopted as shown in detail for the failure mode of static strength in Figure A.2.1. In this figure, the upper level tiers have been greyed, leaving the Tier 1 assessment covered by this process highlighted.

At whatever tier level, the approach involves interaction between the data, load combination, analytical criteria, analytical methods and acceptance criteria; each of these is dealt with in detail in subsections A.2.3 to A.2.8, below. At Tier 1, observed span lengths are judged against span lengths computed from the analytical method, using acceptance criteria, to determine acceptability:

- data, load combinations and analytical criteria are all input into the analytical method
- output from the analytical method is a computed span length, which is compared with the observed span length to determine acceptability of the latter using an acceptance criterion.

A.2.2.2 Considerations In The Tier 1 Static Strength Analytical Method

For the static strength analytical method recommended for pipeline spans in this process document consideration should be given to the following factors:

- loadings
- support conditions
- material characteristic
- cross-section bending resistance
- span mechanical model

- analysis procedure
- analytical method implementation.

Each of these points is addressed in detail in subsection A.2.7, below.

A.2.3 DATA

A.2.3.1 Data Classes

A detailed breakdown of the data into the four classes of: *pipeline*, *operational*, *environmental* and *inspection* is given in Table 2.1. Data in the lines of Table 2.1 that have been greyed are considered to be unnecessary to perform the Tier 1 static strength analysis. The remainder can be viewed as “baseline” data, some of which have to be processed by means of calculation into suitable input data for the analysis.

The **pipeline data** include geometrical and material properties; these are used in the analytical model, the analytical criteria and the material characteristic. The axial restraint factor is used to approximate the degree of suppression of longitudinal strains in the pipe wall due to the interaction of the pipe with the seabed.

The **operational data** encompass installation (residual lay tension) and those related to the pipe contents: its density, pressure and temperature; these are used to derive some of the loadings applied to the span.

The **environmental data** include the parameters that relate to the fluid loading on the pipeline (for example, water depth and various wave and current data). They also contain parameters defining the mechanical interaction between the pipe and the seabed (for example, soil modulus and Poisson's ratio at the span shoulders); these particular parameters influence the support conditions at the shoulder of the pipeline.

The **inspection data** include parameters to locate the span (kilometre start and end points), and freespan length. If marine growth information is included within the inspection data an assessment should be made as to whether this influences the pipeline weight or the hydrodynamic loading on the pipeline.

A.2.3.2 Data Sources

Appropriate sources of pipeline, operational and environmental data are to be used. If no data are available for residual lay tension or axial restraint factor, then these are to be estimated conservatively and included if they adversely affect the pipeline.

A.2.4 LOADINGS AND LOAD COMBINATIONS IN GENERAL

A.2.4.1 General Points

A load combination is built up from *actions* and *loadings* as shown schematically in Table A.2.2. The loading combination to be used is a requirement of the assessment and, as indicated in subsection A.2.5, an *operating* loading is always included in the combination. This will usually correspond to the normal operating conditions of the pipeline, although there may be occasions where other operating conditions need to be considered.

A.2.4.2 Actions

In terms of detailed thermo-mechanical actions there are eight types that require consideration:

- pipeline weight
- external temperature
- external pressure
- current-induced action
- wave-induced action
- contents weight
- internal temperature
- internal pressure.

A.2.4.3 Loadings

Four individual loading classes are to be considered, namely:

- submerged self weight
- environmental: long-term
- environmental: short-term
- operating.

More than one type of operating condition may need to be addressed. As indicated in Table A.2.2, the list covers the following possibilities:

- normal operating
- maximum allowable operating
- shut down (minimum operating)
- hydrotest.

This list may be extended if circumstances dictate.

A.2.5 LOAD COMBINATION IN TIER 1 ANALYTICAL METHOD

A.2.5.1 Load Combination

A load combination is made up from loading classes, and will always comprise the submerged self-weight, environmental long- and short-term load and an operating class, as set out schematically in Table A.2.2.

A.2.5.2 Submerged Self-Weight

The submerged self-weight should comprise the weight of the pipe, anti-corrosion coating and weight coating, minus the displaced weight of seawater. It is calculated from the data as follows:

$$q = q_s + q_e + q_c - q_a \quad (\text{A.2.1})$$

$$q_s = \frac{\rho_s \pi g}{4} [D^2 - (D - 2t)^2] \quad (\text{A.2.2})$$

$$q_e = \frac{\rho_e \pi g}{4} [(D + 2t_e)^2 - D^2] \quad (\text{A.2.3})$$

$$q_c = \frac{\rho_c \pi g}{4} [(D + 2t_e + 2t_c)^2 - (D + 2t_e)^2] \quad (\text{A.2.4})$$

$$q_a = \frac{\rho_a \pi g}{4} (D + 2t_e + 2t_c)^2 \quad (\text{A.2.5})$$

The symbols are explained in Table A.2.1.

The submerged self-weight may be augmented by an estimate of additional gravity load due to marine fouling, if appropriate.

A.2.5.3 Environmental: Long-Term

The only part of the environmental: long-term loading that requires derivation is the external (hydrostatic) pressure. This may be estimated from:

$$p_a = \rho_a gh \quad (\text{A.2.6})$$

A.2.5.4 Environmental: Short-Term

The environmental: short-term loading comprises the hydrodynamic uniformly distributed load resulting from the drag on the pipeline from the moving water particle velocities. Inertia loading is generally small, and in most circumstances may be neglected. It is recommended that directional 50-year return period maximum wave height and period (H_{\max} and T_{\max}), and *associated* maximum surface current velocity are used to determine the maximum combined water particle velocity normal to the heading of the span, which forms the input to Morison's equation to derive the loading on the span. The main steps in this process are as follows:

1. Use directional 50-year return period maximum wave height and period (H_{\max} and T_{\max}), and *associated* maximum surface current velocity
2. Considering the heading of the pipeline span, determine the maximum wave height and corresponding period, and associated surface current velocity normal to the pipeline span
3. Compute the top-of-pipe current velocity V_c using a power-law current profile suggested in the source data
4. Compute the top-of-pipe maximum wave velocity V_w using a wave theory suitable for the H_{\max} - T_{\max} - water depth combination concerned (kinematic spreading may be neglected, and the effect of current velocity on wave period may be ignored)
5. The uniformly distributed load is then derived from:

$$q_h = \frac{1}{2} \rho_a C_d (D + 2t_e + 2t_c) (V_c + V_w)^2 \quad (\text{A.2.7})$$

The environmental: short-term loading may be augmented by an estimate of additional load due to marine fouling, if required.

A.2.5.5 Operating

The only part of the operating loading that requires derivation is the contents self-weight. This is given by:

$$q_i = \frac{\rho_i \pi g}{4} (D - 2t)^2 \quad (\text{A.2.8})$$

A.2.6 ANALYTICAL CRITERIA

A.2.6.1 General

It is recommended that the static strength analytical criteria should embody:

- stress limits
- plastic strain limits
- ovalisation limits
- limits derived from local buckling considerations.

The choice and use of criteria are set out below, and their precise implementation within the analytical method is dealt with in subsection A.2.7, below.

A.2.6.2 Stress Criterion

The output required from the static strength analysis is a computed span length corresponding to a limit set on the peak von Mises stress resulting from all the applied loadings. This peak stress is limited to a percentage of SMYS under this criterion; the following percentages from DNV / BS801 can be used.

	Percentage of SMYS for use in stress analytical criterion			
	DNV		BS8010	
	Fluid category A, C	Fluid category B, D, E	Operating condition NOT hydrotest	Hydrotest operating condition
Within 500 m DNV Zone 2	96	77	72	100
Outwith 500 m DNV Zone 1	96	87	96	100

Reference should be made to BS 8010: Part 3: 1993 and DNV, 1996 for detailed guidance.

A.2.6.3 Strain Criterion

The output required from the static strength analysis is a computed span length corresponding to a limit set on the peak equivalent plastic strain resulting from all the applied loadings. The peak equivalent plastic strain is set to an allowable value under this criterion; an allowable value of 0.1% is suggested.

A.2.6.4 Ovalisation Criterion

The output required from the static strength analysis is a computed span length corresponding to a limit set on the peak cross-section ovalisation resulting from the applied loadings. The peak ovalisation is set to an allowable value under this criterion. It is suggested that an allowable value of 1.5%, corrected for the out-of-roundness (OOR) tolerance from fabrication of the pipe, is used giving a criterion as follows:

$$\frac{D_{\max} - D_{\min}}{2D} \leq (1.5\% - \text{OOR}) \quad (\text{A.2.9})$$

where D_{\max} and D_{\min} are the maximum and minimum diameters, respectively, on the most highly ovalised cross-section.

Given that internal pressure has an ameliorating effect on ovalisation, consideration should be given to a load combination that excludes internal pressure.

A.2.6.5 Local Buckling Criterion

This is related to the collapse of the cross-section. The output required from the static strength analysis is a computed span length such that local buckling of the most highly bent cross-section does not occur under the applied loadings. The peak bending strain is set to an allowable value under this criterion.

Given that internal pressure has an ameliorating effect on local buckling, consideration should be given to a load combination that excludes internal pressure.

A.2.7 TIER 1 STATIC STRENGTH ANALYTICAL METHOD

A.2.7.1 General

The static strength analytical method for implementation at the Tier 1 level uses a strain-based approach, consisting of three aspects:

- a **cross-section bending resistance** model based on an additional plastic strain limitation
- a **span mechanical model** that explicitly embodies span end conditions and the exact effects of effective axial force
- an **analysis procedure** that links the resistance and mechanical models together.

Each of these aspects is dealt with in detail in subsections A.2.7.5, A.2.7.6 and A.2.7.7, below.

A.2.7.2 Loadings

The loadings that should be applied in the analytical method are as follows:

- prestressing due to residual lay tension (to be estimated conservatively and included if it adversely affects the pipeline)
- internal temperature q_i
- internal pressure p_i (which may be the normal operating, maximum allowable operating or hydrotest pressure, whichever is under attention; consideration should also be given to omitting the internal pressure if this is appropriate to the analytical criterion under use, see subsection 2.6)
- external temperature q_a
- external pressure p_a (see subsection A.2.5.3, above)
- total vertical uniformly distributed load $q_v = q + q_i$ (see subsections A.2.5.2 and A.2.5.5, above)
- total horizontal uniformly distributed load q_h (see subsection A.2.5.4, above).

A.2.7.3 Support Conditions

Symmetry at midspan may be assumed. In this case, appropriate symmetry boundary conditions on displacement are enforced at midspan, and one shoulder region considered.

Regarding the shoulder region, consideration must be given to support conditions in the vertical and transverse-horizontal directions. In the present case it is recommended that the supports are modelled as continuous elastic foundations in the vertical and transverse-horizontal planes to represent deformability of the seabed and its interaction with the pipe.

For elastic constants to be used in these types of support it is suggested that the stiffness per unit length of the vertical support should be derived as follows:

$$k_v = \frac{E_f}{2(1 - \nu_f^2)} \quad (\text{A.2.10})$$

and the stiffness per unit length of the transverse-horizontal support should be derived as follows:

$$k_h = \frac{E_f}{2(1 + \nu_f)} \quad (\text{A.2.11})$$

It is in order to use a planar value of transverse stiffness per unit length as the resultant of the above two, i.e.

$$k_f = \sqrt{k_v^2 + k_n^2} \quad (\text{A.2.12})$$

A.2.7.4 Material Characteristic

The stress-strain characteristic for the pipeline steel should be taken as elastic-perfectly plastic, with Young's modulus of E , Poisson's ratio of ν and yield strength of σ_0 .

A.2.7.5 Cross-section Bending Resistance

Physical Model. The cross-section bending resistance model computes an allowable bending moment for a given pipe cross-section (outside diameter and wall thickness), material, subject to pressure and thermal loadings; the resistance is subject to a prescribed limit on maximum strain derived from the analytical criterion. This limit may be elastic (whereupon the allowable bending moment relates to a standard stress limit), or based on an equivalent plastic strain criterion; it is thus completely general.

The mathematical modelling is based on an analysis that is separated out into two phases, as follows:

- prebending analysis, in which the pipeline is fully supported in the vertical and transverse-horizontal directions along its full length by the seabed, and thus involves no bending
- bending analysis, which models the state of stress within the pipeline as a result of spanning, and thus involves bending.

Assumptions. The assumptions used in both phases of the analysis are as follows:

1. The contribution of any weight and/or anti-corrosion coat to stiffness and strength of the pipeline cross-section is ignored.
2. The uniaxial stress-strain response of the pipe steel is elastic-perfectly plastic and material yield is governed by the von Mises yield criterion.
3. Pipe steel plasticity is governed by the Reuss equations for incremental plasticity.
4. Membrane thin-shell calculations based on the pipe median surface are sufficiently accurate for stresses in the pipe wall, with plane stress assumptions taken with respect to the through-thickness direction.
5. Plane cross-sections of the pipe remain plane after bending.

Prebending Analysis. This analysis comprises the loading due to internal and external pressure, internal and external temperature, and axial forces due to restrained longitudinal expansion and residual lay tension. The objectives are to determine:

- the state of stress and strain in the pipe and the net axial force
- the state of stress and strain necessary to just yield the pipe.

The prebending stresses in the pipe will be given by the following formulae:

$$\sigma_{\theta} = (p_i - p_a) \frac{(D - t)}{2t} \quad (\text{A.2.13})$$

$$\sigma_x = \frac{N}{A_s} + \lambda_a \{ \nu \sigma_{\theta} - \alpha E (\theta_i - \theta_a) \} \quad (\text{A.2.14})$$

and the net axial force is

$$N_{\text{netx}} = N + \lambda_a A_s \{ \nu \sigma_{\theta} - \alpha E (\theta_i - \theta_a) \} \quad (\text{A.2.15})$$

where

$$A_s = \frac{\pi}{4} [D^2 - (D - 2t)^2] \quad (\text{A.2.16})$$

The corresponding strains are given by:

$$\varepsilon_{\theta} = \frac{1}{E} (\sigma_{\theta} - \nu \sigma_x) + \alpha (\theta_i - \theta_a) \quad (\text{A.2.17})$$

$$\varepsilon_x = \frac{1}{E} (\sigma_x - \nu \sigma_{\theta}) + \alpha (\theta_i - \theta_a) \quad (\text{A.2.18})$$

The longitudinal stresses at yield for a prescribed hoop stress, from the von Mises ellipse, are as follows:

$$\sigma_{yxt} = \frac{1}{2} \left[\sigma_{\theta} + \sqrt{4\sigma_o^2 - 3\sigma_{\theta}^2} \right] \quad (\text{A.2.19})$$

$$\sigma_{yxc} = \frac{1}{2} \left[\sigma_{\theta} - \sqrt{4\sigma_o^2 - 3\sigma_{\theta}^2} \right] \quad (\text{A.2.20})$$

and the corresponding longitudinal strains are:

$$\varepsilon_{yxt} = \frac{1}{E} (\sigma_{yxt} - \nu \sigma_{\theta}) + \alpha (\theta_i - \theta_a) \quad (\text{A.2.21})$$

$$\varepsilon_{yxc} = \frac{1}{E} (\sigma_{yxc} - \nu \sigma_{\theta}) + \alpha (\theta_i - \theta_a) \quad (\text{A.2.22})$$

Bending Analysis. The objective of the bending analysis is to determine the cross-section bending resistance of the pipe subject to the analytical criterion, and the prebending state of stress described above. To achieve this the longitudinal strain in one fibre of the pipe (the “fixed” fibre) is set such that the analytical criterion on stress or strain is attained. The longitudinal strain in the diametrically opposite fibre (the “adjusted” fibre) is altered iteratively until a distribution of longitudinal stress obtains in the pipe that gives a net axial force equal to the value from the prebending analysis. The bending moment derived from that stress distribution is then the required cross-section bending resistance.

The final state of longitudinal strain in the **fixed fibre** ϵ_{fx} is given by:

$$\begin{aligned}\epsilon_{fx} &= \epsilon_{yxt} + \left(\sigma_{yxt} - \frac{\sigma_{\theta}}{2} \right) \frac{d\epsilon^p}{\sigma_0} \quad \text{if } \sigma_x > \frac{\sigma_{\theta}}{2} \quad \text{or} \\ \epsilon_{fx} &= \epsilon_{yxc} + \left(\sigma_{yxc} - \frac{\sigma_{\theta}}{2} \right) \frac{d\epsilon^p}{\sigma_0} \quad \text{if } \sigma_x \leq \frac{\sigma_{\theta}}{2}\end{aligned}\tag{A.2.23}$$

Where $d\epsilon^p$ is a limiting equivalent plastic strain increment. This, and the value of σ_0 , will be set according to the analytical criterion in use.

- In the case of a **stress** analytical criterion, σ_0 would be set equal to the percentage multiplier in subsection A.2.6.2 times σ_y and $d\epsilon^p$ would be set to zero.
- In the case of a **strain** analytical criterion, σ_0 would be set to σ_y and $d\epsilon^p$ would be set to the value specified in subsection A.2.6.3.
- In the cases of **ovalisation** or **local buckling** analytical criteria, a limiting bending strain e_b is to be derived and the final state of longitudinal strain in the fixed fibre taken as:

$$\begin{aligned}\epsilon_{fx} &= \epsilon_x + \epsilon_b \quad \text{if } \sigma_x > \frac{\sigma_{\theta}}{2} \quad \text{or} \\ \epsilon_{fx} &= \epsilon_x - \epsilon_b \quad \text{if } \sigma_x \leq \frac{\sigma_{\theta}}{2}\end{aligned}\tag{A.2.24}$$

The longitudinal strain in the **adjusted fibre** is changed iteratively until the resulting longitudinal stress distribution gives the required prebending axial force in the pipe. This is achieved by virtue of Assumption 5, given above, which prescribes a linear distribution of longitudinal strain between the diametrically opposite fibres. Thus at any iteration the strain distribution will be fixed, enabling the circumferential extent of yield to be established by comparing strains with the yield values ϵ_{yxt} and ϵ_{yxc} . For fibres of the pipe where the yield strains in tension and/or compression are exceeded, the longitudinal stresses are set to their corresponding yield values σ_{yxt} and σ_{yxc} . Where the yield strains are not exceeded the longitudinal stresses in those fibres

are set from elastic considerations. In this way the distribution of longitudinal stress around the circumference of the pipe is established and integration of this over the cross-section area gives a net axial force that is compared with the prebending value. Once convergence to the required axial force is attained, the longitudinal strain and stress distributions are completely defined, enabling the cross-section bending resistance to be computed by integration.

Calculation Procedure. The calculation procedure for the cross-section bending resistance is iterative. It is judged to be more practical to implement one calculation procedure for stress or strain analytical criteria, despite the fact that for stress criteria elastic response results and an iterative procedure is not, strictly speaking, necessary. The steps that need to be followed to perform the calculation are as follows:

1. Compute the prebending stresses and strains in the pipe, and the net axial force.
2. Compute the total longitudinal stresses at yield using the von Mises ellipse, and their corresponding strains.
3. Compute the bending stresses and corresponding bending strains necessary to cause yield.
4. Set the longitudinal strain in the fixed fibre by **either**:
 - 4a. Select the bending strain that causes first yield, add this to the prebending longitudinal strain and assign the result to the fixed fibre and
 - 4b. Calculate the longitudinal plastic strain increment from the stresses at yield of the fixed fibre and the analytical criterion being enforced and
 - 4c. Add to the strain at first yield in the fixed fibre from Step 3, the longitudinal plastic strain increment from Step 4.b to give the total limiting strain in the fixed fibre;

or add the bending strain corresponding to the analytical criterion to the prebending strain, and assign the result to the fixed fibre.

5. Guess a total longitudinal strain for the adjusted fibre and assume a linear longitudinal strain variation across the pipe diameter between this and the fixed fibre.
6. Compare the strain distribution from Step 5 with the yield strains from Step 2 to deduce the longitudinal stress distribution, including the extent of plasticity.
7. Calculate the net axial force in the pipe wall by integration of the longitudinal stress

distribution from Step 6 (with due regard to the extent of plasticity); if this does not agree with that from Step 1, iterate through Step 5 et seq.

8. Calculate the cross-section bending resistance in the pipe by product integration of the longitudinal stress distribution from Step 6 (with due regard to the extent of plasticity).

A.2.7.6 Span Mechanical Model

Span idealisation. The pipeline span is idealised as an infinitely long beam on a Winkler-type elastic foundation, in which a central portion of the elastic foundation has been removed, leaving a freespan. The loading comprises a uniformly distributed load and an axial compressive force (the effective axial force). In general, deflections (normal to the pipe axis) will occur over the full length of the pipe but will attenuate within the elastically-supported parts (the shoulders) at rate that depends on the elastic foundation stiffness per unit length and the pipe bending rigidity.

Problem parameters. The model input and response parameters are summarised in Table A.2.3. The input parameters are L , EI^* , N_a , q_n , g and l_f and the response parameters are M_{su} , M_{span} , x_{sho} , M_{sho} and M_{gov} .

Some of the input parameters are computed from baseline data as follows:

Equivalent bending rigidity of the pipe EI^* :

$$EI^* = \frac{EI_s}{(1 - \nu^2)} \quad (A.2.25)$$

where

$$I_s = \frac{\pi}{64} [D^4 - (D - 2t)^4] \quad (A.2.26)$$

Effective axial compression in pipe N_a :

$$\begin{aligned} N_a &= \sigma_x A_s - p_i \frac{\pi}{4} (D - 2t)^2 \quad \text{if } \sigma_x \leq 0 \\ N_a &= -p_i \frac{\pi}{4} (D - 2t)^2 \quad \text{if } \sigma_x > 0 \end{aligned} \quad (A.2.27)$$

Uniformly distributed lateral loading q_n :

$$q_n = \sqrt{q_v^2 + q_h^2} \quad (A.2.28)$$

Axial force inverse characteristic length γ :

$$\lambda_f = \left[\frac{k_f}{4EI^*} \right]^{\frac{1}{4}} \quad (\text{A.2.29})$$

Shoulder inverse characteristic length λ_f :

$$L < \frac{\sqrt{2}}{\gamma} \cos^{-1} \left[\left(\frac{\gamma}{\lambda_f} \right)^2 - 1 \right] \quad (\text{A.2.30})$$

Expressions for the various response bending moments are dealt with below.

Bar-buckling and upper range of limiting span length. Owing to the possibility of bar-buckling of the span due the compression caused by the effective axial force, there exists an upper limit to allowable span length that will be determined by this phenomenon. This may be found from the following equation:

$$\begin{aligned} & \frac{q_n}{\sqrt{2} \gamma N_a} \left\{ \tan \left(\frac{\gamma L}{\sqrt{2}} \right) - \frac{\gamma L}{\sqrt{2}} \right\} - M_{su} \frac{\sqrt{2} \gamma \left\{ \cos(\sqrt{2} \gamma L - 1) \right\}}{N_a \sin(\sqrt{2} \gamma L)} + \\ & + \frac{(q_n L - 4 M_{su} \alpha_f)}{2EI^* (3\alpha_f^2 - \beta_f^2)} = 0 \end{aligned} \quad (\text{A.2.31})$$

Bending moment at freespan/shoulder junction M_{su} . The bending moment at the junction between the freespan and the shoulder (i.e. at the end of the span) is determined from:

$$\alpha_f = \sqrt{\sqrt{\frac{k_f}{4EI^*} + \frac{N_a}{4EI^*}}} \quad (\text{A.2.32})$$

where

$$\beta_f = \sqrt{\sqrt{\frac{k_f}{4EI^*} - \frac{N_a}{4EI^*}}} \quad (\text{A.2.33})$$

$$\gamma = \sqrt{\frac{-N_a}{2EI^*}} \quad (\text{A.2.34})$$

Bending moment at midspan M_{span} . The bending moment at midspan is given by:

$$M_{span} = \frac{q_n}{2\gamma^2} \left\{ \frac{1}{\cos\left(\frac{\gamma L}{\sqrt{2}}\right)} - 1 \right\} + 2M_{su} \cos\left(\frac{\gamma L}{\sqrt{2}}\right) \left\{ 1 - \frac{\tan\left(\frac{\gamma L}{\sqrt{2}}\right)}{\tan(\sqrt{2}\gamma L)} \right\} \quad (A.2.35)$$

Location and magnitude of peak bending moment in shoulder x_{sho} and M_{sho} . The location of the peak bending moment in the shoulder portion of the pipe is found from:

$$\cot(\beta_f x_{sho}) = \frac{-(\beta_f M_{su} + \alpha_f M_x)}{(\alpha_f M_{su} - \beta_f M_x)} \quad (A.2.36)$$

$$M_x = \frac{q_n L \lambda_f^2 + \alpha_f (\alpha_f^2 - 3\beta_f^2) M_{su}}{-\beta_f (3\alpha_f^2 - \beta_f^2)} \quad (A.2.37)$$

and the **magnitude** of the corresponding bending moment is computed from:

$$M_{sho} = M_3 + M_4 \quad (A.2.38)$$

where

$$M_3 = \frac{-q_n L}{\beta_f} \frac{\lambda_f^2}{(3\alpha_f^2 - \beta_f^2)} e^{(-\alpha_f x_{sho})} \sin(\beta_f x_{sho}) \quad (A.2.39)$$

$$M_4 = M_{su} e^{(-\alpha_f x_{sho})} \left[\cos(\beta_f x_{sho}) - \frac{\alpha_f (\alpha_f^2 - 3\beta_f^2)}{\beta_f (3\alpha_f^2 - \beta_f^2)} \sin(\beta_f x_{sho}) \right] \quad (A.2.40)$$

Governing bending moment M_{gov} . The governing bending moment in the model is taken as the largest absolute value of the three bending moments given above, as follows:

$$M_{gov} = \text{MAX}(|M_{su}|, |M_{span}|, |M_{sho}|) \quad (A.2.41)$$

A.2.7.7 Analysis Procedure

In the analysis procedure, the span length is determined for which the governing bending moment from the span mechanical model equals the allowable bending moment from the cross-section bending resistance model. In cases where the allowable bending moment corresponds with a stress analytical criterion, this relates to an exact elastic technique. For situations where

a plastic strain limit is used (as determined from strain, ovalisation, or local buckling analytical criteria), the approach corresponds to a lower-bound equilibrium technique. This is because of the three necessary and sufficient conditions for the collapse of a structure:

- **equilibrium** is **satisfied** because the system of bending moments selected for the analysis is in equilibrium with the imposed loads
- **yield** is **satisfied** because the governing bending moment does not exceed the fully plastic moment of the pipe
- the **mechanism** criterion is **violated** because insufficient plastic hinges are present in the pipe for a mechanism to occur.

A.2.7.8 Analytical Method Implementation

The analytical method has been implemented into a spreadsheet program. An example of an analysis proforma is given in Section A.3, ATTACHMENTS.

A.2.8 ACCEPTANCE CRITERION

The output from the Tier 1 static strength analysis method is a computed span length L_{comp} . A percentage of this is compared with the observed span length to determine acceptability of the latter; the percentage suggested is 90%. Hence, the criterion for acceptability of the observed span is:

$$L_{obs} \leq 0.9 L_{comp} \tag{A.2.42}$$

Data	Symbol
Pipeline Data	
Pipe outside diameter	D
Pipe nominal wall thickness	t
Corrosion coat thickness	t_c
Weight coat thickness	t_w
Steel density	ρ_s
Corrosion coat density	ρ_e
Weight coat density	ρ_c
Steel elastic modulus	E
Steel Poisson's ratio	ν
SMYS steel	σ_y
Steel thermal expansion coefficient	α
Axial restraint factor	λ_a
Pipeline heading	ϕ
Operational Data	
Residual lay tension	N
Internal pressure	p_i
Contents density	ρ_i
Contents temperature	θ_i
Design life of pipeline	T_p
Environmental Data	
Minimum water depth at LAT	h
Local seawater density	ρ_a
Local seawater temperature	θ_a
Current velocity data	-
Wave data	-
Hydrodynamic drag coefficient	C_d
Hydrodynamic added mass coefficient	C_a
Soil elastic modulus at span shoulders	E_f
Soil Poisson's ratio at span shoulders	ν_f
Longitudinal friction coefficient at span shoulders	μ_L
Transverse friction coefficient at span shoulders	μ_T
Inspection Data	
Kilometre point at start of span	KP _s
Kilometre point at end of span	KP _e
Freespan length	L _{obs}
Gap beneath span	G
Marine growth information	-

Table A.2.1 Data Classes

Action	Loading	Load Combination			
PIPELINE WEIGHT	SUBMERGED SELF-WEIGHT	•	•	•	•
EXTERNAL TEMPERATURE	ENVIRONMENTAL: LONG-TERM	•	•	•	•
EXTERNAL PRESSURE		•	•	•	•
CURRENT-INDUCED	ENVIRONMENTAL: SHORT-TERM	•	•	•	•
WAVE-INDUCED		•	•	•	•
CONTENTS WEIGHT	NORMAL OPERATING	•			
INTERNAL TEMPERATURE		•			
INTERNAL PRESSURE		•			
CONTENTS WEIGHT	MAXIMUM ALLOWABLE OPERATING		•		
INTERNAL TEMPERATURE			•		
INTERNAL PRESSURE			•		
CONTENTS WEIGHT	SHUT-DOWN (MINIMUM OPERATING)			•	
INTERNAL TEMPERATURE				•	
INTERNAL PRESSURE				•	
CONTENTS WEIGHT	HYDROTEST				•
INTERNAL TEMPERATURE					•
INTERNAL PRESSURE					•

Table A.2.2 Relationship Between Actions, Loading And Load Combinations

Parameter description	Symbol	Formula / note
Freespan length	L	Varies within analytical procedure, see subsection A.2.7.7.
Bending rigidity of pipe	EI^*	$EI^* = \frac{EI_s}{(1-\nu^2)}$ Equivalent bending rigidity, based on hoop inextensibility of pipe.
Axial force in pipe (compression entered as negative)	N_a	$N_a = \sigma_x \frac{\pi}{4} [D^2 - (D - 2t)^2] - p_i \frac{\pi}{4} (D - 2t)^2$ Effective axial force in the pipe. σ_x only to be included if negative; residual lay tension ignored.
Uniformly distributed lateral loading	q_n	$q_n = \sqrt{q_v^2 + q_h^2}$ Resultant of vertical and horizontal uniformly distributed loads.
Axial force inverse characteristic length	γ	$\gamma = \sqrt{\frac{-N_a}{2EI^*}}$
Shoulder inverse characteristic length	λ_f	$\lambda_f = \left[\frac{k_f}{4EI^*} \right]^{\frac{1}{4}}$ k_f is the resultant of vertical and horizontal foundation stiffnesses per unit length, see subsection A.2.7.3.
Yield strength of pipe steel used in computation of cross-section bending resistance	σ_o	Set to pipe steel SMYS, or factored value thereof, depending on analytical criterion in use. See subsections A.2.6 and A.2.7.5.
Bending moment at freespan/shoulder junction	M_{su}	See subsection A.2.7.6.
Bending moment at midspan	M_{span}	See subsection A.2.7.6.
Location of peak bending moment in shoulder	x_{sho}	See subsection A.2.7.6.
Magnitude of peak bending moment in shoulder	M_{sho}	See subsection A.2.7.6.
Governing bending moment	M_{gov}	$M_{gov} = \text{MAX}(M_{su} , M_{span} , M_{sho})$ Governing bending moment is taken as the largest absolute value of freespan/shoulder junction, midspan and shoulder peak bending moments.

Table A.2.3 Input And Response Parameters For Tier 1 Span Mechanical Model

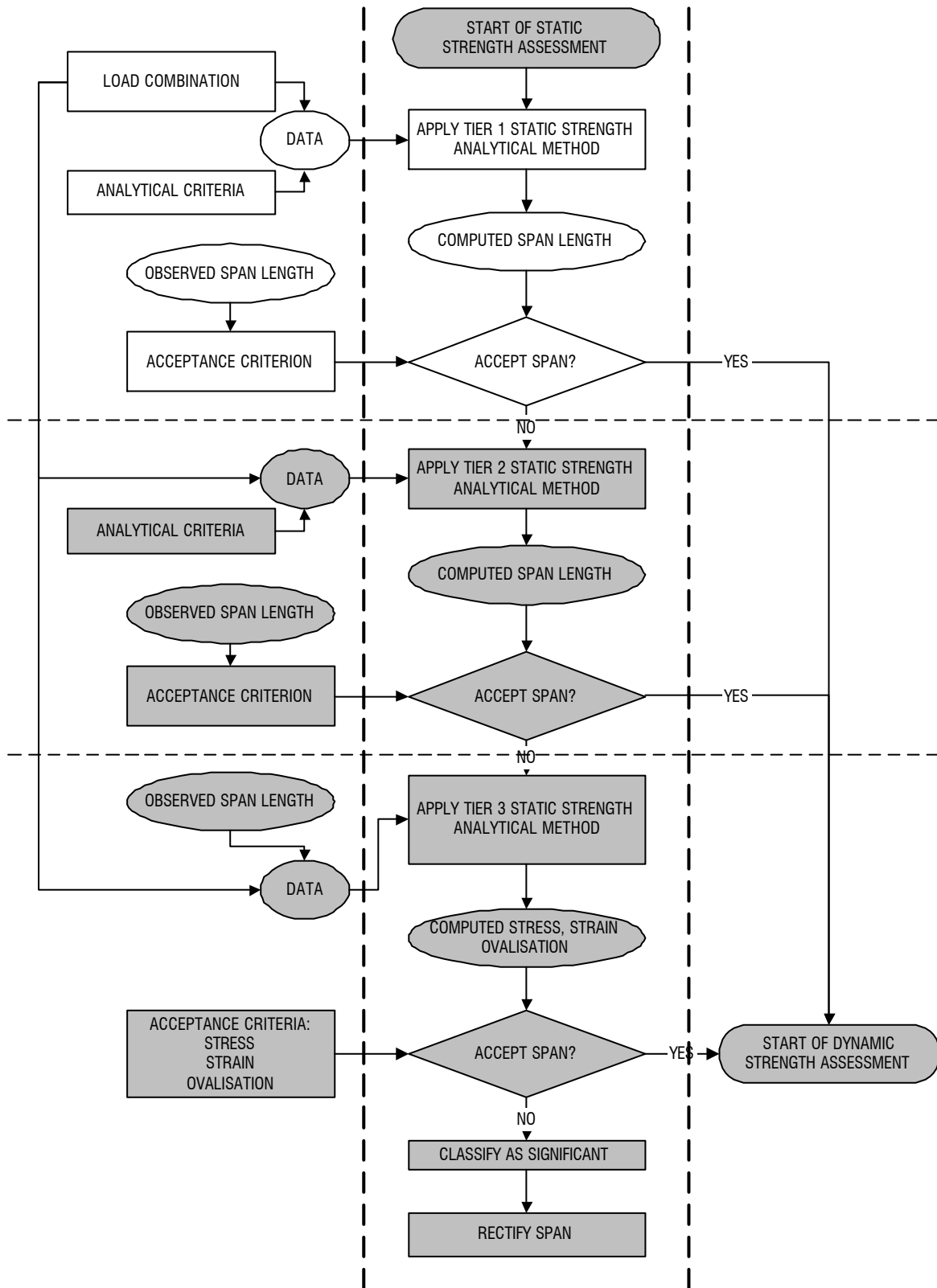


Figure A.2.1 Static Strength Assessment At The Tier 1 Level

A.3 ATTACHMENTS

TIER 1 Beam on elastic foundation STATIC STRENGTH span assessment method			
Pipeline data			
	Symbol	Value	(Units)
Pipeline segment identification	ID	PL-101-A	
Kilometre start point	KPs	0	km
Kilometre end point	KPe	0.16	km
Outside diameter	D	762	mm
Nominal wall thickness	t	15.88	mm
Corrosion coat thickness	te	5.56	mm
Weight coat thickness	tc	48	mm
Steel density	rs	7850	kg/m ^ 3
Corrosion coat density	re	1200	kg/m ^ 3
Weight coat density	rc	3124	kg/m ^ 3
Steel elastic modulus	E	207000	N/mm ^ 2
Steel Poissons ratio	nu	0.3	
Steel SMYS	SMYS	358	N/mm ^ 2
Factor on SMYS	Ksmys2	1	
Factored SMYS	So	358	N/mm ^ 2
Steel coeff. of thermal expansion	alf	1.16E-05	° C ^ -1
Operational conditions data			
			(Units)
Residual lay tension	Nlay	0	N
Contents pressure	pnorm	1.69	N/mm ^ 2
Contents density	ri	585.4	kg/m ^ 3
Contents temperature	thi	15	° C
Environmental data			
			(Units)
Gravitational acceleration	g	9.81	m/s ^ 2
Minimum water depth at LAT	h	37	m
Current speed at top of pipe	Vc	0.57	m/s
Max. wave induced velocity at top of pipe	Vw	1.61	m/s
Local seawater density	rw	1025	kg/m ^ 3
Local seawater temperature	tha	8	° C
Hydrodynamic drag coefficient	Cd	1.05	
Soil elastic modulus at span shoulders	kf	25	N/mm ^ 2
Safety factors etc.			
			(Units)
Weight growth factor	ew	1	
Axial restraint factor	l	1	
Maximum equivalent plastic strain	ep2	0.10%	
Stress/strain criterion being applied is		2	
Safety factor on span (static strength)	lIs	0.9	
P-delta effect switch (0 = off, 1 = on)	Switch	1	
Principal results			
			(Units)
Submerged weight of pipe/unit length	q	3257.9	N/m
Horizontal loading/unit length	qh	2236.94	N/m
Maximum loading/unit length	qmx	3951.94	N/m
Residual lay tension stress	Slit	0	N/mm ^ 2
Hoop stress	Sh	30.97	N/mm ^ 2
Thermal stress	St	-16.81	N/mm ^ 2
Poisson effect stress	Sp	9.29	N/mm ^ 2
Net prebending longitudinal stress	Sn	-7.52	N/mm ^ 2
Membrane axial force		-2.80E+05	N
Bore pressure axial force		-7.08E+05	N
Effective axial force		-9.88E+05	N
Allowable bending moment	Mall	2.86E+06	Nm
Error check on span length calculation	Error	OK	
Factored governing allowable span length	Ls1	73.9	m

Table A.3.1 Example Of Tier 1 Static Strength Analysis Proforma

APPENDIX B

PIPELINE DEFECT ASSESSMENT PROCESS: SPAN ANALYSIS FOR STATIC STRENGTH AT THE TIER 2 LEVEL

TABLE OF CONTENTS

	Page No.
B.1 INTRODUCTION	B.1.1
B.1.1 PURPOSE	B.1.1
B.1.2 SCOPE AND LIMITATIONS	B.1.1
B.1.3 REFERENCES	B.1.1
B.1.3.1 Codes And Standards	B.1.1
B.2 PROCESS	B.2.1
B.2.1 OBJECTIVE	B.2.1
B.2.2 ASSESSMENT STRATEGY AT THE TIER 2 LEVEL	B.2.1
B.2.2.1 Generic	B.2.1
B.2.2.2 Considerations In The Tier 2 Static Strength Analytical Method	B.2.1
B.2.3 DATA	B.2.2
B.2.3.1 Data Classes	B.2.2
B.2.3.2. Data Sources	B.2.2
B.2.4 LOADINGS AND LOAD COMBINATIONS IN GENERAL	B.2.3
B.2.4.1 General Points	B.2.3
B.2.4.2 Actions	B.2.3
B.2.4.3 Loadings	B.2.3
B.2.5 LOAD COMBINATION IN TIER 2 ANALYTICAL METHOD	B.2.4
B.2.5.1 Load Combination	B.2.4
B.2.5.2 Submerged Self-Weight	B.2.4
B.2.5.3 Environmental: Long-Term	B.2.4
B.2.5.4 Environmental: Short-Term	B.2.5
B.2.5.5 Operating	B.2.5
B.2.6 ANALYTICAL CRITERIA	B.2.6
B.2.6.1 General	B.2.6
B.2.6.2 Stress Criterion	B.2.6
B.2.7 TIER 2 STATIC STRENGTH ANALYTICAL METHOD	B.2.6
B.2.7.1 General	B.2.6
B.2.7.2 Loadings	B.2.7
B.2.7.3 Support Conditions	B.2.8
B.2.7.4 Material Characteristic	B.2.9
B.2.7.5 Mechanical Model	B.2.9
B.2.7.6 Analytical Method Implementation	B.2.13
B.2.8 ACCEPTANCE CRITERION	B.2.13
B.3 ATTACHMENTS	B.3.1

LIST OF TABLES

Table B.2.1 Data Classes

Table B.2.2 Relationship Between Actions, Loading And Load Combinations

Table B.3.1 Example Of Tier 2 Static Strength Analysis Proforma

LIST OF FIGURES

Figure B.2.1 Static Strength Assessment At The Tier 2 Level

Figure B.2.2 Schematic Representation Of Tier 2 Analytical Method

B.1 INTRODUCTION

B.1.1 PURPOSE

The purpose of this process is to set down the methodology for the static strength analysis of pipeline spans at the Tier 2 level and to ensure that best practice is applied.

B.1.2 SCOPE AND LIMITATIONS

This process applies to pipelines laid directly onto the seabed. It applies to an individual span; that is, a single clear unsupported length of pipeline that is sufficiently isolated from other spans or features as to be judged to behave as a self-contained entity. It does not apply to pipelines that are trenched, trenched and backfilled, trenched and infilled due to natural soil migration, or pipelines that are piggybacked.

B1.3 REFERENCES

B1.3.1 Codes And Standards

- Rules For Submarine Pipeline Systems. Det Norske Veritas. **DNV, 1996.**
- Code Of Practice For Pipelines Subsea: Design, Construction And Installation. British Standards Institute (BSI). **BS 8010: Part 3: 1993.**
- American Petroleum Institute (API). Recommended Practice For Planning, Designing, And Constructing Fixed Offshore Platforms - Working Stress Design. **RP2A-WSD, 20th ed., July 1993.**

B.2 PROCESS

B.2.1 OBJECTIVE

The objective of this process is to ensure that the static strength analysis of pipeline spans at the Tier 2 level is conducted in a rigorous manner, with due regard to the mechanical characteristics of the problem, using appropriate analytical criteria, and that spans are determined to be acceptable or significant against acceptance criteria.

B.2.2 ASSESSMENT STRATEGY AT THE TIER 2 LEVEL

B.2.2.1 Generic

The recommended Pipeline Defect Assessment Procedure allows a tiered approach to analytical methods and span acceptance. Specifically, up to a three-tiered philosophy can be adopted as shown in detail for the failure mode of static strength in Figure B.2.1. In this figure, Tiers 1 and 3 have been greyed, leaving the Tier 2 assessment covered by this process highlighted.

At whatever tier level, the approach involves interaction between the data, load combination, analytical criteria, analytical methods and acceptance criteria; each of these is dealt with in detail in subsections B.2.3 to B.2.8, below. At Tier 2, observed span lengths are judged against span lengths computed from the analytical method, using acceptance criteria, to determine acceptability:

- data, load combination and analytical criteria are all input into the analytical method
- output from the analytical method is a computed span length, which is compared with the observed span length to determine acceptability of the latter using an acceptance criterion.

B.2.2.2 Considerations In The Tier 2 Static Strength Analytical Method

For the static strength analytical method recommended for pipeline spans in this process document consideration should be given to the following factors:

- loadings
- support conditions
- material characteristic
- mechanical model

- Analytical method implementation.

Each of these points is addressed in detail in subsection B.2.7, below.

B.2.3 DATA

B.2.3.1 Data Classes

A detailed breakdown of the data into the four classes of: *pipeline*, *operational*, *environmental* and *inspection* is given in Table B.2.1. Data in the lines of Table B.2.1 that have been greyed are considered to be unnecessary to perform the Tier 2 static strength analysis. The remainder can be viewed as “baseline” data, some of which have to be processed by means of calculation into suitable input data for the analysis.

The **pipeline data** include geometrical and material properties; these are used in the analytical model, the analytical criteria and the material characteristic. The axial restraint factor is used to approximate the degree of suppression of longitudinal strains in the pipe wall due to the interaction of the pipe with the seabed.

The **operational data** encompass installation (residual lay tension) and those related to the pipe contents: its density, pressure and temperature; these are used to derive some of the loadings applied to the span.

The **environmental data** include the parameters that relate to the fluid loading on the pipeline (for example, water depth and various wave and current data). They also contain parameters defining the mechanical interaction between the pipe and the seabed (for example, soil modulus and Poisson's ratio at the span shoulders); these particular parameters influence the support conditions at the shoulder of the pipeline.

The **inspection data** include parameters to locate the span (kilometre start and end points), and freespan length. If marine growth information is included within the inspection data an assessment should be made as to whether this influences the pipeline weight or the hydrodynamic loading on the pipeline.

B.2.3.2 Data Sources

Appropriate sources of pipeline, operational and environmental data are to be used. If no data are available for residual lay tension or axial restraint factor, then these are to be estimated conservatively and included if they adversely affect the pipeline.

B.2.4 LOADINGS AND LOAD COMBINATIONS IN GENERAL

B.2.4.1 General Points

A load combination is built up from *actions* and *loadings* as shown schematically in Table B.2.5. The loading combination to be used is a requirement of the assessment and, as indicated in subsection B.2.5, an *operating* loading is always included in the combination. This will usually correspond to the normal operating conditions of the pipeline, although there may be occasions where other operating conditions need to be considered.

B.2.4.2 Actions

In terms of detailed thermo-mechanical actions there are eight types that require consideration:

- pipeline weight
- external temperature
- external pressure
- current-induced action
- wave-induced action
- contents weight
- internal temperature
- internal pressure.

B.2.4.3 Loadings

Four individual loading classes are to be considered, namely:

- submerged self weight
- environmental: long-term
- environmental: short-term
- operating.

More than one type of operating condition may need to be addressed. As indicated in Table B.2.5, the list covers the following possibilities:

- normal operating
- maximum allowable operating
- shut down (minimum operating)
- hydrotest.

This list may be extended if circumstances dictate.

B.2.5 LOAD COMBINATION IN TIER 2 ANALYTICAL METHOD

B.2.5.1 Load Combination

A load combination is made up from loading classes, and will always comprise the submerged self-weight, environmental long- and short-term load and an operating class, as set out schematically in Table B.2.2.

B.2.5.2 Submerged Self-Weight

The submerged self-weight should comprise the weight of the pipe, anti-corrosion coating and weight coating, minus the displaced weight of seawater. It is calculated from the data as follows:

$$q = q_s + q_e + q_c - q_a \quad (\text{B.2.1})$$

$$q_s = \frac{\rho_s \pi g}{4} [D^2 - (D - 2t)^2] \quad (\text{B.2.2})$$

$$q_e = \frac{\rho_e \pi g}{4} [(D + 2t_e)^2 - D^2] \quad (\text{B.2.3})$$

$$q_c = \frac{\rho_c \pi g}{4} [(D + 2t_e + 2t_c)^2 - (D + 2t_e)^2] \quad (\text{B.2.4})$$

$$q_a = \frac{\rho_a \pi g}{4} (D + 2t_e + 2t_c)^2 \quad (\text{B.2.5})$$

The symbols are explained in Table B.2.1.

The submerged self-weight may be augmented by an estimate of additional gravity load due to marine fouling, if appropriate.

B.2.5.3 Environmental: Long-Term

The only part of the environmental: long-term loading that requires derivation is the external (hydrostatic) pressure. This may be estimated from:

$$p_a = \rho_a gh \quad (\text{B.2.6})$$

B.2.5.4 Environmental: Short-Term

The environmental: short-term loading comprises the hydrodynamic uniformly distributed load resulting from the drag on the pipeline from the moving water particle velocities. Inertia loading is generally small, and in most circumstances may be neglected. It is recommended that directional 50-year return period maximum wave height and period (H_{\max} and T_{\max}), and *associated* maximum surface current velocity are used. To determine the maximum combined water particle velocity normal to the heading of the span, which forms the input to Morison's equation to derive the loading on the span. The main steps in this process are as follows:

1. Use directional 50-year return period maximum wave height and period (H_{\max} and T_{\max}), and *associated* maximum surface current velocity
2. Considering the heading of the pipeline span, determine the maximum wave height and corresponding period, and associated surface current velocity normal to the pipeline span
3. Compute the top-of-pipe current velocity V_c using a power-law current profile suggested in the source data
4. Compute the top-of-pipe maximum wave velocity V_w using a wave theory suitable for the H_{\max} - T_{\max} - water depth combination concerned (kinematic spreading may be neglected, and the effect of current velocity on wave period may be ignored)
5. The uniformly distributed load is then derived from:

$$q_h = \frac{1}{2} \rho_a C_d (D + 2t_e + 2t_c) (V_c + V_w)^2 \quad (\text{B.2.7})$$

The environmental: short-term loading may be augmented by an estimate of additional load due to marine fouling, if required.

B.2.5.5 Operating

The only part of the operating loading that requires derivation is the contents self-weight. This is given by:

$$q_i = \frac{\rho_i \pi g}{4} (D - 2t)^2 \quad (\text{B.2.8})$$

B.2.6 ANALYTICAL CRITERIA

B.2.6.1 General

It is recommended that the static strength analytical criterion should embody a stress limit.

The choice and use of the criterion is set out below, and its precise implementation within the analytical method is dealt with in subsection B.2.7.

B.2.6.2 Stress Criterion

The output required from the static strength analysis is a computed span length corresponding to a limit set on the peak von Mises stress resulting from all the applied loadings. This peak stress is limited to a percentage of SMYS under this criterion; the following percentages from DNV / BS801 can be used:

	Percentage of SMYS for use in stress analytical criterion			
	DNV		BS8010	
	Fluid category A, C	Fluid category B, D, E	Operating condition NOT hydrotest	Hydrotest operating condition
Within 500 m DNV Zone 2	96	77	72	100
Outwith 500 m DNV Zone 1	96	87	96	100

Reference should be made to BS 8010: Part 3: 1993 and DNV, 1996 for detailed guidance.

B.2.7 TIER 2 STATIC STRENGTH ANALYTICAL METHOD

B.2.7.1 General

The analytical method is shown in outline in the flow-chart given in Figure B.2.2. The purpose of the analysis is to compute a span length for the pipe subjected to the various loadings and an analytical criterion. The analytical method is made up of four computational modules, namely:

- axial model (prebending state)
- membrane model

- bending model
- analytical criterion.

These interact with each other within an overall framework. The framework controls the method iteratively, changing the span length until the analytical criterion is just satisfied. The interaction between the modules and the way the framework operates is outlined in more detail below, and the individual models are given a fuller description in subsection B.2.7.5.

The **axial model** takes as inputs the pipe material properties and cross-section dimensions, and internal and external temperatures and pressures. It computes, and produces as outputs, the pipe wall hoop and longitudinal stresses, and initial effective axial force in the pipe. The latter is aggregated from the longitudinal stress in the pipe wall times the cross-section area, and the internal pressure times the pipe bore area. Since the computations do not involve the span length, the axial model functions outwith the iterative loop that changes this parameter.

A cycle of iteration starts with the **membrane model**. This receives pipe material properties and cross-section dimensions, lateral load, and (from the prebending model) initial effective force as inputs. In addition to these the model uses the span length for the particular iteration cycle; its purpose is to compute the membrane stresses that develop longitudinally in the pipe wall as a result of sag tension, and produces as output the final effective axial force in the span.

The **bending model** takes pipe material properties and cross-section dimensions, lateral load, span length, and (from the membrane model) final effective axial force. The principal output it produces is the peak bending stress in the pipe wall.

The final stage in any cycle of iteration is the application of the **analytical criterion**. In this, the pipe wall hoop stress from the axial model, the final longitudinal stresses from the membrane model and the peak bending stress from the bending model are combined to give the peak von Mises stress. The result is compared with the stress from the analytical criterion, and if the two are significantly close in value, the span length is deemed to be that which is required; otherwise, a revised span length is taken and the cycle of iteration begins again.

B.2.7.2 Loadings

The loadings that should be applied in the analytical method are as follows:

- prestressing due to residual lay tension (to be estimated conservatively and included if it adversely affects the pipeline)
- internal temperature q_i
- internal pressure p_i (which may be the normal operating, maximum allowable

- operating or hydrotest pressure, whichever is under attention)
- external temperature q_a
- external pressure p_a (see subsection B.2.5.3, above)
- total vertical uniformly distributed load $q_v = q + q_i$ (see subsections B.2.5.2 and B.2.5.5, above)
- total horizontal uniformly distributed load q_h (see subsection B.2.5.4, above).

B.2.7.3 Support Conditions

Symmetry at midspan may be assumed. In this case, appropriate symmetry boundary conditions on displacement are enforced at midspan, and one shoulder region considered.

Regarding the shoulder region, consideration must be given to support conditions in the vertical, transverse-horizontal and the longitudinal-horizontal directions.

For the longitudinal-horizontal direction consideration should be given to the interaction of the extensibility of the pipeline supported at the shoulders and the deformability of the supporting soil. It is suggested that the stiffness per unit length of the longitudinal-horizontal supporting soil should be derived as follows:

$$k_h = \frac{E_f}{2(1 + \nu_f)} \quad (\text{B.2.9})$$

The stiffness against longitudinal pull-in at the ends of the span is to be taken for an infinite shoulder length and is given by:

$$K_L = \sqrt{EA_s k_h} \quad (\text{B.2.10})$$

where

$$A_s = \frac{\pi}{4} [D^2 - (D - 2t)^2] \quad (\text{B.2.11})$$

The Tier 2 analytical method requires the specification of an equivalent slip length of pipe at the shoulders, denoted as ℓ , which gives the same stiffness against pull-in as the pipe-foundation combination. This is given by:

$$\ell = \frac{EA_s}{K_L} = \sqrt{\frac{EA_s}{k_h}} \quad (\text{B.2.12})$$

As spans become larger, it is apparent that rotational bending stiffness lessens relative to the vertical and transverse-horizontal stiffnesses of the supporting soil. In these cases, to which the Tier 2 analytical method is most appropriate, it is in order to take fix-fix end conditions with

respect to rotations of the span ends about axes normal to the vertical and transverse-horizontal planes.

B.2.7.4 Material Characteristic

The stress-strain characteristic for the pipeline steel should be taken as elastic, with Young's modulus of E , Poisson's ratio of ν . Where required, the yield strength should be taken as s_0 .

B.2.7.5 Mechanical Model

B.2.7.5.1 Axial Model

Purpose. The purpose of the axial model is to determine the longitudinal and hoop state of stress in the pipe wall and the initial effective axial force in the pipeline.

Assumptions. The assumptions used for the axial model are as follows:

1. The structural effects of anti-corrosion and weight coats are ignored.
2. The stress-strain response of the pipe steel is elastic.
3. The pipe is fully supported along its length by the seabed, and there are no bending-type deformations.
4. Membrane thin shell calculations based on the median surface of the steel pipe are sufficiently accurate for stresses, with plane stress assumptions with respect to the through-thickness direction.
5. There is full axial restraint in the longitudinal direction, leading to thermal and Poisson-effect stresses.

Stresses and initial effective axial force. The pipe wall stresses and initial effective axial force are given by the following expressions:

Hoop stress σ_θ :

$$\sigma_\theta = (p_i - p_a) \frac{(D - t)}{2t} \quad (\text{B.2.13})$$

Longitudinal stress σ_{x0} :

$$\sigma_{x0} = \frac{N}{A_s} + \left\{ \nu \sigma_\theta - \alpha E (\theta_i - \theta_a) \right\} \quad (\text{B.2.14})$$

Initial effective axial force N_{a0} :

$$N_{a0} = \sigma_{x0} A_s - p_i \frac{\pi}{4} (D - 2t)^2 \quad (\text{B.2.15})$$

B.2.7.5.2 Membrane Model

Purpose. The purpose of the membrane model is to determine the sag tension longitudinal stress that develops in the pipe wall as a result of bending in the span, and the final effective axial force.

Idealisation. The spanning portion of the problem is idealised as a planar beam with fix-fix rotational boundary conditions. The ends of the beam are capable of translating horizontally (“pulling-in”), but are restrained from doing so by adjoining lengths of straight pipe (“slip lengths”) on the shoulders that are anchored at their ends remote from the spanning portion. The whole of the model (span plus the two slip lengths) are initially subject to an effective axial force; the span portion is also loaded by a uniformly distributed lateral load.

Assumptions. The assumptions used for the membrane model are as follows:

1. Only longitudinal stresses may occur in the pipe wall within the slip length.
2. There are no rotations at the ends of the freespan portion of the model.
3. There is compatibility of longitudinal displacement at the junctions between the spanning and slip length portions of the model.
4. The stress-strain response of the pipe steel is elastic.
5. The initial effective axial force is uniform along the length of the model.
6. The membrane tension developed in response to the bending is uniform along the length of the model.
7. Euler-Bernoulli beam-bending theory applies to the spanning portion of the model.

Parameters. The parameters are derived using baseline data and other expressions derived in subsection 2.7.5.1, above, as follows:

Equivalent bending rigidity of the pipe EI^* :

$$EI^* = \frac{EI_s}{(1 - \nu^2)} \quad (\text{B.2.16})$$

where

$$I_s = \frac{\pi}{64} [D^4 - (D - 2t)^4] \quad (\text{B.2.17})$$

Pipe cross-section radius of gyration r_s :

$$r_s = \sqrt{\frac{I_s}{A_s}} \quad (\text{B.2.18})$$

Uniformly distributed lateral loading q_n :

$$q_n = \sqrt{q_v^2 + q_h^2} \quad (\text{B.2.19})$$

Normalised span length λ :

$$\lambda = \frac{1}{\pi} \left(\frac{q_n r_s}{4EA_s} \right)^{\frac{1}{4}} \left(\frac{L}{r_s} \right) \quad (\text{B.2.20})$$

Normalised initial effective axial force n_{ao} :

$$n_{ao} = \frac{N_{ao}}{EI^*} \sqrt{\frac{EI^* r_s}{4q_n}} \quad (\text{B.2.21})$$

Governing equations. The equations that govern the response of the membrane model, written in terms of the problem parameters defined above, are as follows:

Equation determining midspan lateral deflection δ_m :

$$\zeta - \lambda^4 + \frac{L}{16(L+2\ell)} \zeta^3 + n_{ao} \lambda^2 \zeta = 0 \quad (\text{B.2.22})$$

where

$$\zeta = \frac{\delta_m}{r_s} \quad (\text{B.2.23})$$

This is a cubic equation in ζ , which can be solved by standard methods.

Longitudinal pull-in deflection at span end u :

$$u = \pi^2 \frac{\ell}{4L(L+2\ell)} \delta_m^2 \quad (\text{B.2.24})$$

Normalised additional membrane force n_a :

$$n_a = \frac{L}{4(L+2\ell)} \zeta^2 \quad (\text{B.2.25})$$

Final effective axial force N_a :

$$N_a = N_{ao} + EI^* \left(\frac{\pi}{L} \right)^2 n_a \quad (\text{B.2.26})$$

Final pipe wall longitudinal stress σ_{xa} :

$$\sigma_{xa} = \sigma_{x0} + \frac{EI^*}{A_s} \left(\frac{\pi}{L} \right)^2 n_a \quad (\text{B.2.27})$$

B.2.7.5.3 Bending Model

Purpose. The purpose of the bending model is to determine the peak longitudinal bending stress in the pipe wall when the span is loaded by the uniformly distributed lateral load and the final effective axial force.

Idealisation. The span portion only is considered. This is treated as a beam with fix-fix end conditions under uniformly distributed lateral load and an axial force.

Assumptions. The assumptions used in the bending model are as follows:

1. There is no rotation at the ends of the span.
2. There is no restraint against pull-in at the ends of the span.
3. The stress-strain response of the pipe steel is elastic.
4. Small deflection theory applies.
5. Euler-Bernoulli beam-bending theory applies.

Governing equations. The equations that govern the response of the bending model, written in terms of the problem parameters defined above, are as follows:

Peak bending stress σ_{xb} :

$$\sigma_{xb} = \frac{D}{2I_s} \frac{q_n L^2}{4} \left(\frac{\theta - \tanh \theta}{\theta^2 \tanh \theta} \right) \quad \text{if } N_a \geq 0 \quad (\text{B.2.28})$$

$$\sigma_{xb} = \frac{D}{2I_s} \frac{q_n L^2}{4} \left(\frac{\tan \theta - \theta}{\theta^2 \tan \theta} \right) \quad \text{if } N_a < 0$$

where

$$\theta = \frac{L}{2} \sqrt{\frac{|N_a|}{EI^*}} \quad (\text{B.2.29})$$

Midspan lateral deflection δ_b :

$$\delta_b = \frac{q_n L^4}{16EI^*} \frac{1}{\theta^3} \left\{ \frac{\theta}{2} - \tanh\left(\frac{\theta}{2}\right) \right\} \quad \text{if } N_a \geq 0$$

$$\delta_b = \frac{q_n L^4}{16EI^*} \frac{1}{\theta^3} \left\{ \tan\left(\frac{\theta}{2}\right) - \frac{\theta}{2} \right\} \quad \text{if } N_a < 0$$
(B.2.30)

B.2.7.5.4 Use Of Analytical Criterion

The span length is deemed to have reached the magnitude necessary to satisfy the analytical criterion when the following condition is satisfied:

$$\left| \begin{array}{c} \left[\sqrt{(\sigma_{xa} + \sigma_b)^2 - (\sigma_{xa} + \sigma_b)\sigma_\theta + \sigma_\theta^2} \right] \\ \text{OR} \\ \left[\sqrt{(\sigma_{xa} - \sigma_b)^2 - (\sigma_{xa} - \sigma_b)\sigma_\theta + \sigma_\theta^2} \right] \end{array} \right| - \sigma_o \leq \xi$$
(B.2.31)

where σ_o is the percentage of SMYS determined using the analytical criterion as set out in subsection B.2.6.2, and ξ is a convergence tolerance close to zero.

B.2.7.6 Analytical Method Implementation

The analytical method has been implemented into a spreadsheet program. An example of an analysis proforma is given in Section B.3, ATTACHMENTS.

B.2.8 ACCEPTANCE CRITERION

The output from the Tier 2 static strength analysis method is a computed span length L_{comp} . A percentage of this is compared with the observed span length to determine acceptability of the latter; the percentage suggested is 90%. Hence, the criterion for acceptability of the observed span is:

$$L_{obs} \leq 0.9 L_{comp}$$
(B.2.32)

Data	Symbol
Pipeline Data	
Pipe outside diameter	D
Pipe nominal wall thickness	t
Corrosion coat thickness	t_c
Weight coat thickness	t_w
Steel density	ρ_s
Corrosion coat density	ρ_e
Weight coat density	ρ_c
Steel elastic modulus	E
Steel Poisson's ratio	ν
SMYS steel	σ_y
Steel thermal expansion coefficient	α
Axial restraint factor	λ_a
Pipeline heading	ϕ
Operational Data	
Residual lay tension	N
Internal pressure	p_i
Contents density	ρ_i
Contents temperature	θ_i
Design life of pipeline	T_p
Environmental Data	
Minimum water depth at LAT	h
Local seawater density	ρ_a
Local seawater temperature	θ_a
Current velocity data	-
Wave data	-
Hydrodynamic drag coefficient	C_d
Hydrodynamic added mass coefficient	C_a
Soil elastic modulus at span shoulders	E_f
Soil Poisson's ratio at span shoulders	ν_f
Longitudinal friction coefficient at span shoulders	μ_L
Transverse friction coefficient at span shoulders	μ_T
Inspection Data	
Kilometre point at start of span	KP _s
Kilometre point at end of span	KP _e
Freespan length	L _{obs}
Gap beneath span	G
Marine growth information	-

Table B.2.1 Data Classes

Action	Loading	Load Combination			
PIPELINE WEIGHT	SUBMERGED SELF-WEIGHT	•	•	•	•
EXTERNAL TEMPERATURE	ENVIRONMENTAL: LONG-TERM	•	•	•	•
EXTERNAL PRESSURE		•	•	•	•
CURRENT-INDUCED	ENVIRONMENTAL: SHORT-TERM	•	•	•	•
WAVE-INDUCED		•	•	•	•
CONTENTS WEIGHT	NORMAL OPERATING	•			
INTERNAL TEMPERATURE		•			
INTERNAL PRESSURE		•			
CONTENTS WEIGHT	MAXIMUM ALLOWABLE OPERATING		•		
INTERNAL TEMPERATURE			•		
INTERNAL PRESSURE			•		
CONTENTS WEIGHT	SHUT-DOWN (MINIMUM OPERATING)			•	
INTERNAL TEMPERATURE				•	
INTERNAL PRESSURE				•	
CONTENTS WEIGHT	HYDROTEST				•
INTERNAL TEMPERATURE					•
INTERNAL PRESSURE					•

Table B.2.2 Relationship Between Actions, Loading And Load Combinations

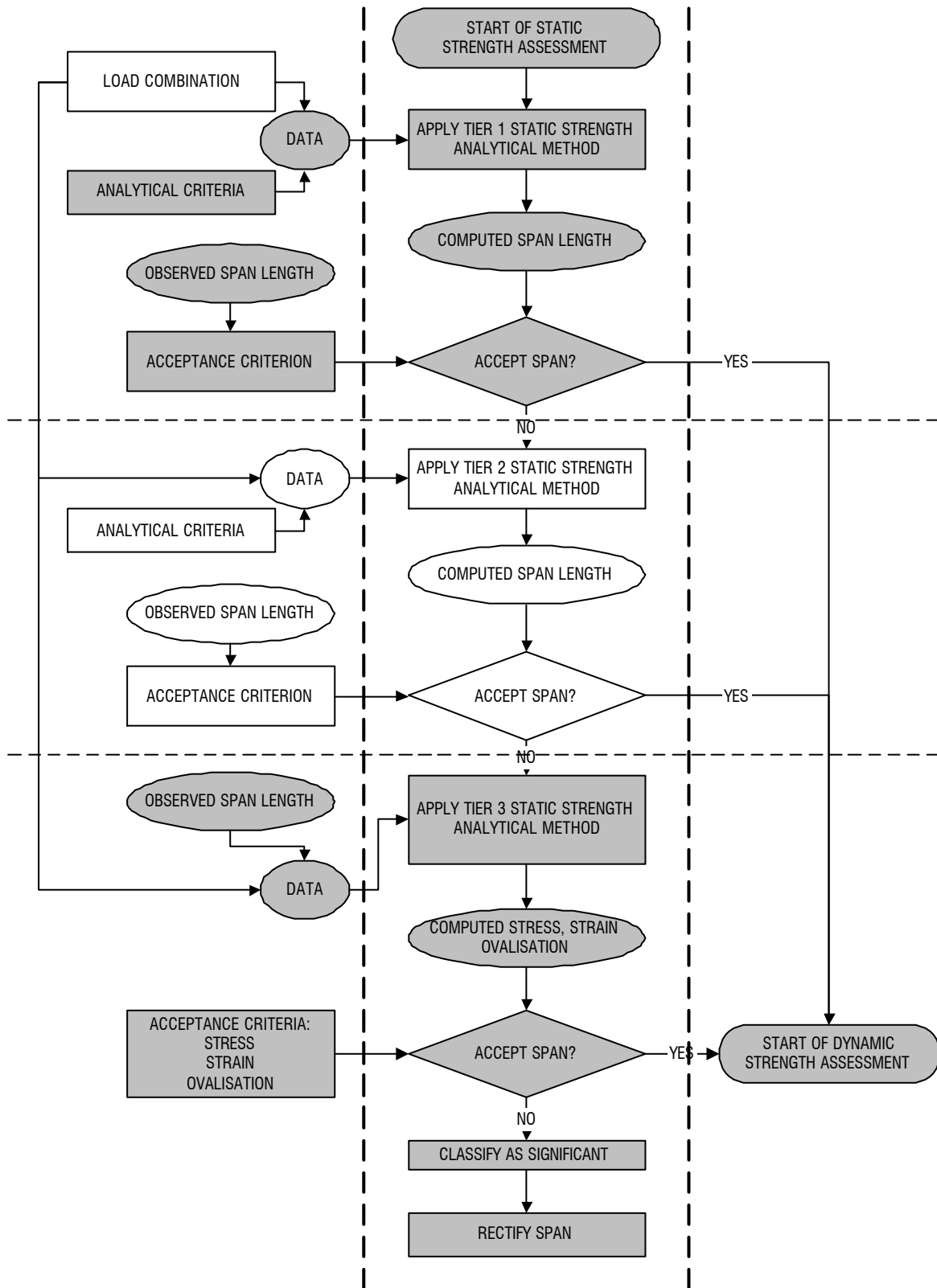


Figure B.2.1 Static Strength Assessment At The Tier 2 Level

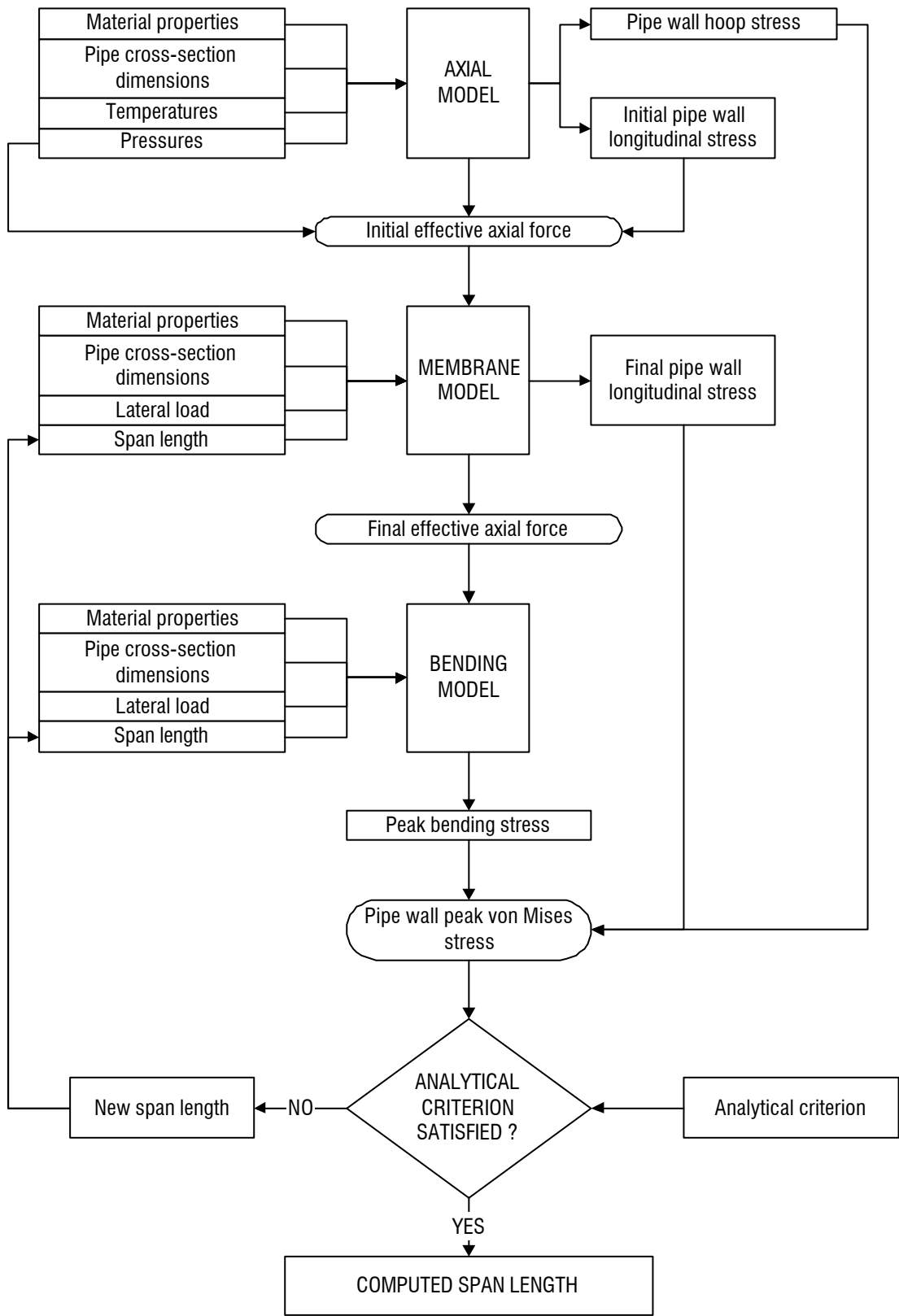


Figure B.2.2 Schematic Representation Of Tier 2 Analytical Method

B.3 ATTACHMENTS

TIER 2 Membrane effects STATIC STRENGTH span assessment method			
Pipeline data			
-	Symbol	Value	(Units)
Pipeline segment identification	ID	PL-774-G	
Kilometre start point	KPs	397	km
Kilometre end point	KPe	404.4	km
Outside diameter	D	914.4	mm
Nominal wall thickness	t	28.4	mm
Corrosion coat thickness	te	6	mm
Weight coat thickness	tc	76	mm
Steel density	rs	7850	kg/m ³
Corrosion coat density	re	1400	kg/m ³
Weight coat density	rc	3040	kg/m ³
Steel elastic modulus	E	207000	N/mm ²
Steel Poissons ratio	nu	0.3	
Steel SMYS	SMYS	448.3	N/mm ²
Steel coeff. of thermal expansion	alf	0.0000116	°C ⁻¹
Operational conditions data			
-			(Units)
Residual lay tension	Nlay	0	N
Contents pressure	pnorm	10	N/mm ²
Contents density	ri	105.4	kg/m ³
Contents temperature	thi	10	°C
Environmental data			
-			(Units)
Gravitational acceleration	g	9.81	m/s ²
Minimum water depth at LAT	h	45	m
Current speed at top of pipe	Vc	0.51	m/s
Max. wave induced velocity at top of pipe	Vw	0.95	m/s
Local seawater density	rw	1025	kg/m ³
Local seawater temperature	tha	4	°C
Hydrodynamic drag coefficient	Cd	1.05	
Pipeline longitudinal slip length	Lslip	50	m
Safety factors			
-			(Units)
Safety factor on span	lls	0.9	
Factor on SMYS	Ksmys1	0.96	
P-delta effect switch (0 = off, 1 = on)	SWPD	1	
Membrane effect switch (0 = off, 1 = on)	SWMB	1	
Convergence norm for solution routine	CONV	0.001	
Principal results			
-			(Units)
Submerged weight of pipe/unit length	q	4876.35	N/m
Horizontal loading/unit length	qh	1237.00	N/m
Maximum loading/unit length	qmx	5030.80	N/m
Hoop stress	Sh	148.93	N/mm ²
Net prebending longitudinal stress		30.27	N/mm ²
Additional membrane stress		75.88	N/mm ²
Bending stress		378.90	N/mm ²
Peak equivalent stress		430.37	N/mm ²
Initial membrane axial force		2.39E+06	N
Bore pressure axial force		-5.78E+06	N
Initial effective axial force		-3.38E+06	N
Additional effective axial force		6.00E+06	N
Final effective axial force		2.61E+06	N
Midspan lateral deflection (from bending)		2.0343	m
Midspan lateral deflection (from membrane)		2.2451	m
End pull-in (at one end)		0.0167	m
Error check on span length calculation		OK	
Factored allowable span length	Ls2	134.5	m

Table B.3.1 Example of Tier 2 Static Strength Analysis Proforma

APPENDIX C

PIPELINE DEFECT ASSESSMENT PROCESS: SPAN ANALYSIS FOR STATIC STRENGTH AT THE TIER 3 LEVEL

TABLE OF CONTENTS

	Page No
C.1 INTRODUCTION	C.1.1
C.1.1 PURPOSE	C.1.1
C.1.2 SCOPE AND LIMITATIONS	C.1.1
C.1.3 REFERENCES	C.1.1
C.1.3.1 Codes And Standards	C.1.1
C.2 PROCESS	C.2.1
C.2.1 OBJECTIVE	C.2.1
C.2.2 ASSESSMENT STRATEGY AT THE TIER 3 LEVEL	C.2.1
C.2.2.1 Generic	C.2.1
C.2.2.2 Considerations In The Tier 3 Static Strength Analytical Method	C.2.1
C.2.3 DATA	C.2.2
C.2.3.1 Data Classes	C.2.2
C.2.3.2 Data Sources	C.2.2
C.2.4 LOADINGS AND LOAD COMBINATIONS IN GENERAL	C.2.3
C.2.4.1 General Points	C.2.3
C.2.4.2 Actions	C.2.3
C.2.4.3 Loadings	C.2.3
C.2.5 LOAD COMBINATION IN FINITE ELEMENT ANALYSIS	C.2.4
C.2.5.1 Load Combination	C.2.4
C.2.5.2 Submerged Self-Weight	C.2.4
C.2.5.3 Environmental: Long-Term	C.2.4
C.2.5.4 Environmental: Short-Term	C.2.5
C.2.5.5 Operating	C.2.5
C.2.6 TIER 3 (FINITE ELEMENT) STATIC STRENGTH ANALYTICAL METHOD	C.2.5
C.2.6.1 Finite Element Package	C.2.5
C.2.6.2 Loadings	C.2.6
C.2.6.3 Element Types	C.2.6
C.2.6.4 Element Mesh	C.2.7
C.2.6.5 Support Conditions	C.2.7
C.2.6.6 Material Characteristic	C.2.9
C.2.6.7 Analysis Options	C.2.9
C.2.6.8 Analysis Procedure	C.2.9

TABLE OF CONTENTS/continued

C.2.7	ACCEPTANCE CRITERIA	C.2.9
C.2.7.1	General	C.2.9
C.2.7.2	Stress Criterion	C.2.9
C.2.7.3	Strain Criterion	C.2.9
C.2.7.4	Ovalisation Criterion	C.2.11
C.2.7.5	Local Buckling Criterion	C.2.11
C.3	ATTACHMENTS	C.3.1

LIST OF TABLES

Table C.2.1	Data Classes
Table C.2.5	Relationship Between Actions, Loading And Load Combinations

LIST OF FIGURES

Figure C.2.1	Static Strength Assessment At The Tier 3 Level
--------------	--

C.1 INTRODUCTION

C.1.1 PURPOSE

The purpose of this process document is to set down the considerations for the finite element static strength analysis of pipeline spans at the Tier 3 level and to ensure that best practice is applied.

C.1.2 SCOPE AND LIMITATIONS

This process applies to pipelines laid directly onto the seabed. It applies to an individual span; that is, a single clear unsupported length of pipeline that is sufficiently isolated from other spans or features as to be judged to behave as a self-contained entity. It does not apply to pipelines that are trenched, trenched and backfilled, trenched and infilled due to natural soil migration, or pipelines that are piggybacked.

C.1.3 REFERENCES

C.1.3.1 Codes And Standards

- Rules For Submarine Pipeline Systems. Det Norske Veritas. **DNV, 1996.**
- Code Of Practice For Pipeline Subsea: Design, Construction And Installation. British Standards Institute (BSI). **BS 8010: Part 3: 1993.**
- American Petroleum Institute (API). Recommended Practice For Planning, Designing, And Constructing Fixed Offshore Platforms - Working Stress Design. **RP2A-WSD, 20th ed., July 1993.**

C.2 PROCESS

C.2.1 OBJECTIVE

The objective of this process document is to ensure that the finite element analysis of pipeline spans is conducted in a rigorous manner, with due regard to the mechanical characteristics of the problem, and that spans are determined to be acceptable or significant against acceptance criteria.

C.2.2 ASSESSMENT STRATEGY AT THE TIER 3 LEVEL

C.2.2.1 Generic

The recommended Pipeline Defect Assessment Procedure allows a tiered approach to analytical methods and span acceptance. Specifically, up to a three-tiered philosophy can be adopted as shown in detail for the failure mode of static strength in Figure 2.1. In this figure, the lower level tiers have been greyed, leaving the Tier 3 assessment covered by this process highlighted.

At whatever tier level, the approach involves interaction between the data, load combinations, analytical criteria, analytical methods and acceptance criteria; with the exception of analytical criteria, each of these is dealt with in detail in subsections 2.3 to 2.7, below. At Tier 3, observed span lengths are analysed with the results judged against acceptance criteria to determine acceptability:

- observed span length forms part of the input to the analytical method
- analytical criteria in the lower tiers are acceptance criteria at the Tier 3 level
- the output from the Tier 3 analytical method relates directly to the acceptance criteria employed.

C.2.2.2 Considerations In The Tier 3 Static Strength Analytical Method

In using finite element methods for the analysis of pipeline spans consideration should be given to the following factors:

- finite element package
- loadings
- element types
- element mesh
- support conditions

- material characteristic
- analysis options
- analysis procedure.

Each of these points is addressed in detail in subsection C.2.6, below.

C.2.3 DATA

C.2.3.1 Data Classes

A detailed breakdown of the data into the four classes of: *pipeline*, *operational*, *environmental* and *inspection* is given in Table C.2.1. Data in the lines of Table C.2.1 that have been greyed are considered to be unnecessary to perform the static strength finite element analysis. The remainder can be viewed as “baseline” data, some of which has to be processed by means of calculation into suitable input data for the finite element analysis.

The **pipeline data** include geometrical and material properties; these are used to construct the finite element model and its material characteristic.

The **operational data** encompass installation (residual lay tension) and those related to the pipe contents: its density, pressure and temperature; these are used to derive some of the loadings applied to the span.

The **environmental data** include the parameters that relate to the fluid loading on the pipeline (for example, water depth and various wave and current data). They also contain parameters defining the mechanical interaction between the pipe and the seabed (for example, soil modulus and Poisson’s ratio at the span shoulders, and longitudinal and transverse coefficients of friction between the pipeline and the seabed); these particular parameters influence the support conditions at the shoulder of the pipeline.

The **inspection data** include parameters to locate the span (kilometre start and end points), and freespan length. If marine growth information is included within the inspection data an assessment should be made as to whether this influences the pipeline weight or the hydrodynamic loading on the pipeline.

C.2.3.2 Data Sources

Appropriate sources of pipeline, operational and environmental data are to be used. If no data are available for residual lay tension, then it is to be estimated conservatively and included if it adversely affects the pipeline.

C.2.4 LOADINGS AND LOAD COMBINATIONS IN GENERAL

C.2.4.1 General Points

A load combination is built up from *actions* and *loadings* as shown schematically in Table C.2.2. The loading combination to be used is a requirement of the assessment, and as indicated in subsection C.2.5 an *operating* loading is always included in the combination. This will usually correspond to the normal operating conditions of the pipeline, although there may be occasions where other operating conditions need to be considered.

C.2.4.2 Actions

In terms of detailed thermo-mechanical actions there are eight types that require consideration:

- pipeline weight
- external temperature
- external pressure
- current-induced action
- wave-induced action
- contents weight
- internal temperature
- internal pressure.

C.2.4.3 Loadings

Four individual loading classes are to be considered, namely:

- submerged self weight
- environmental: long-term
- environmental: short-term
- operating.

More than one type of operating condition may need to be addressed. As indicated in Table 2.5, the list covers the following possibilities:

- normal operating
- maximum allowable operating
- shut down (minimum operating)
- hydrotest.

This list may be extended if circumstances dictate.

C.2.5 LOAD COMBINATION IN FINITE ELEMENT ANALYSIS

C.2.5.1 Load Combination

A load combination is made up from loading classes, and will always comprise the submerged self-weight, environmental long- and short-term load and an operating class, as set out schematically in Table C.2.2.

C.2.5.2 Submerged Self-Weight

The submerged self-weight should comprise the weight of the pipe, anti-corrosion coating and weight coating, minus the displaced weight of seawater. It is calculated from the data as follows:

$$q = q_s + q_e + q_c - q_a \quad (\text{C.2.1})$$

$$q_s = \frac{\rho_s \pi g}{4} [D^2 - (D - 2t)^2] \quad (\text{C.2.2})$$

$$q_e = \frac{\rho_e \pi g}{4} [(D + 2t_e)^2 - D^2] \quad (\text{C.2.3})$$

$$q_c = \frac{\rho_c \pi g}{4} [(D + 2t_e + 2t_c)^2 - (D + 2t_e)^2] \quad (\text{C.2.4})$$

$$q_a = \frac{\rho_a \pi g}{4} (D + 2t_e + 2t_c)^2 \quad (\text{C.2.5})$$

The symbols are explained in Table C.2.1.

The submerged self-weight may be augmented by an estimate of additional gravity load due to marine fouling, if appropriate.

C.2.5.3 Environmental: Long-Term

The only part of the environmental: long-term loading that requires derivation is the external (hydrostatic) pressure. This may be estimated from:

$$p_a = \rho_a gh \quad (\text{C.2.6})$$

C.2.5.4 Environmental: Short-Term

The environmental: short-term loading comprises the hydrodynamic uniformly distributed load resulting from the drag on the pipeline from the moving water particle velocities. Inertia loading is generally small, and in most circumstances may be neglected. It is recommended that directional 50-year return period maximum wave height and period (H_{\max} and T_{\max}), and *associated* maximum surface current velocity are used to determine the maximum combined water particle velocity normal to the heading of the span, which forms the input to Morison's equation to derive the loading on the span. The main steps in this process are as follows:

1. Use directional 50-year return period maximum wave height and period (H_{\max} and T_{\max}), and *associated* maximum surface current velocity
2. Considering the heading of the pipeline span, determine the maximum wave height and corresponding period, and associated surface current velocity normal to the pipeline span
3. Compute the top-of-pipe current velocity V_c using a power-law current profile suggested in the source data
4. Compute the top-of-pipe maximum wave velocity V_w using a wave theory suitable for the H_{\max} - T_{\max} - water depth combination concerned (kinematic spreading may be neglected, and the effect of current velocity on wave period may be ignored)
5. The uniformly distributed load is then derived from:

$$q_h = \frac{1}{2} \rho_a C_d (D + 2t_e + 2t_c) (V_c + V_w)^2 \quad (C.2.7)$$

The environmental: short-term loading may be augmented by an estimate of additional load due to marine fouling, if appropriate.

C.2.5.5 Operating

The only part of the operating loading that requires derivation is the contents self-weight. This is given by:

$$q_i = \frac{\rho_i \pi g}{4} (D - 2t)^2 \quad (C.2.8)$$

C.2.6 TIER 3 (FINITE ELEMENT) STATIC STRENGTH analytical method

C.2.6.1 Finite Element Package

A reputable, well-validated package should be used to conduct the finite element analysis of spans. The principal requirements of the package are that it has an appropriate range of

elements, has non-linear capabilities (both geometric and material) and has facilities for applying the types of loadings required.

C.2.6.2 Loadings

The loadings that should be applied to the finite element model should be as follows:

- prestressing due to residual lay tension (to be estimated conservatively and included if it adversely affects the pipeline)
- internal temperature θ_i
- internal pressure p_i (which may be the normal operating, maximum allowable operating or hydrotest pressure, whichever is under attention; consideration should also be given to omitting the internal pressure if this is appropriate to the acceptance criterion under use, see subsection C.2.7)
- external temperature θ_a
- external pressure p_a (see subsection C.2.5.3, above)
- total vertical uniformly distributed load $q = q + q_i$ (see subsections C.2.5.2 and C.2.5.5, above)
- total horizontal uniformly distributed load q_n (see subsection C.2.5.4, above).

C.2.6.3 Element Types

Elements are required in order to model the pipeline and the seabed.

In general, codes do not allow the weight coat to be considered to contribute structurally to the pipeline (see, BS 8010: Part 3: 1993 and DNV, 1996) and so elements are only required to model the steel pipe. These should have the following capabilities:

- three-dimensional beam action
- P - δ effects
- hoop stress and strain, as well as longitudinal stress and strain
- temperature and pressure effects
- end-cap effects, if necessary
- section deformation (if an acceptance criterion involving ovalisation is being used; see subsection C.2.7.4 below).

In using tailor-made elements, such as PIPE or ELBOW-type elements in ABAQUS for example, consideration should be given to any diameter to thickness limitations inherent in the element formulations.

Possible options for elements used to represent the seabed may be extension/compression

springs, or rigid-surface. In the case of springs, the principal requirement is that they allow a non-linear load-deflection response to be specified. The requirements for rigid-surface elements are that they allow contact with the pipe elements and hence uplift, and that they have the capability of modelling friction between the surface and the pipe elements.

C.2.6.4 Element Mesh

In meshing the finite element model two distinct regions need to be considered: the span region and the shoulder region. Providing that conditions at the two shoulders of the span can be considered to be identical, then symmetry at midspan may be assumed and a half-model built; this will comprise half the span length (as dictated by the value observed in the inspection, L_{obs}) coupled to one shoulder-supported region.

Generally, in the span region, elements to represent the pipe will only be required. A suitably graded mesh for these elements must be used that has regard for the generation of peak bending moments at midspan and around the junction between the span and the shoulder, and the possibility of bar buckling. Aspect ratio (length to diameter) restrictions of the elements are not to be violated in generating the mesh.

In the shoulder region(s) elements will be required to represent both the pipe and the seabed. As such, a number of factors require careful consideration:

- the length of the pipe part of the finite element model should be such as to represent semi-infinite conditions
- the density and node spacing of elements used to represent the pipe must have regard for the generation of peak bending moment around the junction between the span and the shoulder, and aspect ratio (length to diameter) restrictions of the elements
- the spacing of discrete springs, which may be used to represent the seabed (see subsection C.2.6.5, below), must be such as to replicate continuous support
- the extent of rigid surfaces, which may be used to represent the seabed (see subsection C.2.6.5, below), must be such as to represent semi-infinite conditions.

C.6.5 Support Conditions

The support conditions to be enforced depend on whether or not symmetry at midspan of the model has been assumed (see subsection 2.6.4, above). If a full model is to be used then considerations of support conditions are confined to the two shoulder regions. In the event that

a half-model is used, then appropriate symmetry boundary conditions on displacement must be enforced at midspan, and one shoulder region considered.

Regarding the shoulder regions, consideration must be given to support conditions in the vertical, transverse-horizontal and longitudinal-horizontal directions. The use of two main types of support to replicate the pipeline/seabed interaction at the span shoulder is suggested:

1. continuous elastic foundation (or discrete elastic springs) in the vertical plane to model deformability of the seabed; and discrete elastic-perfectly plastic springs in the transverse and longitudinal horizontal directions to model deformability and frictional slip

3. rigid-surface with friction interaction between pipe elements and the surface to provide: restraint in the vertical, and both horizontal directions; and the facility for lift-off of the pipeline from the rigid surface at the shoulders.

For elastic constants to be used in support type 1, above, it suggested that the stiffness per unit length of the vertical support should be derived as follows:

$$k_v = \frac{E_f}{2(1 - \nu_f^2)} \quad (C.2.9)$$

and the stiffness per unit length of the transverse and longitudinal support should be derived as follows:

$$k_h = \frac{E_f}{2(1 + \nu_f)} \quad (C.2.10)$$

The limiting force per unit length of the longitudinal and transverse springs should be determined from:

$$f_{LL} = \mu_L q_v \quad (C.2.11)$$

$$f_{LT} = \mu_T q_v \quad (C.2.12)$$

respectively.

In view of the fact that discrete springs may be used for the vertical, longitudinal- and transverse-horizontal directions, then the stiffness and limiting forces for these springs should be obtained by multiplying the above values by the longitudinal spacing of the springs in the finite element model.

The rigid surface support (type 2, above) requires only the specification of the friction coefficients in the longitudinal and transverse horizontal directions. Appropriate values of m_l and m_T are to be taken.

C.2.6.6 Material Characteristic

The stress-strain characteristic for the pipeline steel should be taken as elastic-perfectly plastic. Care must be taken, however, in that some finite element packages require true (rather than engineering) parameters to be specified.

C.2.6.7 Analysis Options

The analysis options should include full geometric and material non-linearity. Consideration should be given to the use of displacement control, the Riks method, or other non-linear solution procedures if necessary.

C.2.6.8 Analysis Procedure

The analysis procedure to be used depends on the finite element package. Given that material non-linearity may occur in the analysis, it is important to appreciate that if plasticity develops, then the order of load application may affect results. This is a particular consideration if an acceptance criterion involving plastic strain is adopted (see subsection 2.7.3, below). In the light of this, careful consideration needs to be given to the order of load application as it relates to the formation of the span.

Thus in the case of a span formed by soil migration from beneath the pipeline, it may be judged appropriate to apply the internal and external temperatures and pressures, plus the total vertical uniformly distributed load in a single load-step, followed by the total horizontal uniformly distributed load as a separate load-step (this has the effect of separating out the environmental: short-term loading effects from the spanning effects). Another possibility is to apply all loading to the shoulder portion of the model as a first load-step, followed by all the loading on the freespan portion of the model as a second load-step (this has the effect of separating out the as-laid and span formation aspects of the problem).

C.2.7 ACCEPTANCE CRITERIA

C.2.7.1 General

There is a general requirement that the analytical outputs must have the capacity for ready comparison with the acceptance criteria. Precisely how this is handled depends on the exact details of the FEA model employed in the analytical method. It is worth noting that, for example, if the type of elements used in the FE representation are such that ovalisation and local buckling

are modelled, and output variables allow it, then a direct comparison between acceptance criteria and analysis output may be made. Alternatively, if the elements do not allow this, then some indirect comparison must be made, between curvatures or bending strains. Finite element packages, for the most part, will always provide stress and strain as outputs.

The acceptance criterion for Tier 3 may be taken from:

- the computed peak equivalent stress being less than or equal to a percentage of the pipe steel specified minimum yield strength (SMYS); or
- the computed peak equivalent plastic strain being less than or equal to a prescribed limit; or the most onerous of
- the peak computed ovalisation being less than or equal to a prescribed limit; and
- a criterion derived from local buckling considerations.

The choice and use of limits are set out below.

C.2.7.2 Stress Criterion

The output required from the finite element analysis is the peak von Mises stress resulting from all the applied loadings. This peak stress is compared with a percentage of SMYS to determine acceptance under this criterion; the following percentages are suggested:

	Percentage of SMYS for use in stress analytical criterion			
	DNV		BS8010	
	Fluid category A, C	Fluid category B, D, E	Operating condition NOT hydrotest	Hydrotest operating condition
Within 500 m DNV Zone 2	96	77	72	100
Outwith 500 m DNV Zone 1	96	87	96	100

Reference should be made to BS 8010: Part 3: 1993 and DNV, 1996 for detailed guidance.

C.2.7.3 Strain Criterion

The output required from the finite element analysis is the peak equivalent plastic strain resulting from all the applied loadings. This peak strain is compared with an allowable value to determine acceptance under this criterion; an allowable value of 0.1% is suggested.

C.2.7.4 Ovalisation Criterion

The output required from the finite element analysis is the peak cross-section ovalisation resulting from the applied loadings. This peak ovalisation is compared with an allowable value to determine acceptance under this criterion. It is suggested that an allowable value of 1.5%, corrected for the out-of-roundness (OOR) tolerance from fabrication of the pipe, is used giving a criterion as follows:

$$\frac{D_{\max} - D_{\min}}{2D} \leq (1.5\% - \text{OOR}) \quad (\text{C.2.13})$$

where D_{\max} and D_{\min} are the maximum and minimum diameters, respectively, on the most highly ovalised cross-section.

Given that internal pressure has an ameliorating effect on ovalisation, consideration should be given to a load combination that excludes internal pressure.

C.2.7.5 Local Buckling Criterion

This is related to the collapse of the cross-section section. If the finite element model allows it, then this phenomenon can be directly monitored and the acceptance criterion becomes one of determining if there is an adequate margin against local buckling under the applied loadings.

Given that internal pressure has an ameliorating effect on local buckling, consideration should be given to a load combination that excludes internal pressure.

Data	Symbol
Pipeline Data	
Pipe outside diameter	D
Pipe nominal wall thickness	t
Corrosion coat thickness	t_c
Weight coat thickness	t_w
Steel density	ρ_s
Corrosion coat density	ρ_e
Weight coat density	ρ_c
Steel elastic modulus	E
Steel Poisson's ratio	ν
SMYS steel	σ_y
Steel thermal expansion coefficient	α
Axial restraint factor	λ_a
Pipeline heading	ϕ
Operational Data	
Residual lay tension	N
Internal pressure	p_i
Contents density	ρ_i
Contents temperature	θ_i
Design life of pipeline	T_p
Environmental Data	
Minimum water depth at LAT	h
Local seawater density	ρ_a
Local seawater temperature	θ_a
Current velocity data	-
Wave data	-
Hydrodynamic drag coefficient	C_d
Hydrodynamic added mass coefficient	C_a
Soil elastic modulus at span shoulders	E_f
Soil Poisson's ratio at span shoulders	ν_f
Longitudinal friction coefficient at span shoulders	μ_L
Transverse friction coefficient at span shoulders	μ_T
Inspection Data	
Kilometre point at start of span	KP _s
Kilometre point at end of span	KP _e
Freespan length	L _{obs}
Gap beneath span	G
Marine growth information	-

Table C.2.1 Data Classes

Action	Loading	Load Combination			
PIPELINE WEIGHT	SUBMERGED SELF-WEIGHT	•	•	•	•
EXTERNAL TEMPERATURE	ENVIRONMENTAL: LONG-TERM	•	•	•	•
EXTERNAL PRESSURE		•	•	•	•
CURRENT-INDUCED	ENVIRONMENTAL: SHORT-TERM	•	•	•	•
WAVE-INDUCED		•	•	•	•
CONTENTS WEIGHT	NORMAL OPERATING	•			
INTERNAL TEMPERATURE		•			
INTERNAL PRESSURE		•			
CONTENTS WEIGHT	MAXIMUM ALLOWABLE OPERATING		•		
INTERNAL TEMPERATURE			•		
INTERNAL PRESSURE			•		
CONTENTS WEIGHT	SHUT-DOWN (MINIMUM OPERATING)			•	
INTERNAL TEMPERATURE				•	
INTERNAL PRESSURE				•	
CONTENTS WEIGHT	HYDROTEST				•
INTERNAL TEMPERATURE					•
INTERNAL PRESSURE					•

Table C.2.2 Relationship Between Actions, Loading And Load Combinations

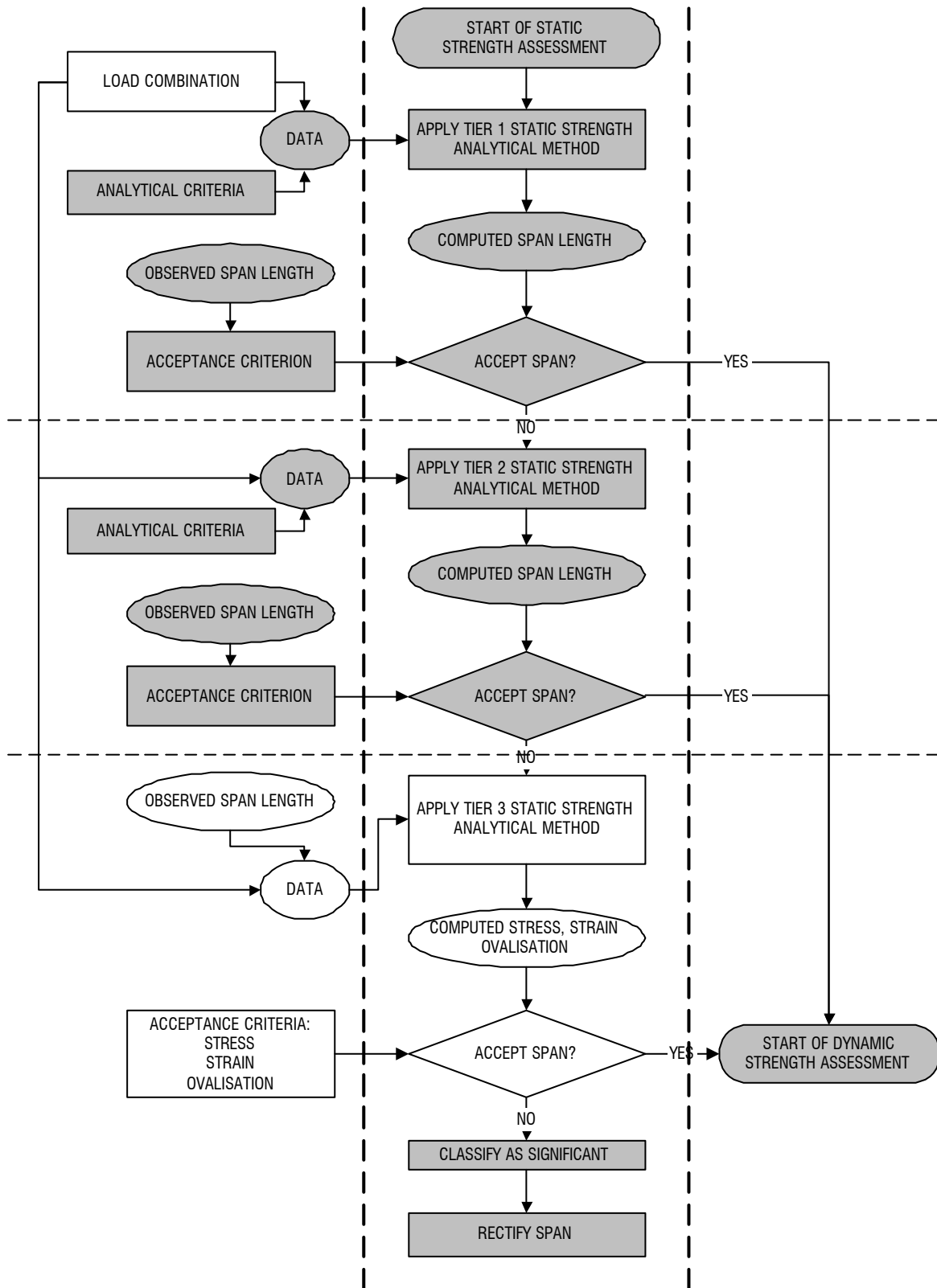


Figure C.2.1 Static Strength Assessment At The Tier 3 Level

C.3 ATTACHMENTS

There are no attachments to this document.

APPENDIX D

PIPELINE DEFECT ASSESSMENT PROCESS: SPAN ANALYSIS FOR DYNAMIC OVERSTRESS AT THE TIER 1 LEVEL (VORTEX SHEDDING)

TABLE OF CONTENTS

	Page No.
D.1. INTRODUCTION	D.1.1
D.1.1 PURPOSED.1.1	
D.1.2 SCOPE AND LIMITATIONS	D.1.1
D.1.3 REFERENCES	D.1.1
D.1.3.1 Codes And Standards	D.1.1
D.2. PROCESS	D.2.1
D.2.1 OBJECTIVE	D.2.1
D.2.2 ASSESSMENT STRATEGY AT THE TIER 1 LEVEL	D.2.1
D.2.2.1 Generic	D.2.1
D.2.2.2 Considerations In The Tier 1 Dynamic Strength Analytical Method	D.2.1
D.2.3 DATA	D.2.2
D.2.3.1 Data Classes	D.2.2
D.2.3.2 Data Sources	D.2.2
D.2.4 LOADINGS AND LOAD COMBINATIONS IN GENERAL	D.2.2
D.2.4.1 General Points	D.2.2
D.2.4.2 Actions	D.2.3
D.2.4.3 Loadings	D.2.3
D.2.5 LOAD COMBINATION IN TIER 1 ANALYTICAL METHOD	D.2.3
D.2.5.1 Load Combination	D.2.3
D.2.5.2 Submerged Self-Weight	D.2.3
D.2.5.3 Environmental: Long-Term	D.2.4
D.2.5.4 Environmental: Short-Term	D.2.4
D.2.5.5 Operating	D.2.5
D.2.6 ANALYTICAL CRITERION	D.2.5
D.2.6.1 General	D.2.5
D.2.6.2 Reduced Velocity Criterion	D.2.5
D.2.7 TIER 1 DYNAMIC STRENGTH ANALYTICAL METHOD	D.2.5
D.2.7.1 General	D.2.5
D.2.7.2 Loadings	D.2.5
D.2.7.3 Support Conditions	D.2.6
D.2.7.4 Material Characteristic	D.2.6
D.2.7.5 Frequency Limitation	D.2.6
D.2.7.6 Span Mechanical Model	D.2.7
D.2.7.7 Analysis Procedure	D.2.9
D.2.7.8 Analytical Method Implementation	D.2.9
D.2.8 ACCEPTANCE CRITERION	D.2.9
D.3. ATTACHMENTS	D.3.1

LIST OF TABLES

Table D.2.1	Data Classes
Table D.2.2	Relationship Between Actions, Loading And Load Combinations
Table D.2.3	Input And Response Parameters For Tier 1 Span Mechanical Model
Table D.3.1	Example Of Tier 1 Dynamic Strength Analysis Proforma

LIST OF FIGURES

Figure D.2.1	Dynamic Strength Assessment At The Tier 1 Level
--------------	---

D.1 INTRODUCTION

D.1.1 PURPOSE

The purpose of this process is to set down the methodology for the dynamic strength analysis of pipeline spans at the Tier 1 level and to ensure that best practice is applied.

D.1.2 SCOPE AND LIMITATIONS

This process applies to pipelines laid directly onto the seabed. It applies to an individual span; that is, a single clear unsupported length of pipeline that is sufficiently isolated from other spans or features as to be judged to behave as a self-contained entity. It does not apply to pipelines that are trenched, trenched and backfilled, trenched and infilled due to natural soil migration, or pipelines that are piggybacked.

D.1.3 REFERENCES

D.1.3.1 Codes And Standards

- Rules For Submarine Pipeline Systems. Det Norske Veritas. **DNV, 1996.**
- Code Of Practice For Pipelines Subsea: Design, Construction And Installation. British Standards Institute (BSI). **BS 8010: Part 3: 1993.**
- American Petroleum Institute (API). Recommended Practice For Planning, Designing, And Constructing Fixed Offshore Platforms - Working Stress Design. **RP2A-WSD, 20th ed., July 1993.**

D.2 PROCESS

D.2.1 OBJECTIVE

The objective of this process is to ensure that the dynamic strength analysis of pipeline spans at the Tier 1 level is conducted in a rigorous manner, with due regard to the mechanical characteristics of the problem, using appropriate analytical criteria, and that spans are determined to be acceptable or significant against acceptance criteria.

D.2.2 ASSESSMENT STRATEGY AT THE TIER 1 LEVEL

D.2.2.1 Generic

The recommended Pipeline Defect Assessment Procedure allows a tiered approach to analytical methods and span acceptance. Specifically, up to a three-tiered philosophy can be adopted as shown in detail for the failure mode of dynamic strength in Figure D.2.1. In this figure, the upper level tiers have been greyed, leaving the Tier 1 assessment covered by this process highlighted. At whatever tier level, the approach involves interaction between the data, load combinations, analytical criteria, analytical methods and acceptance criteria; each of these is dealt with in detail in subsections D.2.3 to D.2.8, below. At Tier 1, observed span lengths are judged against span lengths computed from the analytical method, using acceptance criteria, to determine acceptability:

- data, load combination and analytical criteria are all input into the analytical method
- output from the analytical method is a computed span length, which is compared with the observed span length to determine acceptability of the latter using an acceptance criterion.

D.2.2.2 Considerations In The Tier 1 Dynamic Strength Analytical Method

For the dynamic strength analytical method recommended for pipeline spans in this process document, consideration should be given to the following factors:

- loadings
- support conditions
- material characteristic
- frequency limitation
- span mechanical model
- analysis procedure
- analytical method implementation.
-

Each of these points is addressed in detail in subsection D.2.7, below.

D.2.3 DATA

D.2.3.1 Data Classes

A detailed breakdown of the data into the four classes of: *pipeline*, *operational*, *environmental* and *inspection* is given in Table D.2.1. Data in the lines of Table D.2.1 that have been greyed are considered to be unnecessary to perform the Tier 1 dynamic strength analysis. The remainder can be viewed as “baseline” data, some of which have to be processed by means of calculation into suitable input data for the analysis.

The **pipeline data** include geometrical and material properties; these are used in the analytical model, the analytical criteria and the material characteristic. The axial restraint factor is used to approximate the degree of suppression of longitudinal strains in the pipe wall due to the interaction of the pipe with the seabed.

The **operational data** encompass installation (residual lay tension) and those related to the pipe contents: its density, pressure and temperature; these are used to derive some of the loadings applied to the span.

The **environmental data** include the parameters that relate to the fluid loading on the pipeline (for example, water depth and various wave and current data). They also contain parameters defining the mechanical interaction between the pipe and the seabed (for example, soil modulus and Poisson’s ratio at the span shoulders); these particular parameters influence the support conditions at the shoulder of the pipeline.

The **inspection data** include parameters to locate the span (kilometre start and end points), and freespan length. The gap beneath the span is included and an assessment should be made as to whether this influences the susceptibility of the span to vortex shedding. If marine growth information is included within the inspection data an assessment should be made as to whether this influences the pipeline mass or the hydrodynamic loading on the pipeline.

D.2.3.2 Data Sources

Appropriate sources of pipeline, operational and environmental data are to be used. If no data are available for residual lay tension or axial restraint factor, then these are to be estimated conservatively and included if they adversely affect the pipeline.

D.2.4 LOADINGS AND LOAD COMBINATIONS IN GENERAL

D.2.4.1 General Points

A load combination is built up from *actions* and *loadings* as shown schematically in Table D.2.2. The loading combination to be used is a requirement of the assessment and, as indicated in subsection D.2.5, an *operating* loading is always included in the combination. This will usually correspond to the normal operating conditions of the pipeline, although there may be occasions where other operating conditions need to be considered.

D.2.4.2 Actions

In terms of detailed thermo-mechanical actions there are eight types that require consideration:

- pipeline weight
- external temperature
- external pressure
- current-induced action
- wave-induced action
- contents weight
- internal temperature
- internal pressure.

D.2.4.3 Loadings

Four individual loading classes are to be considered, namely:

- submerged self weight
- environmental: long-term
- environmental: short-term
- operating.

More than one type of operating condition may need to be addressed. As indicated in Table D.2.2, the list covers the following possibilities:

- normal operating
- maximum allowable operating
- shut down (minimum operating)
- hydrotest.

This list may be extended if circumstances dictate.

D.2.5 LOAD COMBINATION IN TIER 1 ANALYTICAL METHOD

D.2.5.1 Load Combination

A load combination is made up from loading classes, and will always comprise the submerged self-weight, environmental long- and short-term load and an operating class, as set out schematically in Table D.2.2.

D.2.5.2 Submerged Self-Weight

The submerged self-weight should comprise the weight of the pipe, anti-corrosion coating and weight coating, minus the displaced weight of seawater. It is calculated from the data as follows:

$$q = q_s + q_e + q_c - q_a \quad (D.2.1)$$

$$q_s = \frac{\rho_s \pi g}{4} \left[D^2 - (D - 2t)^2 \right] \quad (D.2.2)$$

$$q_e = \frac{\rho_e \pi g}{4} \left[(D + 2t_e)^2 - D^2 \right] \quad (D.2.3)$$

$$q_c = \frac{\rho_c \pi g}{4} \left[(D + 2t_e + 2t_c)^2 - (D + 2t_e)^2 \right] \quad (D.2.4)$$

$$q_a = \frac{\rho_a \pi g}{4} (D + 2t_e + 2t_c)^2 \quad (D.2.5)$$

The symbols are explained in Table D.2.1.

The submerged self-weight may be augmented by an estimate of additional weight due to marine fouling, if appropriate.

D.2.5.3 Environmental: Long-Term

The only part of the environmental: long-term loading that requires derivation is the external (hydrostatic) pressure. This may be estimated from:

$$p_a = \rho_a g h. \quad (D.2.6)$$

D.2.5.4 Environmental: Short-Term

The environmental: short-term loading comprises the water particle velocities at or near the seabed. It is recommended that directional 50-year return period significant wave height and mean zero up-crossing period (H_{sig} and T_z), and *associated* maximum surface current velocity are used. These are then used to determine the maximum combined water particle velocity normal to the heading of the span. The main steps in this process are as follows:

1. Use directional 50-year return period significant wave height and period (H_{sig} and T_z), and *associated* maximum surface current velocity
2. Considering the heading of the pipeline span, determine the significant wave height and corresponding period, and associated surface current velocity normal to the pipeline span
3. Compute the top-of-pipe current velocity V_c using a power-law current profile suggested in the source data
4. Compute the top-of-pipe maximum wave velocity V_w using a wave theory suitable for the H_{sig} - T_z - water depth combination concerned (kinematic spreading may be neglected, and the effect of current velocity on wave period may be ignored)

D.2.5.5 Operating

The only part of the operating loading that requires derivation is the contents self-weight. This is given by:

$$q_i = \frac{\rho_i \pi g}{4} (D - 2t)^2 \quad (\text{D.2.7})$$

D.2.6 ANALYTICAL CRITERION

D.2.6.1 General

It is recommended that the dynamic strength analytical criterion at the Tier 1 level should be based on limits on reduced velocity, as related to the mechanics of vortex shedding.

The choice and use of the criterion are set out below, and its precise implementation within the analytical method is dealt with in subsection D.2.7, below.

D.2.6.2 Reduced Velocity Criterion

The output required from the dynamic strength analysis is a computed span length corresponding to a limit set on the lowest natural frequency of vibration subject to all the applied loadings. This frequency is limited to a value that is set by considering the reduced velocity threshold for the onset of cross-flow oscillations; it is suggested that a reduced velocity threshold V_{rn} of 3.5 should be used.

D.2.7 TIER 1 DYNAMIC STRENGTH ANALYTICAL METHOD

D.2.7.1 General

The recommended dynamic strength analytical method implemented at the Tier 1 level consists of three aspects:

- a **frequency limitation** based on a reduced velocity threshold
- a **span mechanical model** that explicitly embodies span end conditions and the exact effects of effective axial force
- an **analysis procedure** that links the frequency limitation and mechanical models together.

Each of these aspects is dealt with in detail in subsections D.2.7.5, D.2.7.6 and D.2.7.7, below.

D.2.7.2 Loadings

The loadings that should be applied in the analytical method are as follows:

- prestressing due to residual lay tension (to be estimated conservatively and included if it adversely affects the pipeline)

- internal temperature θ_i
- internal pressure p_i (which may be the normal operating, maximum allowable operating or hydrotest pressure, whichever is under attention)
- external temperature θ_a
- external pressure p_a (see subsection D.2.5.3, above).

D.2.7.3 Support Conditions

Symmetry at midspan may be assumed. In this case, appropriate symmetry boundary conditions on displacement are enforced at midspan, and one shoulder region considered.

Regarding the shoulder region, consideration must be given to support conditions in the vertical direction. In the present case it is recommended that the supports are modelled as continuous elastic foundations in the vertical plane to represent deformability of the seabed and its interaction with the pipe.

For elastic constants to be used in this type of support, suggested that the stiffness per unit length of the vertical support should be derived as follows:

$$k_v = \frac{E_f}{2(1-\nu_f^2)} \quad (D.2.8)$$

D.2.7.4 Material Characteristic

The stress-strain characteristic for the pipeline steel should be taken as elastic, with Young's modulus of E and Poisson's ratio of ν .

D.2.7.5 Frequency Limitation

The frequency limitation is set by consideration of the reduced velocity threshold for the onset of cross-flow oscillations. Reduced velocity is defined as:

$$V_r = \frac{V}{f(D + 2t_e + 2t_c)} \quad (D.2.9)$$

where

- V_r = reduced velocity
- V = water particle velocity at the top of pipe level
- f = span natural frequency in Hertz

and the other symbols are defined in Table D.2.1.

The water particle velocity is taken as the combined flow velocity stemming from the sum of the current and wave velocities derived according to subsection D.2.5.4. The reduced velocity is set

equal to the limiting value in the analytical criterion (subsection D.2.6.2, above), denoted as V_{rth} , and this gives an allowable frequency, ω_{all} , in radians per second, as:

$$\omega_{\text{all}} = \frac{2\pi(V_c + V_w)}{V_{\text{rth}}(D + 2t_e + 2t_c)} \quad (\text{D.2.10})$$

D.2.7.6 Span Mechanical Model

Span idealisation. The pipeline span is idealised as a planar, infinitely long beam on a Winkler-type elastic foundation, in which a central portion of the elastic foundation has been removed, leaving a freespan. The loading comprises a uniformly distributed load and an axial compressive force (the effective axial force). In general, dynamic deflections (normal to the pipe axis) will occur over the full length of the pipe but their magnitude will attenuate within the elastically-supported parts (the shoulders) at a rate that depends on the elastic foundation stiffness per unit length and the pipe bending rigidity.

Assumptions. The assumptions used in the development of the span mechanical model are as follows:

1. Membrane thin-shell calculations based on the pipe median surface are sufficiently accurate for stresses in the pipe wall, with plane stress assumptions taken with respect to the through-thickness direction.
2. The normal Euler-Bernoulli beam-bending assumptions are presumed to apply.
3. The contribution of any weight and/or anti-corrosion coat to bending rigidity of the pipeline cross-section is ignored.
4. The effects of rotary inertia are not included.
5. The span is assumed to be symmetrical about midspan; thus only symmetric modes of vibration are considered, which will include the one corresponding to the lowest natural frequency of vibration as this comprises a single half-wave along the length of the freespan.
6. The span is under zero or compressive effective axial force only.

Problem parameters. The model input and response parameters are summarised in Table D.2.3. The input parameters are EI^* , N_a , m_e , γ , λ_f and β , and the response parameter is L .

Some of the input parameters are computed from baseline data as follows:

Equivalent bending rigidity of the pipe EI^* :

$$EI^* = \frac{EI_s}{(1-\nu^2)} \quad (\text{D.2.11})$$

where

$$I_s = \frac{\pi}{64} [D^4 - (D-2t)^4] \quad (D.2.12)$$

Effective axial compression in pipe N_a :

$$N_a = \sigma_x A_s - p_i \frac{\pi}{4} (D-2t)^2 \text{ if } \sigma_x \leq 0 \quad (D.2.13)$$

$$N_a = -p_i \frac{\pi}{4} (D-2t)^2 \text{ if } \sigma_x > 0$$

where:

$$\sigma_x = \frac{N}{A_s} + \lambda_a \left\{ \nu \sigma_\theta - \alpha E (\theta_i - \theta_a) \right\} \quad (D.2.14)$$

$$\sigma_\theta = (p_i - p_a) \frac{(D-t)}{2t} \quad (D.2.15)$$

Effective mass of the pipeline m_e :

$$m_e = \frac{1}{g} (q + q_a) + C_a \rho_a \frac{\pi}{4} (D + 2t_e + 2t_c)^2 \quad (D.2.16)$$

Axial force inverse characteristic length γ :

$$\gamma = \sqrt{\frac{-N_a}{2EI^*}} \quad (D.2.17)$$

Shoulder inverse characteristic length λ_f :

$$\lambda_f = \left[\frac{k_v}{4EI^*} \right]^{\frac{1}{4}} \quad (D.2.18)$$

Natural frequency parameter β :

$$\beta = \left[\frac{m_e \omega_{all}^2}{EI^*} \right]^{\frac{1}{4}} \quad (D.2.19)$$

Expressions relating the various input and response parameters are dealt with below.

Bar-buckling and upper range of limiting span length. Owing to the possibility of bar-buckling of the span due the compression caused by the effective axial force, there exists an upper limit to allowable span length that will be determined by this phenomenon. This may be found from the following equation:

$$L < \frac{\sqrt{2}}{\gamma} \cos^{-1} \left[\left(\frac{\gamma}{\lambda_f} \right)^2 - 1 \right] \quad (D.2.20)$$

Frequency determinant. The lowest natural frequency of the span mechanical model is computed from the frequency determinant. This is a four by four array as follows:

$$\begin{vmatrix} a_2 \sinh\left(\frac{a_2 L}{2}\right) & a_2 \cosh\left(\frac{a_2 L}{2}\right) & -b_2 \sin\left(\frac{b_2 L}{2}\right) & b_2 \cos\left(\frac{b_2 L}{2}\right) \\ a_2^3 \sinh\left(\frac{a_2 L}{2}\right) & a_2^3 \cosh\left(\frac{a_2 L}{2}\right) & b_2^3 \sin\left(\frac{b_2 L}{2}\right) & -b_2^3 \cos\left(\frac{b_2 L}{2}\right) \\ -(a_1^2 + b_1^2 + a_2^2) & 2a_1 a_2 & -(a_1^2 + b_1^2 - b_2^2) & 2a_1 b_2 \\ 2a_1(a_1^2 + b_1^2) & -a_2(3a_1^2 - b_1^2 - a_2^2) & 2a_1(a_1^2 + b_1^2) & -b_2(3a_1^2 - b_1^2 + b_2^2) \end{vmatrix} = 0 \quad (D.2.21)$$

where:

$$a_1 = \sqrt{\frac{1}{2} \left[\sqrt{(4\lambda_f^4 - \beta^4) + \gamma^2} \right]} \quad (D.2.22)$$

$$b_1 = \sqrt{\frac{1}{2} \left[\sqrt{(4\lambda_f^4 - \beta^4) - \gamma^2} \right]} \quad (D.2.23)$$

$$a_2 = \sqrt{\left[\sqrt{(\gamma^4 + \beta^4) + \gamma^2} \right]} \quad (D.2.24)$$

$$b_2 = \sqrt{\left[\sqrt{(\gamma^4 + \beta^4) - \gamma^2} \right]} \quad (D.2.25)$$

It will be observed that the elements of the frequency determinant are functions of γ , λ_f , β and L .

D.2.7.7 Analysis Procedure

In the analysis procedure, the span length is determined for which the lowest natural frequency of the span corresponds to the limiting natural frequency. This is achieved by fixing the values of the input parameters γ , λ_f and β in the elements of the frequency determinant, and computing the value of L which causes the expansion of the determinant to be zero.

D.2.7.8 Analytical Method Implementation

The analytical method has been implemented into a spreadsheet program. An example of an analysis proforma is given in section D.3, ATTACHMENTS.

D.2.8 ACCEPTANCE CRITERION

The output from the Tier 1 dynamic strength analysis method is a computed span length L_{comp} . A percentage of this is compared with the observed span length to determine acceptability of the latter; the percentage suggested is 90%. Hence, the criterion for acceptability of the observed span is:

$$L_{obs} \leq 0.9L_{comp} \quad (D.2.26)$$

Data	Symbol
Pipeline Data	
Pipe outside diameter	D
Pipe nominal wall thickness	t
Corrosion coat thickness	t_e
Weight coat thickness	t_c
Steel density	ρ_s
Corrosion coat density	ρ_e
Weight coat density	ρ_c
Steel elastic modulus	E
Steel Poisson's ratio	ν
SMYS steel	σ_y
Steel thermal expansion coefficient	α
Axial restraint factor	λ_a
Pipeline heading	ϕ
Operational Data	
Residual lay tension	N
Internal pressure	p_i
Contents density	ρ_i
Contents temperature	θ_i
Design life of pipeline	T_p
Environmental Data	
Minimum water depth at LAT	h
Local seawater density	ρ_a
Local seawater temperature	θ_a
Current velocity data	-
Wave data	-
Hydrodynamic drag coefficient	C_d
Hydrodynamic added mass coefficient	C_a
Soil elastic modulus at span shoulders	E_f
Soil Poisson's ratio at span shoulders	ν_f
Longitudinal friction coefficient at span shoulders	μ_L
Transverse friction coefficient at span shoulders	μ_T
Inspection Data	
Kilometre point at start of span	KP_s
Kilometre point at end of span	KP_e
Freespan length	L_{obs}
Gap beneath span	G
Marine growth information	-

Table D.2.1 Data Classes

Action	Loading	Load Combination			
PIPELINE WEIGHT	SUBMERGED SELF-WEIGHT	●	●	●	●
EXTERNAL TEMPERATURE	ENVIRONMENTAL: LONG-TERM	●	●	●	●
EXTERNAL PRESSURE		●	●	●	●
CURRENT-INDUCED	ENVIRONMENTAL: SHORT-TERM	●	●	●	●
WAVE-INDUCED		●	●	●	●
CONTENTS WEIGHT	NORMAL OPERATING	●			
INTERNAL TEMPERATURE		●			
INTERNAL PRESSURE		●			
CONTENTS WEIGHT	MAXIMUM ALLOWABLE OPERATING		●		
INTERNAL TEMPERATURE			●		
INTERNAL PRESSURE			●		
CONTENTS WEIGHT	SHUT-DOWN (MINIMUM OPERATING)			●	
INTERNAL TEMPERATURE				●	
INTERNAL PRESSURE				●	
CONTENTS WEIGHT	HYDROTEST				●
INTERNAL TEMPERATURE					●
INTERNAL PRESSURE					●

Table D.2.2 Relationship Between Actions, Loading And Load Combinations

Parameter description	Symbol	Formula / note
Freespan length	L	Varies within analytical procedure, see subsection D.2.7.7.
Bending rigidity of pipe	EI^*	$EI^* = \frac{EI_s}{(1-\nu^2)}$ Equivalent bending rigidity, based on hoop inextensibility of pipe.
Axial force in pipe (compression entered as negative)	N_a	$N_a = \sigma_x \frac{\pi}{4} [D^2 - (D-2t)^2] - p_i \frac{\pi}{4} (D-2t)^2$ Effective axial force in the pipe. σ_x only to be included if negative; residual lay tension ignored.
Effective mass of pipeline	m_e	$m_e = \frac{1}{g} (q + q_a) + C_a \rho_a \frac{\pi}{4} (D + 2t_e + 2t_c)$
Axial force inverse characteristic length	γ	$\gamma = \sqrt{\frac{-N_a}{2EI^*}}$
Shoulder inverse characteristic length	λ_f	$\lambda_f = \left[\frac{k_v}{4EI^*} \right]^{\frac{1}{4}}$ k_f is the vertical foundation stiffnesses per unit length, see subsection D.2.7.3.
Natural frequency parameter	β	$\beta = \left[\frac{m_e \omega_{all}^2}{EI^*} \right]^{\frac{1}{4}}$ Based on allowable natural frequency ω_{all} , calculated as shown in subsection D.2.6.2.

Table D.2.3 Input And Response Parameters For Tier 1 Span Mechanical Model

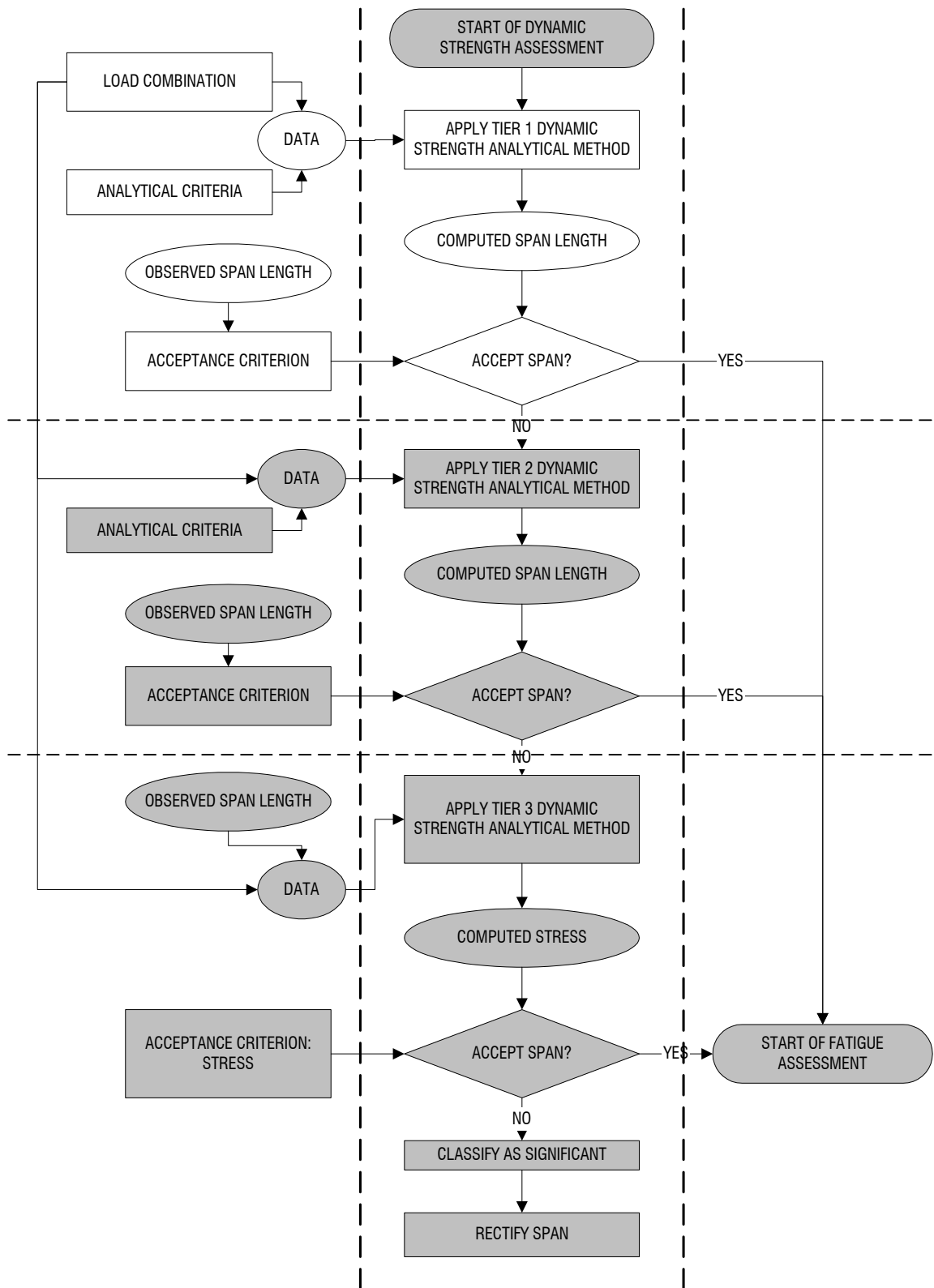


Figure D.2.1 Dynamic Strength Assessment At The Tier 1 Level

D.3 ATTACHMENTS

TIER 1 Beam on elastic foundation VORTEX SHEDDING span assessment method			
Pipeline data			
-	Symbol	Value	(Units)
Pipeline segment identification	ID	PL-101-A	
Kilometre start point	KPs	0	km
Kilometre end point	KPe	0.16	km
Outside diameter	D	762	mm
Nominal wall thickness	t	15.88	mm
Corrosion coat thickness	te	5.56	mm
Weight coat thickness	tc	48	mm
Steel density	rs	7850	kg/m ^ 3
Corrosion coat density	re	1200	kg/m ^ 3
Weight coat density	rc	3124	kg/m ^ 3
Steel elastic modulus	E	207000	N/mm ^ 2
Steel Poissons ratio	nu	0.3	
Steel coeff. of thermal expansion	alf	1.16E-05	° C ^ -
Operational conditions data			
-			(Units)
Residual lay tension	Nlay	0	N
Contents pressure	pnorm	1.69	N/mm ^ 2
Contents density	ri	585.4	kg/m ^ 3
Contents temperature	thi	15	° C
Environmental data			
-			(Units)
Gravitational acceleration	g	9.81	m/s ^
Minimum water depth at LAT	h	37	m
Current speed at top of pipe	Vc	0.57	m/s
Sig. wave induced velocity at top of pipe	Vwsig	0.52	m/s
Local seawater density	rw	1025	kg/m ^ 3
Local seawater temperature	tha	8	° C
Hydrodynamic added mass coefficient	Ca	1	
Soil elastic modulus at span shoulders	kf	25	N/mm ^ 2
Safety factors etc.			
-			(Units)
Weight growth factor	ew	1	
Axial restraint factor	l	1	
Threshold reduced velocity	Vrth	3.5	
Safety factor on span (vortex shedding)	lv	0.9	
P-delta effect switch (0 = off, 1 = on)	Switch	1	
Principal results			
-			(Units)
Submerged weight of pipe/unit length	q	3257.9	N/m
Effective mass of pipe/unit length	me	1548.3	kg/m
Residual lay tension stress	St	0	N/m
Hoop stress	Sh	30.97	N/mm ^ 2
Thermal stress	St	-	N/mm ^ 2
Poisson effect stress	Sp	9.29	N/mm ^ 2
Net prebending longitudinal stress	Sn	-7.52	N/mm ^ 2
Membrane axial force		-2.80E+05	N
Bore pressure axial force		-7.08E+05	N
Effective axial force		-9.88E+05	N
Allowable frequency	Fall	0.3608	Hz
Error check on span length calculation	Error	OK	
Factored span length based on fix-fix ends		65.88	m
Factored governing allowable span length	Lv1	60.3	m

Table D.3.1 Example Of Tier 1 Dynamic Strength Analysis Proforma

APPENDIX E

DEVELOPMENT OF FATIGUE ASSESSMENT METHODOLOGY

CONTENTS

	Page No.
E.1 OVERVIEW	E.1.1
E.1.1 PREAMBLE	E.1.1
E.1.2 BACKGROUND CONSIDERATIONS	E.1.2
E.1.2.1 Fixed Rigid Cylinders in Uniform Steady Flow	E.1.2
E.1.2.1.1 Flow regime	E.1.2
E.1.2.1.2 Vortex shedding	E.1.3
E.1.2.2 Factors Affecting Strouhal Number for Fixed Rigid Cylinders in Uniform Steady Flow	E.1.5
E.1.2.2.1 Reynold's number	E.1.5
E.1.2.2.2 Cylinder roughness	E.1.6
E.1.2.2.3 Boundary proximity	E.1.7
E.1.2.2.4 Turbulence intensity in approach flow	E.1.7
E.1.2.3 Elastically Restrained Rigid Cylinders in Uniform Steady Flow	E.1.7
E.1.2.3.1 Modes of response	E.1.8
E.1.2.3.2 Means of illustration of response	E.1.8
E.1.2.4 Unsteady Flow: General Considerations	E.1.10
E.1.2.4.1 Wave-induced current	E.1.11
E.1.2.4.2 Combined steady and wave-induced current	E.1.12
E.1.3 ANALYTICAL TECHNIQUES	E.1.13
E.1.3.1 Preamble	E.1.13
E.1.3.2 Reduced Velocity Techniques	E.1.14
E.1.3.2.1 DNV (1981)	E.1.15
E.1.3.2.2 Barltrop and Adams (1991)	E.1.17
E.1.3.2.3 OTI 93 614 (HSE, 1993)	E.1.18
E.1.3.2.4 APAL (1993)	E.1.21
E.1.3.3 Structural Mechanics Techniques	E.1.21
E.1.3.3.1 EXXON method	E.1.21
E.1.3.3.2 ABAQUS	E.1.22
E.1.4 LITERATURE REVIEW	E.1.25
E.1.4.1 Preamble	E.1.25
E.1.4.2 Fluid Loading	E.1.26
E.1.4.2.1 Steady current in free stream	E.1.26
E.1.4.2.2 Planar oscillatory flow	E.1.27
E.1.4.2.3 Combined steady current and wave-induced flow	E.1.28
E.1.4.3 Reduced Velocity Techniques	E.1.31

E.1.4.3.1	Steady current and planar oscillatory flow in free stream	E.1.31
E.1.4.3.2	Steady current and plane boundary	E.1.33
E.1.4.3.3	Planar oscillatory flow and plane boundary	E.1.37
E.1.4.3.4	Steady current, planar oscillatory flow and plane boundary	E.1.40
E.1.4.3.5	Steady current and scour trenches	E.1.48
E.1.4.3.6	Planar oscillatory flow and scour trenches	E.1.48
E.1.4.4	General Fatigue Calculations for Pipeline Spans	E.1.50
E.1.4.5	Summary of Literature in Relation to Assessment Issues	E.1.52
E.1.5	FATIGUE LIFE AND DAMAGE CALCULATION	E.1.53
E.1.5.1	Limits Set by Codes and Guidelines	E.1.53
E.1.5.1.1	BS 8010	E.1.53
E.1.5.1.2	DNV	E.1.54
E.1.5.1.3	IP6	E.1.55
E.1.5.2	S-N Curves	E.1.55
E.1.5.3	Damage/Fatigue Life Calculation	E.1.55
E.1.6	SUMMARY AND CLOSING REMARKS	E.1.56
E.1.6.1	Background Considerations	E.1.56
E.1.6.2	Literature Review	E.1.57
E.2	INITIAL PROPOSALS FOR DYNAMIC METHODOLOGY	E.2.1
E.2.1	PREAMBLE	E.2.1
E.2.2	OVERALL DYNAMIC ASSESSMENT STRATEGY	E.2.1
E.2.2.1	Overall Strategy	E.2.1
E.2.2.2	Deterministic, Statistical and Reliability-Based Strategies	E.2.2
E.2.3	DATA, LOADING CASES AND LOAD COMBINATIONS	E.2.2
E.2.3.1	Data	E.2.2
E.2.3.2	Loading Classes	E.2.3
E.2.3.3	Load Combinations	E.2.4
E.2.4	ANALYTICAL METHODS	E.2.4
E.2.4.1	Tier 1	E.2.4
E.2.4.2	Tier 2	E.2.5
E.2.4.3	Tier 3	E.2.5
E.2.5	DETAILED LOADING	E.2.6
E.2.5.1	Data	E.2.6
E.2.5.1.1	Current data	E.2.6
E.2.5.1.2	Wave data	E.2.6
E.2.5.2	Data Processing	E.2.7
E.2.5.2.1	Current	E.2.7
E.2.5.2.2	Wave	E.2.7

E.2.5.2.3	Combined current and wave data	E.2.8
E.2.5.2.4	Further pre-processing	E.2.9

E.3	CONCLUSIONS	E.3.1
------------	--------------------	-------

E.4	RECOMMENDATIONS	E.4.1
------------	------------------------	-------

E.5	REFERENCES	E.5.1
------------	-------------------	-------

E.1 OVERVIEW

E.1.1 PREAMBLE

Figure E.1.1 presents, in generic terms, a framework outlining the key facilities necessary for dealing with fatigue assessment of pipelines, and how these various aspects interact. In broad terms this framework would be the same regardless of what structural system is under consideration. The detail relating to some or all of the individual modules indicated in the figure would render the framework particular to pipelines. Moreover, this detail would also dictate, in an analogous way to the methodology suggested for static strength assessment, the degree of conservatism/complexity of the modules and therefore the tier at which they should be applied. The modules indicated in Figure E.1.1 may be described in general terms in the following.

1. Environmental Data

This module comprises the development and manipulation of data pertaining to sea conditions. It would involve a wide range of sea-states consisting of wave heights and periods, and nominally steady current velocities. Data provision and manipulation would be principally statistical.

2. Analytical Loading

The purpose of this module is to receive data generated by the preceding module and to process it into suitable "loading" for use by the subsequent analytical module. This processing is likely to involve two stages: firstly, the translation of conditions at the sea surface (or some other measuring point) into water particle velocity conditions at the seabed, or top of pipeline level; secondly, the conversion of water particle motions into hydrodynamic loading. Depending on the analytical tools used, only the first or both of these stages may be necessary.

3. Analysis

This module is necessary to predict the response of the pipeline to the analytical loading derived from the previous module given the input of structural data. A great range of analytical tools are available, but the consideration of appropriate ones must be based on the fact that, owing to the nature of the loading, a great deal of repeated analysis will be necessary. In any case the analytical tool must predict the response (in terms of motion) of the pipeline span to the loading.

4. Stress Ranges

This module is required to compute the stress ranges that result in the pipeline span from its motion. This computations may or may not be directly integrated within the previous module

depending on the analytical tools employed there.

5. Fatigue Damage/Life

The procedures within this module are required to receive the stress ranges calculated from the previous module and, using them as input data, compute the fatigue damage and life of the pipeline span.

The preceding represents a simplified view of the problem, but nevertheless provides a valuable framework around which the remainder of this Section of the report is built. Of the above modules the most contentious is probably the analysis and the tools employed therein; this is dealt with in Section E.1.3. Having laid the foundations for this in fairly detailed but more general terms, a comprehensive review of literature is given in Section E.1.4; this is devoted principally to identifying key information relevant to analysis methods and assessment methodologies in general. Section E.1.5 deals with fatigue damage and life calculations and limits imposed by codes and standards. Closing remarks, in which the information is brought together, summarised and preliminary conclusions drawn, are given in Section E.1.6.

The hydrodynamic loading and response of pipeline spans is a highly complex phenomenon, particularly with regard to vortex shedding. The subject area is very demanding as it involves fluid dynamics and structural mechanics in close and complicated interaction. For this reason it was felt important to preface all of the sections referred to above with Section E.1.2, which covers the background considerations. These centre particularly around cylinders in fluid flow of various types and vortex shedding, the principal factors affecting response, the key non-dimensionalised parameters defining flow and response, and the primary means of illustrating response. All of these provide a fundamental basis for the understanding and interpretation of information provided in the later sections of the report.

E.1.2 BACKGROUND CONSIDERATIONS

E.1.2.1 Fixed Rigid Cylinders in Uniform Steady Flow

Although not directly replicating in all aspects the physical reality of the problem, the body of technological knowledge associated with the uniform steady flow of fluid around fixed rigid cylindrical bodies forms the basis of the understanding of the dynamic response of spanning submarine pipelines. Two particular aspects assume primary importance, namely: flow regime (importance of Reynolds number) and vortex shedding (importance of Strouhal number).

E.1.2.1.1 Flow regime

The regimes in free-stream flow past a rigid circular cylinder depend on a non-dimensional

parameter referred to as the **Reynolds number** and given the symbol, R_e . This is a function of three variables, as follows:

$$R_e = \frac{UD}{\nu}$$

where U = approach flow velocity

D = cylinder outside diameter

ν = kinematic viscosity of surrounding fluid.

The Reynolds number provides a measure of the extent to which the viscosity of the fluid damps out instabilities in the flow that would otherwise produce turbulence. Thus for a given cylinder in a fixed free-stream velocity:

high ν < 6 low R_e 6 no turbulence (laminar flow)

low ν < 6 high R_e 6 turbulent flow

Ranges of typical values for the variables listed above corresponding to North Sea pipelines might be as follows (OTI 93 614, 1993).

$$\nu = 1.5 \times 10^{-6} \text{ m}^2/\text{s}$$

$$1.5 \text{ m/s} \# U \# 2.5 \text{ m/s}$$

$$0.3\text{m} \# D \# 1.0\text{m}$$

These lead to the range of possible Reynolds numbers as illustrated in Figure 2.2. Of importance are critical and supercritical R_e values; these correspond to:

$$2 \times 10^5 \# R_e \# 5 \times 10^5 \text{ and}$$

$$5 \times 10^5 \# R_e \# 3 \times 10^6,$$

respectively, and it is seen that the practical range of Reynolds number indicated above encompasses these values.

E.1.2.1.2 Vortex shedding

The range of Reynolds number indicated above includes the stable alternate vortex street where $300 \leq Re \leq 3 \times 10^5$ (see Figure 2.2). In this, vortex pairs are shed alternately in the wake of the cylinder, in the sequence one from the top followed by one from the bottom, according to a well-defined frequency given by:

$$f_s = \frac{SU}{D}$$

where f_s = vortex shedding frequency

S = Strouhal number

the other terms having been defined earlier.

Owing to the pressure differentials created by the shedding vortices, forces are exerted on the cylinder which are periodic and are of two types:

- IN-LINE, parallel to the flow, where the forces are in the same direction for every vortex shed
- CROSS-FLOW, normal to the flow, where the forces generated are in opposite directions alternately for every vortex shed.

Hence the frequencies of the in-line and cross-flow forces are $2f_s$ and f_s , respectively, and they can be expressed as:

$$F_x(t) = \frac{1}{2} \rho U^2 D \{C_D + C'_D(2f_s t)\}$$

$$F_y(t) = \frac{1}{2} \rho U^2 D C'_L(f_s t)$$

where F_x = drag or in-line force as a function of time t

D = density of fluid

- C_D = 'steady' drag coefficient
- C_D' = fluctuating (time dependent) drag coefficient
- F_y = lift or cross-flow force
- C_L' = fluctuating (time dependent) lift coefficient.

Clearly the shedding frequency is of prime importance and, with reference to the formula given above for f_s , central to its value is the non-dimensional parameter referred to as the **Strouhal number** given the symbol S . Given the importance of this parameter the factors affecting it are discussed in more detail in the next section.

E.1.2.2 Factors Affecting Strouhal Number of Fixed Rigid Cylinders in Uniform Steady Flow

The key factors affecting Strouhal number, and consequently vortex shedding frequency, have been listed in OTI 93 614 (HSE, 1993), for example, as:

- Reynolds number
- Cylinder roughness
- Boundary proximity
- Velocity gradient across cylinder
- Turbulence intensity in approach flow
- Cylinder length:diameter ratio

In the case of velocity gradient, there is a trend for S to increase with increasing gradient, but this is eliminated if the approach velocity of the fluid is taken as the value at the top of the cylinder. The cylinder length:diameter ratio is generally considered not to be a significant parameter in spanning situations owing to the fact that the cylinder is compliant. The remaining factors warrant more detailed discussion, as given below.

E.1.2.2.1 Reynolds number

Information on the effects of this factor on Strouhal number for fixed rigid cylinders can be found in Barltrop and Adams (1991), OTI 93 614 (HSE, 1993) and Sheppard and Omar (1992). A figure

representing the dependence of S on R_e is given in Figure E.1.3. This is fairly typical of information given by all references in this respect; all tend to agree that there are regimes of Strouhal number corresponding to ranges of Reynolds number. There is, however, a lack of agreement as to the nomenclature used for the regimes and the values of R_e representing the demarcations between the regimes. This is not surprising given that these matters are a question of interpretation of experimental data.

Also indicated on Figure E.1.3 are power spectral densities for cross-flow spectra versus Strouhal number for a number of fixed values of Reynolds number. These are useful because they indicate the strength of the vortex shedding (magnitudes of the ordinates) and the concentration of values of Strouhal number (shape of curve as related to abscissae).

In terms of regimes of response the following are suggested in OTI 93 614 (HSE, 1993):

- SUBCRITICAL: $3 \times 10^2 < R_e < 2 \times 10^5$, vortex shedding highly regular, S approximately constant and equal to 0.2.
- CRITICAL: $2 \times 10^2 < R_e < 3 \times 10^5$, weak vortex shedding, S approximately equal to 0.46.
- SUPERCRITICAL: $5 \times 10^2 < R_e < 3.5 \times 10^5$, regular weak vortex shedding over a broad band of frequencies, $0.4 < S < 0.46$.
- TRANSCRITICAL: $3.5 \times 10^6 < R_e$, regular vortex shedding, $S \approx 0.2$.

Sheppard and Omar (1992) argue that for all practical purposes vortices are shed at a single frequency for $R_e < 7 \times 10^5$ and for $R_e > 7 \times 10^6$. For $7 \times 10^5 < R_e < 7 \times 10^6$ the spectrum of cross-flow forces is broad-banded, reduced in magnitude and very sensitive to such things as free stream turbulence.

E.1.2.2.2 Cylinder roughness

The preceding has considered cylinders that are hydraulically smooth. Cylinder roughness leads to turbulence and this exerts a major influence on the process of laminar to turbulent flow transition and hence the physical characteristics of the flow regime around the perimeter of the cylinder. The parameter usually used to quantify roughness is the relative roughness as given by k_s/D , where k_s is termed the equivalent sand roughness (and is related to real sand grain diameters)

According to OTI 93 614 (HSE, 1993) the major effect of increasing roughness is to lower the R_e values demarcating the subcritical, critical, supercritical and transcritical regions of

response described above. Within the regions themselves the following effects are observed:

- SUBCRITICAL: vortex shedding regular, S approximately constant and equal to 0.2.
- CRITICAL: vortex shedding eliminated, region disappears for $k_s/D \bullet > 1 \times 10^{-2}$, vortex shedding always present.
- SUPERCRITICAL: introduction of roughness re-establishes regular strong vortex shedding, for $0.75 \times 10^{-3} < k_s/D < 30 \times 10^{-3}$, S in the range $0.2 < S < 0.46$ and is inversely proportional to the relative roughness.
- TRANSCRITICAL: vortex shedding behaviour largely independent of R_e , S in the range $0.21 < S < 0.23$.

Summary diagrams, giving the variation of S with R_e for different k_s/D values and the boundaries between the various flow regimes, are given in Figure 2.4 and are taken from OTI 93 614 (HSE, 1993). It is also worth noting that according to this reference a typical k_s value for a concrete coated pipeline would be around 6.0mm giving a range of relative roughness between 2×10^{-2} and 6×10^{-3} for pipelines with diameters between 0.3 and 1.0m.

E.1.2.2.3 Boundary proximity

It is to be expected that the presence of a rigid plane boundary parallel to the flow will affect the Strouhal number. Moreover as the gap between the cylinder and the boundary is reduced the frequency of vortex shedding (which is proportional to the effective approach velocity) and the Strouhal number will increase. The gap ratio (ratio of gap size to cylinder diameter) is taken as the key parameter and it has been found that the Strouhal number (for subcritical values of R_e) maximises for gap ratios of 0.5 and 0.75, with increases in the Strouhal number of the order of 5% and 10% of the free stream value.

E.1.2.2.4 Turbulence intensity in approach flow

The effects caused by turbulence in the approach flow may be classified as indirect and direct. In the case of indirect effects, turbulence may cause changes in the flow velocity distribution resulting in velocity gradients across the width of the cylinder; the effects of these have been discussed above. Direct effects relate to the physical characteristics of the flow, and little is known about this.

E.1.2.3 Elastically Restrained Rigid Cylinders in Uniform Steady Flow

The preceding has considered rigid cylinders held fixed in uniform flow, a further stage of development towards similitude with a pipeline span is to allow the cylinder flexibility of motion in the in-line and cross-flow directions. This provides the cylinder with the ability to move in response to the hydrodynamic forces imposed upon it by the vortex shedding. Resonance of the cylinder can interact with the vortex shedding process, forcing the vortex shedding into synchronisation with the cylinder motion (at its natural frequency) thereby magnifying the amplitude of vibration. This phenomenon is referred to as **lock-in**. The key point is that the effect of cylinder motion is to enhance and actively assist in the vortex formation and shedding process. It should be noted that the cylinder, owing to its rigidity, possesses only two degrees of kinematic freedom corresponding with the in-line and cross-flow directions.

E.1.2.3.1 Modes of response

Given the behaviour of fixed cylinders, at least two modes of response would be anticipated for cylinders having the ability to move, namely:

- IN-LINE, in which the frequency of vortices shed in the wake of the cylinder is approximately equal to half the natural frequency of vibration of the cylinder
- CROSS-FLOW, in which the frequency of vortices shed is approximately equal to the natural frequency of vibration of the cylinder.

In the event these occur, but in addition a third IN-LINE response is possible which is associated with the shedding of symmetric pairs of vortices, one from the top and one from the bottom of the cylinder, simultaneously. This is a forced phenomenon, which may occur at lower flow velocities, and is caused by low relative velocity between the moving cylinder and the flow.

E.1.2.3.2 Means of illustration of response

Generally, and particularly with regard to the reporting of experimental work involving moveable cylinders in uniform flow, response is illustrated graphically using dimensionless parameters. In the case of moveable cylinders, care must be taken in distinguishing the frequency of vortices shed in the wake of the cylinder from that of vortices that would have been shed had the cylinder been fixed. This is because the phenomenon of lock-in results in the fact that these two frequencies are different under particular flow conditions.

The following frequency parameters are used:

f_n = natural frequency of vibration of the moveable cylinder

f_s = vortex shedding frequency for the fixed cylinder

f_w = dominant frequency of vortices shed in the wake of the cylinder
(these may cover a range).

The convention is to use the natural frequency of vibration of the cylinder as the normalising quantity and to take:

$$V_r = \frac{U}{f_n D} = \text{reduced velocity}$$

$$\frac{f_w}{f_n} = \text{wake vortex shedding frequency ratio}$$

$$\frac{S}{n} = \frac{SU}{f_n D} = SV_r = \text{fixed cylinder vortex shedding frequency ratio}$$

In addition, the amplitude of oscillation, a , may be divided by the cylinder diameter to give a further dimensionless quantity.

$$\frac{a}{D} = \text{amplitude ratio}$$

Various types of amplitudes may be taken including maximum, RMS, double- and single-amplitudes.

Using these various parameters an idealised response of a cylinder may appear as illustrated in Figure 2.5. The response is mapped as a set of two graphs, both take reduced velocity as the abscissa, one takes frequency ratio as the ordinate and the other uses amplitude ratio.

Considering the graph of frequency ratios versus reduced velocity, two frequency plots are given. The fixed cylinder ratio appears as a straight line with a constant of proportionality equal to the Strouhal number. This presumes that the range of V_r is such that the Strouhal number is constant for Reynolds number (which is a function of flow velocity and hence reduced velocity); this may not always be the case.

The wake frequency ratio is also shown and the lock-in phenomenon is demonstrated. As the flow velocity is increased from zero the wake frequency initially follows the fixed cylinder frequency until the first in-line response is encountered; this continues with vortices being shed every time the motion of the cylinder reverses into the flow direction, until with increasing flow velocity the frequency reverts back to the fixed cylinder frequency. Further increases in flow

velocity result in lock-in to the second in-line case where it is seen that the wake frequency remains equal to half the natural frequency of the cylinder over a range of flow velocities. Within this range the actual Strouhal number is reduced by wake circulation, which is built up by the cylinder motion, allowing the wake frequency to be maintained at half the cylinder natural frequency. Eventually a flow velocity is reached where sufficient circulation to achieve this cannot be preserved and a jump back to the fixed cylinder frequency occurs. This situation is maintained until the cross-flow lock-in occurs, for which the mechanisms are similar to those just described, except that over the range of flow velocity corresponding to lock-in the wake frequency is maintained at the cylinder natural frequency.

It is seen that, in general, at lock-in enforced synchronisation over-rides fixed cylinder theory. This is also illustrated by the plot of amplitude ratio versus reduced velocity where it is seen that lock-in is characterised by a series of peaks in the curve that maximise then die away at ranges of flow velocity for which the wake frequency coincides with the fixed cylinder vortex shedding frequency. Given that peaks occur, this indicates that the amplitudes of vibration of the cylinder may be limited in both the in-line and cross-flow directions as a result, say, of mechanical damping in the system. However, during the lock-in phases, the forces applied to the cylinder may be greater than those exerted on fixed cylinders.

The description above represents a somewhat idealised situation in which the modes of response are well-separated and distinguishable. In practice significant response may occur well before cross-flow resonance takes place and in addition to this coupled vibration between in-line and cross-flow motions may occur, giving, depending on oscillation frequencies, elliptical or figure of eight vibration orbits (Lissajous figures).

E.1.2.4 Unsteady Flow: General Considerations

In all the preceding, consideration has been confined to uniform steady flow, ie. the free stream flow velocity does not change with time. In practice currents incident upon a suspended length of pipeline will not, in general terms, be as simple as this. They will comprise flow velocities derived from the following:

- tidal flows, usually based on a long period of variation and, therefore, treated as quasi-static
- storm surge and other similar transient events
- wave-induced, involving a whole spectrum of periods.

In fatigue terms the most important of these will be the more frequently occurring events, ie. the steady current arising from tidal flows, and the flow velocities stemming from waves. Since

steady flow has been dealt with already it remains to address the background considerations pertaining to wave-induced currents, and the combination of steady and wave-induced currents.

E.1.2.4.1 Wave-induced current

In the course of wave action water particle orbits are elliptical in one wave period. Precise orbit shapes depend upon wave period and mean water depth. In deep water, particle orbits are circular having diameters which decrease exponentially towards the seabed to the extent that the water at depths in excess of about one half of a wavelength is hardly affected by waves. In shallow water the orbits become elliptical with their long axis parallel to the mean water surface; at the seabed the excursions made by the water particles in the vertical direction are virtually zero.

This latter situation means that water particles move only horizontally backwards and forwards according to the periodic characteristics of the wave. This type of flow is referred to as plane oscillatory motion, having no velocity component in the vertical direction, and is frequently used in experimental investigations to simulate wave effects.

Of paramount importance is the maximum distance moved by a water particle from the centre of the cylinder during a complete wave cycle. This is also known as the excursion. Thus during a complete wave cycle a water particle will start from an excursion point with zero velocity travel past the centre of the cylinder, reach the opposite excursion point (thereby completing a wave half-cycle), before reversing direction and returning to its starting point and completing the wave cycle. Hence during a wave half-cycle the water particle concerned travels in the same direction, but with a sinusoidally varying velocity. The key points in this respect are whether there is sufficient time or distance (in terms of two excursions per wave half-cycle) and flow velocity during a wave half-cycle to allow vortex shedding to occur and the number that will be shed if conditions are conducive.

This can be assessed by means of a dimensionless parameter referred to as the **Keulegan-Carpenter number** and given the symbol K_c .

This is a function of two variables, as follows:

$$K_c = \frac{U_w T}{D}$$

where U_w = peak flow velocity past the cylinder during a wave cycle

T = wave period

D = cylinder diameter.

It is, in effect, similar in form to the reduced velocity for steady flow with the difference being it embodies wave frequency. Indications from experimentation (OTI 93 614: HSE, 1993) are as follows:

- $K_c < 5$ vortices are shed if at all in a symmetric pattern, cross-flow forces are insignificant
- $5 < K_c < 15$ single vortex shed in each wave half-cycle, cross-flow frequency equals twice wave frequency
- $15 < K_c < 25$ two vortices shed per wave half-cycle, dominant frequency of cross-flow force equals three times wave frequency
- $K_c > 25$ increases in the number of vortices completely formed and shed in each wave half-cycle until wake resembles steady flow situation, and thus becomes independent of wave frequency.

For situations where K_c is greater than 25 spectral analysis of cross-flow forces shows that there are peak contributions at integer multiples of the wave frequency. However, the vortex shedding is closely synchronised and coupled with the wave frequency only for $K_c < 25$.

There is further evidence to suggest that for "high" (>20) values of K_c a form of "quasi-static" vortex shedding occurs where the shedding frequency closely follows the instantaneous cyclical variations in the oscillating flow velocity. Also the wave Strouhal number (for surface roughened cylinders) shows little Reynolds number dependence, remaining essentially constant at about 0.2. In essence this means that the formula given in Section 2.2.1 for the computation of the vortex shedding frequency could be used by substituting the instantaneous velocity for the steady flow velocity.

E.1.2.4.2 Combined steady and wave-induced current

In this situation it is clear that the flow velocity may or may not reverse direction depending on the relative values of the steady and peak oscillatory components of the flow velocity. The overall velocity conditions may be quite different in the two halves of a wave cycle and it is convenient to compute the Keulegan-Carpenter numbers corresponding to each wave half-cycle in the following manner:

$$K_{C1,2} = \left(\frac{\pi}{2} U_c \pm U_w \right) \frac{T}{D}$$

where U_c = the steady current velocity,

and the other terms have been defined previously.

Clearly if $U_c > U_w$ no flow reversal takes place and whilst the vortex generation process may vary during the course of a wave cycle, the wake remains on one side of the cylinder. Quasi-steady flow conditions may prevail providing that the two Keulegan-Carpenter numbers pertaining to the wave half-cycles are sufficiently high.

There is likely to be, however, a reasonable consistency in vortex generation during the entire wave cycle.

On the other hand if $U_c < U_w$ the potential exists for the flow velocity to reverse direction during part of the wave cycle. This will inevitably disrupt any vortex generation built up over a preceding period because the upstream and wake regions relative to the cylinder, and the velocity regimes are forced to change. Again the Keulegan-Carpenter numbers in each wave half-cycle could be computed but values of U_c and U_w may be such as to yield a negative K_c in one case: this should be interpreted as pertaining to a reversed velocity relative to the other wave half-cycle. If the Keulegan-Carpenter numbers pertaining to one or both wave half-cycles are sufficiently high, quasi-steady conditions may prevail.

E.1.3 ANALYTICAL TECHNIQUES

E.1.3.1 Preamble

It is evident from a preliminary appraisal of the literature that two types of analytical techniques either are, or have the potential to be, used in assessment of fatigue in pipeline spans. These may be classified as techniques related to:

- reduced velocity (see Section E.1.3.2)
- structural mechanics.

Reduced velocity techniques are empirical and exploit the fact (observed in Section E.1.3.2) that it is very often the case in experiments that cylinders subject to fluid flow experience limited

amplitudes of vibration. The techniques utilise databases (in the broadest sense) of experimental results to assess in the case of pipelines, firstly, the expectation of significant dynamic response and, secondly (if this is the case) the likely maximum amplitudes of vibration. Two important points must be made regarding this:

- experimentation tends to be predominated by tests on rigid fixed or elastically-mounted cylinders subjected to fairly simplified flow regimes, with comparatively little information related to real pipeline spans
- the techniques give no direct information about stress ranges.

Structural mechanics techniques embody all the dynamic structural analysis that may be available. Broadly speaking these may be classified into two types, namely: time-domain and frequency-domain analyses. They are fundamentally different and this affects their practicability in application to fatigue calculations.

In essence time-domain analyses take a time-varying loading applied to a structural model and compute the response history of the model. The response history may be thought of as a graph of stress, deflection etc., versus time. The method is very powerful, can involve structural and material nonlinearities and so forth, and is useful in investigating the instantaneous response of the structural model. It is not, however, a very practical method in fatigue calculations as it does not allow the computation of stress ranges and their frequencies of occurrence directly.

Frequency-domain analyses, on the other hand, are much more suitable for fatigue computations. The time-varying loading is broken down into its frequency components, each component applied separately and a steady-state response calculated at that frequency. The responses can then be superposed to give the resultant effect, or used individually in fatigue damage calculations because stress ranges can be an automatic product of the analysis. By its nature frequency-domain analysis is a linear dynamic technique, but this does not represent a serious drawback in practical terms.

Structural mechanics techniques may also embody all the bespoke methods developed and programmed on an individual basis by various companies; for example, Snamprogetti (1994).

E.1.3.2 Reduced Velocity Techniques

Techniques of this type are principally empirical and use incident flow velocity of the moving stream of water, natural frequencies of vibration of the pipeline span, pipeline outside diameter, pipeline effective mass per unit length, logarithmic decrement of structural damping and seawater density in a pair of dimensionless parameters, namely: reduced velocity and a stability parameter. These coefficients are then related to databases of experimental results, usually

in graphical form, to assess:

- the expectation of significant in-line and cross-flow dynamic response
- the likely maximum amplitudes of vibration pertaining to in-line and cross-flow vibration.

Approaches of this sort should be regarded as semi-qualitative, although attempts have been made to use them in a more quantitative context to calculate fatigue life.

E.1.3.2.1 DNV (1981)

The guidance given in DNV (1981) is the oldest extant and is contained in Appendix A of the document; it relates to vortex shedding due to current only. Two sets of two graphs are provided pertaining to in-line and cross-flow motions. In each set the first graph is used to estimate the flow velocity at which motion is initiated for a particular natural frequency of vibration of the pipeline, and the second graph is used to estimate the amplitude of vibration as a proportion of the pipeline diameter.

The procedure is illustrated schematically in Figure 2.6. The key parameters with regard to the procedure are as follows:

$$V_r = \frac{U_c}{f_i D}$$

where V_r = reduced velocity (dimensionless)

U_c = incident current velocity normal to the axis of the pipeline

D = pipeline outside diameter

f_i = pipeline natural frequency

$$k_s = \frac{2m_e \delta}{\rho D^2}$$

where k_s = stability parameter (dimensionless)

m_e = effective mass per unit length of pipeline, including structural,

contents and added mass

* = logarithmic decrement of structural damping

D = mass of surrounding seawater

$$R_e = \frac{U_c D}{\nu}$$

where R_e = Reynolds number (dimensionless)

ν = kinematic viscosity of surrounding seawater

$$g = y_{\max} \frac{\int_0^L y^2(x) dx \dot{u}^{1/4}}{\int_0^L y^4(x) dx \dot{u}}$$

where y = mode shape corresponding with the natural frequency concerned

y_{\max} = maximum value of the mode shape

x = distance along a span of length L .

As can be seen from the flow chart, the processes pertaining to in-line and cross-flow motions can be treated separately and their respective logics are derived from the underlying graphs given in Figure E.1.7. After computation of the k_s and V_r parameters, in-line motion is considered first and reference is made to A.4 in Figure E.1.7; no significant motion occurs if $k_s \leq 1.8$.

If, however, $1.2 < k_s < 1.8$ it is apparent from A.3 that motion occurs if $V_r \geq 2.2$, whereupon the maximum amplitude as a proportion of diameter can be read off A.4; no motion occurs if $V_r < 2.2$. Alternatively, if $k_s < 1.2$ then A.3 must be checked to determine if the combination of V_r and k_s is such as to cause motion. If this is the case, then A.4 is used to determine amplitude; if not then no significant motion needs to be taken into account.

When cross-flow motion is considered, then additional computation of Reynolds number is necessary. No significant motion occurs if $V_r < 3.7$. If this is not the case, A.5 is used to

determine if motion occurs, based on R_g and V_r , with A.6 used to estimate the maximum cross-flow amplitude if this is the case.

It is worth pointing out that for a given geometrical configuration of pipeline span (ie. fixed span length) subject to a fixed current velocity, if no in-line or cross-flow motion occurs for the lowest natural frequency of vibration then higher frequencies do not need to be investigated. However, if motion is indicated for the lowest natural frequency, then the higher frequencies need to be assessed until one is reached for which no motion results.

E.1.3.2.2 Barltrop and Adams (1991)

Vortex shedding is covered in Barltrop and Adams (1991), and although broadly directed towards the dynamics of fixed marine structures it provides a comprehensive reference. The procedure distilled from this reference is summarised in Figure E.1.8 and is broadly similar to and uses the same assessment parameters as DNV (1981).

The procedure is governed by an overall loop in which all natural frequencies of vibration are checked until one is reached for which no in-line or cross-flow response is indicated. For an individual natural frequency the reduced velocity is checked against criteria to assess whether vibration is likely to occur; if this is the case, then the amplitude of vibration as a proportion of the pipeline diameter is read off a graph (see Figures E.1.9 and E.1.10). In-line and cross-flow motion are both treated similarly.

Key differences exist between this method and the one suggested by DNV (1981), these relate to:

- the assessment of the onset of motion
- the treatment of wave loading.

In terms of the onset of motion, Barltrop and Adams give fixed values to the ranges of reduced velocity within which the oscillation modes occur. DNV on the other hand indicate that the ranges are functions of the stability parameter k_s and Reynolds number R_g in the cases of in-line and cross-flow vibrations, respectively.

Barltrop and Adams emphasise that considerable uncertainty exists when assessment is required for wave or simultaneous wave and current forces. The central question surrounding wave motion is whether, under velocity variation or reversal every half wave cycle, conditions prevail to allow the build-up of vortex shedding to the same extent that might occur under steady flow conditions.

In terms of wave-only, Barltrop and Adams argue that the Keulegan-Carpenter number (see Subsection E.2.2.4.1) is the key parameter determining whether the flow excursion is sufficient for separation to occur and for vortices to fully form before flow reversal. For Keulegan-Carpenter numbers in the range $0 < K_c < 5$, vortices are shed (if at all) in a symmetric pattern and cross-flow forces are insignificant.

To account for transient behaviour it is suggested that use is made of a factor denoted as Q which deals with intermittent lock-in through the wave cycle. This is indicated on the flow chart in Figure E.1.8 and is introduced as a division in the stability parameter k_s . The computation of Q is based on the assumption that the cyclic wave loading leads to intermittent lock-in over the times when the velocity is in the range for excitation of a particular mode of vibration. The response reaches an equilibrium in which the decay between periods of lock-in just balances the increase during lock-in; on this basis Q is taken as:

$$Q = \frac{e^{-\delta F} - 1}{e^{-\delta F} e^{-\delta M} - 1}$$

where δ = logarithmic decrement of structural damping

F = number of forcing cycles in a half wave cycle

M = number of decay cycles in a half wave cycle

$$M + F = \frac{T_w}{T_n}$$

where T_w = wave period

T_n = natural period of vibration of the pipeline.

Generally speaking in situations of intermittent lock-in the factor Q assumes a value less than unity. This results in an increase in the stability parameter with a consequent reduction in the amplitude vibrations computed from Figures E.1.9 and E.1.10.

E.1.3.2.3 OTI 93 614 (HSE, 1993)

This document takes a similar approach to that given in DNV (1981), but has a number of fundamental differences. The methodology is based principally upon a number of rigorously

performed full-scale experiments on smooth and roughened pipeline spans reported in OTI 92 555 (HSE, 1993) and performed by Hydraulic Research Limited in the Severn Estuary.

OTI 93 614 (HSE, 1993) argues that the reduced velocity approach of, for example, DNV (1981) for the assessment of a span condition is not acceptable, since the characteristics of real span behaviour are not adequately represented. The essence of the argument lies in the fact that the simplistic view of response, that oscillations of the pipeline can be distinguished into distinct, well-separated regimes of behaviour according to the magnitude of reduced velocity, is not borne out by the full-scale experimental results.

In the case of smooth pipelines, hysteresis effects were found to occur in the wake frequency response. In these, dynamic jumps took place between responses associated with in-line and cross-flow vortex shedding frequencies with both increasing and decreasing reduced velocity. Observations showed, however, that the spans responded at an approximately constant frequency (nominally the still water natural frequency) throughout the changing regimes of vortex shedding. It was also shown that whilst the initial response region was marked by in-line vibrations, this was accompanied by smaller amplitude, but significant, cross-flow components. Moreover, the tests revealed a significant increase in in-line response amplitude over commonly suggested limiting values. This was ascribed to the fact that critical flow conditions gave rise to much lower C_D values than would normally be expected, the consequences of which being that the in-line damping components due to hydrodynamic drag were reduced, thereby increasing the corresponding vibration amplitude.

Initial findings from the experiments on stationary rough pipeline spans gave reason to expect that the dynamic behaviour of a span at low gap ratios (ratio of gap between the underside of the pipeline and the seabed, and the pipeline diameter G/D) differed from the behaviour for larger gap ratios due to differences in the characteristics of the vortex-induced excitation mechanisms. This expectation was borne out by the experiments in which spans were free to vibrate. In the case of high gap ratios, progressive (rather than dynamic) wake frequency variations with reduced velocity were observed between responses associated with in-line and cross-flow vortex shedding frequencies. The span response was much more complex than in the case of smooth pipelines: initially the span responds to increasing reduced velocity such that motions in both the in-line and cross-flow directions are at the span still water natural frequency; for further increases in reduced velocity the in-line span response exhibits a dynamic jump in order to remain synchronised with the wake frequency, whilst the cross-flow response maintains synchronisation with twice the wake frequency. This sequence of events is essentially retraced upon reduction of reduced velocity.

For small gap ratios in conjunction with rough pipelines some similarities to the responses of smooth pipelines were exhibited but differences were observed. Upon increasing the reduced

velocity an abrupt jump to a higher frequency is displayed by the wake response; following this jump the span responds in both the in-line and cross-flow directions at roughly the still water natural frequency.

In terms of practical response characteristics, the report recommended the following:

- the relationships for in-line motion in, for example, DNV (1981) should remain applicable
- the cross-flow onset thresholds in DNV (1981) are judged to be non-conservative for full-scale pipelines spans and, owing to the possibility of hysteresis effects and the coupled interaction between the motions in the in-line and cross-flow directions leading to an early threshold of large amplitude response, limitations should be based solely on a reduced velocity criterion as related to gap ratio
- the incident velocity to be used for assessment should be based on the conservative assumption of adding the steady current velocity to the maximum wave induced velocity.

Based upon this, the potential for a pipeline span to undergo vortex-induced vibration should be assessed using the reduced velocity parameter V_r against two threshold limits V_{r1} and V_{r2} , as follows:

$V_r < V_{r1}$ No significant vortex-induced vibration takes place

$V_{r1} \# V_r < V_{r2}$ Vortex-induced vibration of relatively low amplitude may take place

$V_{r2} \# V_r$ Large amplitude and potentially catastrophic vortex-induced vibration may take place.

V_{r1} is derived from A.3 of Figure E.1.7 and V_{r2} is given by:

$V_{r2} = 2.4$ if $G/D \# 2.0$

$V_{r2} = 3.0$ if $G/D > 2.0$

In cases where $V_{r1} \# V_r < V_{r2}$ the amplitude of response may be estimated from A.4 in Figure 2.7, and it is to be emphasised that there is no provision for amplitude calculation in the situation when $V_{r2} \# V_r$.

The procedure thus follows the flowchart depicted in Figure E.2.11; this is similar to that in

Figure 2.6 except that complete distinction is not made between in-line and cross-flow motions.

E.1.3.2.4 APAL (1993)

This particular reference suggests a fatigue methodology based around the use of the graphs provided in DNV (1981) or the data on response amplitudes given in OTI 92 555 (HSE, 1993). No provision is made for dealing with waves and current velocity only is considered.

The fatigue calculation consists of a basic loop which is repeated for all of a finite number of current velocities as defined in a probability distribution function, ie. from current velocity scatter data. Thus each current velocity taken has a probability of occurrence associated with it.

The basic loop involves carrying out the DNV (1981) assessment procedure as described earlier in terms of critical reduced velocities, and using either the DNV (1981) graphs, or the data set in OTI 92 555 (HSE, 1993) to estimate the corresponding amplitudes of vibration in the in-line and cross-flow directions. These are then combined to estimate the peak stress range and from this an endurance limit from a suitable S-N curve. The computation is performed using the lowest natural frequency of vibration of the pipeline span, firstly to compute the reduced velocity at the head of the process, and finally to estimate the number of cycles actually undergone as the product of the natural frequency and the probability of occurrence of the current velocity under consideration. The ratio of the actual number of cycles to the endurance limit gives the contribution made to the total fatigue damage by the particular current velocity considered.

The total fatigue damage will be the sum of all the individual contribution made by the current velocities as defined in the probability distribution function. The damage will be in effect a rate per length of time used in the derivation of the current velocity probability distribution function.

It is worthwhile noting that no indication is given in this document as to whether, within an individual current velocity calculation, attention should be given to higher frequencies of vibration of the pipeline span as indicated in the preceding subsections. Finally, the above methodology, or an extension thereof, appears to form the basis of the assessment procedures outlined by Kaye, Galbraith, Ingram and Davies (1993).

E.1.3.3 Structural Mechanics Techniques

E.1.3.3.1 EXXON method

This particular paper, by Pantazopoulos et al (1993) (all staff members at Exxon Production Research Company, Houston), is significant principally for its usage of a vortex induced loading formulation that involves combined steady and wave-induced current. This particular aspect is dealt with in detail in Section E.2.4.3 of this report.

In addition to this, however, the paper advocates the use of a frequency-domain technique for the solution of beam-column equations of motion used to model the response of the pipeline span. These are two in number, corresponding to the in-line and cross-flow directions, and the respective responses are coupled by virtue of relative velocity effects between the moving pipeline and the flow.

In essence the loading, as a function of time, is decomposed into its Fourier components, ie. loading amplitudes at a series of frequencies of oscillation. The solutions, in terms of deflected shapes, for each loading frequency are taken to be the superpositions of the eigenfunctions of the beam-column multiplied by unknown deflection response amplitudes. The deflection amplitudes are then determined using the equations of motion. This yields the response of the pipeline to a loading amplitude of a fixed frequency in terms of steady state amplitude of deflection, which can readily be converted to stress ranges for subsequent analysis for fatigue damage or life. This process can be repeated for as many frequency components of the loading as are deemed necessary for an accurate representation of behaviour.

It should be noted that this analytical technique is, in fact, a fairly standard type of approach that may be determined from many textbooks on structural dynamics or mechanical vibrations. What makes this particular paper stand out, however, is the use of this method in combination with a novel loading representation as described later.

E.1.3.3.2 ABAQUS

ABAQUS is a very powerful, general purpose finite element analysis package. It is capable of linear and nonlinear calculations involving geometric (large deflections) and material (plasticity) effects. BOMEL has used it successfully in pipeline applications, both in terms of static strength (BOMEL 1996a and 1996c) and in the computation of natural frequencies of vibration (1996d).

It should be emphasised that ABAQUS is an analytical tool, and so has no facility for applying criteria in a direct manner to limit the configuration of the system being analysed. In the case of static strength assessments of pipeline spans the procedure adopted by BOMEL was to increase the span length of the pipeline being considered, repeatedly analyse, and monitor key variables (stress, strain etc) against criteria. A similar procedure has been adopted by BOMEL for the computation of natural frequencies. This approach is successful in both these situations providing that the number of analyses to be performed is not too large.

ABAQUS has no facility for the computation of fatigue damage, but its strength lies in its wide range of capabilities in dynamic analysis. Broadly speaking dynamic analyses may be divided into two types: linear and nonlinear, in much the same way as static analyses. Facilities exist in ABAQUS for conducting frequency-domain or time-domain analyses.

Linear analyses are described as linear perturbation procedures; generally this means that they are small deflection, elastic material responses about some base state. The base state may have been arrived at by means of a nonlinear procedure, however. In the case of the analyses undertaken by BOMEL, natural frequencies of vibration were computed via a linear procedure after having applied a nonlinear static analysis to simulate the response to the applied load. In this way the effects of membrane tension on natural frequency were evaluated.

Within **linear dynamic analyses** four options are provided, namely: response spectrum analysis, time history analysis, steady-state response analysis and random response analysis.

Response spectrum analysis provides an estimate of the peak response of a structure to steady-state dynamic motion of its fixed points: ie. base motion. All points constrained by boundary conditions are assumed to move in phase in any one of three orthogonal directions (two, in planar models) according to user-specified input spectra. These spectra are defined as functions of frequency for different values of damping. The peak responses are first computed independently for each direction of excitation for each natural mode of vibration of the system, which are then combined to create an estimate of the actual peak response of any variable chosen for output, as a function of frequency and damping.

Time history analysis gives the response of a model as a function of time, based on a specified time-dependent loading. The response is obtained from a procedure in which the model amplitudes are integrated through time and synthesised. So long as the system under analysis is correctly represented by the vibration modes being used (which are generally only a small subset of the total modes of the finite element model), and the forcing functions vary piecewise-linearly through time (achievable by means of a small enough timestep), the method can be very accurate.

Steady-state response analysis provides the response of the system when it is excited by harmonic loading at a given frequency. Usually such analysis is done as a frequency sweep, by applying the loading at a series of different frequencies and recording the response. The input for the procedure allows for such sweeping, also enabling sampling points on the frequency scale to be spaced closer together at the natural frequencies of the system, thus allowing detailed definition of the response close to resonance.

Random response analysis predicts the response of a system which is subjected to a nondeterministic continuous excitation that is expressed in a statistical manner using a power spectral density function. In the most general case this type of excitation is defined as a frequency dependent power spectral density matrix, giving the correlation between the loadings at the various degrees of freedom to which the excitation is applied. It is assumed by ABAQUS that the frequency dependence and the spatial dependence of the loading can be separated.

The random response of the model is expressed as power spectral density values of nodal and element variables, as well as their root mean square values.

When **nonlinear dynamic response** is being studied, in which large geometrical deflections and material plasticity must be accounted for in the analysis, direct integration of the system must be used. All of the equations of motion of the system must be integrated through time, and because of this, direct integration methods are generally significantly more expensive than the modal methods that are usually chosen for linear studies (see above). Within the general category of nonlinear dynamic analysis ABAQUS provides three methods, referred to as: direct method, subspace projection method and explicit method.

The "standard" **direct method** is an implicit one, meaning that the nonlinear dynamic equilibrium equations must be solved at each increment of time. This is done iteratively, using either Newton's method or the quasi-Newton method. This equation solving process is expensive, but because nonlinearities are usually more simply accounted for in dynamic situations (because the inertia terms provide mathematical stability to the system) the method is successful in all but a few cases of extreme nonlinearity. The principal advantage of this method lies in the fact that variable-length time increments may be used during the course of an analysis, enabling in some cases of sudden events, a long time record to be analysed.

In the case of the **subspace projection method** the eigenmodes of the linearised system are used as a small set of global basis vectors. For some cases this method can be very effective, and is often significantly less expensive than the direct integration of all the equations of motion of the model. Within ABAQUS the method is implemented using a central difference operator to integrate the equations of motion projected onto the eigenmodes of the linear system. A fixed time increment is used throughout an analysis which is the smaller of a user-specified value or one derived from the highest frequency of the eigenmodes that are used as the basis of the solution. The effectiveness of the method depends on the value of the eigenvectors of the linear system as a set of global interpolation functions for the problem. This relies on judgement on the part of the user analogous to deciding the sufficiency of a particular mesh of finite elements. The method is, however, valuable for mildly nonlinear systems.

The **explicit method** uses a central difference scheme but is subject to a maximum time increment that can be taken without the method generating large, rapidly growing errors. This is closely related to the time required for a stress wave to cross the smallest element dimension in the model; thus the time increment may be very short if the finite element mesh contains small elements, or if the stress wave propagation velocity in the material is high (for steel this is 5000 m/s). The method is only computationally attractive for problems where the total dynamic response time that must be modelled is only a few orders of magnitude longer than this maximum time-step limit. There are also limitations in the implementation of the method

with respect to the types of elements that may be used.

Broadly speaking the use of a tool like ABAQUS requires a definition of the loading. This could be done by means of, for example, the Exxon loading model (see 2.4.3, below) or exploiting the potential to couple the program to computational fluid dynamics (CFD) software.

E.1.4 LITERATURE REVIEW

E.1.4.1 Preamble

As stated earlier, the purpose of this subsection of the report is to perform a comprehensive review of literature relevant to the dynamic response of pipeline spans, with a view to identifying key information relevant to analysis methods, and assessment methodologies in general. The approach taken has been to appraise information that usefully contributes both in terms of direct application, (ie. specific formulations that may be used), and in a phenomenological sense, ie. that provide behavioural understanding as a precursor to model development.

In assessing the information it is useful to have an overall appreciation of the important issues that bear on the problem, and the way that they interact. This appreciation may be gained from Figure E.1.12, which represents some of the major issues that require consideration in the dynamic response of pipeline spans. Owing to the enormous complexity that the problem presents, the great majority of the work that has been carried out by researchers has been experimental, with a comparatively small amount that could be described as theoretical. For this reason it is the experimental work that has dictated the choice of upper-level issue categories indicated on the figure, namely:

- flow conditions

- cylinder type

- degrees of kinematic freedom

- seabed effects.

Other, more arcane effects stemming from detailed fluid dynamics considerations, for example: Reynolds number, surface roughness, turbulence and so forth, have been dealt with in Subsections E.1.2 and E.1.3.

Thus a piece of information from the literature which may relate to a particular experiment or practical physical situation, would be a combination of flow conditions, cylinder type, degrees of kinematic freedom and seabed effects. Each of these categories has been further divided into a number of sub-categories, so that the physical situation can be classified more finely.

For the further subdivision, flow conditions may be: steady current, regular wave (planar oscillatory), irregular wave or steady current plus wave (regular or irregular). The cylinder type may be rigid (it is common practice in experimentation to test short lengths of bar or pipeline) or flexible (actual pipelines or appreciable lengths of bar). The degrees of kinematic freedom may be limited by a particular experimental set-up; rigid cylinders may be fixed, elastically-supported in either the in-line or cross-flow directions, or in both (0, 1 and 2 degrees-of-freedom, respectively); flexible cylinders possess up to an infinite number of kinematic degrees-of-freedom. Finally, seabed effects may be categorised according to whether: the seabed is remote enough for the cylinder to be considered as being in a free stream; or the seabed is in close proximity and can be considered as a plane rigid boundary; or the seabed geometry results from a close-proximity scour trench.

There are 120 combinations of these categories possible and the body of literature has not yet covered all of these. The remaining part of this subsection deals with, on the whole, the principal combinations for which information does exist and covers fluid loading aspects; reduced velocity aspects and general fatigue calculations for pipeline spans.

E.1.4.2 Fluid Loading

E.1.4.2.1 Steady current in free stream

In steady flow (as indicated in Subsection E.1.2, above) the forces on a rigid fixed cylinder may be approximated as (see, for example, Faltinsen, 1990):

$$F_x = \frac{1}{2} \rho D V_c^2 \left\{ C_{DM} + C_{DD} \sin \left(4\pi \frac{S_c}{D} V_c t + \phi \right) \right\}$$

$$F_y = \frac{1}{2} \rho D V_c^2 C_{LD} \sin \left(2\pi \frac{S_c}{D} V_c t + \psi \right)$$

where F_x = in-line force per unit length

F_y = cross-flow force per unit length

- D = density of seawater
- D = outside diameter of pipeline
- V_c = steady current velocity
- C_{DM} = steady (mean) drag coefficient
- C_{DO} = oscillatory drag coefficient
- S_c = Strouhal number for steady current
- N,R = phase angles
- C_{LO} = oscillatory lift coefficient

E.1.4.2.2 Planar oscillatory flow

Bearman et al (1984) and **Verley (1982)** and others have found that for a rigid cylinder in a planar oscillatory flow given by:

$$V_x = V_w \cos T_w t$$

the cross-flow force can be reasonably well described by extending the ideas developed in steady flow to:

$$F_y = \frac{1}{2} \rho D C_L \cdot \sin \left(\int_0^t 2\pi \frac{S_w}{D} |V_x| dt + \phi \right) \cdot V_x^2$$

- where V_x = instantaneous flow velocity
- V_w = peak wave velocity
- T_w = wave circular frequency
- t = time
- F_y = cross-flow force
- D = density of seawater

D = outside diameter of pipe

C_L = lift coefficient

S_w = Strouhal number for wave

N = constant phase angle

This model predicts the lift force magnitude to modulate with the dynamic pressure ($\frac{1}{2} \rho V_x^2$) and the frequency of vortex shedding to modulate through the wave cycle with one vortex being shed each time the free stream displaces $D/(2S_w) \cdot 2.5D$ past the cylinder (Bartrop and Adams, 1991). Generally the value of C_L and N are chosen to optimise the fit of the model to experimental results.

Bearman and Obasaju (1989) have also applied this same model to the analogous problem of estimating the cross-flow forces on a circular cylinder oscillating in an in-line direction in a steady current. In this the instantaneous flow velocity in the above equation is replaced by the relative velocity between the steady flow and the vibrating cylinder. The theory can then very accurately predict experimentally measured response providing, as above, C_L and N are adjusted to match the predicted and measured forces at a peak or a trough.

E.1.4.2.3 Combined steady current plus wave-induced flow

Pantazopoulos et al (1993) have been referred to above in terms of the frequency-domain analytical technique the paper advocates (see Section E.1.3.3.1). However, as stated before, the paper is probably more notable for its representation of loading. Expressions were given for loading in both in-line and cross-flow directions. The in-line force model was the familiar Morison equation based on relative velocity. The cross-flow force model was similar to those proposed by Verley (1982) and Bearman et al (1984) for planar oscillatory flow, but differed from these insofar as steady and oscillatory flow were combined.

The starting point for either type of force was expressing the instantaneous flow velocity as:

$$V_x = V_c + V_w \sin T_w t$$

where V_x = instantaneous flow velocity

V_c = steady current velocity

V_w = peak wave velocity

T_w = wave circular frequency

t = time

The in-line force, as a function of time, was taken as:

$$F_x(t) = F_{DX} + F_{IX}$$

where F_x = in-line force per unit length

F_{DX} = hydrodynamic drag force per unit length

F_{IX} = hydrodynamic inertia force per unit length.

Allowing for relative velocity effects between the moving flow and pipeline, the drag force was given by:

$$F_{DX} = \frac{1}{2} \rho D C_D \{ (V_x - \dot{x})^2 + (\dot{y})^2 \}^{1/2} (V_x - \dot{x})$$

where D = density of seawater

D = outside diameter of pipeline

C_D = drag coefficient (non-transient)

\dot{x} = velocity of the vibrating pipeline in the in-line (x) direction

\dot{y} = velocity of the vibrating pipeline in the cross-flow (y) direction

Assuming that the instantaneous flow velocity is much greater than the pipeline velocities, then the drag force was linearised to give:

$$F_{DX} = \frac{1}{2} D D C_D * V_x * (V_x - 2\dot{x})$$

The inertia force per unit length, with allowance for relative velocity effects, was given by:

$$F_{IX} = D A_p \{ V_x + C_A (V_x - \dot{x}) \}$$

- where A_p = net cross-section area of the pipe
- V_x = instantaneous flow acceleration
- \ddot{x} = acceleration of vibrating pipe
- C_A = added mass coefficient (non-transient).

It is seen that the two components of the force equation contain coupling terms involving the pipe motion (\dot{x} and \ddot{x}). The paper implies that these terms can be subsumed into the equations of motion of the pipe as hydrodynamic damping and added mass effects. This leaves the transient force equation as follows:

$$F_x = \frac{1}{2} DDC_D \dot{V}_x^* / V_x + DA_p(1 + C_A) \ddot{V}_x$$

This is, in fact, the standard Morison equation using only the instantaneous flow velocity and acceleration.

Similar arguments were applied to the cross-flow force, the equation for which appears as:

$$F_y = \frac{1}{2} DDC_L(t) \dot{V}_x^* (V_x - \dot{x})$$

There are two key features of this equation that require further discussion: firstly, the presence of the in-line pipe velocity in the definition of the cross-flow force; and, secondly, the time-dependent lift coefficient $C_L(t)$.

The presence of the in-line pipe velocity in the equation for the cross-flow force builds into the analysis two complicating factors. Firstly, that motions of the pipeline in the in-line and cross-flow directions are coupled; ie. in-line velocities affect cross-flow force and, consequently, cross-flow motions. Secondly, the in-line velocity term is spatially as well as temporally dependent; this would mean that unlike the in-line force given above, which is a function of time alone and can therefore be regarded as a time dependent uniformly distributed load, the cross-flow force per unit length varies not only with time but also along the length of the pipeline. However, providing that the equations of motion of the pipe are uncoupled, in principle, the in-line equations could be solved for \dot{x} which could be inserted into the F_y expression prior to solution of the cross-flow equation of motion.

The time-dependent lift coefficient was given by:

$$C_L(t) = C_{LM} + C_{LO} \sin T_s t$$

where C_{LM} = mean lift coefficient

C_{LO} = oscillatory lift coefficient

T_s = vortex shedding circular frequency.

The vortex shedding frequency was assumed to be defined as:

$$\omega_z = 2\pi S_c \frac{V_c}{D} \pm \alpha S_w \omega_w K_c$$

where S_c = Strouhal number for current

S_w = Strouhal number for wave

K_c = Keulegan-Carpenter number for the wave.

The positive sign is used when $V_w \sin T_w t$ is positive and vice-versa, and " α " assumes the following values:

" α " = 1 when $V_c < V_w$ (flow reversal)

" α " = 2/B when $V_c \geq V_w$ (no flow reversal)

The two different Strouhal numbers recognise the fact that vortex shedding for waves and currents have inherent differences. The " α " parameter defines the wave contribution to the vortex shedding frequency and approximates the continuous variation of velocity during a complete wave cycle. The sign differences indicate that two different vortex shedding frequencies govern, one in each wave half cycle, during a complete wave cycle.

Noting the definition of Keulegan-Carpenter number given in Subsection 2.2.4.1, the expression for vortex shedding frequency becomes:

$$\omega_z = \frac{2\pi}{D} (S_c V_c \pm \alpha S_w V_w)$$

E.1.4.3 Reduced Velocity Techniques

E.1.4.3.1 Steady current and planar oscillatory flow in free stream

Sumer and Fredsøe (1987) conducted experiments on a rigid, spring-mounted cylinder,

principally in oscillating flow, but also with a limited number in steady flow. The spring support arrangements were such that the cylinder possessed a degree of kinematic freedom only in the cross-flow direction. The effects on frequency response and vibration amplitude of Keulegan-Carpenter number, K_c (peak flow velocity as a proportion of cylinder diameter times wave frequency) and reduced velocity, V_r (peak flow velocity as a proportion of cylinder diameter times cylinder natural frequency) were investigated. In addition to this, the roles played by support spring stiffness and cylinder specific gravity were also examined briefly.

Results, in the form of graphs of various response frequency ratios, vibration amplitude ratios and RMS cylinder displacement ratios, versus reduced velocity at fixed values of K_c were presented. However, it should be noted that by fixing K_c in this way and varying V_r meant for each V_r taken, a different wave frequency had to be imposed to maintain constant K_c . Thus, in the graphs presented, the V_r axis represented not only varying peak flow velocity but concomitant wave frequency variation.

For K_c equal to 10 it was found that the frequency response of the cylinder modulated with the wave frequency by exhibiting two vibrations per wave cycle across a range of reduced velocities between two and ten. The response amplitude and RMS displacement each attained a single sharp peak.

For an intermediate range of K_c numbers the frequency response of the cylinder depended on the reduced velocity. At low V_r the number of response vibrations per wave cycle tended to be around five times the K_c number (ie. the Strouhal frequency) and as the V_r number increased, the number of response vibrations stepped down until two was reached, whereupon this value was maintained for further increases in reduced velocity. Within the ranges of reduced velocity for which constant ratios of response frequency to wave frequency were found, individual peaks of response amplitude and RMS displacement occurred. This gave a multi-peaked appearance to the graphs of response amplitude versus reduced velocity over a range of reduced velocity, which varied with K_c number. This was followed by a very much less sharp increase in response amplitude with reduced velocity increased outside of this range. The height of the peaks seemed to be allied closely to the opportunity for the response frequency to resonate with the natural frequency.

For high K_c numbers these trends were repeated, but individual peaks in the response amplitude curves become less distinctive, looking more like smooth curves. The propensity for the response frequency to modulate at twice the wave frequency was always evident at high reduced velocities, however, along with the maximum amplitudes of vibration tending to coincide with resonance. The trend for high K_c numbers (eg. $K_c = 100$) was for the frequency response to be very similar to that for steady current, ie. initial response at the Strouhal frequency followed by lock-on to the natural frequency for an intermediate range of reduced velocity. The

amplitude response was characterised by a sharp rise to a peak approximately at lock-on, but the decay from the peak for increasing reduced velocity was much less steep in the case of high K_c number when compared with the steady flow case.

Interesting results were also obtained for $K_c = 5$. The response frequency was found to be always equal to the wave frequency, indicating that the vibrations were caused by lift force variations. Moreover, self-excited vibrations with large amplitudes tended to occur at much higher values of reduced velocity than was the case for the higher K_c numbers. These vibrations could be initiated at reduced velocities similar in value to those corresponding to the high K_c cases if a sufficiently large external disturbance was applied to the cylinder.

Regarding the effects of spring stiffness it was found that the two set-ups where the stiffness of one was three times the other differed very little in terms of frequency response and maximum amplitude of vibration. It appeared that lock-in occurred at systematically lower reduced velocities in the case of the system with the stiffer spring than the softer spring; this was attributed to the lighter damping in the stiff spring case.

It was also noted that the results obtained in the study reported in this paper were very similar to corresponding ones in which a plane boundary was in proximity at a gap ratio of unity. The authors concluded from this that no substantial change occurs in the response characteristics of the cylinder when the gap ratio is increased from unity to infinity.

E.1.4.3.2 Steady current and plane boundary

Tsahalis and Jones (1981) have performed experiments on a flexible pipe in proximity to a plane wall under steady flow conditions and investigated the effects of gap ratio on response frequency and amplitude of vibration. The gap ratios studied were 50 (to represent free-stream conditions), 6, 4, 3, 2 and 1. The end support conditions were simply-supported with respect to rotation, and full axial restraint, thus allowing some degree of membrane tension to develop in cases of large vibration amplitudes.

In the case of the gap ratio of 50 the pipeline exhibited a frequency jump phenomenon. As the flow velocity was increased, first perceptible vibrations occurred with the response frequency close to the Strouhal frequency; with further increases in flow velocity both the amplitude of vibration and the response frequency increased (but the latter remained smaller than the corresponding Strouhal frequency). This situation continued until at a particular reduced velocity the amplitude of vibration peaked, and a further increase in flow velocity resulted in a sudden reduction in vibration amplitude, accompanied by a sudden increase in response frequency. Further increase in flow velocity resulted in relatively constant amplitudes and frequency responses. The authors suggest that this jump phenomenon is attributable to the nonlinearities introduced into the bending rigidity of the pipe by the membrane tension, rendering the system

similar in behaviour to a stiffening Duffing oscillator. This particular point highlighted the potential problems of hydro-elastic dissimilarity in applying results from rigid, spring-mounted cylinders to flexible pipelines.

The authors also highlight the dependence of response in terms of frequency and amplitude of vibration on specific gravity of the pipe. As the specific gravity is lowered, critical reduced velocity (the conditions of flow under which maximum vibration amplitude occurs) tends to increase. Lower specific gravity would occur for a pipe in water as opposed to the same pipe in air. The authors argue for a less limited definition of lock-in; rather than being defined as response and vortex shedding frequencies coalescing into a single value close to the natural frequency, the definition should be that the vibrating body "takes control" of the vortex shedding in apparent violation of the Strouhal relationship.

A number of observations on the response of the pipe in the presence of a plane boundary as compared to that of the isolated (no boundary proximity) pipe, were made as follows:

- the increase of response frequency with flow velocity is less steep
- first perceptible vibrations take place at a higher reduced velocity
- the increase of vibration amplitude with flow velocity is less steep
- the maximum amplitude is attained at a higher reduced velocity
- the maximum amplitude is reduced
- once the maximum amplitude is attained it remains constant for higher flow velocities.

A direct consequence of this last point is that curves of vibration amplitude versus reduced velocity tended to appear S-shaped rather than bell-shaped as for the isolated pipe.

All of these trends were exhibited by gap ratios decreasing from 6 to 2, as compared with 50, but for a value of 1 they were reversed with the exception of the reduction of the maximum amplitude. This appeared to be very nearly halved compared with the isolated case.

Fredsøe et al (1985) have conducted experiments on rigid, spring-supported cylinders exposed to a steady current and possessing one degree of kinematic freedom by virtue of a system of spring supports in the cross-flow direction. Two spring stiffnesses were used: designated as "soft" and "hard", and three sets of experiments performed comprising the two spring types and a cylinder specific gravity of one, and the soft spring combined with a cylinder specific gravity

of 1.89. Gap ratios in the range zero to 1.7 were investigated.

Overall, the paper suggests that the vibrations are partly induced by vortex shedding and partly self-excitation (particularly in the case of very small gap ratios). In the latter case the vibrations are caused by rapidly changing displacements which, because of the inability of the downstream wake to adjust rapidly enough to accommodate the necessary changes in fluid discharge through the gap, lead to upward pressures on the cylinder when it is moving away from the boundary. These types of vibration, however, may not occur spontaneously over a range of flow velocities; in the experiments, perturbations in the form of an applied and then released displacement, were necessary to instigate them.

Principal observations made from the experiments were as follows:

- the response frequencies were generally higher than the corresponding Strouhal frequency except for reduced velocities less than 3 and greater than 8
- the response frequency increased with decreasing gap ratio
- there were no significant differences between results for the soft and hard spring cases, except that there was a small tendency to larger frequencies in the stiff spring case
- the cylinder specific gravity has some influence on the response frequency: at large reduced velocities, the frequency decreases with increasing specific gravity; the effect is more pronounced for small gap ratios
- the maximum amplitude of vibration occurred at larger values of reduced velocity as the gap ratio was reduced
- the maximum amplitude of vibration increased as the gap ratio was reduced
- as the gap ratio was reduced from 1.7 down to 0.14 the curve of amplitude of vibration versus reduced velocity tended to change from S-shaped to bell-shaped (similar to what might be expected for an isolated pipe).

Large amplitude vibrations were only stimulated in the case of small gap ratios by artificially introduced perturbations, as mentioned earlier. In general the size of perturbation (in the form of initial displacement to diameter ratio) necessary to obtain vibrations depended upon gap ratio and reduced velocity; for a given gap ratio the perturbation reduced linearly with increasing reduced velocity, with a slope that reduced with reducing gap ratio. These relationships were

such that threshold reduced velocities were determined at which no perturbations were required to induce the self-excited vibrations. The threshold reduced velocities increased as the gap ratio decreased and, for a fixed gap ratio were greater for the soft configuration than for the stiff one.

The differing vibration mechanisms in the case of a rigid cylinder in steady flow and in close proximity to a plane boundary have also been investigated experimentally by **Tørum and Anand (1985)**. The cylinder in their case was fixed in the in-line direction and the main purpose of the work reported in the paper was to investigate the effect of turbulence intensity on the mean drag force and vibration amplitudes. Two sets of experiments were reported, referred to as Case 1 and Case 2, involving gap ratios of 0.5, 0.75, 1.0 and 3.0 for a turbulence intensity of 3%, and a fixed gap ratio of 0.5 with turbulence intensities of 3.4, 5.5 and 9.5%. Turbulence intensity in this case was defined as the ratio of the RMS velocity to the mean velocity. The experimental set-up had an arrangement involving a dummy pipe (which moved above the free stream, in air, in sympathy with the submerged cylinder) and a sand box which acted as an "impact preventer" that restricted the gap to greater than about 10% of the cylinder diameter, thereby limiting the motion of the cylinder.

For the Case 1 results, it was shown that the maximum value of mean drag coefficient was not much affected by gap ratio; the magnitude of reduced velocity at which the maximum occurred seemed to shift to a higher value as the gap ratio reduced. Whilst reduction in gap ratio appeared to reduce maximum amplitude of vibration, the responses for gap ratios of 0.75 and 0.5 were found to be amplified in the upward direction and asymmetric; the authors attributed this to the possible existence of steady lift due to flow constriction in the gap plus possible vortex shedding (see the account of Fredsøe et al (1985), earlier). In addition to this the occurrence of the maximum amplitude of vibration shifts to a higher reduced velocity as the gap ratio decreases from 1.0 to 0.5.

For the Case 2 results, it was found that:

- the maximum amplitudes of vibration did not seem to be much affected by turbulence intensity
- the occurrence of the maximum amplitude of vibration and subsequent amplitudes of vibration at other levels shifted to a lower reduced velocity at the turbulence intensity of 9.5 compared with the lower values
- bottom proximity affects the lock-in range of the vibrating cylinder such that the vortex shedding frequency did not lock-on to the natural frequency, but continued to increase and control the cylinder motion; vibrations took place at the vortex shedding frequency up to the maximum amplitude of vibration and differed only after the

cessation of large amplitude vibrations.

E.1.4.3.3 Planar oscillatory flow and plane boundary

Sumer et al (1986) carried out experiments on a rigid, spring-mounted cylinder that was restricted to cross-flow vibrations only. The flow conditions were principally wave-induced currents, with Keulegan-Carpenter numbers in the range 10 to 100, but steady current results were presented to allow comparison. A plane wall was also present in the experiments, with gap ratios taken of 1.0, 0.4 and 0.15. The flow conditions were achieved by means of carriage action in a water-filled flume. In the support arrangements for the cross-flow direction, two types of springs were used: referred to as "soft" and "stiff". Some additional experiments were executed on the soft spring set-up but with a different cylinder mass, this allowed the effects of changing specific gravity to be investigated. Except in the cases of steady current, the reduced velocity was defined in terms of the maximum velocity (amplitude) of the wave motion, the cylinder diameter and its natural frequency; the Keulegan-Carpenter number was defined similarly but using the wave frequency. In the experiments, the reduced velocity was changed by altering the peak velocity; in order to keep the K_c number constant for variable reduced velocity it was necessary, therefore, to change the wave frequency for each value of reduced velocity.

In the case of a gap ratio of unity the following observations were made:

- For $K_c = 10$, the response frequency was twice the wave frequency (ie. the cylinder underwent two oscillations per wave cycle) for reduced velocities in the range zero to 10, following the Strouhal frequency. The amplitude versus reduced velocity curve exhibited a sharp spike, maximising at around response and natural frequency equality.
- For $K_c = 20$ and 40, the response frequencies were initially four and seven times the corresponding wave frequencies, ie. corresponding fairly well with the Strouhal frequency; however, with increasing reduced velocity the response frequencies "jumped down" exhibiting ratios of 3 and 5 respectively; during these jumps, the response frequencies reduced to being approximately equal to the cylinder natural frequency. The amplitude versus reduced velocity curves exhibited two sharp spikes, and the large amplitude regime extended over larger ranges of reduced velocity than was the case at the lower value of K_c .
- For $K_c > 60$ (specifically = 100) the response frequency was initially 20 times the wave frequency and corresponded with the Strouhal frequency; with increasing reduced velocity, rather than the stepwise change in response frequency exhibited by the lower Keulegan-Carpenter numbers, there was a gradual reduction in response

frequency to 10 times the wave frequency. The response frequency during this gradual change, was maintained roughly at the cylinder natural frequency. The amplitude versus reduced velocity curve rose very rapidly after onset of vibrations, before maximising when the response frequency equalled the cylinder natural frequency; thereafter, the amplitude remained at the maximum value over the full range of reduced velocity tested.

- For the steady current case the response frequencies followed the Strouhal frequency before a lock-on condition was attained for a short range of reduced velocity; thereafter, response frequency corresponded to values less than the Strouhal frequency. The amplitude versus reduced velocity curve rose very steeply in the range of reduced velocity leading up to lock-in, peaked during lock-in, before reducing more gradually for further increases in reduced velocity
- the response frequencies were found to correspond very closely with the vortex-shedding frequencies of fixed rigid cylinders in a free stream (ie. a cylinder held stationary with no boundary in proximity)
- in comparing the soft and stiff spring results it was found that there was little difference between the response frequencies for the two cases; however, the vibration amplitudes for the stiff spring cases tended to be generally larger and this was ascribed to the lighter damping in that case
- the maximum amplitude for $K_c = 10$ was very close to that pertaining to the current case and, generally, the effect of increasing K_c was to reduce the maximum amplitude (by a factor of two for a change in K_c from 10 to 100)
- the initiation of vibration of the cylinder under wave-induced current generally occurred at smaller reduced velocities than for steady current; this was attributed to the fact that the reversal of wake may create flow velocities larger than the free stream velocity.

In the case of gap ratios of 0.15 and 0.4, the following observations were made:

- for small values of reduced velocity, and for all of the Keulegan-Carpenter numbers tested, the mean gap ratio was maintained at the equilibrium value in still water, ie. there was no overall lift of the cylinder
- as the reduced velocity was increased, however, the mean gap ratio increased, indicating that (on average) the cylinder was repelled away from the boundary; also,

the smaller the K_c number, the larger the mean gap ratio; thus, the overall lift force on the cylinder increased with increasing reduced velocity, but decreased with increasing Keulegan-Carpenter number.

The following conclusions were drawn from the experiments involving the gap ratios of 0.15 and 0.4 concerning the frequency response and vibration amplitude of the cylinder:

- the response frequencies generally did not follow the vortex shedding frequencies
- the vibration amplitudes increased significantly as the gap ratio decreased (the converse of this occurred for the steady current case, the maximum amplitudes were very similar in value for gap ratios of 0.15 and 0.4)
- the curves of amplitude of vibration versus reduced velocity in the cases of the gap ratios less than one were "S"-shaped rather than "peaked" as was the case for a gap ratio of unity
- the vibration amplitudes were significantly reduced at times when the wave velocity passed through its zero crossing points
- the mechanism of vibration differed depending on gap ratio; for the gap ratio of 0.15 the cylinder experiences a lift force mechanism that stems from wall proximity effects
- incipient vibration appeared to occur at values of reduced velocity that were smaller in the case of waves than in the case of currents for small values of Keulegan-Carpenter numbers only (10, 20); this earlier initiation was attributed to the larger lift forces present for the smaller K_c numbers.

As mentioned above, a number of tests were carried out to investigate the effects increased cylinder specific gravity (increased mass) had on the response characteristics. It has to be borne in mind that an increase in mass will also increase the reduced damping or stability parameter. The specific gravity was, in fact, changed from 1.0 to 1.72 and experiments undertaken for steady current and wave-induced flow with a K_c number of 40. The following observations were made:

- In the case of steady current, it was found that the increase in specific gravity:
 - reduced the maximum amplitude of vibration significantly, and increased the reduced velocity at which large amplitude vibrations were induced in the case of a gap ratio of unity

- had negligible effects on the vibration amplitude versus reduced velocity curve in the case of a gap ratio of 0.4.
- changed the amplitude versus reduced velocity curve from S-shaped to continuously rising with increasing reduced velocity in the case of a gap ratio of 0.15 (this meant that the magnitudes of the vibration amplitudes were not limited)
- In the case of wave-induced flow with a Keulegan-Carpenter number of 40, it was found that the increase in specific gravity
 - reduced the maximum amplitude of vibration most significantly for a gap ratio of unity; smaller reductions were evident at the smaller gap ratios
 - the onset value of reduced velocity was increased most significantly for a gap ratio of unity; the increases became progressively smaller as the gap ratio decreased.

Although no direct investigation of vortex shedding was made, the indications from the work were that vibration of the cylinder was by vortex shedding in the cases of a gap ratio of unity. For the gap ratio of 0.15, wall proximity/lift force effects were the main mechanism of vibration of the cylinder. For the intermediate gap ratio of 0.4, a combination of these two influences was responsible for the vibration.

E.1.4.3.4 Steady current, planar oscillatory flow and plane boundary

Tsahalis (1984) investigated the vortex-induced vibrations of a flexible cylinder near a plane boundary exposed to steady current and wave flow. The cylinder had a length:diameter ratio of 113:1; it was simply-supported with respect to bending moment in both the in-line and cross-flow directions, but fixed in the axial direction. Despite this the pipe natural frequencies were the same in the in-line and cross-flow directions, indicating negligible membrane tension due to sag. The response of the model to vortex-induced vibrations was determined for a wide range of values of gap ratio and Keulegan-Carpenter number. In the paper, however, results only for gap ratios of infinity and unity in combination with K_c numbers of 0 (steady current) and 20 were presented. In all tests the wave frequency was kept constant and the K_c variation was achieved by varying the wave height.

In the case of steady flow and an infinite gap ratio it was found that the first perceptible cross-flow vibrations took place at a reduced velocity of 3 with a response frequency close to the Strouhal frequency, and a maximum amplitude occurred at a reduced velocity of about 7 with a frequency of about 0.92 of the natural frequency. In-line response was the same in character, but with the exceptions that the frequency was twice that of the cross-flow vibration and the

amplitude was one-quarter of the cross-flow amplitude. These results were much as expected, and indicated that, in displacement terms, the pipe underwent a figure-of-eight type motion.

For the situation of a gap ratio of unity, and under steady flow conditions, the response in the cross-flow direction was similar to that for the corresponding case of a flexibly-mounted rigid cylinder (Tsahalis and Jones, 1981). The proximity of the plane boundary had the following effects on the cross-flow response compared with the isolated pipe:

- the maximum single amplitude was reduced by a factor of two and persisted over a wider range of reduced velocity
- the first perceptible vibrations took place at a higher reduced velocity.

In the case of the in-line direction the response was similarly affected, however, the response frequencies were found to be equal to those in the cross-flow direction. This suggests that, while the vibrations are induced by vortex shedding, the wake and interaction between the wake and the vibrating pipe are influenced by the presence of the plane boundary and it appeared that the pipe underwent oval-shaped (rather than figure-of-eight) motion.

In the case of combined steady and wave-induced flow on the pipe with an infinite gap ratio it was found that the major effect of superimposed flow was to give rise to vortex-induced vibration over the whole range of reduced velocity. Specifically in the cross-flow direction it was found that in comparison with the steady flow case:

- the single amplitude was larger for reduced velocity less than 6
- the maximum single amplitude was reduced in value, but still occurred at a reduced velocity of 7
- the single amplitude was smaller for reduced velocities greater than 7
- the dominant response frequencies were the same as in the steady flow case, except for reduced velocity greater than nine, where they become larger.

In the in-line direction, it was found that:

- the single amplitude was larger for all reduced velocities
- the maximum single amplitude was increased by 50% and it persisted over a wider range of reduced velocity

- the dominant response frequencies change dramatically and follow closely the dominant response frequencies in the cross-flow direction, except for reduced velocity greater than 8 where they become larger.

It was also found that in addition to the dominant frequency of vibration in the in-line and cross-flow directions, additional neighbouring frequencies (with energy contents of at least 10% of the dominant) were present, indicating that the pipe did not undergo pure harmonic vibrations.

For the final situation of the pipe exposed to combined steady and wave-induced flow and a gap ratio of unity it was found that the flow regime, in combination with the boundary proximity, had a tremendous effect of the vortex induced vibration of the pipe. The flow regime was such that for reduced velocities in excess of 2.3 the flow did not reverse; ie. the current velocity always exceeded the amplitude of the wave velocity.

In comparison with the steady flow free-stream conditions (no boundary proximity) it was found that in the cross-flow direction:

- the maximum of the single amplitude was reduced by a factor of about three
- the maximum persisted over almost the whole range of reduced velocity tested (this had the effect of "flattening" the amplitude versus reduced velocity graph, making it less "peaky")
- the dominant response frequencies were larger, but their trend remained unchanged.

In the in-line direction, it was found that:

- the maximum of the single amplitude was reduced by a factor of around two
- the maximum persisted over almost the whole range of reduced velocity tested
- the dominant response frequencies followed the trend of their counterparts in the cross-flow direction.

The frequency content of the responses in both the in-line and cross-flow directions indicated that the pipe did not undergo pure harmonic vibrations.

Tsahalis (1985) also reported an extension to the series of tests summarised above, in which steady currents were superimposed with wave-induced currents corresponding to Keulegan-Carpenter numbers of 0, 5, 10, 15, 20, 25 and 30, along with proximities to a boundary with gap

ratios of 1, 2, 4, 6 and 4. The test conditions were as described above.

In the case of steady current and regular waves where the gap ratio was held constant and Keulegan-Carpenter number was varied, it was found that:

- in the cross-flow direction
 - the maximum amplitude of vibration generally decreased with increasing K_c
 - the first perceptible vibrations took place at smaller reduced velocities as K_c increased
 - vibration frequencies remained basically unchanged

- in the in-line direction
 - the maximum amplitude of vibration generally increased with increasing K_c
 - the first perceptible vibrations took place at smaller reduced velocities for increasing K_c
 - frequencies of vibration remained basically unchanged.

For the situation of steady current and regular waves in which the Keulegan-Carpenter number was held constant and the gap ratio was varied, it was found that for both cross-flow and in-line directions

- the maximum amplitude of vibration decreased slightly with decreasing gap ratios in the range 2 to 4; however, it decreased dramatically for a further reduction in gap ratio to unity.

- The frequencies of vibration remained basically unchanged.

Jacobsen et al (1984) carried out tests on an elastically-supported cylinder in proximity to a plane rigid boundary in flows stemming from steady current, waves and waves superimposed on steady current. Some results from an irregular wave train are also reported. The cylinder appeared to be allowed degrees of freedom in the in-line and cross-flow direction, although in the paper, only the results of the analysis of the displacements (in terms of maxima and RMS values) in the cross-flow direction are included. Gap ratios of zero (cylinder just touching the plane boundary in its equilibrium state), 1.0 and 0.5 were tested. In presenting results, the wave conditions were characterised by the Keulegan-Carpenter number and the reduced velocity

based on the maximum oscillatory velocity. The combined wave and current experiments were performed at steady flow velocities of 0.2 m/s and 0.6 m/s, the reduced velocities for these were expressed in terms of the wave parameters. For the waves, Keulegan-Carpenter numbers of 30, 60, 90 and 120 were investigated.

It was found that in comparing the results for steady current with those for waves:

- for a gap ratio of unity, and in steady current, peak maximum oscillations occurred between reduced velocities of 5 and 6 and after passing through a second lower plateau, movements almost ceased for V_r above about 9; in the case of the wave motion, the vibration amplitudes were significantly less than the steady current case in the resonance range, but were larger at the low and high range of reduced velocities; maximum and maximum RMS amplitudes appeared to reduce with increasing K_c numbers
- for a gap ratio of 0.5 unsymmetrical responses occurred, owing to the close proximity of the boundary; instead of the typical "bell"-shaped maximum amplitude versus reduced velocity curve obtained for the steady current, the curve for wave flows was more S-shaped with a peak similar in value to that of the current which was independent of Keulegan-Carpenter number; similar traits were displayed by the corresponding RMS amplitude curves
- for a gap ratio of zero the forcing mechanism changed and was judged to be not related to the regular shedding of vortices; it was found that the response amplitudes almost increased continuously with increasing reduced velocity regardless of Keulegan-Carpenter number; moreover, the amplitudes increase for decreasing K_c numbers for V_r below 5, meaning that the excitation force is larger and stems from a lift away from the boundary.

For steady current superimposed on wave compared with steady current, it was found that:

- for a gap ratio of unity, significant changes in curves of RMS amplitude versus reduced velocity occurred for both current velocity cases; larger amplitudes of vibration were found for the current velocity of 0.2 m/s for almost all reduced velocities; for the 0.6 m/s current velocity radical changes were introduced into the response curves, the maximum values of RMS amplitude disappeared giving more constant values over the range of reduced velocities investigated
- for a gap ratio of 0.5, the response curves for a current velocity of 0.2 m/s were found to be very similar to the steady current ones, regardless of the Keulegan-Carpenter

number; the application of the 0.6 m/s current had a similar effect to the one found for a gap ratio of unity.

Some of the most revealing results, in phenomenological terms, however, stem from the displacement time series given in this paper. In the case of regular waves, it was shown that vibration amplitudes vary within each half-wave period and that the variation depends on reduced velocity: vibrations almost decay to zero for small V_r , whereas for large V_r , vibrations were sustained. Similar patterns were displayed by results from flow conditions of regular wave combined with steady current, and irregular waves. Thus "pulses" of high frequency vibration resulted, that modulated to half periods of velocity variation during which the reduced velocity was of sufficient value to cause resonance. In the case of irregular waves particularly this meant that it was feasible for long periods to elapse without any vibrations, but vibrations could build up and decay during the passage of a large wave.

The distributions of response double amplitudes also showed very interesting features. For the regular wave example given (which corresponded to a Keulegan-Carpenter number of 90) over the range of reduced velocity taken (3.8 to 6.5) there was little difference between the value of the peak amplitudes; the distribution changed quite radically however as reduced velocity was altered from 3.8 to 6.5, from having the major part of the amplitudes concentrated at small values to being concentrated at larger values.

Response to irregular waves is, by definition, a complex phenomenon. The authors suggest in this paper an ingenious way of dealing with irregular waves by first dividing the time series up into a sequence of single oscillations (by means of a zero up-crossing analysis) each described by a period and maximum velocity. These, in turn define a Keulegan-Carpenter number and reduced velocity for that oscillation. The corresponding vibrations are then computed from the regular wave test results assuming that each irregular oscillation contributes to the total vibrations as one regular wave with identical parameters. An example amplitude distribution computed in this way was compared with a measured result, and the correlation was found to be very good, but it tended to underpredict the number of small amplitudes and overpredict the number of large amplitudes. This was because the use of the regular wave did not include the build-up and decay of amplitudes, but used the maximum; this tended to overemphasise the larger amplitudes at the expenses of the smaller ones. Nevertheless this method showed great promise in terms of adaptation to fatigue analysis.

Bryndum et al (1989) carried out a large number of tests in both a flume and a towing tank. Two types of model were tested: a short segment of pipe (essentially a rigid cylinder) that was spring-mounted in such a way to allow displacements in the in-line and cross-flow directions; a long flexible pipe suspended between low-friction hinges which gave simple-support for out-of-straight bending. A flat plate was put in proximity to the models to represent the seabed. In both model types the following flow types were used:

1. Steady current
2. Regular waves
3. Combined steady current and regular waves
4. Irregular waves
5. Combined steady current and irregular waves

and the effects of reduced velocity, Keulegan-Carpenter number and current ratio (ratio of current and maximum wave velocity in the case of combined flow) were investigated.

In the specific case of the rigid pipe tests, a total number of 2550 individual experiments were performed covering the variation of a wide range of parameters: gap ratio, roughness ratio, stability parameter, turbulence intensity, presence of scour or relative scour hole depth. In addition, tests with no (fixed) or one degree-of-freedom, or in transient conditions, or with different specific masses were carried out.

In the specific case of the flexible pipe tests, a total number of 240 individual experiments were carried out covering the effects of: incident angle of flow, pipe length to diameter ratio, effective axial stiffness at the supports, pipe tension and gap ratio.

For the rigid pipe tests under steady current it was found that:

- the gap ratio imposed geometrical limitations on pipe displacements; for small gaps (ratio < 0.4) impact energy absorption occurred and regular vortex shedding did not take place, with pipe motions initiated by fluctuating hydrodynamic lift; for large gaps (ratio > 0.8) vortex shedding occurred with the response resembling that of a cylinder in a free stream
- the effects of increased stability parameter (damping) were to reduce displacements at resonance in the cases of large gap ratio.

For the rigid pipe tests under regular wave conditions it was found that:

- in a reference test with a Keulegan-Carpenter number of 10 and a gap ratio of 0.8, the converse of what normally happens in steady flow occurred in that the in-line vibration amplitudes were potentially much larger than the cross-flow ones; moreover, the in-line amplitude versus reduced velocity curve increased monotonically with increasing

reduced velocity and did not exhibit a maximum

- the response was highly dependent on the Keulegan-Carpenter number; for a small K_c of 5 resonance with the wave frequency was possible at suitable reduced velocities, thus giving the in-line amplitude versus reduced velocity curve a local peak; this effect disappeared with increased K_c number where the response curve reverted to a monotonic form, but the rate of increase with reduced velocity diminished with increasing Keulegan-Carpenter number
- the cross-flow amplitudes were generally much lower than the in-line ones; the cross-flow amplitude versus reduced velocity curves occasionally displayed local peaks which are associated with shifts in the number of cylinder oscillations per wave period
- the effect on the in-line vibrations of reducing the gap ratio was not very significant; in the cross-flow direction, however, amplitudes of vibration increased with reducing gap ratio owing to the lift force effects referred to earlier
- the effects of increased damping were negligible, owing to the relative magnitudes of the damping and resonance forces
- the introduction of combined steady current had little effect on the cross-flow response over a range of current ratios between zero and 2; steady current appeared to reduce the vibration amplitudes compared to the pure wave case with reductions becoming greater as the current ratio increased.

For steady flow tests on the flexible pipe there were found to be some differences between the responses of the flexible pipe and the rigid cylinder. Significant vibrations for the flexible pipe did not occur until larger reduced velocities than those necessary for the rigid cylinder; moreover, relatively high in-line responses were observed in the case of the pipe, that were absent for the cylinder. The authors ascribe these differences to the fact that, for the long flexible pipe, the fundamental frequencies in the in-line and cross-flow directions were different.

In those cases of steady flow it was found that the effect of pipe tension was quite profound. Increased pipe tension tended to increase the amplitudes of vibration very significantly in both the cross-flow and in-line directions.

For the flexible pipe subjected to regular wave flow it was found that the measured response was independent of the wave incident angle within the range zero to 45 degrees.

E.1.4.3.5 Steady current and scour trenches

Sumer, Mao and Fredsøe (1988) conducted an experimental investigation of the effects of the proximity of a scour trench on the vibration characteristics of a rigid cylinder in steady flow. The cylinder was spring-supported in the cross-flow direction and held fixed in the in-line direction. The scour holes used in the experiments were produced with the cylinder held fixed against motion and sitting on an erodible bed comprising a sediment with $d_{50} = 0.36\text{mm}$ and $\sigma(d_{85}/d_{15}) = 1.4$ (d is the particle diameter) and allowing a steady flow to pass for 30 minutes. In conducting a vibration test the cylinder was freed in the cross-flow direction and the test then performed in a typical sequence; the scour profile remained virtually unchanged during this. Three gap ratios (relative to the line of the undisturbed bed) were tested: 0.9, 0 and -0.3. The paper is not clear over the depth of the scour trench, but indications were that it was of the order of 0.6 times the cylinder diameter. Data are given in the paper in terms of frequency and double amplitude.

It was found that:

- the amplitude and frequency responses did not resemble those of a cylinder placed near a plane boundary; instead of S-shaped amplitude response curves (plane boundary), the curve for gap ratios of zero and -0.3 were bell-shaped; response frequencies were lower than in the case of plane boundary experiments
- the response behaviour was found to be quite similar to that observed for boundary-free cylinders where vortex shedding is the only agent responsible for the vibrations; flow visualisation revealed that vortex shedding was present for every gap ratio tested
- the range of reduced velocity within which appreciable vibration amplitudes occurred changed significantly with gap ratio, even though the maximum amplitude experienced remained unchanged
- incipient vibrations started relatively early for larger gaps
- the value of reduced velocity at which the maximum vibrations occurred increased as the gap ratio decreased
- the responses of cylinders with gap ratios of 0.9 and infinity were virtually identical.

E.1.4.3.6 Planar oscillatory flow and scour trenches

In a series of papers **Sumer et al (1988, 1989)** have studied experimentally the vibrational response of rigid, elastically-supported cylinders to wave-induced fluid motion and in proximity to an idealised scour trench. Both regular (sinusoidal) and irregular waves were modelled at

Keulegan-Carpenter numbers of 10 and 40, along with gap to diameter ratios ranging from -0.8 to 2 (where a negative number indicates immersion of the cylinder within the scour trench). Reduced velocities were taken in the range 3-8, with the definition of V_r related to the amplitude of velocity in the regular wave case, and the significant velocity amplitude in the case of irregular waves.

They noted that for cross-flow vibrations in regular waves, and for $K_c = 10$, the frequency of vibration was always maintained at twice the wave frequency across the gap ratio and reduced velocity ranges tested. Moreover, the number of in-line vibrations per wave cycle was one more than the number of cross-flow vibrations, ie. three.

It was found that amplitudes of vibration in the cross-flow direction increase as V_r increased, attaining their peak values when the frequency of vibration and the natural frequency approximately coincide in value. At high negative gap ratios (-0.5, -0.8) amplitudes of vibration tended to become limited by impact of the cylinder with the sidewalls of the scour trench. Two kinds of in-line motion of the cylinder were evident: those modulated with the wave frequency, and superimposed higher frequency motions modulated with the vortex shedding (when it occurred). Peaks of vibration amplitude in the in-line direction tended to be when the frequency of vibration was approximately half the natural frequency.

An alternative pattern of response was exhibited by the cylinder for flow regimes corresponding to $K_c = 40$ in regular waves. The cross-flow response depended upon the gap ratio: for gap ratio positive the cross-flow frequency of vibration was 10-11 times the wave frequency at small values of reduced velocity, with this factor reducing as V_r increased (the vibrations were due to vortex shedding); for gap ratios between zero and -0.5, the vortex shedding was suppressed owing to trench wall proximity and flow blockage, and the cylinder experienced a cross-flow force oscillating at twice the wave frequency (cf. $K_c = 10$), thus the frequency of vibration is twice the wave frequency; with gap ratios between -0.5 and -0.8 the vortex shedding reappeared, and the frequency of vibration followed the same kind of variation as was the case for a positive gap ratio, although peak amplitudes of vibration were somewhat smaller. Overall in-line vibration amplitudes tended to be distinctly smaller for $K_c = 40$ than for $K_c = 10$.

In general terms it was found that for regular waves, and comparing the results for scour trench with those for flat seabed proximity:

- when the gap ratio was two-diameters there was little difference between the two sets of results
- when the cylinder is placed in a scour trench the amplitudes and frequencies of vibration (for a given reduced velocity) are greatly reduced compared with those

corresponding to a flat bed.

For irregular waves, and $K_c = 10$, the cross-flow vibrations depended on the gap ratio. For a positive gap ratio the vibrations were driven by vortex shedding; lock-in occurred and the cylinder simply started to vibrate at its natural frequency when the vortex shedding frequency coincided with this. For negative gap ratios the vortex shedding was suppressed and the cylinder was subjected to a cross-flow force oscillating at twice the wave frequency. The maximum amplitudes of cross-flow vibrations were, in general, greater than the corresponding values for regular waves. The in-line vibration responses were virtually indistinguishable from those obtained from the regular waves and, in overall terms, the above response was the same for conditions where $K_c = 40$.

The authors of these two papers draw the following conclusions:

1. The position of the cylinder relative to the trench is an important determining factor for the vibratory response of the cylinder.
2. For a cylinder exposed to irregular waves, the pattern of frequency response appears to be the same as in regular waves when the gap ratio is negative. The cross-flow vibration amplitudes are generally larger for irregular waves. The same is also true for the in-line movements of the cylinder.
3. The response of a cylinder placed in a trench is markedly different from that near a flat boundary. The amplitudes of vibration are greatly reduced when the cylinder is placed in a trench. The cross-flow frequencies are also reduced.

E.1.4.4 General Fatigue Calculations for Pipeline Spans

Tsahalis and Jones (1982) have made fatigue life calculations for pipeline spans exposed to steady flow and undergoing vortex-induced vibrations. The effect of the proximity of the bed was taken into account by utilising the results of model tests. They used a very simple structural model involving a simply-supported beam to estimate strain ranges corresponding to a single mode of vibration. A formula for fatigue life in years was developed that is a function of a number of normalised parameters, including span length over outside diameter, steel pipe diameter over outside diameter, vortex shedding frequency over span natural frequency, and vibration amplitude over outside diameter. Fatigue lives were calculated over a twelve-hour tidal cycle using what amounted to a reduced velocity technique (see Section 2.4.3 above). In this, graphical results from experiments on a flexible pipe were used to estimate vortex shedding frequency and amplitude ratios for different proximities between pipeline and seabed, and different span lengths. It was shown that fatigue life was extremely sensitive to span length (increases in span length reduced fatigue life or conversely increased fatigue damage). Most

interestingly, curves of fatigue life versus span length exhibited minimum fatigue lives (around 0.2 to 0.3 years) for finite ratios of gap beneath span to pipeline outside diameter.

Rather curiously, the calculations of **Orgill et al (1990)** indicated the opposite to the above, namely that fatigue damage reduced (and hence fatigue life increased) with increasing span length. They used an equivalent lumped parameter system obtained by considering only the mode of vibration corresponding to the lowest frequency of vibration in the cross-flow direction along with an equation of motion involving a time-dependent force modulated at the vortex shedding frequency. Idealised fatigue damage was taken as a stress range raised to a power. Expressions were developed to relate the response of a prototype span to that of a simpler experimental model (rigid elastically-supported cylinders, for example) by means of the ratio of various key non-dimensionalised parameters.

For the purposes of parametric studies, however, model parameters were set to unity and mode shapes corresponding to assumed conditions of simple support and clamped ends were taken. Parametric evaluations were made of the effects of mode shape, span length, axial load and damping on fatigue damage, all of which (unsurprisingly) were shown to be important in fatigue calculations. As mentioned earlier, the results indicated (rather perversely) reductions in fatigue damage with increasing span length (this would only be the case if membrane tension were allowed to participate at longer span lengths thereby leading to possible reductions in stress ranges, an effect not present in their model). The effects of fixed value axial load were investigated, and it was found that increasing tension resulted in very little change to fatigue damage (probably for reasons outlined above); curiously, for the simply supported spans, compressive axial forces caused reductions in fatigue damage. As might be expected, damping tended to reduce fatigue damage.

Tsahalis (1983) extended the ideas developed in **Tsahalis and Jones (1982)** into the concept of "generalised" fatigue damage. This is based on the fact that, excluding geometric parameters such as outside diameter, pipe diameter, span length and natural frequency of vibration, fatigue damage is a function of the ratios of response frequency to natural frequency and vibration amplitude to pipe diameter. By dividing out the geometric parameters and a time period over which a particular flow velocity is sustained, a generalised damage parameter results which is a function of response frequency ratio and amplitude ratio. From experimental data these ratios are available (in principle, if not in fact) as functions of reduced velocity and, say, gap ratio between pipe and seabed. Such data then allows the generation of a generic graph of generalised fatigue damage versus reduced velocity for different values of gap ratio from which damage can be determined for a given flow condition. Multiplication of this by the normalisation factors and the period over which the flow condition occurs gives the fatigue damage. Repetition of this for all flow regimes and periods of interest, summing the damages and taking the inverse yields the fatigue life.

E.1.4.5 Summary of Literature in Relation to Assessment Issues

At this stage it is worth summarising the literature covered in Subsection E.1.2.4, particularly that contained in E.2.4.3 and concerned with, in effect, reduced velocity techniques. There is a tremendous amount of detail in the reviews presented, and a technical summary would be part of the process of forming a database that can be quantitatively interrogated. The building of this database is judged to be outwith the scope of the present work and is proposed as a recommended piece of work in Section E.4. For the present purposes, therefore, the summary is confined to the relationship between the literature reviewed and the important issues in dynamic response of pipeline spans raised in Subsection E.1.4.1 and illustrated in Figure E.1.12.

The summary addresses whether the literature covers the ground in terms of the issues identified earlier and, therefore, contributes to an assessment of the feasibility of any database derived from the literature. The summary is presented in Figure E.1.13; this comprises a matrix made up from combinations of flow conditions, cylinder type and seabed effects; degrees of kinematic freedom are indicated as superscripts on the entries in the matrix.

It can be seen that the majority of information is related to rigid cylinder experimentation, with the minority covering flexible cylinders or quasi-pipelines. In the case of rigid cylinders, most seabed effects are well covered, but it would appear that there is insufficient information on scour trenches in amalgamation with combined steady current and wave flow conditions. For flexible cylinders in combination with a plane boundary, it is seen that all flow conditions are reasonably well-covered, but there is an absence of information connected with free stream conditions and scour trenches. The lack of free stream flow conditions information is not seen as a serious shortfall because many of the references involving the influence of a plane boundary generally include, in effect, free stream conditions at sufficiently large gap ratios.

All-in-all there is probably sufficient literature of enough quality to cover the main aspects of many practical problems of pipeline span assessment by reduced velocity techniques. This would be able to provide a body of information to form a database that would represent a significant advance over the limited information currently held in codes of practice and design guidelines (eg DNV, 1981).

E.1.5 FATIGUE LIFE AND DAMAGE CALCULATION

E.1.5.1 Limits Set by Codes and Guidelines

Three codes were considered in this respect; these are as follows:

- BS 8010 : Part 3 : 1993
Code of Practice for Pipelines Subsea: design, construction and installation
- Det Norske Veritas (DNV) : 1981 (reprint with corrections 1982)
Rules for Submarine Pipeline Systems
- Institute of Petroleum, 4 edition, 1982
Pipeline Safety Code (IP6)

These documents contain various degrees of guidance, although none were deemed to be comprehensive.

E.1.5.1.1 BS 8010

BS 8010 is very specific regarding strain-based design. Clause 4.2.7.1: use of allowable strain in design, states that:

"...This approach is only permissible where geometric considerations limit the maximum strain to which the pipeline can be subjected and where the controlled strain is not of a cyclic or repeated nature".

This would appear very definitively to rule out the application of strain-based approaches to fatigue calculations.

For actual fatigue calculations, Clause 4.2.8 applies; two sub-clauses follow, dealing with fatigue loads and fatigue life.

Clause 4.2.8.1 covers fatigue loads stating that all fluctuating loads should be considered in establishing the effect of fatigue on the pipeline, except those that produce stresses below the threshold for fatigue damage. Many S-N curves for welded tubulars, however, do not incorporate a threshold. Typical sources of fluctuating loads are suggested to include:

- wave forces
- vibrations caused by vortex shedding, product flow, or other phenomena
- operation cycles

- alternating movement of platforms and other structures

Clause 4.2.8.2 covers fatigue life. A general statement is given first that consideration should be given to the fatigue life of pipelines to ensure that minor defects do not grow to a critical size under the influence of cyclic loading. The code gives multiplying factors corresponding to fixed ranges of stress variations which are applied to the number of daily stress cycles occurring for the principal stresses within the ranges. The total sum of factored and unfactored cycles should not exceed 15000. This simplistic approach is suggested as an alternative to more comprehensive fatigue analyses based on fracture mechanics or S-N curve approaches.

Spanning pipelines are dealt with under Clause 4.6, with vortex shedding and fatigue covered by 4.6.4. The clause states specifically that:

"Pipeline ... oscillations induced by internal or external fluid flow should be considered".

The pipeline design should either prevent pipeline oscillations, or show that if they occur they are acceptable with respect to the following:

- service considerations
- strength
- fatigue
- coating integrity.

As most of the loads contributing to fatigue are of a random nature, statistical considerations will normally be required for determination of the long-term distribution of fatigue loading effects. The code allows the use of deterministic or spectral analysis methods, subject to acceptance.

The code is specific regarding the effects of dynamic response and that these effects are properly accounted for, particularly in the determination of stress ranges for pipelines excited in the resonance range. In such cases the amount of damping assumed in the analysis is to be conservatively estimated.

S-N curves in the code are also referred to as "characteristic resistances" normally based on a 95% confidence limit. Accumulated damage may be computed using Miner's rule and limited to a usage factor, the value of which depends upon the access for inspection: values of 0.1 and 0.3 are specified for no access and access, respectively.

E.1.5.1.2 DNV

Pipeline spanning is covered under Clause 4.2, which deals with pipeline/riser during operation. Fatigue is dealt with specifically under Clause 4.2.4. The first sub-clause of this states that:

"All stress fluctuations of magnitude and number large enough to have a significant fatigue effect on the pipeline are to be investigated".

The typical causes of stress fluctuations suggested in DNV are precisely the same as in BS 8010. The code states that the aim of fatigue design is to ensure adequate safety against fatigue failures within the planned life of the pipeline. It suggests that fatigue analysis methods may be based on either fracture mechanics approaches or fatigue test (S-N curve) data.

Methods based on fatigue tests generally consist of three main steps:

- determination of the long term distribution of stress range
- selection of appropriate S-N curves
- determination of accumulated damage.

E.1.5.1.3 IP6

Clause 4.2.5.3 of this document states that pipelines are not usually subject to a large number of significant stress changes and, therefore, fatigue failures are extremely rare; the effects of repeated stress changes of an appreciable magnitude should be the subject of a special examination. The code further states, but offers no specific guidance on how to undertake the necessary analysis, that the effect of vortex shedding on spans may need special examination with regard to fatigue.

E.1.5.2 S-N Curves

A great variety of these exist, for example, those referred to as API-X and API-X' (API RP2A LRFD, 1993), F2 (UK, Department of Energy, 1989), AWS-X (AWS D1.1, 1983) and those suggested for boiler and pressure vessel design (ASME, 1986).

For high stress low cycle fatigue, the design S-N curves may be extrapolated back linearly to a stress range equal to twice the material yield strength. In the event that a welded joint is in a region of simple membrane stress, the linear extrapolation is up to twice the tensile stress limitations.

It must be emphasised that the ASME curves are for un-notched components; whereas curve F2, AWS-X, API-X and API-X' are all for welded joints. Of these, AWS-X, API-X and API-X' are in

general applicable to tubular welded joints, and F2 can be used for pipelines with circumferential welds.

E.1.5.3 Damage/Fatigue Life Calculation

The Palmgren-Miner fatigue model appears to be well-suited for fatigue calculations. According to this linear, cumulative damage rule failure will occur when the damage D_t reaches unity. The damage is calculated from:

$$D_t = \sum_i \frac{n(\Delta\sigma)_i}{N(\Delta\sigma)_i}$$

where D_t = cumulative damage

n = number of cycles occurring in a time T at a stress range of $\Delta\sigma_i$

N = number of cycles to failure at a stress range $\Delta\sigma_i$ (as determined from an S-N curve)

The fatigue life of the pipeline will be the time period over which the damage is calculated, divided by the cumulative damage, as follows:

$$L = \frac{T}{D_t}$$

where L = fatigue life

T = time period of cycled stress application.

E.1.6 SUMMARY AND CLOSING REMARKS

E.1.6.1 Background Considerations

- Generally speaking, approaches to fatigue assessment may be based on two techniques, namely: reduced velocity and structural mechanics. The former is more well-developed than the latter.
- Reduced velocity techniques are mainly empirical and make use of experimental databases, principally on short lengths of cylinders (although some pipeline results

exist) in idealised flow conditions, to assess onset, and likely amplitude and frequency of vibration.

- Implementation of these techniques is either to the extent of limiting the situation so that vibration will not occur, for example, DNV (1981), Barltrop and Adams (1991) and OTI 93 614 (HSE, 1993); or, beyond this, using the data as further input to structural models to compute fatigue damage from stress ranges, for example APAL (1993).
- The data on which the DNV (1981) method is based are ageing, and stem from cylinders in a free stream with various other effects not accounted for. Barltrop and Adams (1991) endeavour to allow for combined wave and current. OTI 93 614 (HSE, 1993) is similar to DNV (1981) but is generally accepted to be more cautious in what is deemed acceptable.
- Two key questions emerge from the implementation of reduced velocity techniques:
 - firstly, the validity of extrapolating the data from simplified experimental situations to the more complex environmental conditions of real pipeline spans
 - secondly, the validity of using such extrapolated data for more detailed calculations involving stress ranges and fatigue.
- Structural mechanics techniques are inherently more sophisticated and complex than reduced velocity techniques insofar as they take hydrodynamic loading and attempt to predict dynamic response. All-in-all, owing to the statistical nature of the loading, structural mechanics techniques based around frequency-domain analysis are likely to be most tractable for fatigue problems.
- The EXXON method (Pantazopoulos, 1993) offers potential, principally in terms of a loading description; the analysis method is a standard modal technique.
- ABAQUS offers great potential as an analytical tool, with a wide range of sophisticated capabilities suitable for the problem. It does not provide pre-processing for developing the loading, nor post-processing for fatigue damage calculation.

E.1.6.2 Literature Review

- To comment that the response of cylinders/pipelines under various flow regimes and in proximity to boundaries is complex is an understatement. Key influencing factors appear to be the introduction of wave effects, gap ratio, and the shape of boundary in proximity with the pipeline (plane boundary or scour trench).

- Differences in response under similar flow conditions may occur depending on the model: rigid cylinder with one or two degrees of freedom, or flexible cylinder (actual pipeline). In the case of the latter, for instance, it may be possible for non-linearities (membrane stretching, for example) to enter the reckoning, introducing dynamic jumps into the response. The difference highlights the point made earlier regarding the extrapolation of data from simplified experiments to more complex real-life situations.
- Regardless of flow conditions and boundary type, there appears to be a threshold value of gap ratio above which response of a cylinder appears to be little different from its response in a free-stream. This threshold gap ratio appears to be around unity.
- The effects of gap ratio appear to be profound for values smaller than the threshold, particularly in the case of a plane boundary. It is often stated that vortex shedding does not occur, but this does not mean that potential oscillations do not have to be considered. For very smaller gap ratios a lift force type of stimulus might be possible.
- The presence of oscillating flows offers a cylinder the potential for vibrations that are modulated with the wave frequency, with the number of vibrations executed per wave cycle dependent on the Keulegan-Carpenter number. High frequency pulses that rise and decay within combined wave and current cycles are possible.
- The responses of cylinders in proximity with scour trenches are quite different from those pertaining to a plane boundary under the same flow conditions; this is significant because a scour trench is more likely to correspond to a real situation.
- There is probably sufficient literature of enough quality to cover the main aspects of many practical problems of pipeline span assessment by reduced velocity techniques. This would provide a body of information to form a database that would represent a significant advance over the limited information currently held in codes of practice and design guidelines.
- Indications are that fatigue life is extremely sensitive to span length and gap ratio. Smaller gap ratios tend to increase fatigue life for a fixed span length; fatigue life is reduced by increasing span length. In combination the two effects tend to produce a curve of fatigue life versus span length that displays a minimum.

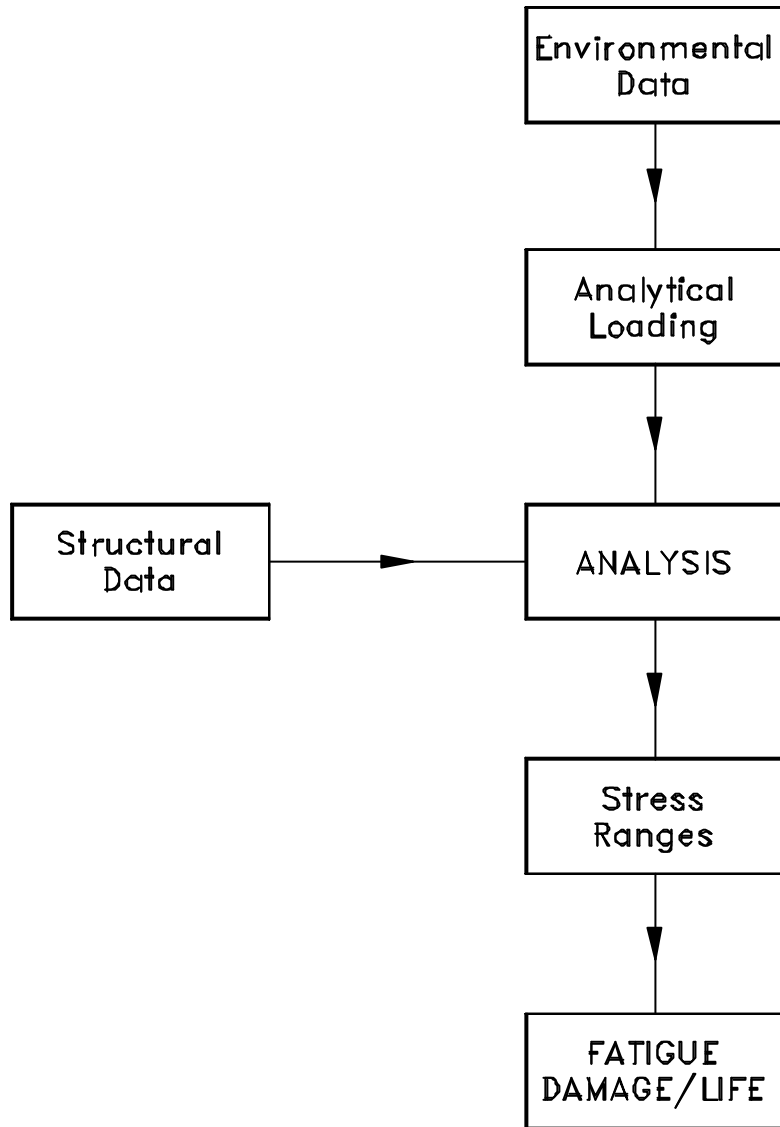


Figure E.1.1 Overall Fatigue Assessment Approach

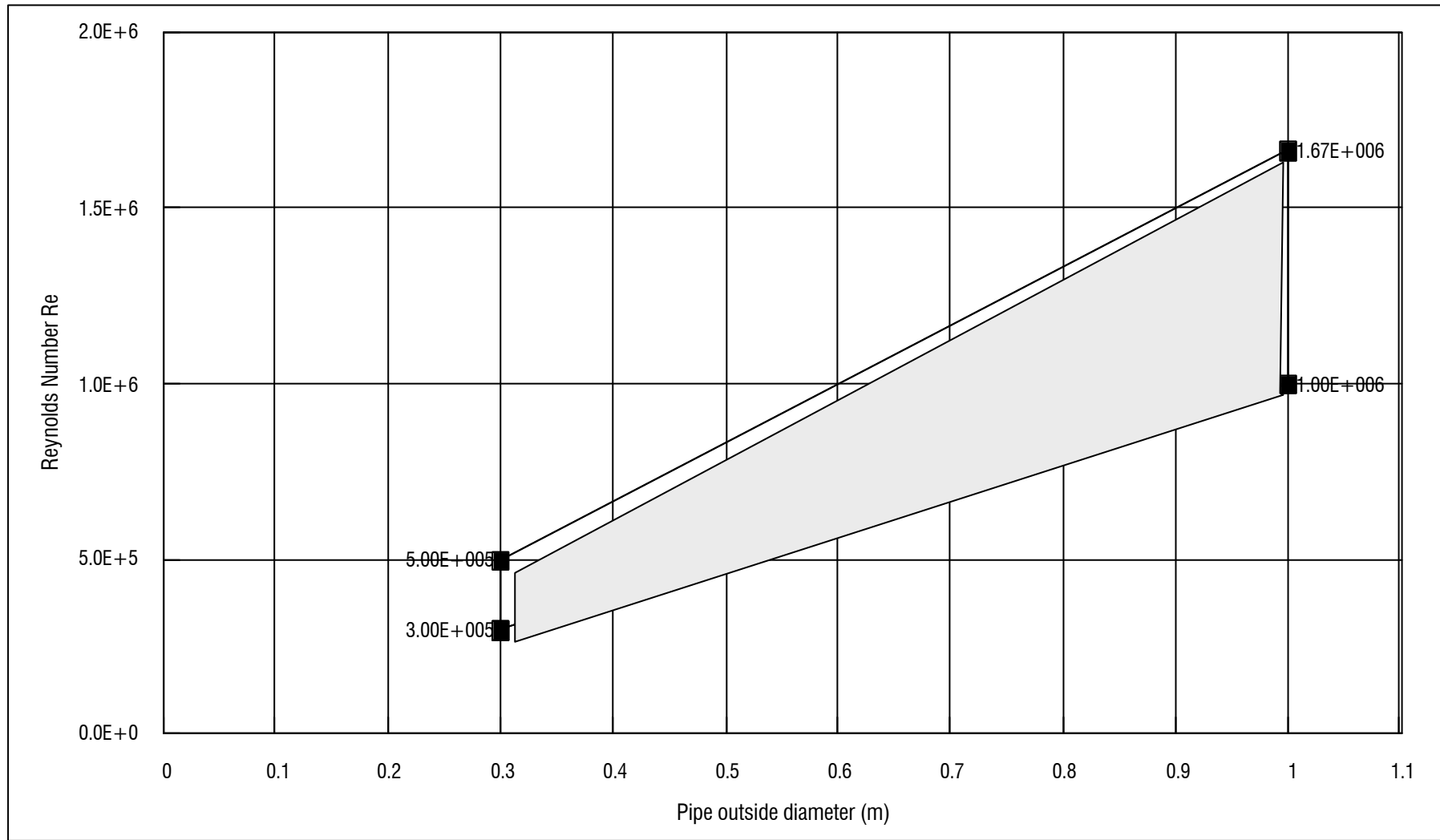


Figure E.1.2 Range of Reynolds Number Typical of Pipelines in the North Sea

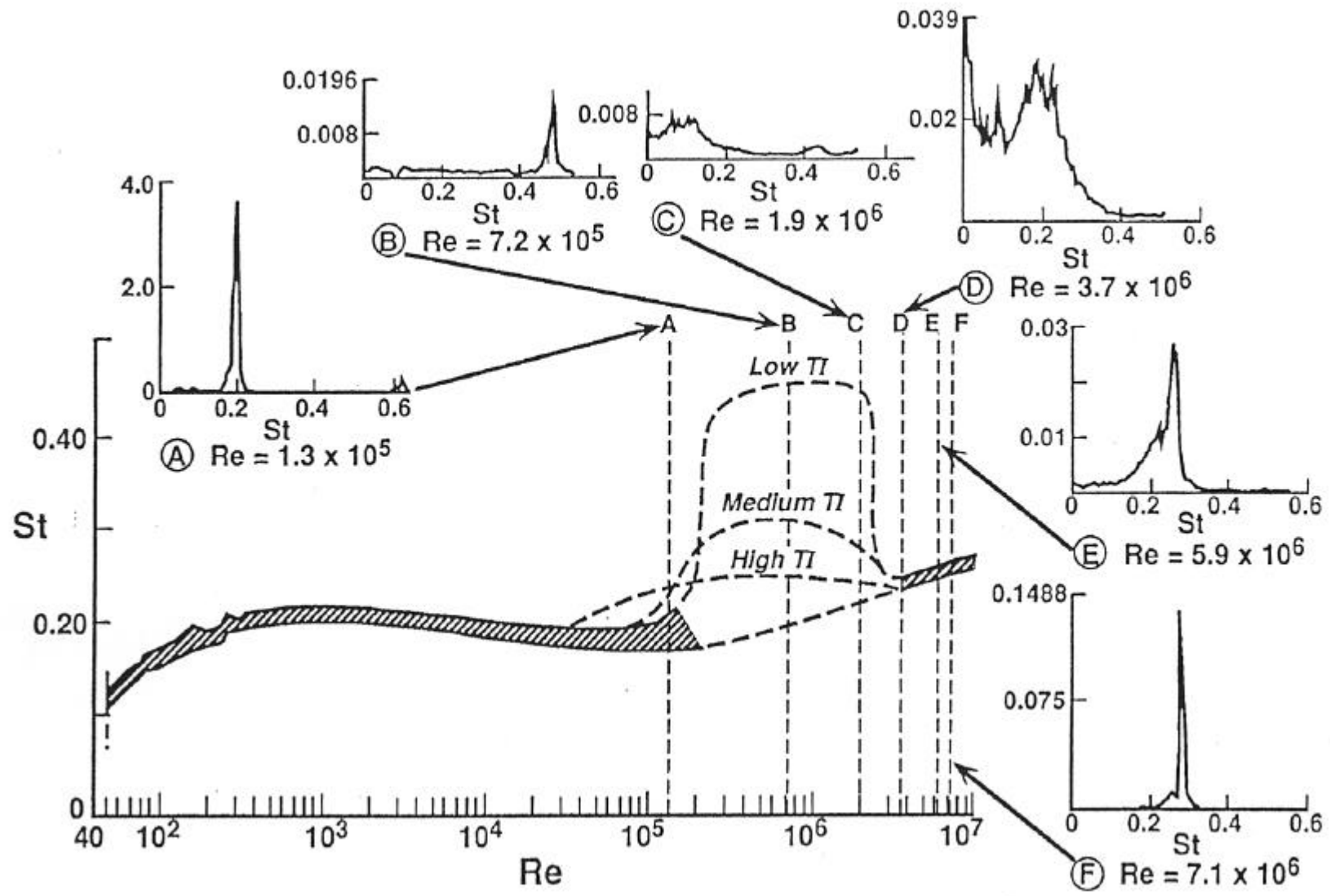


Figure E.1.3 Strouhal Number as a Function of Reynolds Number for Fixed Rigid Smooth Cylinders in Uniform Flow (Sheppard and Omar, 1992)

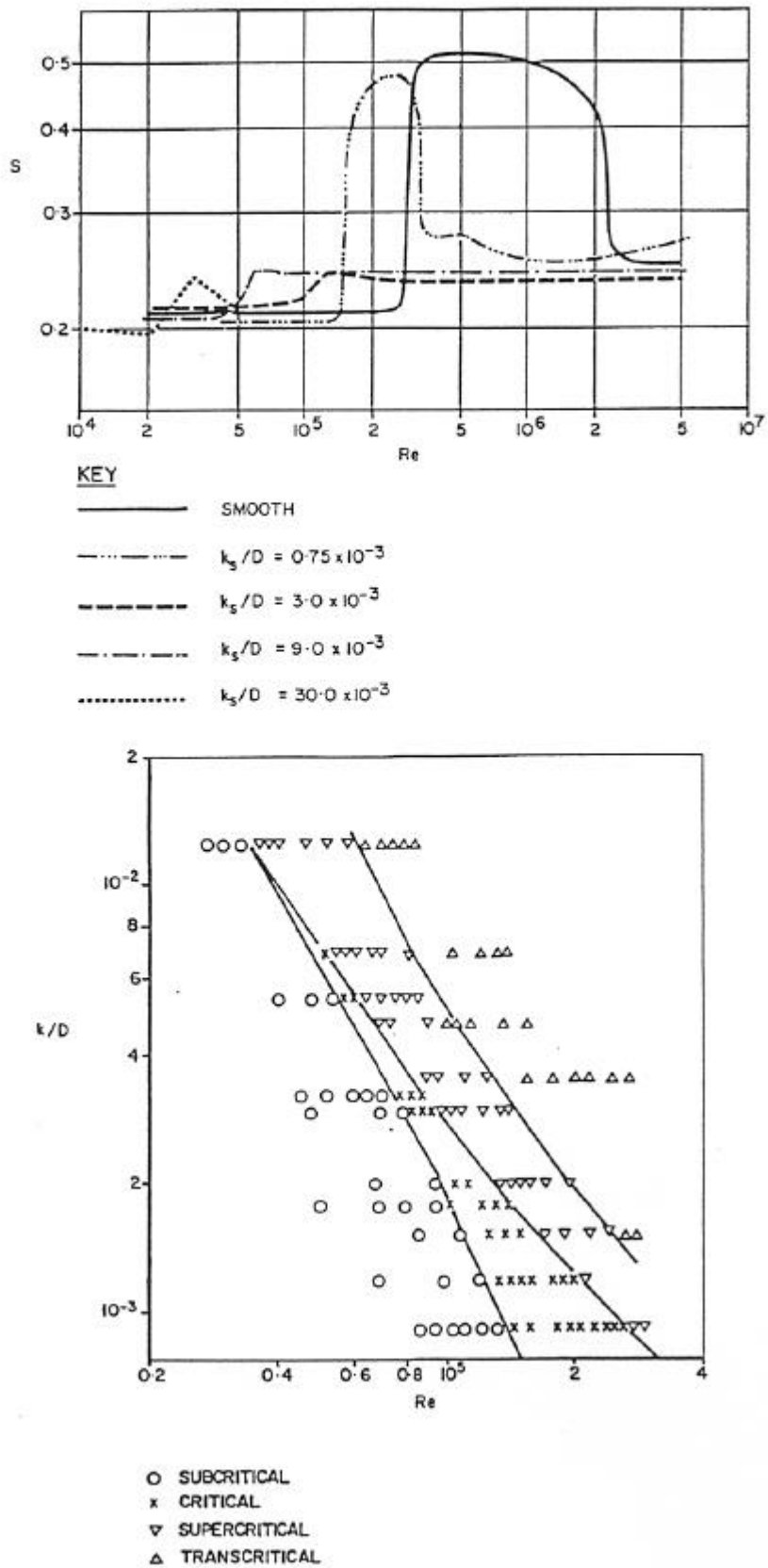


Figure E.1.4 Effects of Relative Roughness on the Strouhal Number as a Function of Reynolds Number for Fixed Rigid Cylinders in Uniform Flow

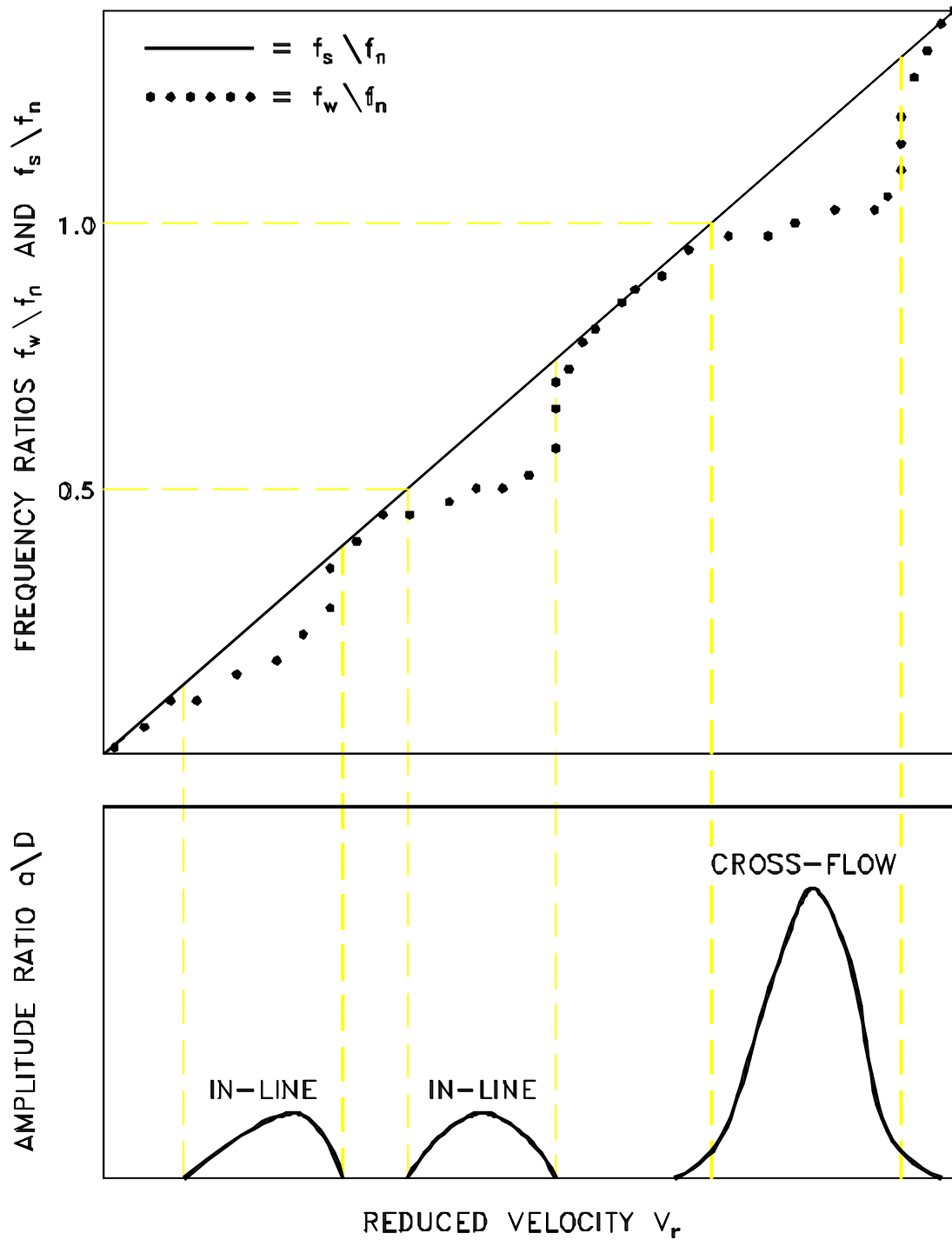


Figure E.1.5 Idealised Response of a Moveable Cylinder in Uniform Flow

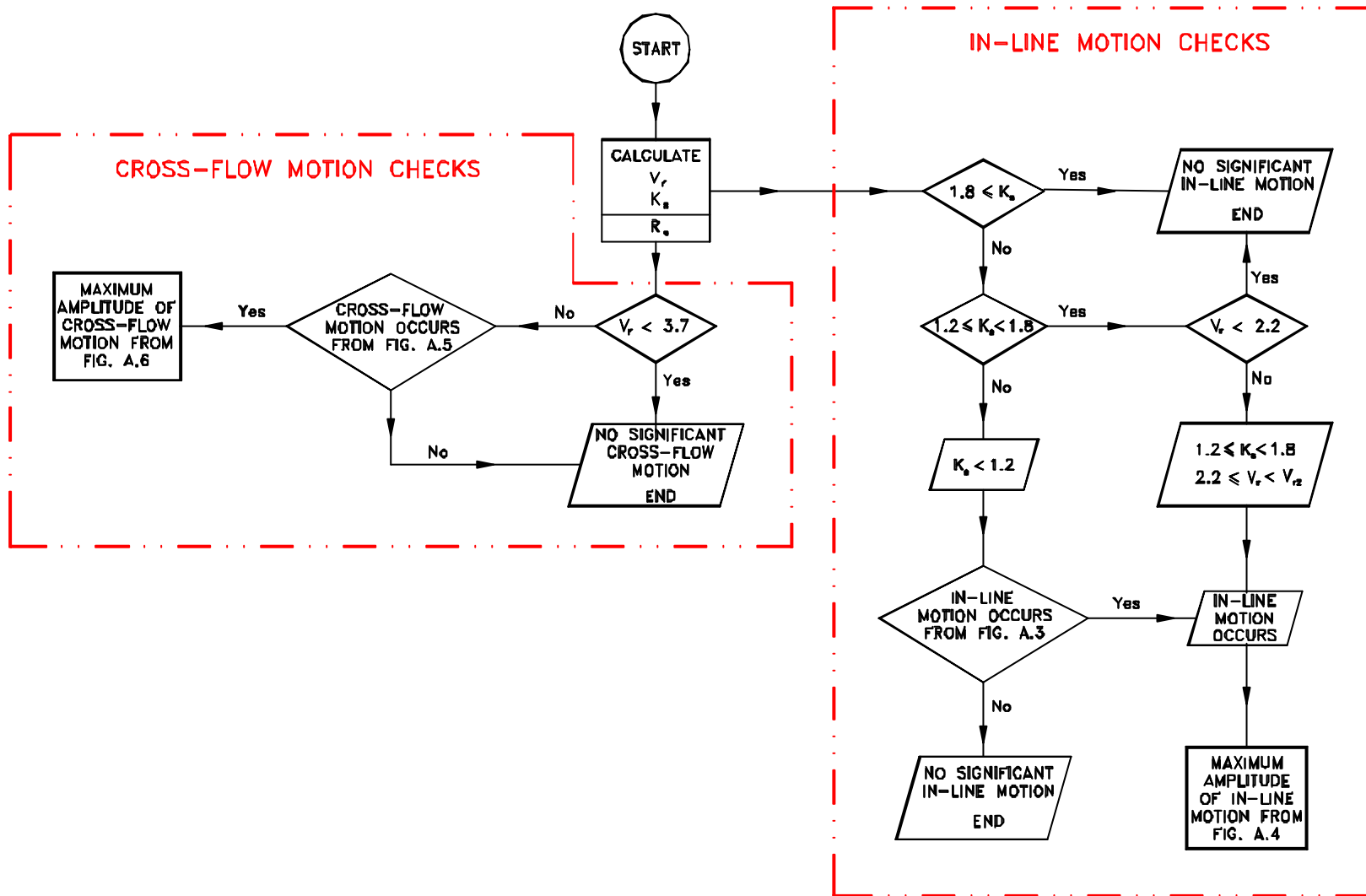


Figure E.1.6 Flow Chart for Vortex Shedding Checks According to DNV (1981)

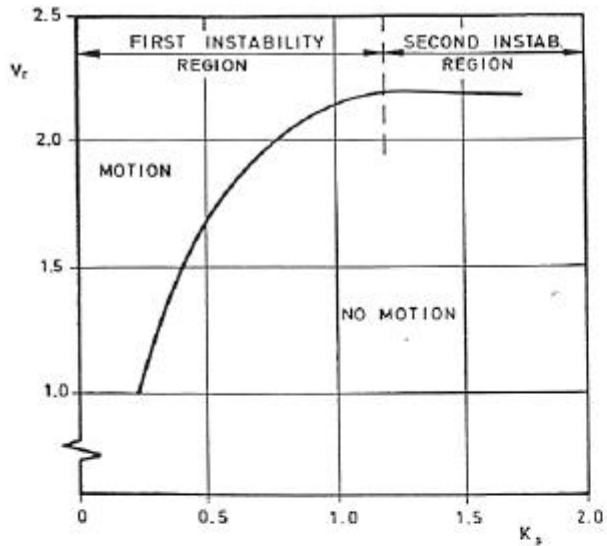


Fig. A.3. Flow velocity for onset of in-line motion.

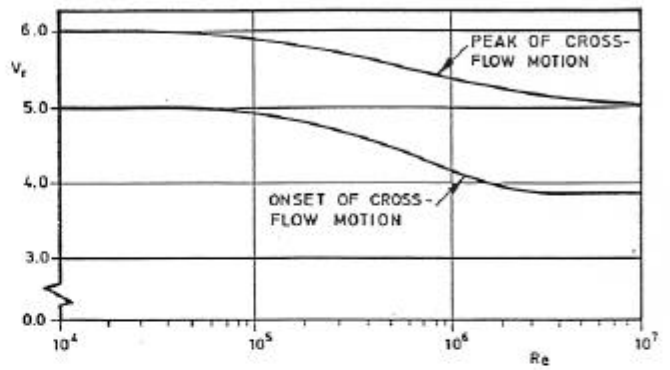


Fig. A.5. Flow speed for onset of cross flow motion.

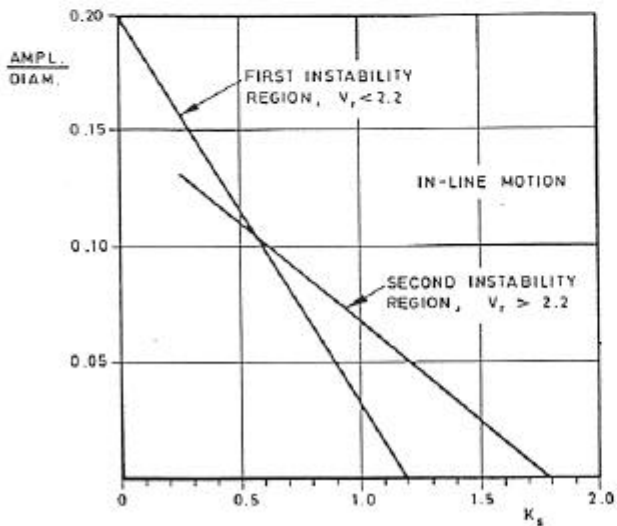


Fig. A.4. Amplitude of in-line motion as a function of K_s

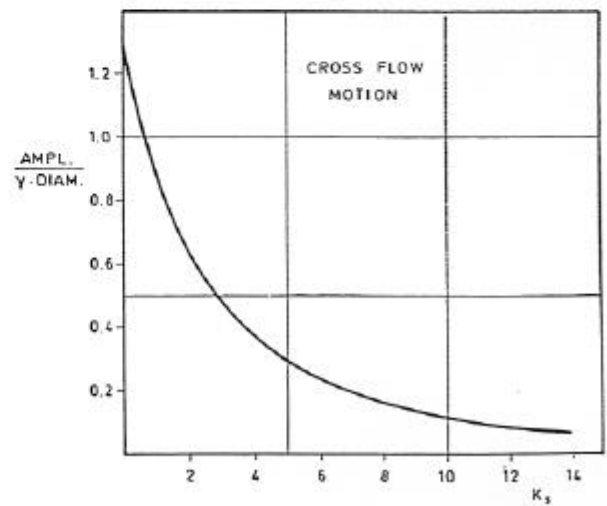


Fig. A.6. Amplitude of crossflow motion as a function of K_s

Figure E.1.7 Underlying Graphs for In-Line and Cross-Flow Excitation of Pipelines taken from DNV (1981)

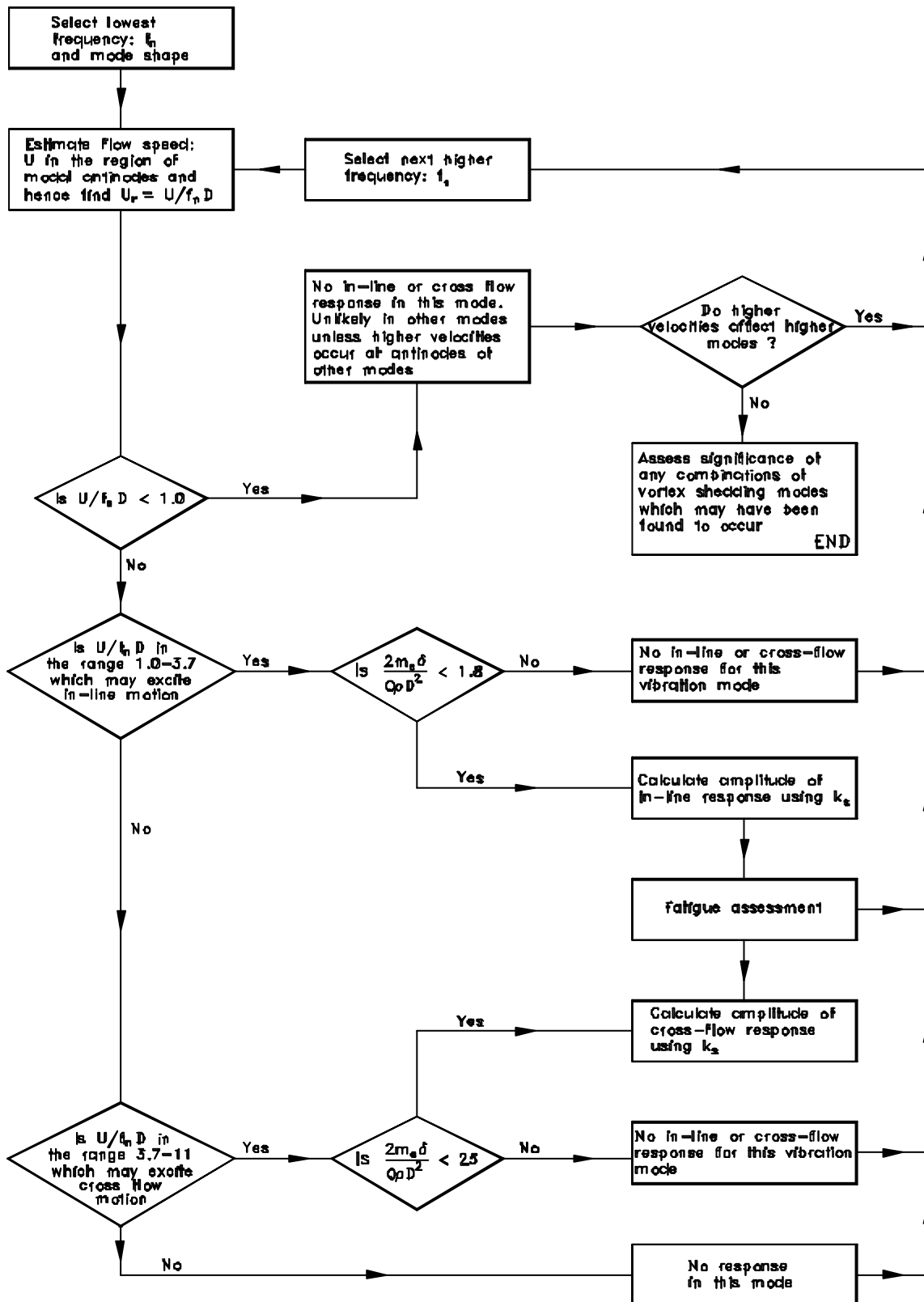


Figure E.1.8 Flow Chart for Vortex Shedding Checks According to Barltrop and Adams (1991)

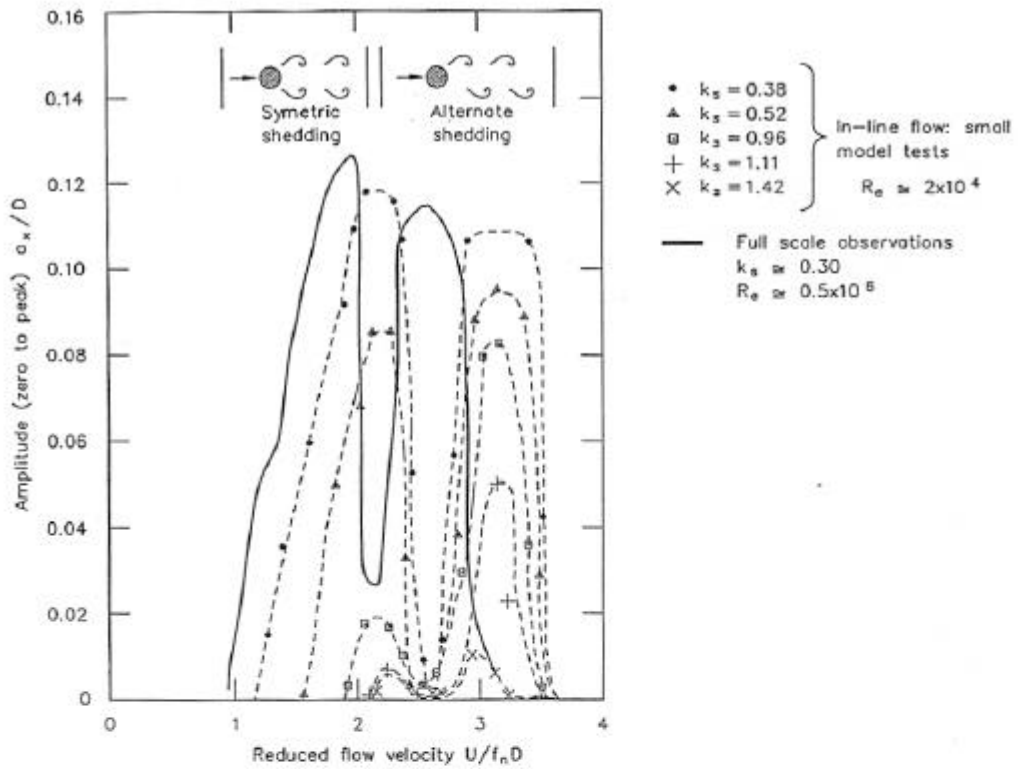


Figure 7.8 Response of cylinder in-line with flow

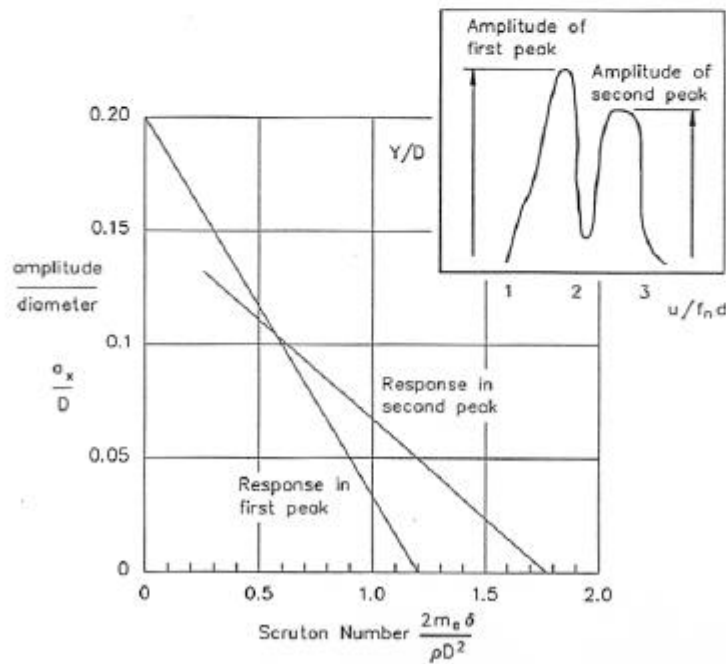


Figure 7.9b Amplitude of in-line response based on data

Figure E.1.9 In-Line Vortex Shedding Graphs from Bartrop and Adams (1991):

Upper: Criteria, Lower: Amplitude of Response

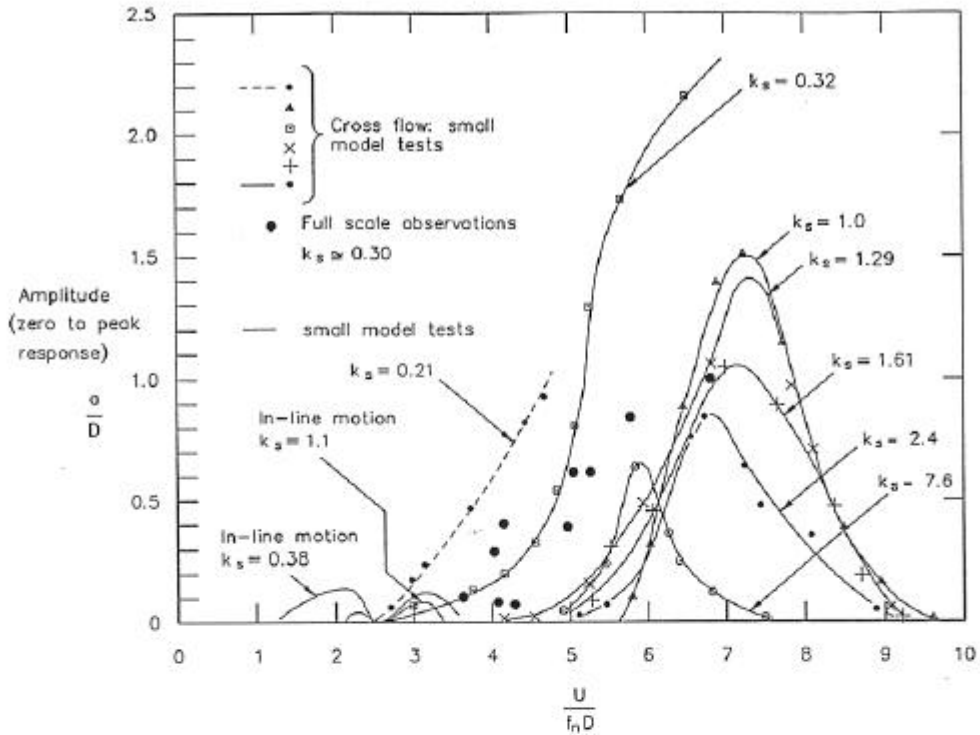


Figure 7.6 Response of model and full-scale cylinder in-line and cross-flow

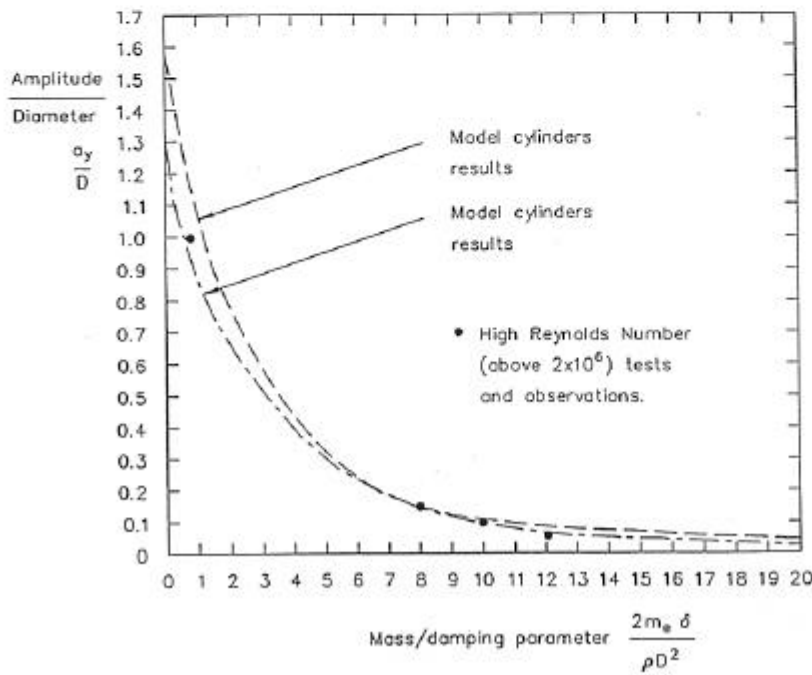


Figure 7.9a Amplitude of response against mass/damping parameter for large motion cross-flow response

Figure E.1.10 Cross-Flow Vortex Shedding Graphs from Barltrop and Adams (1991).

Upper: Criteria, Lower: Amplitude of Response

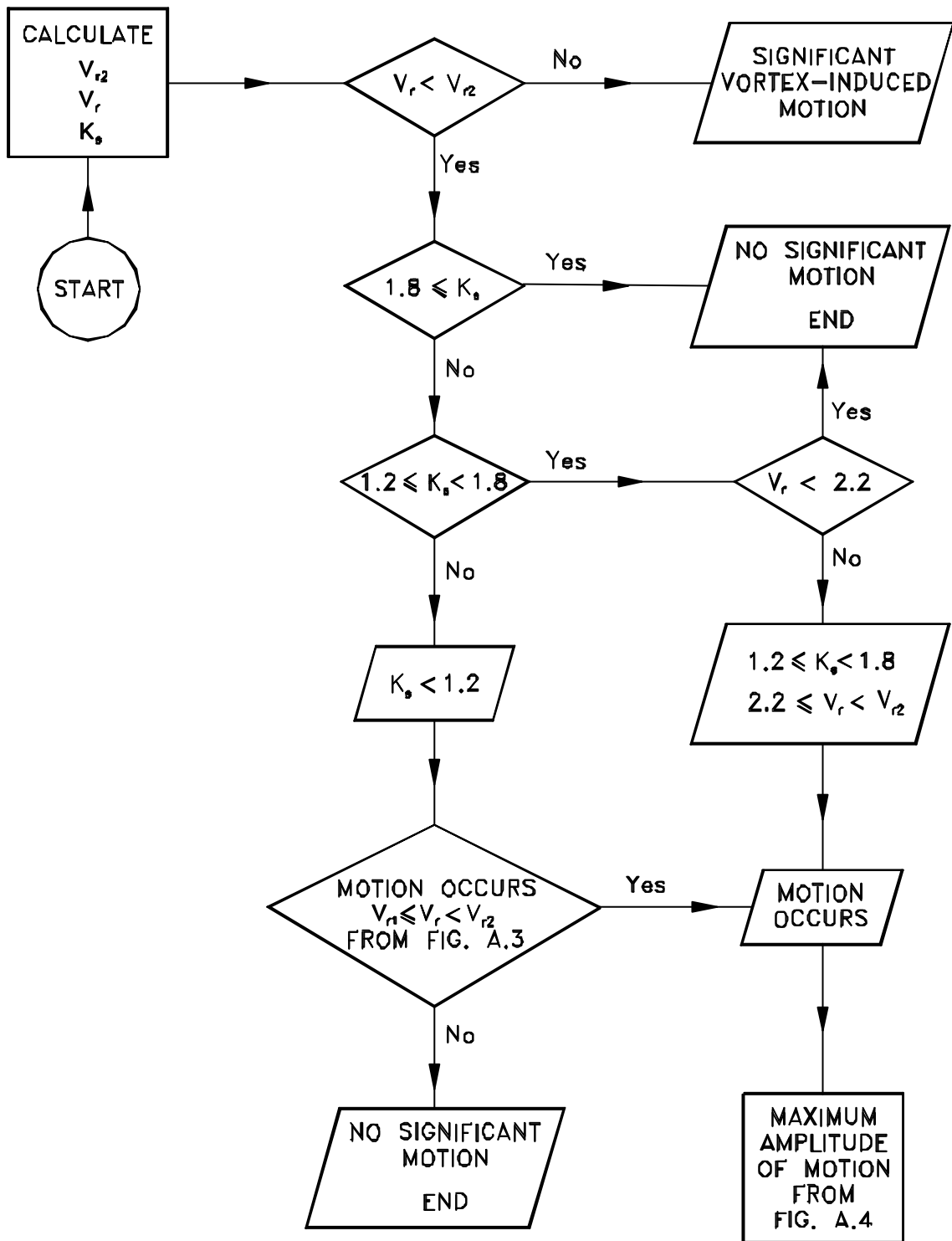


Figure E.1.11 Flow Chart for Vortex Shedding Checks According to OTI 93 614 (HSE, 1993)

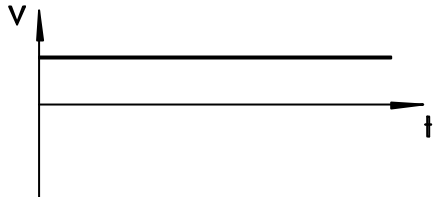
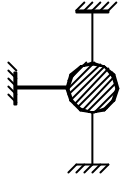
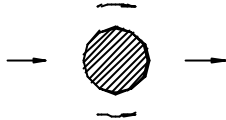
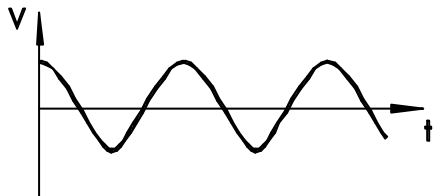
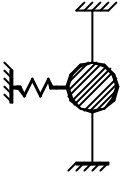
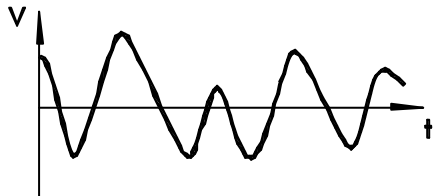
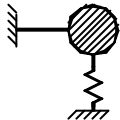
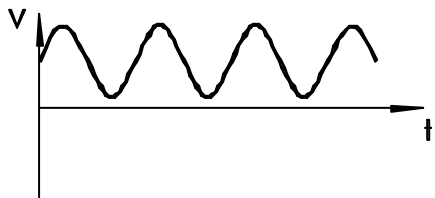
FLOW CONDITIONS	CYLINDER TYPE	DEGREES OF KINEMATIC FREEDOM		SEABED EFFECTS	
<p>STEADY CURRENT</p> 	RIGID	0 FIXED		FREE STREAM	
<p>REGULAR WAVE (PLANAR OSCILLATORY)</p> 		1 FREE IN-LINE			PLANE BOUNDARY
<p>IRREGULAR WAVE</p> 		1 FREE CROSS-FLOW		SCOUR TRENCH	
<p>STEADY CURRENT AND WAVE</p> 		FLEXIBLE (QUASI-PIPELINE)	$\ll 8$		

Figure E.1.12 (1 of 2) Issues in Assessment of the Dynamic Response of Pipeline Spans

CYLINDER TYPE	DEGREES OF KINEMATIC FREEDOM			
RIGID	0 FIXED			
	1 FREE IN-LINE			
	1 FREE CROSS-FLOW			
2 FREE IN-LINE. FREE CROSS-FLOW.				
FLEXIBLE (QUASI-PIPELINE)	$\leq \infty$			

Figure E.1.12 (2 of 2) Issues in Assessment of the Dynamic Response of Pipeline Spans

CYLINDER TYPE						
Rigid Cylinder				Flexible Cylinder/Quasi-pipeline		
SEABED EFFECTS				SEABED EFFECTS		
FLOW CONDITION	Free Stream	Plane Boundary	Scour Trench	Free Stream	Plane Boundary	Scour Trench
Steady Current	eg: DNV (1981), and Barltrop and Adams (1991)	Fredsøe et al (1985) ^X Tørum and Anand (1985) ^X Bryndum et al (1989) ^{IX}	Sumer, Mao and Fredsøe (1988) ^X		OTI 92 555 (HSE, 1993) ^{IX} Tsahalis and Jones (1981) ^{IX} Jacobsen et al (1984) ^X Bryndum et al (1989) ^{IX}	
Regular Wave	Bearman et al (1984) ^X Verley (1982) ^X Bearman and Obasaju (1989) ^F	Sumer et al (1986) ^X Bryndum et al (1989) ^{IX}	Sumer et al (1988, 1989) ^{IX}		Jacobsen et al (1984) ^X Bryndum et al (1989) ^{IX}	
Irregular Wave		Bryndum et al (1989) ^{IX}			Bryndum et al (1989) ^{IX}	
Steady Current and Wave	Sumer and Fredsøe (1987) ^X	Bryndum et al (1989) ^{IX}			Tsahalis (1984) ^{IX} Tsahalis (1985) ^{IX} Jacobsen et al (1984) ^X Bryndum et al (1989) ^{IX}	

F = fixed, I = in-line degree-of-freedom, X = cross-flow degree-of-freedom, IX = in-line and cross-flow degrees-of-freedom

Figure E.1.13 Summary of Literature in Relation to Assessment Issues

E.2 INITIAL PROPOSAL FOR DYNAMIC METHODOLOGY

E.2.1 PREAMBLE

The purpose of this section of the report is to set out an initial proposal for a dynamic assessment strategy of pipeline spans, based partly on the review of information contained within the preceding sections. The scope of the methodology has been widened to cover not only fatigue but dynamic overstress assessment.

Subsection E.2.2 sets out the generic overall dynamic assessment strategy; this embodies, within a tiered approach, the interaction between data, load combinations, criteria, analytical methods and span acceptance. The dynamic overstress and fatigue aspects run in parallel through the strategy. Attention is paid primarily in this report to the fatigue aspects.

The various components that make up the strategy are dealt with both generically, and in terms of specifically recommended technologies, in Subsections E.2.3 to E.2.5. Some important observations regarding the relationship between the proposed and existing methodologies are made in Subsection E.2.6. Closing remarks are given in Subsection E.2.7. Some areas are dealt with in reasonable detail, and some in overview terms because the precise make-up will be a matter of very detailed development, which is outwith the scope of the present work.

E.2.2 OVERALL DYNAMIC ASSESSMENT STRATEGY

E.2.2.1 Overall Strategy

The overall dynamic assessment strategy is summarised in Figure E.2.1, by means of a flow chart. It adopts a three-tiered philosophy, consistent with the static strength assessment strategy recommended by BOMEL. As can be seen, the dynamic overstress and fatigue aspects form two parallel strands within the strategy which dovetail with the static strength assessment strategy at the points indicated.

The strategy is, in effect, a screening process involving three tiers of assessment which, in order of application, involve successively less conservatism and more sophisticated analytical and modelling techniques. In this way pipeline spans that pass conservative tests, that are designed to be easily and rapidly applied, to bulk-processing of large numbers of spans, are screened out at an early stage, leaving fewer spans to be analysed using the more complex techniques of the higher tiers. Thus the basic structure of each tier is similar insofar as it involves the interaction between data, loading, criteria and an analytical method before a

decision is made whether to accept a span. A span must be deemed acceptable with respect to *both* dynamic overstress and fatigue computations before it is passed to the static strength assessment strategy. If it is not acceptable in dynamic terms it is passed to the next higher tier for processing. If a span is determined to be not acceptable at the Tier 3 level, then it must be rectified.

Differences do exist between the tiers, and these are discussed in more detail in the subsection referred to in the preamble. In the meantime it is worth noting a few general points regarding the tiers.

The particular structure of Tiers 1 and 2 is similar. Data form input to the loading, the criteria and the analytical method. The load combinations are input into the criteria and analysis elements, and the criteria input into the analytical method. The output from the analytical method is an allowable span length, which is compared with the observed span length (as measured in the field survey) to determine the acceptability of the latter.

Three key differences exist between Tier 3, and Tiers 1 and 2. The first is that the observed span length has been removed from the decision regarding span acceptability, and instead forms part of the input to the Tier 3 analytical methods. Secondly, instead of the criteria forming input to the analytical method, they form part of the decision-making process as to whether the span is acceptable. Thirdly, the output from the Tier 3 analytical methods relate directly to the criteria employed. Thus observed span lengths are analysed with the results judged against criteria to determine acceptability.

The key features of this strategy are the fact that it is generic and modular. At this level it is not tied to particular technologies; advances in terms of criteria, analytical developments, and improvements in knowledge concerning data and loading can be readily incorporated.

E.2.2.2 Deterministic, Statistical and Reliability-Based Strategies

The overall dynamic assessment strategy proposed offers sufficient scope and flexibility so as to allow implementation within a conventional deterministic framework, or a reliability-based context. In simple terms this is usually regarded as the difference between entering single values and distributions into governing mathematical models. Notwithstanding this, sight must not be lost of the fact that all methodologies are statistically based: deterministic values are generally derived from percentiles of the parameter statistical distributions. These would stem from a finite, sample population and would be subject to some variation that would generate the reliability aspects of the problem (see Figure E.2.2).

Fatigue is a somewhat different problem insofar as it is necessary to consider the damage resulting from the full range of the distribution of the initiating parameters. The statistics need to be considered in more depth in what corresponds to a deterministic approach; reliability only enters the picture if the variability of the statistics, considered as a whole, is also taken into account.

E.2.3 DATA, LOADING CASES AND LOAD COMBINATIONS

E.2.3.1 Data

With reference to Figure E.2.3 data are divided into three classes: pipeline, environmental and operational. A more detailed breakdown of the parameters within each class is given in Table E.2.1. The pipeline data include geometrical and material properties, both mechanical and those connected with weight. The operational data encompass installation (residual lay tension) and input related to the pipe contents: its density and pressure. The environmental data include the parameters that relate principally to the fluid loading on the pipeline (for example, water depth and various fluid particle motion statistics). It might also contain parameters defining the mechanical interaction between the pipe and the seabed (for example, the soil modulus at the span shoulders).

The list is not definitive; it depends on which approaches are taken in the analytical methods within particular tiers. In such circumstances it may be necessary, for example, to add longitudinal and transverse friction coefficients between the pipe and the seabed soil to the parameters listed.

E.2.3.2 Loading Classes

These are also covered in Figure E.2.3. Detailed loadings are those which are either taken directly from the relevant class of input data, for example: internal pressure, which as shown comes from the operational data, or are derived using base-level calculations using input from one or more of the data classes. An example of the latter is external (hydrostatic) pressure, which is calculated from water depth and local seawater density as contained in the environmental data class. In terms of detailed thermo-mechanical loads there are seven types that require considerations:

- submerged weight per unit length
- external temperature
- external pressure
- current and wave-induced uniformly distributed load
- contents weight uniformly distributed load

- internal temperature
- internal pressure

The data sources for each of these individual loads are indicated by connecting arrows to the various data classes.

Loading classes incorporating groups of the detailed loadings are also suggested in Figure E.2.3. Four classes are given, namely:

- self-weight: dead
- environmental: dead
- environmental: live
- operating

The classes are largely self-explanatory and have been designed to differentiate between loadings that are by and large invariant, or subject to only minor variations (dead), and those that are more likely to vary with time (live).

The operating class is also live, and it is suggested that more than one type of operating condition may be need to be addressed. The list given covers normal and maximum allowable operating conditions, shut down and hydrotest. Between these, differences will exist in internal temperatures and pressures, and in some cases contents density and hence contents weight UDL. In some operating conditions some detailed loadings will be absent completely.

E.23.3.3 Load Combinations

Classifying loadings in the way described above allows load combinations to be considered, as indicated in the figure. Generically speaking, a load combination is made up from a number of loading classes, and will always comprise both dead loading classes, an operating class, and the environmental: live loading class. Without the latter there would, of course, be no dynamic effects to be considered.

E.2.4 ANALYTICAL METHODS

E.2.4.1 Tier 1

This being the lowest tier in the overall assessment strategy, it is essential that the analytical methods employed are:

- conservative

- relatively (compared to the high tiers) uncomplicated
- easily and rapidly applied.

These requirements are necessary to allow the bulk-processing of large numbers of spans and the screening out as acceptable of a large majority at an early stage.

For these reasons it is recommended that for the Tier 1 fatigue method (see Figure E.2.1) a reduced velocity technique is used. In broad terms the approach taken should be similar to that already employed, whereby a comparison is made between an allowable reduced velocity, obtained from the span properties and an experimental database, and imposed reduced velocities stemming from the water particle kinematics. Owing to the inherent uncertainties in the whole process the comparison should be statistically based involving the probability of exceedance of the allowable reduced velocity by the imposed conditions. The reliability aspects can be introduced by assigning the appropriate variability to the allowable reduced velocity.

E.2.4.2 Tier 2

At this tier level the technology to be used should be more complex and less conservative than that recommended for Tier 1, but should still be readily applicable and involve a dedicated spreadsheet or high-level computer language programmes. Owing to the statistical nature of the fatigue process it is recommended that analysis methods should be based around frequency-domain, rather than time-domain analyses, as these are particularly suited to the purpose.

Loading should be derived using the model suggested by Pantazopoulos et al (1993), and the structural model should be based upon theirs but with developments necessary to convert it to function in the frequency-domain. Careful calibration studies of the overall analytical method should be made against experimental data with a view to possible simplification to equivalent single and two degree-of-freedom systems.

E.2.4.3 Tier 3

The highest level of analytical sophistication should be applied at this tier in anticipation that the fewest number of spans will require assessment. On this basis it is recommended that finite element methods are applied at this stage. ABAQUS (see Subsection E.1.3.3.2) should be used, and advantage taken of the use of an equilibrium base state of the pipeline arrived at by means of a nonlinear static analysis. This allows advantage to be taken of higher-order effects, such as membrane stretching, on the stiffness properties of the pipeline.

Random response analysis should be used, taking as input power spectral density functions derived from loading defined using the EXXON loading model (Pantazopoulos et al, 1993). The

principal output from such analyses would be stress-range power spectral densities that would require post-processing analysis (that is not performed by ABAQUS) to compute fatigue damage. Modules would need to be developed to undertake these calculations, as well as modules to pre-process the loading into a form suitable for ABAQUS input.

E.2.5 DETAILED LOADING

E.2.5.1 Data

E.2.5.1.1 Current data

Current data are usually available in the form of scatter diagrams containing current velocity (measured at some height above the seabed), direction and number of occurrences at each combination of direction and velocity, as measured at a particular sampling rate over a fixed period of time. The word diagram is something of a misnomer because the data may be in tabular form with, for example, the columns corresponding with cardinal compass directions and the rows with bin ranges of current velocity.

In certain circumstances a degree of processing may have been applied to the data. For example, individual directional data may have been taken and Weibull distributions fitted. The two Weibull parameters may then be tabulated against direction.

E.2.5.1.2 Wave data

The random nature of the water surface means that it can only be quantified statistically (see Subsection E.2.2.2). The statistics do not change very much over a period of about 3 hours and a particular *seastate* may be described by the:

- significant wave height (H_s), and
- the mean zero crossing period (T_z).

The significant wave height is the average height of waves that observers will typically report (Bartrop and Adams, 1991). However, it is biased towards the higher waves and is found to correspond to the average height of the highest one-third of the waves in the seastate.

The mean zero crossing period is obtained from the mean time between up-crossings of the mean water level. It is dependent on the frequency at which the water surface elevation is sampled. Various useful relationships regarding the make-up of the wave heights within a seastate can be derived under the assumption of a Rayleigh distribution.

The significant wave height and mean zero crossing period are typically measured every one

or three hours. Results are presented in an array, as a seastate scatter diagram; these relate H_s and T_z to frequency of occurrence at each combination of these two parameters. This may correspond to a total fixed period of time over which measurements were taken (1 year, 3 years, etc), and directional variation may also be introduced.

The key points to appreciate with regard to fatigue/dynamic response of pipelines are, therefore:

- over an extended period of time an appreciable number of distinctive seastates may occur
- an individual seastate is itself statistically based and may be regarded as built-up from combinations of wave heights and periods.

E.2.5.2 Data Processing

The preceding refers to, in a sense, raw current and wave data. This will require pre-processing into forms suitable as input in the form of "loads" to the various dynamic analysis methods. The term load is meant here in its most general sense, because some of the dynamic analysis methods suggested for use above involve reduced velocity techniques; load in that sense therefore means water particle velocity. Not only this, but the precise requirements as to pre-processing depend on the details of the analytical methods employed.

A further, and vitally important, question also arises as to the combination of wave and current to be taken. So far the statistics of current and wave have been discussed individually; the question as to how joint statistics are to be determined needs to be addressed.

E.2.5.2.1 Current

The principal first step in dealing with the current scatter data is relating the velocities as recorded at the measurement depth to the velocities at the top of pipe level. According to OTI 93 614 (HSE, 1993) this may be done using either an empirical power law approximation (the errors produced by which can be of low significance when compared with the uncertainties inherent in the velocity data), or a logarithmic velocity profile (which is based on a more realistic physical reasoning, involving turbulent boundary layer theory and seabed roughness, but requires a reasonable estimate of the latter from available seabed data).

In addition to this allowance must be made for the yaw angle of the pipeline span under consideration. This could be achieved by resolving the current velocities to directions normal and tangential to the span and only considering those normal components. This would need to be followed by the derivation of a new scatter diagram that eliminates current directional aspects. What results, therefore, is a one-dimensional array that gives for particular current

velocities the number of occurrences per year (and, implicitly, the corresponding probabilities).

E.2.5.2.2 Wave

Current data are very easily translated to water particle velocities at the top-of-pipe level. The situation for wave data is not so straightforward; it would require a number of intervening steps and calculation loops to perform the required translation from seastate to water particle velocities and periods at the top-of-pipe level.

As mentioned above the description of a particular seastate is itself a statistical representation of a distribution of component sinusoidal wavelets. The first step in the pre-processing of a particular seastate is to decompose it to its component wavelets and generate an individual wave height-period joint probability diagram. This can be achieved using the Longuet-Higgins formula (see Bartrop and Adams, 1991), which can be applied to calculate the probabilities and, from the wave periods, the number of waves per year for each seastate occurring in a year. From this the total number of waves of various heights and periods can be determined by summing each set of seastate results weighted by each seastate's probability. The final result of this step is a single array, each element of which gives the total number of wavelets having particular combinations of wave height and period occurring during one year.

The second step would be, for each wave height and period in the array, to compute the corresponding peak water particle velocity at the top of the pipe. Strictly speaking, for each pair of wave height and period, reference to the water depth should be made and the appropriate wave theory selected for the computation of the peak horizontal particle velocity at the top of pipe (Bartrop and Adams, 1991). APA (1996) limit the calculation of wave kinematics to Airy (linear) and Stokes 5th-order wave theories only.

The results of these computations are, therefore, two arrays giving for combinations of wave height and period in one year:

- the number of waves that occur per year (the probability distribution of combinations of wave height and period)
- the corresponding peak horizontal velocities.

The combination of these two arrays gives the number of sinusoidal waves per year having a given peak horizontal velocity at the top of pipe level and period and, implicitly, their corresponding probability of occurrence as *events*.

E.2.5.2.3 Combined current and wave data

Combining current and wave data is, in principle, a simple matter of combining the *events* of a particular wavelet having a peak velocity and period with a particular current velocity. The probability of the combined event occurring, assuming that the two are uncorrelated, will be the product of the probabilities of the individual events occurring.

Thus for a wavelet corresponding with a wave height of H_j and a period of T_j , having a peak velocity of $V_{w,ij}$ normal to the pipeline and a probability of occurrence (per year) of $P_{w,ij}$, combined with a current velocity of $V_{c,k}$ normal to the pipeline having a probability of occurrence (per year) of $P_{c,k}$, then the combined event, E_{ijk} , in terms of velocity is given as:

$$V_{ijk} = V_{c,k} + V_{w,ij} \sin \left(\frac{2\pi t}{T_j} \right)$$

where V_{ijk} = instantaneous water particle velocity

t = time variation

The probability of this event occurring P_{ijk} will be given by:

$$P_{ijk} = P_{c,k} P_{w,ij}$$

This probability is directly related to the period of time T_{ijk} over which the event occurs in one year, which will be given by:

$$T_{ijk} = P_{ijk} J$$

where J is the total time in one year. The expected number of half-cycles that the combined wavelet is able to execute will be:

$$N_{ijk} = 2P_{ijk} J / T_j$$

If this value is less than unity, then the event could be treated as steady current only.

E.2.5.2.4 Further pre-processing

Further pre-processing of the combined data may be necessary depending on the analytical methods employed in the tiers of the strategy. It may be sufficient, in the case of reduced velocity techniques for example, to conduct further pre-processing to allow for randomisation of the phase angles between the different wavelets.

In the case of structurally-based analytical methods it may be necessary to transform the velocities into forces, by means for example of the expressions suggested by Pantazopoulos et al (1993). These in turn may need to be converted to spectra or power density spectra in order to be in a form suitable for the analytical method concerned.

Pipeline data	
Pipe outside diameter	D
Pipe nominal wall thickness	t
Corrosion coat thickness	t_b
Weight coat thickness	t_c
Steel density	D_s
Corrosion coat density	D_e
Weight coat density	D_c
Steel elastic modulus	E
Steel Poisson's ratio	<
SMYS steel	F_y
Steel thermal expansion coefficient	"
Axial restraint factor	8
Operational data	
Residual lay tension	N
Internal pressure	p_i
Contents density	D_i
Contents temperature	2_i
Environmental data	
Minimum water depth at LAT	h
Local sea water density	D_w
Local sea water temperature	2_a
Hydrodynamic drag coefficient	C_d
Hydrodynamic added mass coefficient	C_m
Soil modulus at span shoulders	K_s
Current statistics	
Wave statistics	

Table E.1.1 Data Classes for Dynamic Strategy

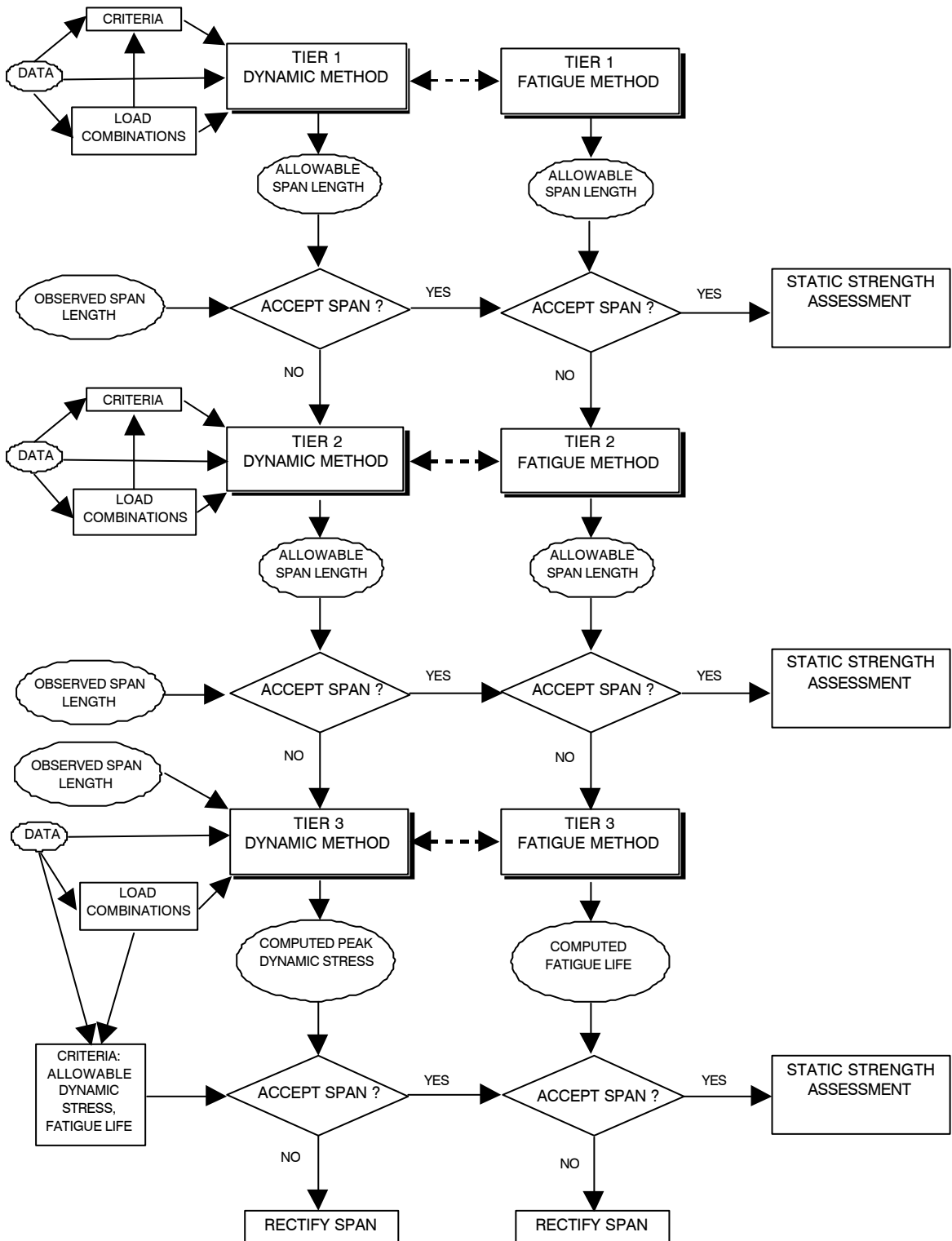


Figure E.2.1 Overall Dynamic Assessment Strategy

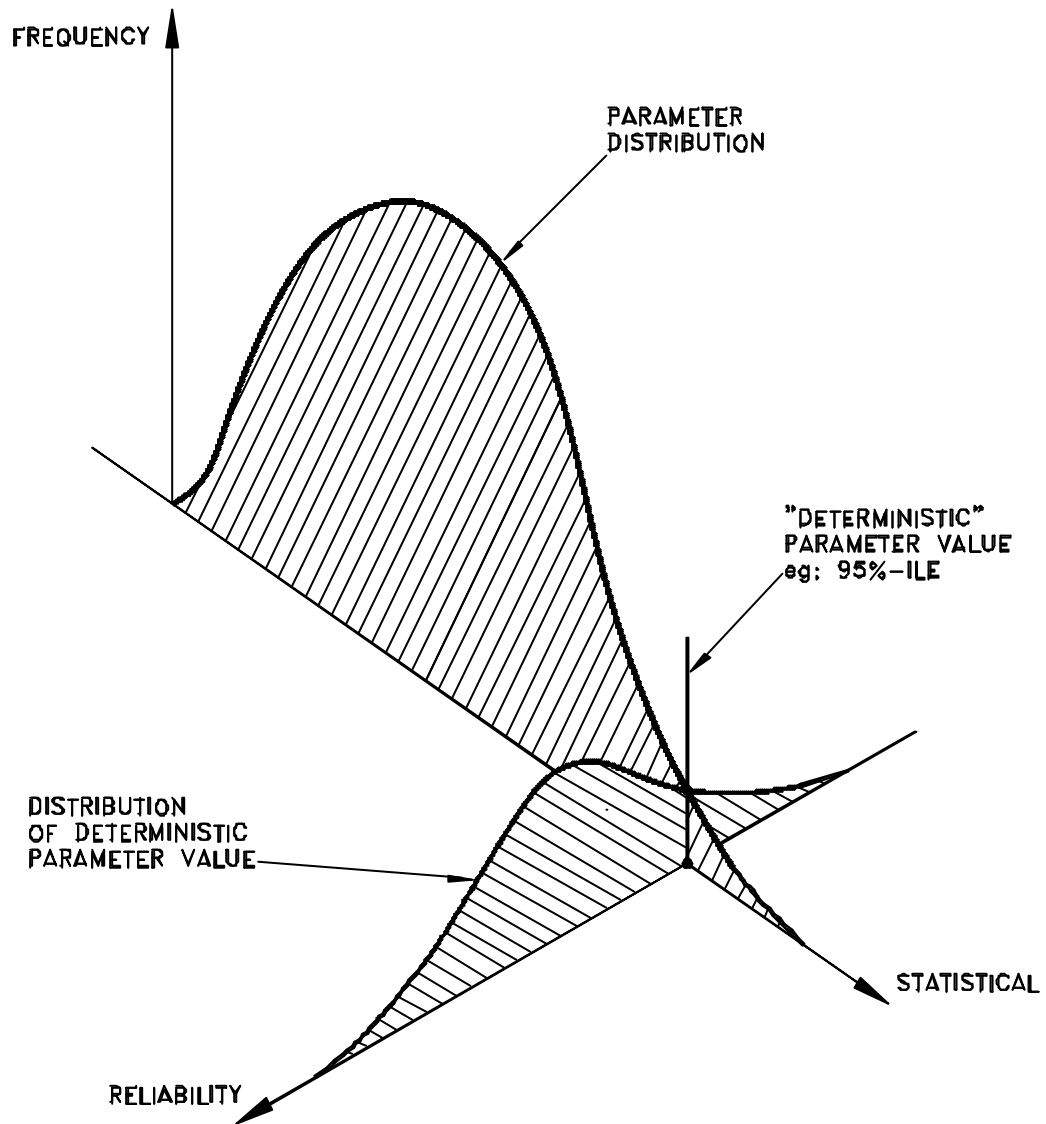


Figure E.2.2 Concepts of Deterministic, Statistical and Reliability-Based Strategies

DATA SOURCE	DETAILED LOADING	LOADING CLASS	LOAD COMBINATIONS				
ENVIRONMENTAL	SUBMERGED WEIGHT PER UNIT LENGTH	SELF WEIGHT: DEAD	●	●	●	●	
	EXTERNAL TEMPERATURE	ENVIRONMENTAL: DEAD	●	●	●	●	
	EXTERNAL PRESSURE		●	●	●	●	
PIPELINE	WAVE AND CURRENT-INDUCED	ENVIRONMENTAL: LIVE	●	●	●	●	
	CONTENTS WEIGHT UDL	NORMAL OPERATING	●				
	INTERNAL TEMPERATURE		●				
	INTERNAL PRESSURE		●				
	OPERATIONAL	CONTENTS WEIGHT UDL	MAXIMUM ALLOWABLE OPERATING		●		
		INTERNAL TEMPERATURE			●		
INTERNAL PRESSURE				●			
OPERATIONAL	CONTENTS WEIGHT UDL	SHUT DOWN (MINIMUM OPERATING)			●		
	INTERNAL TEMPERATURE				●		
	INTERNAL PRESSURE				●		
OPERATIONAL	CONTENTS WEIGHT UDL	HYDROTEST				●	
	INTERNAL TEMPERATURE					●	
	INTERNAL PRESSURE					●	

Figure E.2.3 Dynamic Loading Considerations

E.3. CONCLUSIONS

- E.3.1 Pipeline dynamic response is a complex phenomenon involving fluid dynamics and structural mechanics in close and complicated interaction. The state of knowledge is far from certain and reliance has been placed in the past (and for the foreseeable future) on the results of experimentation.
- E.3.2 To date analytical techniques have centred around empirical reduced velocity techniques founded on the experimental bases referred to above. Whilst this approach is probably acceptable for threshold vibrations, the data has also been extrapolated for use in more complex situations to compute fatigue life and damage. The validity of this has not been established.
- E.3.3 Fatigue assessment strategies currently employed place complete reliance on a single analytical technique and in that sense are restrictive because they do not allow for the flexibility offered by introducing a range of different analytical approaches; in one particular case, use is made of data from codes of practice that may be judged as outdated.
- E.3.4 Much of the data in codes of practice is now out of date. However, there is probably sufficient literature of quality to cover the main aspects of many practical problems of pipeline span assessment by reduced velocity techniques.
- E.3.5 Codes of practice do not currently allow strain-based types of approaches in fatigue assessment.
- E.3.6 From the limited number of reliable analyses reported in the open literature fatigue life of pipeline spans is extremely sensitive to span length; life decreases as span length increases
- E.3.7 Fatigue is inherently statistical in nature and this, coupled to the complexity and uncertainty of the physical situation, means that probabilistic approaches recommend themselves.
- E.3.8 The rational manipulation of environmental data, seastates and current scatter diagrams, and their appropriate combination and transformation to seabed kinematics and loads, is central to the rigour of any analytical tool.
- E.3.9 The development of structural mechanics techniques is much less well-advanced. This is principally because of the difficulties that exist in defining the loading. The EXXON method may help to remedy this.

E.3.10 Owing to the statistical nature of fatigue any structural mechanics techniques should be based around spectral or power spectral density approaches, ie. frequency-domain analysis.

E.4. RECOMMENDATIONS

On the strength of the work contained in this report, the following recommendations are made:

- E.4.1 The three-tiered overall dynamic assessment strategy as set out above should be adopted. The benefits are that the strategy is flexible, modular and rational; it will allow the usage of reliability techniques in areas where most benefit will accrue, and given the variety in analytical methods suggested for inclusion it does not place reliance on one single analytical technique. A modular approach should be taken to its development, as set out below.
- E.4.2 Loading should be treated as a separate module that services all the tiers of the overall assessment strategy. Methodologies should be devised and implemented to transform wave and current data into combined seabed kinematics in a rational manner (Tier 1), transform them into seabed hydrodynamic loads using the EXXON method and process them into spectra or power spectral densities (Tiers 2 and 3).
- E.4.3 It is recommended that the Tier 1 fatigue method developed should be a reduced velocity approach. The level of conservatism should be such as to reduce the risk of pipeline span vibrations occurring to "as low as reasonably practicable". To this end a database of experimental results should be formed so as to extend the base of knowledge beyond DNV and other current codes of practice. The approach should embody threshold of vibration techniques applied in a statistical/reliability context.
- E.4.4 The level of conservatism appropriate to the Tier 2 fatigue method should be such that pipeline vibrations are admitted, but the damage that they do over a predefined period of time is limited. The method developed should be based around spectral or power spectral density approaches and should be founded on a suitably adapted modal solution method. The method should first be prototyped on a one or two degree-of-freedom basis for calibration against the experimental database mentioned above.
- E.4.5 A fatigue damage/life calculation module should be developed, based on S-N curves, to service all three of the tiers within the overall strategy.
- E.4.6 The Tier 3 fatigue method should be based around finite element models. Once the loading and fatigue life modules have been developed (see items E.4.2 and E.4.5, above), investigations should be performed using the FE models to determine the effects of various modelling approaches on fatigue life and its sensitivity to certain parameters.

E.5. REFERENCES

1. ABB Global Engineering (1994). 'Amoco (UK) Exploration Company. Pipeline engineering support services. Span assessment procedure for Amoco pipelines', ABBGEL Document No 1723/RPT/0.31 Rev A2, January 1994.
2. American Petroleum Institute (API) (1993). 'Planning, designing and constructing fixed offshore platforms - Load and Resistance Factor Design', API RP2A LRFD, First Edition, 1993.
3. American Welding Society (1983). 'Structural welding code', AWS D1.1, 1983.
4. Andrew Palmer and Associates (APAL) (1993). Private communication.
5. Andrew Palmer and Associates (1996). 'Amoco (UK) Exploration Co, CATS gas trunkline: deterministic span fatigue analysis'. Document No. 606.11.1/TR/300/01/00, 1996.
6. ASME (1986). 'Boiler and pressure vessel: Code Section III', 1986.
7. Barltrop N D P and Adams A J (1991). 'Dynamics of fixed marine structures', Butterworth Heineman, Oxford, 3rd Edition, 1991.
8. Bearman P W, Graham J M R, and Obasaju E D (1984). 'A model equation for the transverse forces on cylinders in oscillatory flow', Applied Ocean Research, Volume 6, No 3, 1984.
9. Bearman P W and Obasaju E D (1989). 'Transverse forces on a circular cylinder oscillating in-line with a steady current', Proceedings Offshore Mechanics and Arctic Engineering Conference, 1989.
10. British Standards Institution (1993). 'BS 8010 : Part 3 : 1993 Code of practice for pipelines subsea: design, construction and installation, 1993.
11. Bryndum M B, Bonde C, Smitt L W, Tura F and Montesi M (1989). 'Long free spans exposed to current and waves: model tests', OTC Paper 6153, Proceedings 21st Annual Offshore Technology Conference, 1989.

12. Department of Energy (1989). 'Offshore installations: Guidance on design, construction and certification', 4th edition, 1989.
13. Det Norske Veritas (DNV) (1981). 'Rules for submarine pipeline systems', 1981.
14. Faltinsen O M (1990). 'Sea loads on ships and offshore structures', Cambridge University Press, 1990.
15. Fredsøe J, Sumer B M, Andersen J and Hansen E A (1985). 'Transverse vibrations of cylinder very close to a plane wall', Proceedings 4th Offshore Mechanics and Arctic Engineering Symposium, 1985.
16. Health and Safety Executive (1993). 'Evaluation of vortex shedding frequency and dynamic span response, development of guidelines for assessment of submarine pipeline spans, Background Document One', OTI 93 614, London: HMSO, 1993
17. Health and Safety Executive (1993). 'Vibration of pipeline spans, Development of guidelines for assessment of submarine pipeline spans, Background document three', OTI 92 555, London: HMSO, 1993.
18. Institute of Petroleum (1982). 'Pipeline safety code (IP6)', 4th edition, 1982.
19. Jacobsen V, Bryndum M B, Nielsen R and Fines S (1984). 'Vibrations of offshore pipelines exposed to current and wave action', Proceedings 3rd Offshore Mechanics and Arctic Engineering Symposium, 1984.
20. Kaye D, Galbraith D, Ingram J and Davies R (1993). 'Pipeline freespan evaluation: a new methodology', Offshore European Conference, Aberdeen, 1993.
21. Orgill G, Lambrakos K F, Chao J C and Hyden A M (1990). 'Effects of structural boundary conditions on fatigue life of pipeline spans undergoing vortex-induced vibrations', Proceedings 9th Offshore Mechanics and Arctic Engineering Symposium, 1990.
22. Pantazopoulos M S, Crossley C W, Orgill G and Lambrakos K F (1993). 'Fourier methodology for pipeline span vortex-induced vibration analysis in combined flow', Proceedings Offshore Mechanics and Arctic Engineering Conference, 1993.

23. Sheppard D M and Omar A F (1992). 'Vortex-induced loading on offshore structures: a selective review of experimental work', OTC Paper 6817, Proceedings 24th Annual Offshore Technology Conference, 1992.
24. Snamprogetti Limited (1994). 'Report to Amoco on: Study to investigate free spanning of Southern North Sea pipelines'.
25. Sumer B M, Fredsøe J and Jacobsen V (1986). 'Transverse vibrations of a pipeline exposed to waves', Proceedings 5th Offshore Mechanics and Arctic Engineering Symposium, 1986.
26. Sumer B M and Fredsøe J (1987). 'Transverse vibrations of an elastically mounted cylinder exposed to an oscillating flow', Proceedings 6th Offshore Mechanics and Arctic Engineering Symposium, Vol II, 1987.
27. Sumer B M, Mao Y and Fredsøe J (1988). 'Interaction between vibrating pipe and erodible bed'. Journal of Waterway, Port, Coastal and Ocean Engineering, Proceedings ASCE, Vol 114, No 1, 1988.
28. Sumer B M and Fredsøe J (1988). 'Vibrations of pipelines in scour trenches', Proceedings BOSS, Vol 2, 1988.
29. Sumer B M, Fredsøe J, Gravesen H and Bruschi R (1989). 'Response of marine pipelines in scour trenches', Journal of Waterway, Port, Coastal and Ocean Engineering, Proceeding ASCE, Vol 115, No 4, 1989.
30. Tørum A and Anand N M (1985). 'Free span vibrations of submarine pipelines in steady flows - effect of free-stream turbulence on mean drag coefficients', Journal of Energy Resources Technology, Transactions ASME, Vol 107, 1985.
31. Tsahalis D T and Jones W T (1981). 'Vortex-induced vibrations of a flexible cylinder near a plane boundary in steady flow', OTC Paper 3991, Proceedings 24th Annual Offshore Technology Conference, 1981.
32. Tsahalis D T and Jones W T (1982). 'The effect of sea-bottom proximity on the fatigue life of suspended spans of offshore pipelines undergoing vortex-induced vibrations', OTC Paper 4231, Proceedings 25th Annual Offshore Technology Conference, 1982.

33. Tsahalis D T (1983). 'The effect of sea bottom proximity of the vortex-induced vibrations and fatigue life of offshore pipelines', Journal of Energy Resources Technology, Transactions ASME, Vol 105, 1983.
34. Tsahalis D T (1984). 'Vortex-induced vibrations of a flexible cylinder near a plane boundary exposed to steady and wave-induced currents', Journal of Energy Resources Technology, Transactions ASME, Vol 106, 1984.
35. Tsahalis D T (1985). 'Vortex-induced vibrations due to steady and wave-induced currents of a flexible cylinder near a plane boundary', Proceedings 4th Offshore Mechanics and Arctic Engineering Symposium, 1985.
36. Verley R L P (1982). 'A simple model of vortex-induced forces in waves and oscillating currents', Applied Ocean Research, Vol 4, No 2, 1982.

APPENDIX F

CRITERIA DETERMINING THE STATIC STRENGTH OF PIPELINE SPANS

TABLE OF CONTENTS

	Page No
F.1 CRITERIA DETERMINING THE STATIC STRENGTH OF PIPELINE SPANS	F.1
F.1.1 PREAMBLE	F.1
F.1.2 STRESS AND STRAIN CRITERIA SET BY CODES	F.1
F.1.2.1 Stress Criteria	F.2
F.1.2.2 Strain Criteria	F.2
F.1.3 OFFSHORE TECHNOLOGY REPORT OTN 94 186 (1994)	F.4
F.1.3.1 Review of Codes and Guidelines	F.4
F.1.3.2 Reviews of Technical Information related to Pipeline Ovalisation and Strength	F.7
F.1.3.3 Effects of High Strain Bending on Material Properties	F.10
F.1.3.4 Initial Proposal for Strain-Based Assessment Framework	F.11
F.1.4 JIP ON THE ESTABLISHMENT OF STRAIN-BASED CRITERIA AND ANALYSIS FOR THE ASSESSMENT OF SUBSEA PIPELINES	F.12
F.1.4.1 Objective of the Project and Scope of Work	F.12
F.1.4.2 Review of Principal Sections of Final Report	F.13
F.1.5 COMPARISON OF STRAIN LIMITS	F.18
F.1.5.1 Pipeline Considered	F.18
F.1.5.2 Preliminary Results and Basis of Comparison	F.18
F.1.5.3 Results from Comparison	F.22
F.1.6 CLOSING REMARKS	F.23
F.1.7 REFERENCES	F.23

LIST OF TABLES

Table F.1.1	Coverage detail of strain-based assessment in codes reviewed in OTN 94 186 (1994)
Table F.1.2	Coverage detail of strain-based assessment in AME (1996) [As Table 3.1, but updated to include RP 1111]
Table F.1.3	Pipeline data
Table F.1.4	Pipeline results (full axial fixity assumed)
Table F.1.5	Pipeline Results: strain limits from AME formulae (AME, 1996) and BS8010/DNV formulae in terms of bending strain and equivalent plastic strain increment

F.1. CRITERIA DETERMINING THE STATIC STRENGTH OF PIPELINE SPANS

F.1.1 PREAMBLE

The purpose of this appendix is to address the criteria available to determine the limiting span length of pipelines with respect to static strength. Attention has concentrated on strain limits, as this approach appears to offer more scope for the safe relaxation of criteria than the more conventional stress-based methods.

Section F.1.2 presents an overview of two codes that would be the most important in terms of North Sea practice. These have been taken because they represent the best level of detail offered by all of the pipeline codes taken together. This fact is confirmed by Section F1.3, which gives a summary of a review undertaken for the UK Health and Safety Executive on structural and material implications of bending pipelines to large strains. This involved a review of design codes/guidelines, as well as relevant technical information. Section F1.4 reviews the Final Report of a large Joint Industry Project conducted by a third party contractor of which Amoco was one of the sponsors. The objective of the project was to establish a capability and provide information for the analysis and assessment of pipelines based on strain criteria. The scope of work covered pipe and material testing and finite element work. A comparison between the strain limits proposed by the JIP document, and those from codes and guidelines, is made for an example pipeline segment from Amoco's operations in Section F1.5. Closing remarks are to be found in Section F.1.6.

F.1.2 STRESS AND STRAIN CRITERIA SET BY CODES

The two codes considered in this respect are typical of those available, they are:

- BS 8010 : Part 3 : 1993
Code of Practice for Pipelines Subsea: design, construction and installation.

- Det Norske Veritas (DNV) : 1981 (Reprint with corrections 1982)
Rules for Submarine Pipeline Systems

Within these document the design conditions that are relevant to the spanning situation are referred to as:

- Functional and environmental loads
including: self-weight, thermal effects, pressure effects, transient operations effects, environmental pressure, residual installation loads; current, wave and wind loadings (BS 8010)
- Pipeline system during operation
[presumably acted upon by the same set of effects and loadings as listed above for BS 8010] (DNV).

Both codes allow the use of stress and strain criteria applied to their respective design conditions as summarised below.

F.1.2.1 Stress Criteria

The same stress criterion is used by both codes; the maximum equivalent stress in the pipeline (computed from the von Mises expression) should be less than a design or usage factor times the specified minimum yield stress (SMYS) of the pipe steel. This is expressed mathematically as:

$$\sqrt{F_x^2 + F_2^2 - F_x F_2} \leq 8F_y$$

where F_x = longitudinal stress
 F_2 = hoop stress
 8 = design/usage factor = 0.96
 F_y = specified minimum yield stress

F.1.2.2 Strain Criteria

BS 8010 allows alternative design for strain for conditions other than construction loads and hydrostatic testing and states that:

"The limit on equivalent stress recommended above may be replaced by a limit on allowable strain, provided that the following conditions are met".

It sets out four conditions that must be adhered to, plus a warning in respect of upheaval buckling, as follows:

- Under maximum operating temperature and pressure, the plastic component of the equivalent strain does not exceed 0.1%. The reference state for zero strain is the as-built condition (after pressure testing).

- b. Any plastic deformation occurs only when the pipeline is first raised to its maximum operating pressure and temperature, but not during subsequent cycles of depressurisation, reduction in temperature to the minimum operating temperature, or return to the maximum operating pressure and temperatures.
- c. The ratio of outside diameter to thickness of the pipe does not exceed 60.
- d. Welds have adequate ductility to accept plastic deformation.

Finally, the influence of the plastic deformation on the pipeline's resistance to upheaval buckling should be checked if this phenomenon is likely to occur.

DNV also allows the use of strain criteria in respect of design for the operation condition and states that:

"...In cases where possible strain (displacement) does not exceed the permissible strain ... stresses need not be used as a criterion against excessive yielding..."

The permissible strain is not quantitatively prescribed, but its magnitude must:

- a. Take account of the material ductility
- b. Take account of previously experienced plastic strain (during installation, for example)
- c. Result in acceptable fracture toughness after deformation under this condition
- d. Not lead to violation of out-of-roundness limitations.

These requirements apply to conditions of permanent strain (arising from, for example, permanent curvature) and to pipelines in (almost) continuous contact with the seabed, and to pipelines not in continuous contact provided that yielding would lead to contact that arrested strains before they exceed the permissible values.

To summarise: strain limits are set explicitly by BS 8010, but DNV only gives criteria on which to base limiting strain centred around material requirements, ovalisation and local buckling.

F.1.3 OFFSHORE TECHNOLOGY REPORT OTN 94 186 (1994)

This document constituted a comprehensive review of the design codes/guidance and available technical literature relevant to the structural and material implications of bending pipelines to large strains. It covered the following areas:

- Review of codes and guidelines

- Reviews of technical information related to
 - Ovalisation in response to bending
 - Pipeline strength under individual and/or combined loading actions

- Tests elucidating the effects of high strain bending on material properties

- Initial proposal for strain-based assessment framework.

In addition to these, Appendices covered representation of material stress-strain behaviour, plasticity equations and methods for ovalisation computation.

The subsections that follow summarise the principal areas listed above.

F.1.3.1 Review of Codes and Guidelines

The review of codes and guidelines covered the following six documents:

1. Submarine Pipeline Guidance Notes. Issued by the Pipeline Inspectorate, Petroleum Engineering Division, Department of Energy, October 1984 (DEnGN).

2. Model Code of Safe Practice in the Petroleum Industry: Part 6 Pipeline Safety Code. Institute of Petroleum, 4th Edition, December 1982. Plus Supplement, August 1986 (IP6).

3. Gas Transmission and Distribution Piping Systems. ASME code for Pressure Piping, B31 ANSI/ASME B31.8 - 1989. Plus addenda, B31.8a - 1990, B31.8b - 1990 and B31.8c - 1992 (B31.8).

4. Liquid Petroleum Transportation Piping Systems. ASME Code for Pressure Piping, B31. ANSI/ASME B31.4 - 1979 (B31.4).

5. Rules for Submarine Pipeline Systems. Det Norske Veritas, April 1981, reprint with corrections 1982 (DNV).
6. Code of Practice for Pipelines. Part 3. Pipelines subsea design, construction and installation. BSI, BS 8010 : Part 3 : 1993 (BS8010).

A seventh document:

7. Recommended Practice for Design, Construction, Operation and Maintenance of Offshore Hydrocarbon Pipelines. American Petroleum Institute API RP1111, 1993 (RP1111)

is relevant but was not included in the review.

Each of the codes and guidelines listed above was reviewed under the following headings:

- a. Conditions under which strain-based design would be acceptable
- b. Allowable strain limits in combination with other loads
- c. Buckling
- d. Ovalisation
- e. Effects of cumulative plastic strain
- f. Requirements for straightness following bending/straightening
- g. Effects on material properties, including toughness
- h. Requirements for welded sections.
- i. Recommendations on relevant testing, eg strain ageing, Charpy etc.
- j. Guidelines on the implications of low cycles fatigue for cases of repeated cycles of bending/straightening.

The detailed conclusions in respect of codes/guidelines as they relate to pipeline spanning (assuming that spanning is relevant to clauses related to pipeline systems during operation) were as follows:

- Most codes reviewed are similar in that design is divided into two phases: installation and operation. BS8010, DNV and B31.8 allow strain-based design to be used in both phases, the other codes make no reference to it. For the most part strain-based design is allowed in situations of predictable, non-cyclic, strain-limited displacement. BS8010, in the operation design phase, sets a limit to the pipe D/t ratio of 60.

- Allowable strain limits are dictated, non-specifically, by:
 - material ductility
 - weld properties
 - plastic strain history
 - fracture toughness
 - buckling
 - ovalisation limitations.

BS8010 limits the additional equivalent plastic strain in the operation phase to 0.1%. DNV places no limit other than as determined by the above criteria in the operation phase (see Section F.1.2.2, above).

- Most codes reviewed in the study require that the following modes of buckling are checked:
 - local pipe wall buckling
 - propagation buckling
 - restrained bar buckling.

Only BS8010 and DNV provide a range of formulations for these calculations, but of these only some of the BS8010 formulae are written in terms of strains. IP6 provides a pressure-only formula for local buckling.

- Codes reviewed require that ovalisation be limited. BS8010 provides a formula for calculations, but sets no prescribed limits, except that a minimum of 2.5% is to be used in buckling calculations. DNV prescribes a permissible ovalisation (BS8010 definition) of 1%. IP6 insists on a minimum ovalisation in buckling calculations of 1%.
- Guidelines on cumulative plastic strain are given only in the case of BS8010.
- There are no requirements for straightness following bending/straightening except as may be embodied in residual strain limitations.
- In general there is no specific guidance in respect of the effects on material properties of large straining. Guidance is limited to the specification of testing to ensure that material properties are still acceptable.
- The requirements for welded sections are, in general, restricted to the provision of adequate ductility and fracture toughness, and to the limiting of hardness. For straining in excess of 5% of C-Mn and C-Mn fine grain treated steels DNV requires

that welds are heat treated and are to have a hardness not exceeding 260 HV5.

- Most codes reviewed allow for the provision of additional testing if service conditions dictate that it is required, and this may encompass hardness, Charpy V-notch impact and crack tip opening displacement (CTOD) testing. DNV recommends strain ageing testing for materials that have been strained in excess of 3%.
- No particular recommendations are made in respect of the implications of low cycle fatigue in cases of repeated cycles of bending and straightening. Most codes state that such effects should be incorporated within the normal fatigue check calculations.

In general terms it was concluded that:

- Many of the currently available Codes incorporate the possibility of the use of strain-based criteria in the assessment of the strength and deformation of pipelines.
- There is no consistency from one Code to another with regard to the strain levels which may be permitted in assessment.
- There is not a comprehensive set of formulations which could be used together with strain-based criteria for the assessment of pipelines.

Table F.1.1, taken from OTN 94 186, summarises the findings of the document review.

Columns of the table correspond to the documents reviewed, whilst the rows correspond to the headings listed (a) to (j), above. Each row/column intersection is given a subjective grading according to the detail of coverage given to the subject by the document.

It should be borne in mind that the category given to subject areas must be viewed within the context of its detailed level of coverage as it relates to strain-based assessment techniques. For example, the DNV document gives a well-detailed formulation for addressing the problem of local buckling [part of subject © in the table] under load combinations, but it is stress-based and would be extremely difficult (if not impossible) to alter its make-up to be expressed in terms of strains. Coverage of the same subject by BS8010 has been deemed to be 'better' by virtue of the fact the formulations given are partially strain-based.

F.1.3.2 Reviews of Technical Information related to Pipeline Ovalisation and Strength

The purpose of this section of the OTN document was to survey and review the technical

information in the public domain (that was current at the time) which would allow engineers to evaluate the strength and safety of pipelines at large strains. Attention was concentrated on information related to ovalisation and strength under individually or collectively applied bending, pressure and axial force.

The principal conclusions from this review were as follows:

- The Brazier type of elastic analysis (with Poisson's ratio taken as 0.3 and 0.5) greatly overestimates ovalisations and, whilst conservative, may be uneconomic in practice.
- In modelling ovalisation analytically the following features should be included:
 - elasto-plastic material constitutive behaviour
 - longitudinal and circumferential stress/strain interaction
 - plasticity growth
 - longitudinal bending and ovalisation interaction
 - pressure and axial loading
 - initial states of out-of-roundness, strain and stress and longitudinal curvature
 - cycles of bending, unloading followed by re-bending or reverse bending.
- Few analytical techniques developed to date are able to model the majority of the effects listed above. Results from most of the techniques have poor correlation with experimental data, and currently are not in a form that would permit their application to pipeline assessment.
- Of the techniques examined in this study a particular analytical approach was shown to provide promising potential in respect of ovalisation calculation. It gives very good predictions when validated with the limited amount of good experimental data available. However, it would require fairly extensive development in order to incorporate the structural aspects listed above for a pipeline subjected to pressure and axial loading including initial states and cycles of bending.
- The experimental data currently available are focused on buckling and, to a less extent, on ovalisation. Little data is available in respect of extensive strain measurement in order to assess strain interaction and plasticity growth.
- Few tests have been performed to relate material properties (yield strength, ultimate strength, toughness and so forth) post-straining to those extant in the as-received condition. Results from available tests indicated that straining had the effects of

increasing the yield and ultimate strength, reducing the toughness, and increasing the brittle/ductile transition temperature but these effects are related to older material properties and may not be relevant to current pipeline steels.

- In respect of pure bending a flexure collapse formula must account for the differing responses of low and high diameter-to-thickness ratio pipes. It will be required to highlight the different failure modes for the full practical range of D/t ratios.
- There is a body of evidence that for the low D/t ratio pipes, collapse under pure flexure may occur at a bending strain very close to that of the collapse axial strain under pure axial compression. Verification of this is not currently possible owing to the lack of adequate experimental data for the flexural collapse of pipelines in the range $10 < D/t < 40$.
- Assessment of collapse under pure external pressure needs to consider the fact that low diameter-to-thickness ratio pipes, in the absence of initial imperfections, collapse in a plastic bifurcation mode rather than a hoop yield mode. Design formulae based on this latter concept may have a built-in lack of conservatism.
- Pressure collapse is imperfection sensitive. In the light of the fact that installation techniques may induce appreciable residual ovalisations, a rational basis for the computation of collapse pressure for ovalised pipes should account for this.
- To become relevant to a strain-based assessment regime, formulae for predicting collapse under individual loading (for example, axial compression and pressure) must reflect material response adequately in terms of plastic buckling (rather than through attainment of yield stress) through the use of tangent/secant moduli approaches.
- Simplified theories (ie. those not involving FE analysis) for computing strains when pipes are stressed inelastically and in which geometric non-linearities (buckling) can be ignored, can be evolved from the mathematical theory of plasticity and be designed to be perfectly general in terms of loads applied, boundary conditions and so forth.
- In all cases involving the plastic deformation of pipes under load combinations it is important to emphasise that the order, and manner, of load application affects the results in terms of plasticity growth and the magnitude of forces necessary for collapse.

- The effect of axial tension, when in a situation of combined tension and bending, is beneficial. It increases the magnitude of bending strain at which buckling occurs in a power-law manner. Formulae available in codes of practice to cover this form of inter-action either ignore this, or are not clear on the fundamentally different effects of axial tension and compression.
- Virtually no information was then available to formulate the basis of collapse envelopes for pipes under the combined action of flexure and axial compression.
- No simple formulations were then available to cover the situation of internal pressure combined with flexure. Evidence does exist, in the form of a limited quantity of experimentation and finite element studies (insufficient in total to provide a basis for the development of rational rules), that the presence of internal pressure has an ameliorating effect on the consequences of bending: ovalisation may be greatly reduced and bending buckling strains increased (possibly to the extent that, to all practical purposes, buckling is eradicated).
- External pressure has a profound effect on collapse under flexure, and this is due to the interaction of two destabilising force actions. Experimentation and finite element studies tend to suggest that collapse pressures are reduced by bending strains. This produces a collapse envelope that is convex-in, thus rendering linear collapse envelopes (as used in some codes of practice to quantify this interaction) inherently un-conservative.
- Successful analytical techniques have been evolved in the literature for the prediction of collapse envelopes, particularly so for the combined external pressure and flexure combination of loading. These techniques appear to correlate well with experimental results. However, development of these techniques into design office tools would require considerable effort.

F.1.3.3 Effects of High Strain Bending on Material Properties

The OTN report presented the results of various tests to evaluate the effects on material properties of bending pipe to high strain levels and straightening. The results relate to only two grades of steel, viz X42 and X52. The tests included:

- Bending of pipe during which the applied moments and strains were measured
- Tensile tests on specimens of material cut from pipes after bending and straightening and also from pipes in the as-delivered state

- Charpy impact tests on coupons machined from sections of pipes both prior to bending and after bending and straightening.

The following conclusions are drawn from a study of the results of the tests:

- The material yield stress is affected by straining to high levels, but not in a manner such as to reduce the strength of the material
- The ultimate stress of the material is not affected by bending pipes to high levels of strain
- The ductility of the material is reduced, but not significantly when the pipe is bent and straightened
- The toughness of the material, as measured by the failure energy in the Charpy impact test, is not significantly affected by subjecting the material to high levels of pre-strain of the bending-type used in the tests
- The toughness of the material in the weld affected zone is well in excess of that required in Codes for the material tests reported in the document.

Generally it should be noted that the tests reported and the conclusions relate to one cycle of bending and straightening. That is, the results are relevant to the assessment of the effects on material properties due to installation by reeling or passing through a J-tube or by the pipe conforming to the seabed contour. There is no information available to guide engineers on the assessment of the fitness for purpose of pipelines which have been subjected to moderate or large strains during a number of cycles of loading. Such situations may occur due to operational start-up and shut-down processes.

This last situation is very relevant to the design and assessment of high-pressure high-temperature pipelines and it was recommended that tests on materials likely to be used in pipelines during the next ten years should be tested under realistic conditions of applied strains to determine the effects on the material properties over a practical number of cycles.

F.1.3.4 Initial Proposal for Strain-Based Assessment Framework

The OTN document also presented some preliminary guidance to engineers involved in the assessment of pipelines who wished to use the state of knowledge, that was current at that time, of strain-based criteria. The guidance took the form of a number of points, some of which recommended the use of calculation techniques developed and detailed in the document. These

comprised: simplified elasto-plastic strain analyses in cases where no large geometric changes under loading occur; various Perry-based formulations for the strength of pipelines under individually applied bending, external pressure and axial compression; and formulations for the strength under load combinations. It was recommended that none of the preliminary guidance should be applied to situations where large strains are imposed during more than two cycles of bending or application of pressure and temperature loading.

F.1.4 JIP ON THE ESTABLISHMENT OF STRAIN-BASED CRITERIA AND ANALYSIS FOR THE ASSESSMENT OF SUBSEA PIPELINES

F.1.4.1 Objective of the Project and Scope of Work

The objective of the project (AME, 1996) was to establish a capability and provide the information for, the analysis and assessment of pipelines based on strain criteria. The scope of work covered the following:

- i. Perform tests on a range of pipe geometries and materials and assemble details of other tests to provide a basis for the validation of numerical and other analysis used during design and assessment.
- ii. Validate using the test results a range of finite element models which can be used to simulate the behaviour of pipelines.
- iii. Establish, using parametric studies undertaken with a standard finite element program, a comprehensive description of the structural and material behaviour of pipelines which are strained beyond the elastic limit in a variety of loading conditions.
- iv. Derive simplified relationships between loading and response for pipelines based on the finite element parametric studies.
- v. Establish strain-based criteria which can be used in design and assessment
- vi. Provide guidance on the use of strain-based criteria in the design and assessment of pipelines.

The Final Report for the project (AME, 1996) was very comprehensive and detailed, running to nine sections (Section 1 being the introduction, and Section 9 providing the references) and nine appendices (Appendix A to Appendix I). The Appendices covered detailed information not central

to the main thrust of the report, and these are not reviewed here. The other Sections of the report contained the following:

Section No	Scope
2	Review of design codes and guidelines
3	Review of previous work on pipeline behaviour
4	Pipeline testing
5	Finite element modelling
6	Parametric studies
7	Reliability-based assessment methodology
8	Design guidance

F.1.4.2 Review of Principal Sections of Final Report

F.1.4.2.1 Sections 2 and 3

These sections essentially repeat much of the information contained in the Offshore Technology Report OTN 94 186 (see Subsection F.1.2, above). The principal exception, however, was the fact that RP1111 was also reviewed under the same basis as the other documents. It added very little to the background information, as may be seen from Table F.1.2 (taken from Table 2.8 in the Final Report) where its coverage of strain-based approaches has been classified as no detail to poorly detailed, or poorly detailed to partly detailed.

F.1.4.2.2 Section 4: Pipeline testing

The objective of the tests was to obtain information on the behaviour of pipelines loaded in bending beyond their elastic limit. Overall, the tests were divided into two types: bending tests on prototype scale pipeline segments and material tests on tensile coupons extracted from the pipes.

The bending test programme comprised different pipe geometries (diameter to thickness ratios in the range 10-35) and different materials (API grades X52 to X70 and a single Duplex test). A total of 36 tests was undertaken with a view to determining the response to bending, including local buckling and ovalisation. The tests involved cycles of bending and reverse bending to various levels of strain. Both high and low strain cyclic bending were considered. The key parameters from the bending tests were:

- a. moment versus curvature (longitudinal strain) curve
- b. pipeline collapse behaviour

- c. diameter changes/ovalisation
- d. hoop strains

Material tests were performed on specimens taken from each section of pipe involved in the bending tests, with the intention of determining the effect of applied strain on material properties. Thus, coupons were extracted from regions of a tested pipe that had been subjected to maximum strain and least strain. The material properties/characteristics evaluated were:

- a. stress-strain curve
- b. elastic modulus
- c. yield strength
- d. strain hardening modulus
- e. Charpy V-notch impact toughness.

The detailed results from the bending tests can be found in the report, but it is worth noting some of the principal findings from the material tests, as follows:

- the strained materials displayed more rounded stress-strain curves between elastic and plastic regions, whereas the unstrained materials showed more pronounced characteristic yield points
- despite these difference near the yield point, the strained and unstrained materials have similar values of Young's moduli, and the different stress-strain curves tend to converge in the plastic region
- the stress at which the stress-strain curve becomes non-linear appears to be reduced following plastic deformation
- the Bauschinger effect reduces the yield strength of pipe to below API specified minimum values because of the rounding-off of the stress-strain curve compared with that of the unstrained material
- as regards material toughness, it was found that strain ageing and straining resulted in a general reduction in toughness of between 0% and 10%, although some showed a greater change than this.

F.1.4.2.3 Sections 5 and 6: Finite Element Modelling and Parametric Studies

Section 5 summarises the work undertaken on the development and verification of the finite element models used in the project. The general purpose finite element package ABAQUS was

used along with models which (via the supporting documents for ABAQUS) had already demonstrated their suitability for bending problems. Verification of the models was performed using the test results.

The models developed were based on two generic elements in the ABAQUS element library: ELBOW and SHELL. These were incorporated into three main finite element models, as follows:

- a. Elbow Element Model: these elements are similar to the PIPE elements used successfully in other pipeline engineering projects, but with the difference that deformation of the cross-section is permitted.
- b. 'Slice' finite element model: this model comprises a single element in the longitudinal direction and twelve around the circumference; the model was made to replicate the behaviour of an infinitely long pipeline segment by means of a user-subroutine that controlled the boundary conditions.
- c. Full shell finite element model: this had a number of elements in both the longitudinal and circumferential directions.

In addition to the performance of the various elements, the main plasticity models were also assessed during the course of the investigation. There are two main models both of which establish the onset of yielding using the von Mises yield surface in the standard way. The methods differ in the way that they handle work hardening: the manner in which the yield surface changes with plastic straining. Isotropic hardening assumes that the yield surface changes uniformly in all stress space directions as plastic straining occurs. In kinematic hardening the yield surface maintains its size but shifts its position according to plastic straining; in ABAQUS the kinematic model uses a bi-linear elastic-plastic equivalent stress-strain curve, ie it is a linear kinematic hardening rule.

Generally good agreement was obtained between the results generated by ABAQUS and the measured test data, especially for the moment-strain relationship during low-strain cyclic loading, and loading to high strain. The measured moment versus strain relationship for cyclic loading at high strain was the most difficult to replicate, the most success in these situations was achieved using a kinematic hardening model to simulate the Bauschinger effect associated with such loading patterns.

The validity of the finite element slice model for cyclic bending of pipelines was investigated. It was found that under constant curvature cycles the pipe progressively ovalised, with each increment of ovalisation being approximately constant for each cycle of loading. This was in

agreement with experiments in the literature, and after several cycles of loading a residual ovality became present in the pipeline, which subsequently built up until collapse occurred. The number of cycles required for a pipe to reach a level of ovalisation was found to be sensitive to the yield strength of the material specified. The isotropic hardening model was considered to be the most appropriate of the material representations for use in the parametric study of cyclic ovalisation.

In **Section 6** of the report the results of detailed parametric investigations made using the validated finite element models were set out. The objectives were to determine the effect of several parameters on the collapse behaviour of pipelines under flexure and develop simple mathematical expressions for the effects. The main mechanisms covered were:

- pure bending
- combined loading
- ovalisation under cyclic loading
- wrinkling

Of most relevance to the static strength of submarine pipeline spans are the mechanisms of pure bending, combined loading and wrinkling.

In the case of pure bending and combined loading the objective was to determine simple expressions for:

- critical or maximum moment (moment at collapse)
- critical curvature (curvature at collapse)
- ovalisation-curvature relationship during bending.

In the case of pure bending the following variables were considered in the analysis:

- i. outside diameter and D/t ratio
- ii. initial ovalisation
- iii. residual stress
- iv. material anisotropy (differing yield strengths for the material in the hoop and longitudinal directions)
- v. material strain hardening parameter
- vi. steel grade

It was found that normalised critical curvature was a quadratic function of pipe median diameter to thickness ratio, whereas initial ovalisation entered the ovalisation-curvature relationship as

a constant term. Residual stress had no significant effect on critical moment or curvature, but affected the ovalisation-curvature relationship once the yield stress was exceeded. It was found that the ratio of yield strengths in the circumferential and longitudinal directions had a significant effect on critical moment and curvature. The normalised moment and curvature increased in a nonlinear fashion with an increase in the reciprocal of the strain hardening parameter; this is because this affects the tangent modulus of the material which in turn critically determines collapse. The effects of steel grade were shown to correspond to the influences of the strain hardening parameter particular to the grade.

The combined loading studies determined pipeline collapse interaction relationships between bending moment or bending curvature and the force action concerned, and the influence of the force action on the ovalisation-curvature relationship. The forces considered were:

- axial force
- internal pressure
- external pressure

Thus, only bending in combination with one of these force actions was considered; flexure in co-existence with axial force and internal or external pressure (a very practical possibility) was not considered.

Axial force was shown to affect critical moment, critical curvature and the ovalisation-curvature relationship; the effects differed for axial tension and compression in the case of critical curvature. An increase in the internal pressure resulted in a drop in the critical moment accompanied by an increase in the critical curvature, the effects on the latter were found to be inconsistent and a lower-bound fit to the finite element results was obtained; the ovalisation-curvature relationship was shown to be highly dependent on the applied internal pressure, it reduced significantly the ovalisation for a given curvature. External pressure had a profound effect on critical moment, critical curvature and moment-curvature relationship; in general, the consequences of external pressure were the opposite of internal, but were more exaggerated owing to the instability phenomenon coupled to the influence of imperfections.

Wrinkling of a pipe occurs under compressive stress and, unlike sectional collapse described earlier, corresponds to the formation of short wavelength buckles in the longitudinal direction within the compressed region. Wrinkling is thus possible under bending, axial force, and a combination of the two. No finite element studies were performed in connection with this mechanism, but formulae from the literature were proposed for computing the onset of wrinkling as a result of axial compression or combinations of longitudinal and hoop stress.

F.1.4.2.4 Sections 7&8: Reliability-Based Assessment Methodology and Design Guidance

Section 7 of the report sets out the framework for the reliability-based assessment of pipelines and, as such, is considered to be outside the scope of the present work. **Section 8** presented design guidance for pipelines based on the information generated by the project; its principal value lies in the fact that the formulae relating to critical moment, critical curvature and ovalisation-curvature are summarised.

F.1.5 COMPARISON OF STRAIN LIMITS

F.1.5.1 Pipeline Considered

The purpose of this subsection is to make a comparison between the strain limits applicable to the static strength of a pipeline span derived from BS8010, DNV and AME (1996). The principal data relevant to this pipeline segment are summarised in Table F.1.3.

F.1.5.2 Preliminary Results and Basis of Comparison

The results from preliminary calculations on the pipeline segment are given in Table F.1.4.

The results cover the wall stresses in the pipeline for the prebending condition, in the hoop and longitudinal directions. Also shown are various pressures covering: the net internal pressure (difference between internal and external), internal yield pressure and the external pressure necessary to buckle the pipeline elastically. The prebending longitudinal force in the pipeline is given, along with the force necessary to yield it.

The principal observations to be made from these preliminary results are that:

- there is a net internal pressure in the pipeline giving a tensile hoop stress
- the longitudinal wall stress and force are both negative, indicating compression (this stems from an assumption of full axial fixity of the pipeline in the prebending condition in the longitudinal direction).

These observations are important because they dictate the usage of formulae necessary to compute the various strain limits, as indicated below.

The strain limits calculated relate to bending from the prebending membrane state. Two sets of formulae are used: the first set are taken from the AME Joint Industry Project Report reviewed above (AME, 1996); the second set are derived from limits dictated by BS8010 and DNV. In either case the bending strain limit and the corresponding equivalent plastic strain increment

were calculated; this allows comparison between the different formulations on two differing bases. The criteria used for setting strain limits were as follows:

- first yield
- 0.1% equivalent plastic strain increment
- 1% ovalisation
- collapse.

In the cases of the 1% ovalisation and collapse criteria, where formulae are available, the strain limits were computed for: pure flexure, flexure plus axial force, and flexure plus internal pressure.

BS8010/DNV Formulae

The first criterion used was a stress criterion where the maximum equivalent stress is set equal to the material yield strength. This is a first yield condition taken as follows:

$$\sqrt{[F_x^2 + F_2^2 - F_x F_2]} = F_0$$

where F_x = total longitudinal stress (membrane plus bending)
 F_2 = hoop stress
 F_0 = material yield strength.

The following formula was used for ovalisation (taken from BS8010):

$$\epsilon_o = \left[\frac{\delta}{C_p C_f} \right]^4 \left(\frac{t}{D} \right)$$

where ϵ_o = limiting ovalisation strain
 δ = ovalisation limit = 1% (from DNV)
 C_f = $0.06 \{1 + D/(120t)\}$
 C_p = $1/(1-P/P_e)$
 P = net external pressure
 P_e = $2E/(1 - \nu^2) \cdot (t/D)^3$
 t = pipe wall thickness
 D = pipe outside diameter.

For the example pipeline segment the net pressure is internal, so two calculations were performed with C_p set equal to unity, and P set equal to the negative of the net internal pressure.

This gave a benefit from the stabilising influence of the internal pressure.

Collapse under pure flexure only was considered for the BS8010/DNV formulae as follows:

$$\epsilon_{b, \text{lim}} = 15 (t/D)^2$$

where $\epsilon_{b, \text{lim}}$ = limiting ovalisation strain.

Joint Industry Project Formulae

For the example pipeline segment it was calculated that yield occurred first at the longitudinal compression fibre, and the following expression was derived relating total longitudinal bending strain and equivalent plastic strain increment.

$$\epsilon_{b, \text{bend}} = - (1.018 \times 10^{-3} + 0.894 d,^p)$$

where $\epsilon_{b, \text{bend}}$ = total longitudinal bending strain

$d,^p$ = equivalent plastic strain increment.

This formula was also used to calculate $d,^p$ from a given $\epsilon_{b, \text{bend}}$, and is based on the plasticity theory set out previously.

In the case of ovalisation calculations formulae were extracted from AME (1996) and rearranged to give the following bending strain limitations:

- ovalisation flexure only:

$$\epsilon_b = \left[\frac{\delta}{t_0} \right]^{\frac{1}{n_0}} \frac{Dt}{2D_m^2}$$

- ovalisation flexure plus compressive axial force:

$$\epsilon_m = \left[\frac{\delta}{t_0 A_4} \right]^{\frac{1}{n_0 + n_4}} \frac{Dt}{2D_m^2}$$

- ovalisation flexure plus internal pressure:

$$\epsilon_{of} = \left[\frac{\delta}{f_8 A_s} \right]^{\frac{1}{(k_1 + B_3)}} \cdot \frac{Dt}{2D_m^2}$$

- collapse flexure only:

$$\epsilon_c = f_7 f_{14} f_{19} \cdot \frac{Dt}{2D_m^2}$$

- collapse flexure plus compressive axial force:

$$\epsilon_{ca} = f_7 f_{14} f_{19} (1 - n_2 F_a^{n_2}) \cdot \frac{Dt}{2D_m^2}$$

- collapse flexure plus internal pressure:

$$\epsilon_{ci} = f_7 f_{14} f_{19} (1 + n_5 P_k^{n_5}) \cdot \frac{Dt}{2D_m^2}$$

where

$$f_7 = 0.853 + 0.00809 D_m/t$$

$$f_8 = 0.0108 + 0.00037 D_m/t$$

$$f_9 = 1.64 + 0.00296 D_m/t$$

$$f_{14} = 1$$

$$f_{19} = 0.592$$

$$n_2 = 6.71 - 0.321 D_m/t + 0.0041 D_m/t$$

$$n_3 = 2.33 - 0.036 D_m/t$$

$$n_5 = 1.98$$

$$n_6 = 1.28$$

$$A_4 = 1 + 0.0258 F_a + 2.32 F_a^2$$

$$B_4 = 0.0637 F_a + 0.946 F_a^2$$

$$A_5 = 1 - 1.2 P_{ix} + 0.401 P_{ix}^2$$

$$B_5 = -1.15 P_{ix} + 0.736 P_{ix}^2$$

$$F_a = F_{co} / (BF_o D_m t)$$

$$P_{ix} = (p_i - p_a) / P_{iy}$$

$$D_m = \text{pipe median diameter}$$

$$F_o = \text{material yield strength}$$

$$F_{co} = \text{axial force in pipe wall}$$

$$p_i = \text{internal pressure}$$

$$p_a = \text{external pressure}$$

$$P_{iy} = F_o (2t/D) \text{ for } D/t > 20$$

$$= F_o (D^2 - D_i^2) / (D^2 + D_i^2) \text{ for } D/t \# 20$$

$$D = \text{pipe outside diameter}$$

$$D_i = \text{pipe inside diameter}$$

F.1.5.3 Results from Comparison

The results of all the strain calculations are summarised in Table F.1.5. Strain limits are given for the criteria indicated and the two sets of formulae. Total bending strain and equivalent

plastic strain increment are given in per cent.

In comparing the bending strain limits it is seen that, for obvious reasons, first yield and 0.1% equivalent plastic strain set the lowest limits. For the AME formulae the 1% ovalisation limit is always less than the corresponding collapse limit. The opposite of this is true for the BS8010/DNV formulae, where only the flexure-only results may be compared between these two criteria.

The effects of axial force in the case of the AME formulae are seen to reduce the strain limits from the pure flexure ones; the reduction is negligible in the case of the ovalisation limit, but is larger in the collapse case. The beneficial effects of internal pressure, in terms of increased limits from those set by pure flexure, are shown by the AME formulae; the limit is very nearly doubled in the case of the collapse criterion. Similar gains are shown by the BS8010/DNV formulae in the case of ovalisation.

Generally the AME limits are more onerous than those set by BS8010/DNV in the case of ovalisation, but allow larger limiting strains for the collapse criterion.

F.1.6 CLOSING REMARKS

Criteria are available from existing pipeline design codes and guidelines for determining the static strength of pipeline spans. It is broadly agreed that the criteria from these sources are overly conservative and very limited in their scope.

BS8010, for example, sets the equivalent plastic strain increment as 0.1% plus other material requirements after high straining. Indications are, however, that strains of up to 5% can be tolerated in X52 and X46 pipeline materials without undermining their safety (OTN 94 186, 1994). Whilst this would represent a large step change in term of material limitation, it does throw more emphasis onto the criteria set by, for example, ovalisation and section collapse which tend to set limits in excess of the 0.1% plastic strain increment criterion, but much less than a 5% total strain limit.

Some formulations are available in the codes/guidelines for ovalisation and local buckling calculations but these do not cover the whole range of force combinations that a pipeline span is subject to. The JIP work (AME, 1996) represents the most comprehensive approach to date in terms of the influence of load combinations on ovalisation and section collapse. This too has its limitations insofar as it covers loadings combining flexure with pressure or axial force in pairs, but does not deal with flexure, axial force and pressure acting simultaneously.

Nevertheless it would be extremely useful to extract from the JIP report a subset of criteria relevant to pipeline spanning and to develop the strain limitations across the full range of pipelines in Amoco's North Sea operations, as a precursor to investigating the effects these have on allowable span length.

F.1.7 REFERENCES

1. AME (1996). 'Establishment of strain-based criteria and analysis for the assessment of subsea pipelines. Final report'. Project Review Report AME/26563/R/04, August 1996.
2. BS8010: Part 3 (1993). 'Code of Practice for Pipelines. Part 3. Pipelines subsea: design, construction and installation'. BSI 1993.
3. Det Norse Veritas (DNV) : 1981 (Reprint with corrections 1982). Rules for Submarine Pipeline Systems.
4. OTN 94 186 (1994). 'Investigation of structural and material implications of bending pipelines to large strains'. Offshore Technology Report OTN 94 186. Commercial in Confidence PEN/K/3066, September 1994.

		BS8010	DNV	B31.8	B31.4	DEnGN	IP6
a	Acceptable conditions	T	T	?	x	x	x
b	Strain limits	?	?	x	x	x	x
c	Buckling	T	?	x	x	x	x
d	Ovalisation	?	?	x	x	x	x
e	Cumulative plastic strain	x	T	x	x	x	x
f	Out-of-straightness	x	x	x	x	x	x
g	Material properties	T	T	x	x	x	x
h	Welded sections	?	?	x	x	x	x
l	Testing	T	T	x	x	x	x
j	Low cycle fatigue	x	x	x	x	x	x
k	Availability of strain-based criteria	?	?	x	x	x	x
<p>Key: x = No detail to poorly detailed coverage ? = Poorly detailed to partly detailed coverage T = Partly detailed to well detailed coverage * = Well detailed to explicitly detailed coverage</p>							

Table F.1.1 Coverage detail of strain-based assessment in codes reviewed in OTN 94 186 (1994)

		BS8010	DNV	B31.8	B31.4	DEnGN	IP6	RP1111
a	Acceptable conditions	T	T	?	x	x	x	?
b	Strain limits	?	?	x	x	x	x	x
c	Buckling	T	?	x	x	x	x	?
d	Ovalisation	?	?	x	x	x	x	x
e	Cumulative plastic strain	x	T	x	x	x	x	x
f	Out-of-roundness	x	x	x	x	x	x	x
g	Material properties	T	T	x	x	x	x	x
h	Welded sections	?	?	x	x	x	x	?
l	Testing	T	T	x	x	x	x	x
j	Low cycle fatigue	x	x	x	x	x	x	x
k	Availability of strain-based criteria	?	?	x	x	x	x	x
<p>Key: x = No detail to poorly detailed coverage ? = Poorly detailed to partly detailed coverage T = Partly detailed to well detailed coverage * = Well detailed to explicitly detailed coverage</p>								

Table F.1.2 Coverage detail of strain-based assessment in AME (1996) [As Table 3.1, but updated to include RP 1111]

Pipe outside diameter	D	762 mm
Pipe wall thickness	t	17.5 mm
Steel Young's modulus	E	207 GPa
Steel Poisson's ratio	ν	0.3
Steel yield strength	F_o	358 MPa
Steel coefficient of thermal expansion	"	$1.16 \times 10^{-5} //C$
Maximum internal operating pressure	p_i	9 MPa
Contents temperature	2_i	38 /C
Minimum water depth at LAT	d	28m
Local seawater density	D_w	1025 kg/m ³
Local seawater temperature	2_a	8 /C

Table F.1.3 Pipeline data

External pressure on pipe	p_a	0.281 MPa
Net internal pressure on pipe	p_{ico}	8.719 MPa
Hoop stress	F_2	185.5 MPa
Prebending longitudinal stress	F_{xo}	-16.4 MPa
Prebending longitudinal force	F_{co}	-0.671 MN
Longitudinal yield force	F_{aco}	14.65 MN
Internal yield pressure	P_{iy}	16.4 MPa
Elastic buckling pressure	P_e	5.5 MPa

Table F.1.4 Pipeline results (full axial fixity assumed)

CRITERION	AME FORMULAE		BS8010/DNV FORMULAE	
	Bending Strain (%)	Equivalent Plastic Strain Increment (%)	Bending Strain (%)	Equivalent Plastic Strain Increment (%)
First yield ($F_{eqv} = F_o$)	0.102	0.000	0.102	0.000
0.1% equivalent plastic strain	0.191	0.100	0.191	0.100
1% ovalisation: pure flexure	0.692	0.660	0.803	0.785
1% ovalisation: flexure plus axial	0.691	0.659	-	-
1% ovalisation: flexure plus internal pressure	1.013	1.019	1.291	1.330
Collapse: pure flexure	0.853	0.840	0.791	0.771
Collapse: flexure plus axial	0.818	0.801	-	-
Collapse: flexure plus internal pressure	1.602	1.678	-	-

Table F.1.5 Pipeline Results: strain limits from AME formulae (AME, 1996) and BS8010/DNV formulae
In terms of bending strain and equivalent plastic strain increment

APPENDIX G

RECOMMENDED INSPECTION STRATEGY

TABLE OF CONTENTS

Page No

G.1 PROPOSED IRM STRATEGY

- G.1.1 SUMMARY
- G.1.2 SYSTEM DEFINITION
- G.1.3 STAGE 1: INITIAL ANALYSIS
- G.1.4 STAGE 2: PROPOSED INSPECTION AND MAINTENANCE SCHEDULE
- G.1.5 STAGE 3: UPDATED ANALYSIS

G.2 INPUT REQUIRED

- G.2.1 SUMMARY
- G.2.2 PIPELINE DATA
- G.2.3 DEFINITION OF PIPELINE FAILURE MODES, LIMIT STATES AND TARGET RELIABILITIES
- G.2.4 PROBABILITY ANALYSIS
 - G.2.4.1 Assessment of hazard likelihood of occurrence
 - G.2.4.2 Failure models
 - G.2.4.3 Basic variable statistics
 - G.2.4.4 Component and system reliability analysis
- G.2.5 CONSEQUENCE MODELS
 - G.2.5.1 Fire and blast analysis results
 - G.2.5.2 Economic considerations
 - G.2.5.3 Life-safety considerations
- G.2.6 INSPECTION METHODS, COSTS AND MEASUREMENT UNCERTAINTY
- G.2.7 MAINTENANCE AND REPAIR METHODS, AND COSTS

G.3 REFERENCES

LIST OF TABLES

Table G.1.1 'Acceptable' failure probabilities (for design) from the SUPERB project [31]

LIST OF FIGURES

Figure G.1.2 Illustrative variation of predicted reliability index with time for a single failure mode
Figure G.1.3 Years to next inspection
Figure G.1.4 Illustrative variation of evaluated reliability index with time throughout pipeline life
Figure G.1.5 Flowchart for STAGE 1 : Initial analysis
Figure G.1.6 Flowchart for STAGE 2 : Propose and assess IRM schedule (Preposterior analysis)
Figure G.1.7 Flowchart for STAGE 3 : Update analysis based on inspection results (Posterior analysis)
Figure G.2.1 Illustration of the joint failure point for the intersection of two events

G.1 PROPOSED IRM STRATEGY

G.1.1 SUMMARY

This appendix outlines a risk and reliability-based integrity management system to optimise planning strategy for application to pipeline inspection. The strategy considers both:

- the long term reliability of the pipeline system to ensure that confidence in the integrity of the pipeline is maintained, and
- cost-based risk so that the expected costs of alternative inspection schemes can be compared and minimised on a rational basis.

The proposed strategy is generic in nature, flexible and modular. The strategy can be applied to major transmission lines as well as infield lines, and the methodology can be applied to platform pipework, risers and spool pieces, as well as subsea pipelines. Statutory, Company, or Asset Manager inspection requirements can be readily included in the procedure. A preliminary assessment or 'first-pass' can be undertaken with simple engineering models and published/existing company data, and once critical areas have been identified, more sophisticated models and analysis techniques can be used to improve the assessment. The basic methodology is modular so that future analysis techniques, data and knowledge can be incorporated.

The strategy is based on structural reliability theory which is widely recognised as providing a rational basis for a decision process. Application of reliability techniques enables an appropriate and organised treatment of uncertainties and thus facilitates a consistent assessment of the safety and serviceability of the pipeline.

Essentially, there are three main stages to the strategy which are aimed at the following questions:

- i. What is the present state of the pipeline? (Initial analysis)
- ii. How do we plan for the future? (Inspection schedule preparation)
- iii. How do we monitor the state of the pipeline and update the plan when new information becomes available? (Schedule updating)

The aim of each of the stages is briefly outlined below, and flowcharts illustrating the main steps for each of the three stages are shown in Figures G.1.5 to G.1.7. Each stage is discussed in detail, and a number of examples and Figures have been included to illustrate the techniques involved and typical results that may be obtained - *all examples in this appendix are purely illustrative.*

1) Initial analysis

The first stage of the procedure is to assess both the existing present-day reliability, the risk to life and the cost-based risk of the pipeline, and to assess the variation in these quantities with time (assuming that no inspection or maintenance is undertaken).

The purpose of this task is to identify critical areas and effects dominating the reliability or risk of the pipeline, and to serve as a baseline against which to compare alternative inspection schemes. The results may also show how quickly the reliability of the pipeline becomes unacceptable without any inspection or intervention.

2) Inspection schedule preparation

Based on the results of the first stage, the second stage is to assess and propose a strategy for future inspection and maintenance.

By predicting or forecasting the results of each planned inspection, the reliability assessment of the pipeline can be updated. The plan should ensure that the forecast reliability of the pipeline is acceptable throughout the (anticipated) operating lifetime, and that the risk to life and the environment remains *tolerable*.

Using the costs of inspection, maintenance tasks and repair methods, and based on the (forecast) likelihood of defects/anomalies occurring, the pipeline cost-based risk can also be updated. Alternative inspection schemes can be proposed and then assessed and compared on a rational basis. Thus, risk analysis can be used as a tool for decision making to define the 'best' inspection schedule on the basis of existing knowledge.

3) Schedule updating

The third stage is undertaken once new knowledge is available about the pipeline. New knowledge may, for instance, be due to a change in the operating conditions of the pipeline, or may arise from the results of the first inspection(s). This new information reduces the uncertainty about the state of the pipeline, and can be used to update the reliability and risk assessment using Bayesian theory. Hence, the

inspection schedule can be redefined for the remaining life of the pipeline.

Thus, although initially a full inspection schedule is produced, it may only be the first inspection that is carried out to plan. The schedule for the remaining life of the pipeline is updated based on the best available information at the time, and consequently a number of schedules may be produced at intervals throughout the life of the system.

G.1.2 SYSTEM DEFINITION

The first task is to split the pipeline into zones or segments with *common attributes*; that is:

- hazards,
- failure modes,
- failure consequences, and
- inspection methods.

A typical zoning scheme for a transmission pipeline might be:

- i. platform pipework;
- ii. above water riser - from the topside ESD valve to MSL;
- iii. below water riser - from MSL to the spool piece/riser flange;
- iv. the spool piece;
- v. subsea pipeline in platform safety zone (within 500m of the platform);
- vi. mid-line or open water pipeline;
- vii. shore zone;
- viii. land pipeline.

Each zone can then be analysed individually, and an inspection and maintenance schedule could be defined for each zone. Alternatively, the approach is flexible enough that the reliability and risk results for a number of zones can be compared and combined to define inspection schedules for larger segments of the pipeline, or for one schedule encompassing the whole pipeline. (However, lumping failure consequences together for different zones may not lead to the most economic solution.)

G.1.3 STAGE 1: INITIAL ANALYSIS

Step 1.1 Identify hazards, failure modes and limit states

For each pipeline zone, the first step is to identify all of the hazards that can affect the integrity and operation of the pipeline.

It is important that **all** of the hazards are identified since the omission of a hazard will mean that the study will be incomplete, and the resulting inspection schedule may not be capable of detecting a potential failure mechanism in time.

For each hazard the potential failure modes need to be identified, and these need to be linked with limit states.

A number of definitions for the limit states for operating pipelines have been proposed. One of the most popular definitions, which has been adopted by the SUPERB project (for Submarine Pipeline Reliability Based Design Guideline) [1, 2], is based on four limit states which are defined as follows.

The *Serviceability Limit State* (SLS) requires that the pipeline must be able to remain in service and operate normally (although the integrity may be impaired), and includes the following modes:

- yielding;
- section ovalisation which prevents pigging;
- ratcheting;
- loss of concrete coating.

The *Ultimate Limit State* (ULS) generally corresponds to the maximum load bearing capacity criteria, and includes the following failure modes:

- bursting;
- buckling;
- plastic collapse;
- unrestrained plastic flow;
- unstable fracture;
- tensile rupture.

The *Fatigue Limit State* (FLS) results from excessive fatigue crack growth and damage accumulation under cyclic loading. This is an ULS referring to the entire life time of the pipeline.

The *Accidental Limit State* (ALS) corresponds to ultimate failure due to accidental

loads and/or local damage of the pipeline with loss of structural integrity and rupture.

The limit states are used in the definition of target reliabilities (Step 1.2). Alternative definitions for limit states may be adopted with appropriate targets.

When it comes to assessing the likelihood of a hazard occurring (Step 1.3), it may be helpful to identify both the event initiating each hazard and the possible effects that may be caused. For example, an event initiation due to a trawl beam impact may lead to weight coat damage, anode damage, pipe denting, gouging, or rupture.

It is also useful to identify whether the hazard leads to a failure mode which is instantaneous or whether it leads to a mode which affects the long term integrity of the pipeline.

- Hazards leading to instantaneous failure generally affect the *Accidental Limit State*, and include: dropped objects, dragged anchors, and severe trawl beam impacts.
- Hazards which are solely a time-varying effect leading to the long term degradation of the pipeline include: external and internal corrosion, erosion, and fatigue.
- Hazards which may be both include gouging due to trawl beam impact leading potentially to instantaneous rupture or to a stress-raiser for fatigue. Scour leading to pipeline spanning is also a hazard that may lead either to very rapid failure if the span and wave and current conditions are such that severe cross flow vortex shedding 'locks-on', or if the vibration is less serious and occurs infrequently it may lead to fatigue degradation.

Step 1.2 Assess target reliabilities

For each pipeline zone and limit state, the next step is to assess an acceptable target reliability.

An assessment of the target reliability(s) should consider the actual consequences and nature of failure, economic losses and the potential for human injury or environmental pollution. Ideally, targets should be calibrated with well-established designs that are known to have adequate safety, and actual failure statistics are useful in the assessment if interpreted carefully.

A number of organisations have proposed target reliabilities for use in the absence of better information for a wide variety of structures, including offshore platforms and pipelines. For submarine pipelines, the most recent and comprehensive assessment has been undertaken as part of the SUPERB project, and their target failure probabilities are shown in Table G.1.1. (It should be noted that appropriate units have to be considered to ensure system safety).

SUPERB's proposed targets for the various limit states are based on the *safety class* of the pipeline zone. A *low* safety class corresponds to a pipeline conveying nonflammable water-based products (ie not a Major Accident Hazard Pipeline); a *high* safety class corresponds to the (subsea) sections of oil or gas pipelines within the platform safety zone, ie within 500m of the platform; and the *normal* safety class corresponds to oil or gas pipelines in open water.

The SUPERB targets were primarily developed for the design of new submarine pipelines and they may not be directly applicable to the reassessment of existing pipelines. Nevertheless, they offer a very useful reference point.

Limit State Category	Safety Class		
	Low	Normal	High
Serviceability (SLS)	$10^{-1} - 10^{-2}$ (per year)	$10^{-2} - 10^{-3}$ (per year)	$10^{-2} - 10^{-3}$ (per year)
Ultimate (ULS)	$10^{-2} - 10^{-3}$ (per year)	$10^{-3} - 10^{-4}$ (per year)	$10^{-4} - 10^{-5}$ (per year)
Fatigue (FLS)	10^{-3} (per lifetime)	10^{-4} (per lifetime)	10^{-5} (per lifetime)
Accidental (ALS)	10^{-4} (per km per year)	10^{-5} (per km per year)	10^{-6} (per km per year)

Table G.1.1 'Acceptable' failure probabilities (for design) from the SUPERB project [31]

Step 1.3 Assess likelihood of each hazard and probability of failure

For each hazard or potential cause of failure, the next step is to estimate the probability of exceedence for each relevant limit state.

For a preliminary assessment, generic databases of pipeline failures can be used; the most recent and comprehensive database for North Sea pipelines and risers is PARLOC (Pipeline and Riser Loss of Containment study) [3]. PARLOC is based on data relating to 17,245km of pipelines since 1975, and can be used to assess the likely loss of containment frequency due to different failure causes in the various pipeline or riser zones, depending on the pipeline type, diameter, length, contents, and age.

Whilst generic data is acceptable for a preliminary assessment, these data must be used with care since the particular circumstances of failure incidents may not be known. In addition, the PARLOC database at least, does not record the inspection and maintenance systems for the incidents.

More detailed analyses related to a specific pipeline can be undertaken by assessing the likelihood of a hazard or cause of failure occurring, and then evaluating the probability of failure given that the hazard scenario has occurred. Thus, the probability of failure due to a hazard **A** is evaluated from:

$$P[A] = L[H] \times P[A|H] \quad (G.1.1)$$

where **L[H]** is the likelihood of a hazard occurring per year per km,
and **P[A|H]** is the probability of failure of the pipeline given that the hazard has occurred.

For some hazards it is almost certain that they are likely to occur, ie **L[H] = 1.0**, for instance internal corrosion and fatigue. For other hazards the likelihood of occurrence can be based on subjective judgement, historical records, or by a detailed assessment of all of the relevant data. For example:

- trawling hazards can be assessed by studying historical records of fishing activity in the area, and the depth and extent of burial/exposure of the pipeline;
- the likelihood of a dropped container hitting the pipeline can be assessed from the number of seaboard movements made by the platform crane per year, crane failure rate statistics, and by using hydrodynamic analysis of a free-falling object to assess the probability of hitting the pipeline on the seabed.

It is also necessary to estimate or evaluate the probability that the pipeline will exceed the limit state criterion under the scenario that a hazard has occurred, ie **P[A|H]**. For a preliminary 'first-pass' analysis a subjective assessment may be made; for a more detailed assessment structural reliability methods may be used, which may be made as sophisticated as necessary.

The main requirements for undertaking a structural reliability analysis are:

- an analytical model for assessing exceedence of the limit state criterion, this is known as the *failure function*;
- an assessment of the natural variability and uncertainty of all of the parameters influencing the failure criterion.

At its simplest, a failure function, **Z**, can be defined as:

$$Z = R - S \quad (G.1.2)$$

where R is the strength or strength effect,
and S is the load or load effect.

R and S , and/or Z may of course be complicated functions. For all of the main failure modes adequate failure functions can be formed from the deterministic analysis models presently used in assessment. More sophisticated models can be substituted if necessary.

The (annual) probability of failure due to a failure mode or hazard i , P_{f_i} , is given by:

$$P_{f_i} = P[Z_i \leq 0] = \int_{Z_i=0} f_x(x) dx \quad (\text{G.1.3})$$

where $f_x(x)$ is the probability density function for the basic variables.

There are basically three main types of uncertainty that are relevant and which should be included in the analysis, these are:

- i. Physical uncertainty which is due to the natural variability of the input quantities, such as: SMYS, wall thickness, ovalisation, wave and current velocity parameters, span length etc.;
- ii. Statistical uncertainty which arises from the uncertainty in estimating the parameters of the probability distributions due to limited data;
- iii. Model uncertainty which arises from the idealisations and inaccuracies of the engineering models used to predict loading and resistance.

A number of well-researched techniques have been developed for undertaking structural reliability analysis, including first and second order methods (FORM/SORM), and a variety of Monte Carlo simulation approaches.

The failure probability may be defined on an annual basis or for some other reference period depending on how the failure function and the basic variables, and the likelihood of occurrence, are defined. When probabilities of failure are compared with target probabilities it is clearly important that they are compared on a consistent basis, that is annual targets with annual probabilities, lifetime with lifetime, etc.

Step 1.4 Evaluate system failure probability

For each failure mechanism, for example cross-flow vortex shedding due to spanning, the failure

probabilities for each span are then combined to evaluate the total failure probability for the pipeline zone (or for the whole pipeline). Then for each limit state the system probability is derived by combining the failure probabilities for each failure mechanism.

Pipelines can be considered to be *series systems*, since the failure of any one part due to any failure mode is failure of the system. Thus, strictly the union of the probabilities for each failure event should be computed. Simple bounds on the system probability may be evaluated as:

$$\max_{i=1}^q (P_{f_i}) \leq \left(P_{f_{sys}} = \bigcup_{i=1}^q (P_{f_i}) \right) \leq 1 - \prod_{i=1}^q (1 - P_{f_i}) \quad (G.1.4)$$

In practice the bounds are likely to be too wide for practical use. However, they can be improved by judging the likely correlation between the events. Thus, for events which are highly correlated, for instance general corrosion between one section and the next, the combined probability will be dominated by the maximum individual failure probability.

For highly correlated events:

$$P_{f_{sys}} = \max_{i=1}^q (P_{f_i}) \quad (G.1.5a)$$

However, for different failure modes and hazards most of the failure events will be largely uncorrelated, and a reasonable and conservative estimate can be obtained by evaluating and combining the probabilities for the individual events thus:

For largely uncorrelated events:

$$P_{f_{sys}} = 1 - \prod_{i=1}^q (1 - P_{f_i}) \quad (G.1.5b)$$

Step 1.5 Evaluate time-varying probability

Based on estimates of corrosion rates, scour rates, crack growth, etc., the reliability analysis can be repeated to assess the likely deterioration in reliability with time by undertaking the analysis at yearly (or more frequent) intervals. The uncertainty in predicted corrosion rates, scour rates, etc., should of course be included in the reliability analysis; the uncertainty in these rates is one of the main reasons for undertaking inspections.

The likelihoods and failure probabilities for most of the events affecting the Accidental Limit State are, or can be assumed to be, constant from year-to-year. However, this is not so for most of the events affecting the other limit states.

The variation in system probability with time can then be evaluated using Eqns (G.1.5a) or (G.1.5b) for each time interval.

Step 1.6 Reliability-based assessment

At this stage, for each limit state it is possible to plot the variation in (annual) failure probability and/or reliability index against time, and to compare these with the target probabilities or equivalent reliability indices.

On the same plots it is also useful to show curves for each of the contributing failure hazards and/or failure modes. This gives a graphical indication of the most dominant failure modes, the critical hazards, and indicates the time when the predicted reliability of the pipeline becomes unacceptable.

An illustration of such a plot is shown in Figure G.1.1. In the Figure, failure modes 1 and 2 show little or no deterioration in reliability with time. Initially failure mode 3 is the least likely to occur, however after 5 years this mode dominates the system reliability and leads to a rapid fall in reliability. The reliability becomes unacceptable after 12 years in this example, indicating that an inspection is necessary before this time.

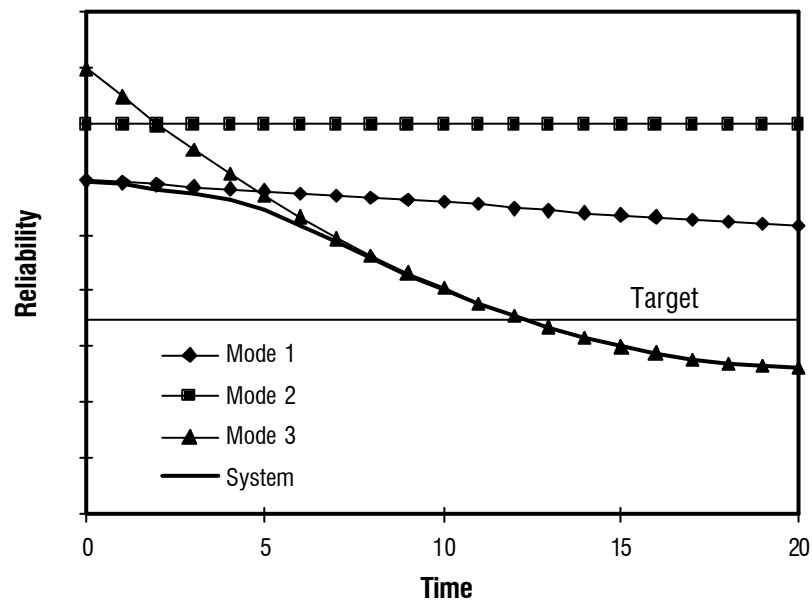


Figure G.1.1 Illustrative variation in reliability for different failure modes with time

Step 1.7 Assess consequences of failure

For a risk-based assessment it is necessary to assess the consequences of failure. Depending on the contents and pressure of the pipeline, and the type and location of the failure, the consequences may be purely economic, they may involve environmental damage, and/or they may lead to injury and / or loss of life.

For mid-line or open water pipelines, and for all zones of pipelines to / from unmanned platforms, the consequences of failure are largely economic.

The cost of failure of a pipeline is likely to include:

- loss of production,
- non-delivery penalty charges,
- loss of product,
- environmental pollution clean-up/mitigation,
- legal fees/fines,
- negative publicity,
- equipment damage,
- property damage.

For most pipelines the majority of the cost associated with a mid-line failure may be associated with lost production which can be readily assessed. For shared lines, non-delivery penalty charges are also likely to be significant, and again these can be readily defined. The cost of the lost product, ie the volume of product within the pipeline and lost before flow can be shut off, can also be easily estimated.

Pollution clean-up costs relate primarily to oil flowlines; whilst it may be difficult to estimate clean-up costs, they are unlikely to be a significant contribution to the total cost of failure. Environmental damage may lead to negative publicity, boycotting of the operator's products etc., and may also lead to significant fines and increased effort and costs in securing future operating licences. In the worst case scenario these costs are almost impossible to estimate.

For risers, sections of pipeline within the platform safety zone, and high pressure gas lines the consequences of a pipeline rupture are more serious; they may affect the integrity of the platform, wells and other flowlines, and may be such that human lives are put at risk. More detailed analyses of failure scenarios may be undertaken to assess the likelihood of jet/pool fires, flash fires, explosions, toxic clouds, etc., and to estimate their effects to the platform and to the personnel onboard. Consequence analysis of this type is often undertaken using Event Tree Analysis (ETA).

The consequences to human life / injury should be reported separately since these are treated differently in the risk analysis from economic consequences.

For onshore sections of pipeline, the hazard to the general population is an additional consideration.

As in inspection schedule for a pipeline is over the long term, inflation or the real rate of return should be taken into account. It is usual practice for expected costs to be discounted to nett present-day values.

Step 1.8 Assess present risk and time-varying risk

There are many definitions of *risk*. Of relevance here is a definition based on a function of the probability of failure and the consequences of failure. Conventionally, the function is defined as the product of the two terms. Thus,

$$\text{Risk} = \text{function}(P_f, \text{Consequences}) = P_f \times \text{Consequences} \quad (\text{G.1.6})$$

As discussed above, the consequences of failure for pipelines are primarily economic losses, but for risers and pipework within the platform safety zone there is the potential for human injury or loss of life.

One approach to treating different types of consequences is to define a utility function which ranks different combinations of cost and life loss according to their perceived impact. By its very nature, such an approach is highly subjective. Furthermore, in a complex risk assessment for a long pipeline it is possible that the economic consequences may have the effect of outweighing the effects to life.

A different approach, which may be considered a 'Best Practice', is to seek to *minimise* the expected costs whilst *constraining* the potential for life loss to be below an acceptable limit - *an ALARP limit* (As Low As considered Reasonably Practicable). This is known as *constrained optimisation*. It is clear that the constraint limits or target reliabilities for pipeline zones where there is potential for loss of life should be particularly carefully assessed to ensure that they are ALARP.

Risk at a time t can be measured by the *expected cost of failure*, $E[C_f(t)]$. The expected cost of failure is given by:

$$E[C_f(t)] = P_{f_{\text{net}}}(t) \frac{C_f}{(1+r)^t} = \sum_{i=1}^m P_{f_i}(t) \frac{C_{f_i}}{(1+r)^t} \quad (\text{G.1.7})$$

where $P_{r_{\text{sys}}}(t)$ is the system probability of failure for time t ,
 $P_{r_j}(t)$ is the probability of failure due to hazard or failure mode j for time t ,
 C_{r_j} is the consequential cost of failure (discounted to NPV) for hazard or failure mode j ,
 r is the real rate of return,
and m is the total number of hazards or failure modes.

The expected cost of failure can be regarded as the average cost incurred through failure over a long period of time.

Step 1.9 Risk-based assessment

It is useful to plot graphs of cost-based risk against time. On the same plots it is also useful to show curves for each of the contributing hazards and / or failure modes.

While in the early years of a pipeline's life the consequences of failure are high, and (once the pipeline settles down and stabilizes) the failure probability is low. With time the consequential costs of failure of the pipeline may fall, however the failure probability increases due to material degradation etc. Typically, a plot of risk against time shows risk falling initially, then levelling off, and after a time the risk starts to increase as the strength of the pipeline deteriorates and the pipeline becomes more likely to fail (see the 'Failure Costs' curve in Figure G.1.2). A rapidly rising curve should be avoided, and indicates that an inspection or reduction of the operating pressure may be beneficial.

G.1.3.1 Sensitivity measures

As well as graphical plots of the variation in reliability and risk with time, the rate of change of reliability $(\partial B/\partial t)$ or failure probability $(\partial P_r/\partial t)$ may be a useful measure; by including the consequences of failure the rate of change in cost-based risk can also be assessed. The rate of change of reliability and risk can also be assessed for each hazard which may help to indicate rapidly changing effects. The hazard rate function $h(t)$, which is defined as:

$$h(t) = \frac{(\partial P_r(t)/\partial t)}{1 - P_r(t)}$$

expresses the likelihood of failure in the time interval t to $t+dt$ as $dt \ll 1$, and is a popular sensitivity measure.

If FORM/SORM reliability analysis is undertaken, parametric sensitivities can be obtained for any statistical (eg. mean or standard deviation) or deterministic parameter entering the reliability analysis. This is useful in identifying dominant parameters, and may indicate where improved inspection or knowledge may be useful.

G.1.4 STAGE 2: PROPOSED INSPECTION AND MAINTENANCE SCHEDULE

Step 2.1 Propose inspection and maintenance schedule

Based on a detailed assessment of the results from the first stage, a *candidate* inspection and maintenance schedule can be proposed. An initial assessment of the existing inspection schedule can be used as a comparison with other schemes, and as a basis for schedule optimisation.

Step 2.2 Assess inspection measurement uncertainties

The measurement uncertainties associated with the proposed inspection techniques need to be considered since each method has different capabilities for observing and reporting defects. The inspection capabilities that need to be addressed include:

- detection limits,
- probability of detection,
- sizing accuracy,
- repeatability,
- locational accuracy.

Step 2.3 Estimate probability of maintenance or repair

Based on the estimated growth rate and the type and quality of the inspection planned, it is possible to assess the probability that the defect will be so substantial that maintenance or repair will be required. This can be evaluated using an event margin, J , which may be based on the failure function, or may be more simply defined.

For example, for spanning the failure function, Z , may be defined in terms of frequency of vibration, pipe stress in the span, and/or fatigue damage. However, the event margin J may be simply defined in terms of span length.

In order to define the event margins, J , a strategy for repair needs to be proposed and defined for each type of defect. The definition of each maintenance and repair event depends on the type of defect.

For example, consider general corrosion. If the corrosion depth is greater than the corrosion limit the pipeline will be derated, otherwise a corrosion inhibitor will be added. Thus, the events may be defined as:

$$J_{inhibitor} = W_{corrode} + e_{insp} - w(T_{insp}) > 0 \quad (G.1.8a)$$

$$J_{derate} = W_{corrode} + e_{insp} - w(T_{insp}) \leq 0 \quad (G.1.8b)$$

where W_{corrode} is the limiting depth for general corrosion,
 $w(T_{\text{insp}})$ is the predicted corrosion depth at the inspection time T_{insp} ,
 e_{insp} is the measurement error associated with the inspection method.

Of course more complex margins can be defined if necessary to cover a range of options.

Step 2.4 Update reliability estimates

Using the results of the previous step, the reliability evaluated from the first stage can be updated to account for the predicted results of the first and subsequent planned inspections - this type of analysis may be referred to as a *preposterior analysis*.

For any time, t , up to the time of the first inspection, ie for $0 \leq t \leq T_1$, the failure probability is evaluated as Stage 1, thus:

$$P_f(t) = P[Z(t) \leq 0] \quad (\text{G.1.9})$$

For any time after the first planned inspection, T_1 , and up to the second planned inspection, T_2 , ie $T_1 \leq t \leq T_2$, the failure probability is evaluated as:

$$\begin{aligned} P_f(t) = & \text{(probability of failure up to } T_1) \\ & + \text{(probability of failure after } T_1 \text{ given that the defect repair criterion is not} \\ & \text{exceeded at } T_1) \\ & + \text{(probability of failure after } T_1 \text{ given defect found and repaired at } T_1) \end{aligned}$$

That is,
$$\begin{aligned} P_f(t) = & P_f(T_1) + \Delta P_f^0(T_1, t) + \Delta P_f^1(T_1, t) \\ & - P[Z(T_1) \leq 0] \\ & + P[Z(T_1) > 0 \cap J > 0 \cap Z^0(t) \leq 0] \\ & + P[Z(T_1) > 0 \cap J \leq 0 \cap Z^1(t) \leq 0] \end{aligned} \quad (\text{G.1.10})$$

where $Z^0(t)$ is the failure function for the pipe in the original condition,
 $Z^1(t)$ is the failure function for the pipe after the defect has been repaired,
and J is the event margin (see Step 2.3)

For any time after the second planned inspection, T_2 , and up to the third planned inspection, T_3 , ie $T_2 \leq t \leq T_3$, the failure probability is evaluated as:

$$\begin{aligned}
P_f(t) = & \text{(probability of failure up to } T_2) \\
& + \text{(probability of failure after } T_2 \text{ given defect criterion not exceeded at } T_1 \text{ or } T_2) \\
& + \text{(probability of failure after } T_2 \text{ given defect found and repaired at } T_2) \\
& + \text{(probability of failure after } T_2 \text{ given defect found and repaired at } T_1) \\
& + \text{(probability of failure after } T_2 \text{ given defects found and repaired at } T_1 \text{ and } T_2)
\end{aligned}$$

That is, $P_f(t) = P_f(T_2) + \Delta P_f^{00}(T_2, t) + \Delta P_f^{01}(T_2, t) + \Delta P_f^{10}(T_2, t) + \Delta P_f^{11}(T_2, t)$ (G.1.11)

As the number of planned inspections increases, the number of combinations of events increases.

Step 2.5 Evaluate system failure probability

For each pipeline zone, and for each limit state, the probabilities can then be combined to evaluate the system reliability. For the types of combined events discussed above it can be difficult to evaluate the system reliability accurately. However, most of the failure modes and hazards will be largely uncorellated, and a reasonable and conservative estimate can be obtained by combining the probabilities for the individual failure events.

Step 2.6 Reliability-based assessment

From Step 2.4, the analysis can be repeated to assess the likely deterioration in reliability with time by undertaking the analysis for yearly (or more frequent) intervals.

An illustration of the variation of predicted reliability index with time for a single failure mode is shown in Figure G.1.2. For the example shown in the Figure, three inspections are planned at times T_1 , T_2 and T_3 .

Until the first planned inspection the reliability behaviour is identical to that evaluated in Stage 1. After the first and each subsequent inspection the curve of reliability index versus time has a marked reduction in slope. This is because the failure rate following an inspection is very small, since:

- either a defect has not been found at all,
- or a defect has been found, measured and assessed to be 'safe',
- or a significant defect has been found and the pipeline has been derated or repaired.

The extent that the predicted failure rate slope is reduced depends on the quality of the inspection method. A poor, inaccurate and unreliable method will have little effect on the failure rate and is of little benefit, whilst a very accurate and dependable method capable of finding and

accurately measuring all defects will reduce the slope almost to zero.

Note, there is no step change in predicted reliability following an inspection since, from Eqn (G.1.10), the predicted probability of failure at a time δt after an inspection can effectively be given by:

$$P_f(T_{insp} + \delta t) = P_f(T_{insp}) p + P_f(T_{insp}) (1-p) \quad (G.1.12)$$

where p is the probability of exceeding the event margin.

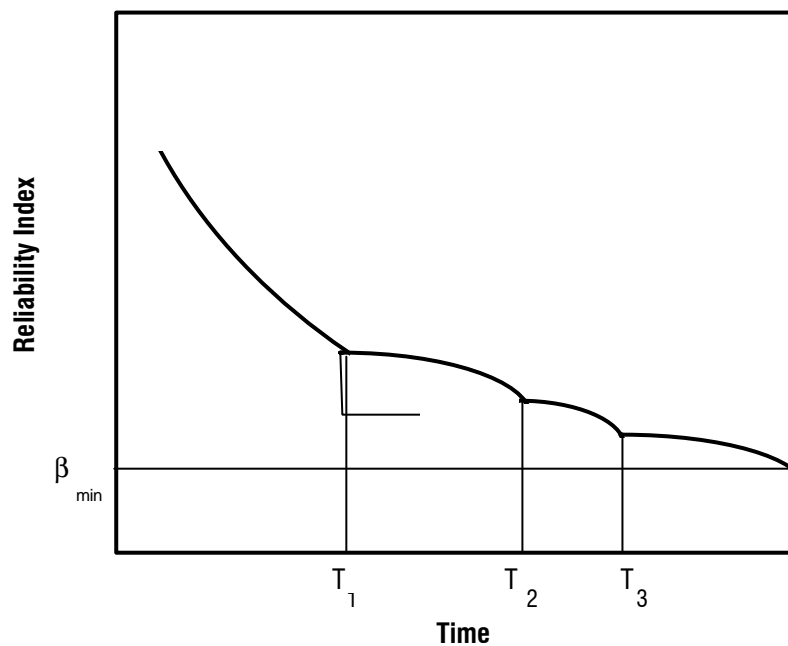


Figure G.1.2 Illustrative variation of predicted reliability index with time for a single failure mode

Step 2.7 Estimate cost of inspection

The cost of inspection depends on the type and quality of inspection undertaken, and should include the costs of assessing and interpreting the results.

Step 2.8 Estimate costs of maintenance and repair

The costs of maintenance or repair clearly depend on the method adopted.

If a shutdown of the pipeline is necessary whilst, or until, the repair or maintenance is undertaken, then the costs should take into account the cost of lost production and penalty charges. The increased costs associated with de-rating the pipeline should also be considered.

Step 2.9 Estimate total expected cost

The expected total future costs for a pipeline associated with a single planned inspection at time T_{insp} is given by:

$$E[C_r(t_d)] = E[C_f(t_d)] + E[C_i(t_d)] + E[C_r(t_d)] \quad (G.1.13)$$

where $E[C_f(t_d)]$ is the expected cost associated with failure,
 $E[C_i(t_d)]$ is the expected cost of inspection,
 $E[C_r(t_d)]$ is the expected cost associated with maintenance or repair.

$$E[C_f(t_d)] = \sum_{i=1}^m \left(P_{r_i}(T_{insp}) \frac{C_{r_i}}{(1+r)^{T_{insp}}} + \{P_{r_i}(t_d) - P_{r_i}(T_{insp})\} \frac{C_{r_i}}{(1+r)^{t_d}} \right) \quad (G.1.14)$$

$$E[C_i(t_d)] = \{1 - P_r(T_{insp})\} \frac{C_i}{(1+r)^{T_{insp}}} \quad (G.1.15)$$

$$E[C_r(t_d)] = P_r(T_r) \frac{C_r}{(1+r)^{T_r}} \quad (G.1.16)$$

where t_d is the expected design operating life of the pipeline,
 $P_{r_i}(t_d)$ is evaluated from Eqn (4.10) for time t_d ,
 m is the total number of failure modes or hazards,
 T_r is the time of repair (typically this may be assumed to be a set time after T_{insp}),
 $P_r(T_r)$ is the probability of repair or maintenance. Assuming that repair is undertaken if the defect tolerance is exceeded, the repair probability is evaluated from:

$$P_r(T_r) = P[Z(T_r) > 0 \cap J \leq 0] \quad (G.1.17)$$

For additional planned inspections Eqn (G.1.14), for the total cost of failure, is modified (for each hazard) as follows:

$$E[C_r(t_p)] = \sum_{i=1}^{n+1} \{P_r(T_p) - P_r(T_{i-1})\} \frac{C_r}{(1+r)^{T_i}} \quad (G.1.18)$$

where n is the total number of planned inspections.

The total cost of the inspections, Eqn (4.15), becomes:

$$E[C_r(t_p)] = \sum_{i=1}^n \{1 - P_r(T_p)\} \frac{C_i}{(1+r)^{T_i}} \quad (G.1.19)$$

Eqn (G.1.16) is similarly modified.

Figure 4.3 shows a typical plot of the expected costs against time to the next inspection, T_{insp} ; the example is based on fatigue of a tubular joint (the Figure is taken from [4]). The repair and inspection costs have been discounted to nett present value. As the pipeline becomes older the expected costs of failure rise as it becomes more likely fail.

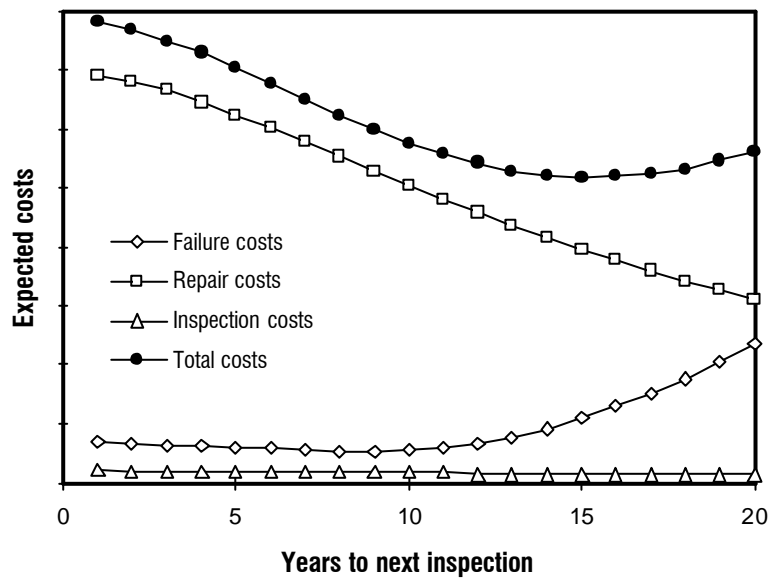


Figure G.1.3 Illustration of variation of expected cost-based risk with time to the next inspection (from [4])

Step 2.10 Optimise inspection and maintenance scheduling

Following a review of the assessment results undertaken, alternative IRM schedules can be suggested and analysed. A number of alternative objectives can be defined, however it is likely that the “best” scheme is the one which leads to minimum expected cost whilst maintaining the reliability of the pipeline at an acceptable level for all of the limit states.

It is possible to propose and define a formal, mathematical model to find *the* “optimum” inspection schedule which, for instance, minimises cost-based risk subject to the constraint that the minimum predicted reliability is greater than the target reliability for each limit state throughout the life of the pipeline for the whole of the system.

However, given the complexity of the problem and the number of items that can be optimised, (eg. inspection times, inspection method, inspection quality, etc.), an approach aimed at seeking *the* optimum solution is not recommended. Most mathematical optimisation techniques have difficulty in treating mixtures of variable types (ie real numbers and integers), the computational effort involved in optimising such a large problem is likely to be excessive, and numerical problems may develop.

Instead a trial-and-error approach is proposed with the selective use of optimisation techniques. For instance, for a particular inspection technique and assumed number of inspections, the times of inspection can be optimised to minimise the expected costs. (The convergence tolerance need only be coarse since inspections are generally undertaken annually, thus the optimisation analysis should require minimal computation effort.) This can be repeated for different numbers of inspections, and then for different methods of inspection.

With such an approach it is much easier to incorporate statutory requirements, Company or Asset Manager requirements, and preferred inspection methods.

G.1.4.1 Sensitivity measures

As well as the sensitivity measures discussed earlier, a useful measure for comparing the importance of a planned inspection is to consider how much the system failure probability for the zone, or whole pipeline, is reduced by the inspection. Thus, for a planned inspection I_k the Importance Factor is:

$$IF_k = \frac{\Delta P_{f_{sys}} | I_k}{P_{f_{sys}}} = 1 - \frac{P_{f_{sys}} | I_k}{P_{f_{sys}}} \quad (G.1.20)$$

where $P_{f_{sys}}$ is the system failure probability for the design life of the pipeline, eg. evaluated

from Eqn (G.1.9),

$P_{f_{\text{sys}}} | I_k$ is the system failure probability given the planned inspection, eg. evaluated from Eqn (G.1.10).

G.1.5 STAGE 3: UPDATED ANALYSIS

Following the results of an inspection, or a change of state of the pipeline, for instance due to a change in operating conditions, or as a result of a major repair to the pipeline, the inspection schedule may be updated.

Step 3.1 Assess measurement error uncertainty

For many types of defect the results of an inspection are presented as a measurement of some sort, eg. span length, corrosion pitting depth, etc. With any measurement there is an associated measurement error or uncertainty which depends on the quality of the measurement and the technique employed.

Step 3.2 Update reliability

Using the results of the previous step, along with the results from the first stage, the reliability can be updated using Bayesian techniques.

The updated probability of failure conditioned on an inspection event I is given by:

$$P_{f_{\text{sys}}} = P[F|I] = \frac{P[F \cap I]}{P[I]} \quad (\text{G.1.21})$$

where $P[I]$ includes the measurement uncertainty associated with the new information.

For example, consider that an inspection for internal corrosion was undertaken at time T_1 and the measured corrosion depth was not considered large enough to warrant remedial action, ie see Eqn (4.8a). Since the pipe has not failed at time T_1 , this information can be expressed as:

$$I = \{Z(T_1) > 0 \cap J > 0\} \quad (\text{G.1.22})$$

For any time after the first planned inspection, T_1 , and up to the second planned inspection, T_2 , ie $T_1 \leq t \leq T_2$, the updated failure probability is evaluated as:

$$\begin{aligned}
P_r(t|\Lambda) &= \Delta P_r^0(T_1, t | \Lambda) \\
&= P[Z(T_1) > 0 \cap J > 0 \cap Z^0(t) \leq 0 | \Lambda] \\
&= \frac{P[Z(T_1) > 0 \cap J > 0 \cap Z^0(t) \leq 0 \cap \Lambda]}{P[\Lambda]} \\
&= \frac{P[Z(T_1) > 0 \cap J > 0 \cap Z^0(t) \leq 0]}{P[\Lambda]} \\
&= \frac{\Delta P_r^0(T_1, t)}{P[\Lambda]} \tag{G.1.23}
\end{aligned}$$

Similarly, if the measured corrosion depth was larger than the tolerance, see Eqn (4.8b), and the pipeline was derated, this information can be expressed by:

$$I = \{Z(T_1) > 0 \cap J \leq 0\} \tag{G.1.24}$$

The updated reliability is then evaluated as:

$$P_r(t|\Lambda) = \Delta P_r^1(T_1, t | \Lambda) = \frac{\Delta P_r^1(T_1, t)}{P[\Lambda]} \tag{G.1.25}$$

Step 3.3 Evaluate system failure probability

For each pipeline zone, and for each limit state, the probabilities can then be combined to evaluate the updated system reliability. As before, most of the failure modes and hazards will be largely uncorrelated, and a reasonable and conservative estimate can be obtained by summing the probabilities for the individual failure events.

Step 3.4 Reliability-based assessment

At this stage, for each limit state it is possible to plot the variation in failure probability and/or reliability index against time. As before, on the same plots it is useful to show curves for each of the contributing failure hazards and/or failure modes.

Figure G.1.4 shows a typical plot of the variation in total evaluated reliability index with time following three inspections at time T_1 , T_2 and T_3 . After each inspection there is a marked rise in reliability because of the increased knowledge and reduced uncertainty about the state of the pipeline. The Figure also shows the effect of a repair to the pipeline following the results of the

inspection at time T_2 - after the repair the reliability is restored to a similar level to the initial condition in this case.

The effect of updating on evaluated reliability based on actual knowledge of the pipeline contrasts with the predicted reliability based on forecast behaviour illustrated in Figure G.1.4.

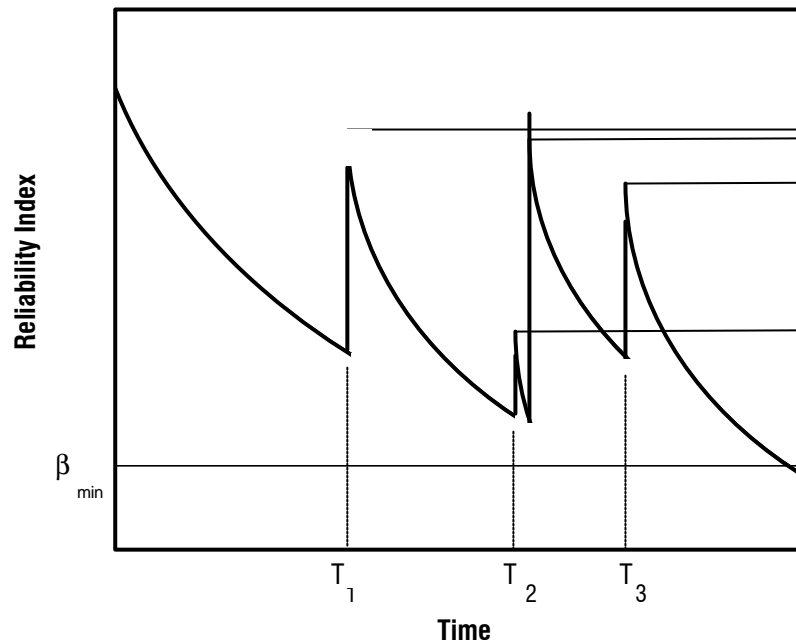


Figure G.1.4 Illustrative variation of evaluated reliability index with time throughout pipeline life

Step 3.5 Estimate cost of further inspection and maintenance

Following the results of an inspection the IRM schedule can be updated. Thus, as before the costs of further inspections need to be estimated.

Step 3.6 Estimate total expected cost

The expected total cost for the remaining life of the pipeline following the results of an inspection I , as before, is given by:

$$E[C_r(t_d)] = P_{r_{*1}}(t_d) \frac{C_r}{(1+r)^t} \quad (G.1.26)$$

If further inspections are planned, the expected costs can be evaluated from Eqns (G.1.14) to (G.1.16) using the updated probabilities in-place of the predictions.

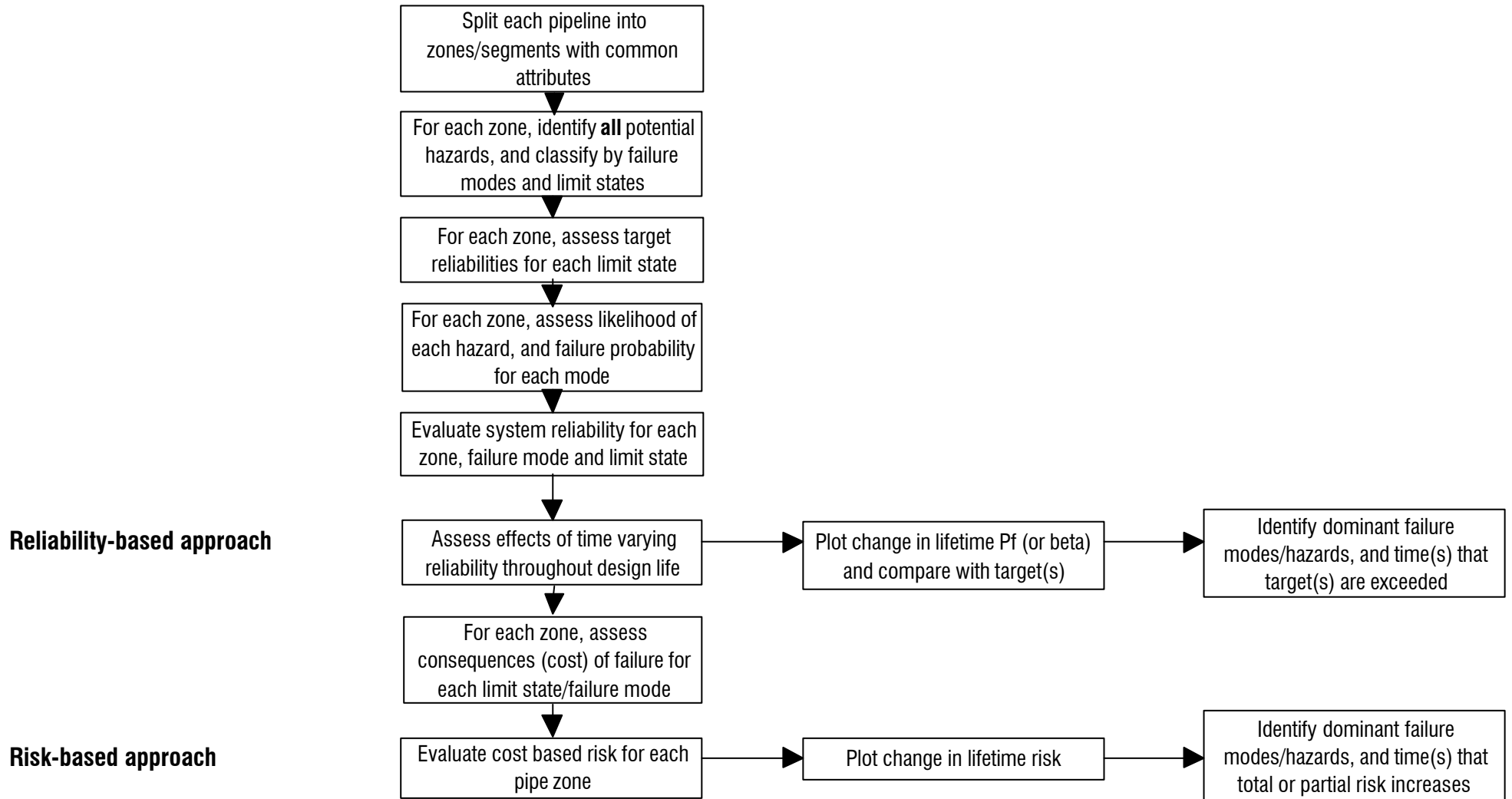


Figure G.1.5 Flowchart for STAGE 1: Initial analysis

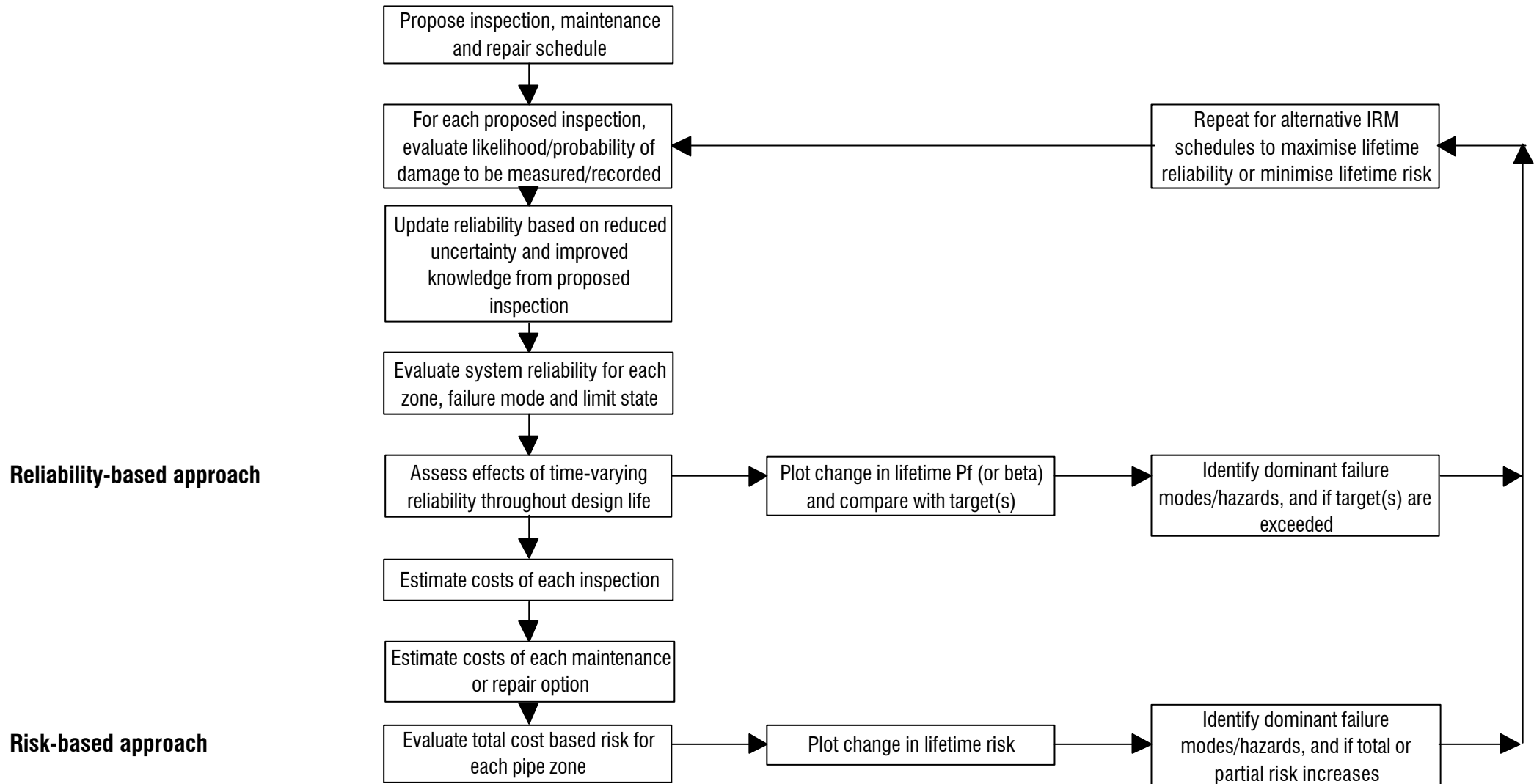


Figure G.1.6 Flowchart for STAGE 2: Propose and assess IRM schedule (Preposterior analysis)

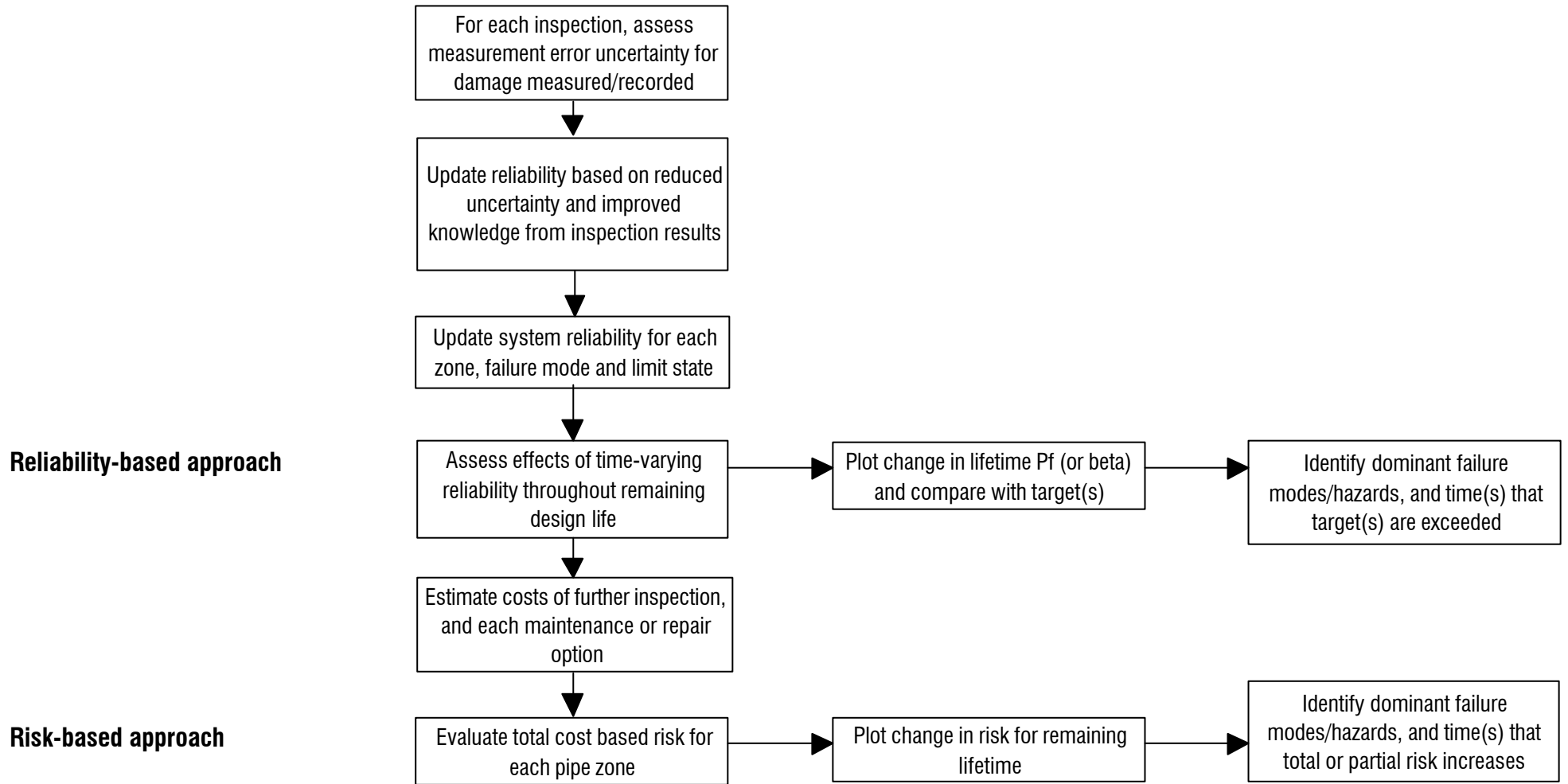


Figure G.1.7 Flowchart for STAGE 3: Update analysis based on inspection results (Posterior analysis)

G.2 INPUT REQUIRED

G.2.1 SUMMARY

This chapter discusses the input data and analysis models that are required for use with a risk and reliability-based inspection planning procedure.

G.2.2 PIPELINE DATA

The following data are required for each pipeline:

- as-built material and geometry data, and details of pipeline coatings, anodes, etc.,
- fabrication data,
- trenching method and burial details, if any,
- soils data and seabed topography,
- metocean data along the pipeline,
- operating history and any forecast changes,
- previous inspection records,
- records of previous interventions, maintenance and repairs.

Some of the data may be incomplete, and it is important that the system should be flexible enough to allow for this.

Results of previous analyses or assessments may be useful for comparison, and details of the present inspection schedule should also be included.

G.2.3 DEFINITION OF PIPELINE FAILURE MODES, LIMIT STATES AND TARGET RELIABILITIES

The failure modes and limit states need to be defined, and all of the hazards that can affect the pipeline need to be identified. This information will be very similar for all subsea pipelines.

For each pipeline corresponding target reliabilities need to be agreed. The target reliabilities are usually chosen to reflect the importance of the asset and the potential consequences of failure. Targets may be defined for individual pipelines; however a more useful approach may be to introduce a categorisation system with targets defined for each level, for example see the

SUPERB targets shown in Table G.1.1.

Where life-safety is a consideration the targets should be particularly carefully defined, and the ALARP principle should be used.

G.2.4 PROBABILITY ANALYSIS

G.2.4.1 Assessment of hazard likelihood of occurrence

Failure rate data from generic databases, such as PARLOC, are useful for preliminary or first-pass analyses, and such data may be useful to store as default data for use in the absence of more specific information.

However, for more detailed analyses, the likelihood of occurrence of a hazard is required for use with reliability analysis to evaluate the probability of failure given that a hazard has occurred.

Many hazards are almost certain to occur, eg. fatigue, corrosion, etc., and thus the likelihood of occurrence is 1.0. For other hazards, particularly those affecting the Serviceability and Ultimate Limit States, the likelihood may be judged subjectively, or if the results of more detailed assessments are available these may be used instead. Likelihood data is particularly important for the Accidental Limit State.

G.2.4.2 Failure models

The structural reliability analysis for the various failure modes requires accurate models to predict failure. For the most part, the failure models may be adapted from the existing deterministic models used for assessment.

It is anticipated that a separate *module* will be developed for each failure mode and/or hazard - modules can then readily be replaced with more sophisticated models.

G.2.4.3 Basic variable statistics

The uncertainty and variability of the basic variables also needs to be assessed. Physical, statistical and model uncertainty need to be accounted for. The modelling can be derived from statistical analysis of available observations of the individual variables, and may provide mean, standard deviation, correlation with other variables, and in some cases distribution type. Other relevant Company and public-domain information may also be useful.

Basic variables include:

- geometric parameters: eg. wall thickness, span length, etc.,
- material parameters: eg. SMYS, Young's modulus, fracture toughness, etc.,
- hydrodynamic parameters and metocean data: eg. drag coefficient, added mass, wave height, current velocity, etc.,
- model uncertainties for the various failure models,
- scour rates, corrosion rates, etc.

Most of the variables are specific to individual pipelines. However, some of the variables are more widely applicable, eg. hydrodynamic coefficients and model uncertainties.

G.2.4.4 Component and system reliability analysis

Software to evaluate component reliability and system reliability is required. Since many of the calculations involve evaluating the probability of intersection for a number of events, reliability software capable of handling multiple constraint and finding the joint "failure point" directly, would be an advantage.

Figure G.2.1 illustrates the joint failure point for the intersection of two events; the shaded area shows the failure region.

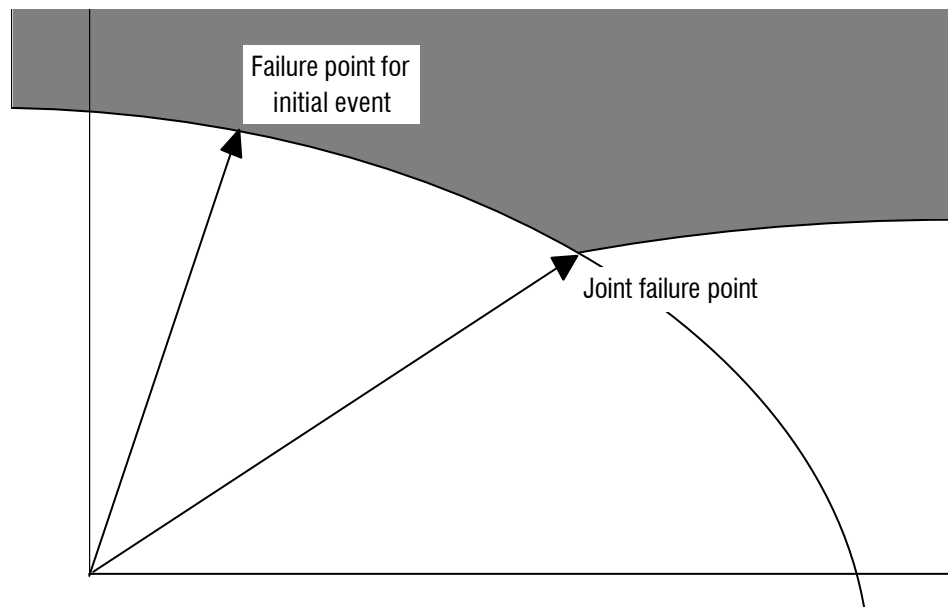


Figure G.2.1 Illustration of the joint failure point for the intersection of two events

G.2.5 CONSEQUENCE MODELS

G.2.5.1 Fire and blast analysis results

For high pressure gas lines, and for sections of pipe within the platform safety zone, risers and platform pipework the consequences of failure need to be considered. Separate quantified risk assessments may be undertaken to assess the likelihood of leaked contents igniting, and fire and blast analyses may be undertaken to assess the effects of various scenarios.

G.2.5.2 Economic considerations

The costs of pipeline failure need to be assessed. As discussed above, the costs of failure should include:

- loss of production,
- non-delivery penalty charges,
- loss of product,
- environmental pollution clean-up/mitigation,
- legal fees/fines,
- negative publicity,
- equipment damage,
- property damage.

G.2.5.3 Life-safety considerations

Where life-safety is a consideration, the potential consequences may need to be carefully evaluated using quantified risk assessments. The results should be stored and treated separately from the economic consequences.

G.2.6 INSPECTION METHODS, COSTS AND MEASUREMENT UNCERTAINTY

A database of information needs to be created containing details of all of the potential inspection methods. The data should contain the following information:

- each potential inspection method available, or in common use,
- all of the defect types that each inspection method is capable of detecting,
- for each of the above, an assessment of the measurement accuracy or uncertainty, together with an assessment of the probability of detecting a defect,
- for each method, an estimate of the present day costs of undertaking an inspection, including the assessment and interpretation of the results.

G.2.7 MAINTENANCE AND REPAIR METHODS, AND COSTS

For each type of defect and level of damage an estimate of the expected repair or maintenance costs is required. Where production needs to be de-rated or shutdown whilst the repair is being undertaken, the costs associated with lost production should be included. Details of the likely effectiveness of the repair or maintenance method should also be stored.

G.3 REFERENCES

1. Sotberg T, Bruschi R, & Mørk, "The SUPERB Project: Reliability-based design guideline for submarine pipelines", Proc 28th OTC, 1996, Houston.
2. Jiao G, Stoberg T, "Risk and reliability based pipeline design", Proc Conf on Risk & Reliability & Limit States in Pipeline Design & Operations, 1996, Aberdeen.
3. "The Update of Loss of Containment Data for Offshore Pipelines (PARLOC '93)", HSE Books, Sheffield, OTH 95 468, 1995.
4. Goyet J, Faber MH, Paynard J-C, & Maroini A, "Optimal inspection and repair planning: Case studies using IMREL software", Proc 13th OMAE Conf, 1994, ASME, Houston.

APPENDIX H

COPY OF REFERENCE: BOMEL, 1995

REDUCING CONSERVATISM IN PIPELINE SPAN ASSESSMENT

Philip J Wicks

Billington Osborne-Moss Engineering Limited
Maidenhead, Berkshire
UK

Helen M Bolt

Billington Osborne-Moss Engineering Limited
Maidenhead, Berkshire
UK

J K Smith

Amoco (UK) Exploration Company
London
UK

ABSTRACT

Conventional pipeline assessments investigate the acceptability of spans against static and dynamic criteria. Each involves many parameters often selected conservatively reflecting subjective uncertainty in the conditions. Detailed information on all parameters would be costly to assemble and a rational approach would be to refine knowledge on key parameters which influence the conservatism of assessments.

To identify these parameters, a probabilistic assessment approach was taken using existing span criteria. Absolute bounds on parameters and statistical data from the literature were used to develop appropriate distributions for each input variable. Monte-Carlo simulations were undertaken to determine the importance of individual parameters and the dependent sensitivity to input assumptions. These systematic screening analyses demonstrated priority areas warranting further investigation and offering a possible direct route to less conservatism.

This paper presents the methodology and illustrates the significance of the findings in relation to example spans in which dynamic and static criteria variously govern. Conclusions are presented for both short term continuance of deterministic methods and longer term development of probabilistic assessment strategies.

INTRODUCTION

Large sums of money may be spent every year in correcting

pipeline free spans. However, there has very often been no evidence of damage or failure in these spans before any remedial work has been undertaken. This would suggest, therefore, that assessment procedures currently in use for spans may be unnecessarily conservative.

Conservatism may arise from three principal sources.

- The restrictions set out in codes of practice and guidelines.
- The analytical techniques, and assumptions made within them, used in performing the assessments.
- The data itself or the way data are used within a given technique; for example, taking bounds or characteristic values for input data values.

Over the last twenty years, much research and development work has been devoted to the problem, both in terms of theory and model/full-scale testing. Attention has been paid on an individual basis to the statics and dynamics of freespan and also to evolving overarching methodologies.

Methods for static evaluation have been suggested by Skomedal (1991) and Irvine (1993), whilst the dynamic problem has been addressed by Bryndum et al (1989), Tassini et al (1989), Reid (1990) and Sheppard and Omar (1992). Both the static and dynamic aspects have been covered by Orgill et al (1992) and by the UK Health and Safety Executive (1993). A very notable attempt to provide rigorous and generalised pipeline spanning guidelines is to be found in descriptions of the GUESP Project (Tura et al, 1994a and 1994b).

ASSESSMENT PROCEDURE

Amoco's Southern North Sea pipeline span assessments are currently carried out according to a procedure that comprises the computation of an allowable span length. This is taken as the lesser of critical span lengths arising from the application of two criteria: limiting static stress and onset of vortex shedding excitation. Both spans are multiplied by a factor of 0.9 to provide an additional margin of safety. In its preliminary form, the procedure follows closely that reported by Kaye et al (1993). The calculations associated with the imposition of the two criteria are dealt with separately below.

Critical span length due to static stress

In this criterion the span is limited such that the maximum von Mises equivalent stress is restricted to 0.96 times the specified minimum yield strength (SMYS) of the pipe material. This is a criterion set by current codes of practice, for example BS 8010 (1993) and DnV (1981).

The pipe wall is assumed to be in a state of plane stress, with the hoop and longitudinal stresses being principal. The hoop stress derives from net pressure on the pipeline; and the longitudinal stress prior to span formation arises from thermal and Poisson effect stresses. This combination of stresses, in conjunction with the von Mises yield criterion, determines an allowable bending stress which, in turn, dictates the critical span length.

The critical span length corresponding with this criterion is computed from:

$$L_{ss} = 0.9 \left(\frac{2IpF_b}{q_{max}D} \right)^{1/2}$$

where

- L_{ss} = critical span length due to static stress
- I = pipe second moment of area
- p = factor in calculating maximum bending moment in the span
- q_{max} = uniformly distributed load per unit length of the span
- D = pipe outside diameter
- F_b = allowable bending stress.

Critical span length due to vortex shedding

In applying this criterion the span is limited such that the first mode fundamental frequency of the span coincides with the onset of cross-flow oscillations; ie. a condition of resonance. The equations for the two frequencies are as follows, for the first

mode fundamental frequency and the onset of cross-flow oscillations:

$$f_s = \frac{f}{2B} \left(\frac{EI}{m_0 L^4} \right)^{1/2}$$

$$f_0 = \frac{V_c + V_{wsig}}{V_m D_0}$$

Equating equations for the two frequencies yields the critical span:

$$L_{cv} = 0.9 \left(\frac{V_m^2 D_0^2 EI}{2B (V_c + V_{wsig})^2 m_0} \right)^{1/4}$$

where

- L_{cv} = critical span length due to vortex shedding
- f = factor in calculating first natural frequency of span
- V_m = reduced threshold velocity for onset of cross-flow oscillations.
- D_0 = pipeline outside diameter, including corrosion and weight coat thickness
- E = pipe Young's modulus
- I = pipe second moment of area
- V_c = current velocity at top of pipe
- V_{wsig} = significant wave induced velocity at top of pipe
- m_0 = effective pipeline mass per unit length.

It is to be noted that various methods exist for combining the current velocity and the water particle velocity due to wave action (see, for example, Chen et al (1994)). The above uses what may be viewed as the conservative approach of summing the two contributions to obtain the combined flow velocity.

In application of the procedure the minimum value of V_m set by DnV (1981) is usually used. For the combined flow of current and waves, there have been suggestions for higher values, Bruschi et al (1989) and Sarpkaya and Isaacson (1981). Moreover, for small ratios of gap below the span to pipeline outside diameter, V_m may be reduced (Raven et al, 1985). The latter is accommodated by setting a gap ratio below which vortex shedding induced cross-flow oscillations are not considered.

The base parameters that are used in the computation of the static stress and vortex shedding limited critical spans are

summarised in Table 1. The axial restraint factor δ , is a parameter introduced for the purpose of assessing the conservatism implicit in assuming full axial restraint at the ends of the pipeline span. This assumption relates to the computation of the longitudinal thermal and Poisson stresses in the pipeline. The factor may only vary between zero (representing complete axial freedom) and unity (representing complete axial fixity).

The parameters p and f appear independently in the equations pertaining to static stress and vortex shedding. However, insofar as they embody the effects of span end conditions and effective axial force they are not totally independent variables. Moreover, the effects of axial force on those parameters can be very significant. Kaye et al (1993) have suggested a formula relating f to effective axial force in the pipeline and span length. In current practice, the choice of values assigned to p and f has been influenced by field measurement data provided by Murray (1992).

SENSITIVITY METHODOLOGY

The purpose of the work was to identify the conservatism in Amoco's assessment procedure. Attention was focused, however, on the data itself and its use within the assessment method. In the work reported here no attempt was made to appraise the relative conservatism between the method currently used and others. The objectives were to gain insight into which variables exerted the greatest (and the least) influence on limiting spans, and to appraise the extent to which those with the greatest influence contributed to the conservatism of the limiting span magnitudes.

The sensitivity methodology chosen for the present requirement is Monte Carlo simulation. This has the advantages of being easy to understand conceptually, rapidly applied, and enabled the required objectives to be met.

The technique used, therefore, corresponds with a Level Three reliability method. It should be reemphasised, however, that reliability analysis per se is not being performed. The approach represents the application of a reliability technique to assess the sensitivity of a deterministically-based assessment procedure, as it is applied in practice. Its value is in helping to distinguish those parameters which govern the assessment and for which more accurate data might reduce the conservatism in current assessments. A software package called "Crystal Ball" marketed by Decisioneering was used to perform the calculations.

ANALYSES PERFORMED AND RESULTS

Three types of analyses were performed on two pipelines. The pipelines are referred to in this paper as 'A' and 'B' and the analyses were denoted as follows:

- deterministic
- primary sensitivity
- secondary sensitivity

In the deterministic analyses each of the chosen pipelines was subjected to the assessment procedure as detailed earlier. Each of the parameters listed in Table 1, however, took a single fixed value as dictated by the normal requirements of the procedure. The limiting span lengths due to static stress, vortex shedding and the governing of the two were computed. The purpose of obtaining these was to provide reference critical spans around which observations concerning the span distributions (obtained from the sensitivity analyses) could be based.

In primary sensitivity analyses, Monte Carlo simulations were performed wherein each of the parameters listed in Table 1, was assigned a frequency distribution. For the purposes of these primary analyses it was felt that, where appropriate, distributions should be set to as wide a spread as was reasonable. The aims of the primary analyses were:

- To identify key parameters to which the computation of limiting spans is most sensitive, thereby highlighting parameters to be concentrated upon in the secondary analyses.
- Equally importantly, the converse of the above.
- To determine, subject to the input distributions used, the key statistics of the limiting span distributions.
- To highlight within the distributions of critical span the predominance of one of the governing criteria: static stress or vortex shedding.

The reason for setting the parameter distributions to have a wide spread was that, if a parameter turned out to be highly ranked in sensitivity terms, the effect of its spread was to be investigated in the secondary sensitivity analyses. Conversely, if a parameter turned out to have a low sensitivity rating based on a wide spread of data, then it could be reasonably dismissed from further consideration.

In the secondary sensitivity analyses, Monte Carlo simulations were again performed, but adjustments were made to the frequency distributions used in the primary analyses for parameters identified as highly ranked. In broad terms, the purpose of making these adjustments was to investigate their effect on sensitivity, distributions of limiting spans and governing criterion.

Deterministic analyses

The magnitude of the input values used in the deterministic analyses are summarised in Table 2. It is seen that the principal differences between the two pipelines relate to:

- geometry and dimensions
- steel yield strength
- water depth
- current and wave velocities

The values used correspond with those that would actually be taken in performing the assessment procedure. Thus the following apply:

- The wave and current velocities were derived from the 50 year return period data.
- In combining the current and wave velocities, the critical wave phase angle was assumed to be zero.
- The magnitude of the axial restraint factor δ was taken as 1.
- The bending moment factor p represented end conditions between simply-supported and fully fixed combined with an amount of axial compression.
- The natural frequency parameter f was treated in a similar way to p .
- The significant wave induced velocity V_{wsig} was derived from 10 year return period data.

The results from the deterministic analyses of the two pipelines are given in Table 3.

As can be seen both pipelines are governed by the static stress criterion and have similar critical span lengths. However, for pipeline A the ratio of static stress span to vortex shedding span is 69% and the corresponding figure for pipeline B is 97%.

Primary Sensitivity Analysis

The distributions used for the input parameters are summarised in Table 4. To obtain these distributions careful searches of the literature and other sources of information were made in order to model these as realistically as possible. For parameters where inadequate detail was forthcoming engineering best-judgement was used. It will be seen from Table 4 that three parameters were given deterministic values: steel elastic modulus, Poisson's ratio and coefficient of thermal expansion. It was judged that these are generally well known and display small coefficients of variation; they would thus bear little influence on the overall results.

For the most part normal distributions were taken for parameters with means set at the nominal values. Notable exceptions to this were the axial restraint factor (half-normal distribution rendering a value of unity more probable), and the use of uniform distributions for some environmental parameters (eg. current velocity).

The bending moment factor p and natural frequency parameter f were more problematic. They are similar in their influences in

that they represent the rotational fixity at the ends of the span and the magnitude of axial force present. The distribution for p was taken as triangular with minimum, mode and maximum values of 4, 12 and 20, respectively. That for f was taken as normal with a mean equal to the nominal value (16.33) and a coefficient of variation of 13%. It was felt that these distributions corresponded with an end condition/axial force regime that generally reflected the assumptions of the deterministic analyses.

Monte Carlo simulations taking 5000 trials were performed on each of the two pipelines using the input parameter distributions summarised in Table 4. The following outputs were obtained in respect of the static stress, vortex shedding and governing criteria:

- sensitivity ratings for each of the input parameters
- statistics of the limiting span length frequency distributions
- the proportions of the total number of trials that were governed by either of the static stress and vortex shedding criteria.

The input parameter sensitivities are summarised in Table 5. The top six ranking parameters are tabulated for the static stress and vortex shedding assessments considered in isolation, and for the governing criterion.

In respect of the static stress assessment it can be seen that the top-ranking parameter for both pipelines was predominantly the bending moment factor p . This was by a very large margin in the case of pipeline B.

Three additional parameters appeared in the top six for both pipelines, but not necessarily with the same rank, namely: pipe wall thickness (t); maximum wave induced velocity (V_w) and hydrodynamic drag coefficient (C_d). The hydrodynamic added mass coefficient (C_m) appeared in the pipeline A rankings by virtue of its correlation with C_d .

For the vortex shedding assessment the top five parameters were the same, and have the same rankings, for both pipelines. The top-ranking parameter was the natural frequency parameter (f), but, it should be noted that the margin over the second-ranked parameter was far greater in the case of pipeline B.

With regard to the governing criterion it can be seen that five of the same parameters appeared in the top six rankings for both pipelines. Of these three were ranked the same for both pipelines (V_w , t and C_d); the remaining two (p and f) were interchanged in ranking between the pipelines. Thus p and f were first and fifth, respectively for pipeline A, whereas they were fifth and first for pipeline B. The suggestion from these rankings, therefore, is that pipeline A is principally governed by the static stress criterion, and pipeline B is principally governed by the vortex shedding criterion.

The statistics of the limiting span length frequency distributions are summarised in Table 6. Information is given on mean and coefficient of variation, as well as the span lengths corresponding with the 2.5%, 5.0% and 50% percentiles.

The mean span lengths tended to reflect the dominance of one or other of the static stress or vortex shedding criteria. Pipeline A had a lower mean for static stress than for vortex shedding with the governing mean closer in value to that of the static stress. The converse of this was true for pipeline B. For both pipeline cases the coefficient of variation for static stress exceeded that for vortex shedding, and it is noticeable that for pipeline B the coefficients of variation for vortex shedding and that corresponding with the governing criterion were very close in value.

The pattern exhibited by the percentile values for the governing limiting span distributions tended to follow the dominant criterion. Thus governing percentiles were close in value to static stress criterion ones for pipeline A, whereas they were close in value to vortex shedding criterion ones for pipeline B. In comparing the deterministically computed governing span lengths with the corresponding percentile values it is seen that for pipeline A the deterministic value lies between the 2.5% and 5.0% percentile values, whereas for pipeline B the deterministic value exceeds the 5.0% percentile value.

Finally the dominance of a particular criterion for each pipeline was confirmed by the percentage of trials results. Of these pipeline B is the most significant in that 90% of the trials were governed by the vortex shedding criterion; this is in contrast with the simple deterministic calculations performed earlier which determined pipeline B to be governed by the static stress criterion.

Secondary Sensitivity Analyses

It is evident from the primary sensitivity analyses that the principal parameters that affected limiting span distributions the most and, therefore, were investigated further in the secondary analyses were as follows:

- bending moment factor p
- natural frequency parameter f
- pipe wall thickness t
- current velocity V_c
- maximum wave induced velocity V_w
- significant wave induced velocity V_{wsig}

The additional distributions used for these parameters are summarised in Table 7. This table reiterates the fact that some parameters (t and V_c) are common to both limiting span calculations whereas others are unique to one or other. Hence, changes to individual input parameter distributions were

assessed in the following way: p and V_w on A only; f and V_{wsig} on B only; and t and V_c on both A and B.

The principal reasons for making the changes to the distributions were to observe the effects of changing mean, mode, COV and distribution of the key input parameters. In the secondary analysis the distributions relevant to each pipeline were changed individually; thus seven analyses were carried out for pipeline A, and 6 analyses for pipeline B.

The following results were observed for the parameters t , V_c , V_w , V_{wsig} :

t A significant reduction in the COV of the pipe wall thickness distribution had the effect, for both pipelines, of removing t from the top six ranking parameters. The reduction had a negligible effect on the variability of the critical span length and the governing criteria.

V_c The change in distribution tended to give a slightly increased ranking percentage, but had little effect on the critical span statistics or governing criteria for both pipelines.

V_w Increasing the COV of the distribution had the effects of: promoting the parameter up the sensitivity rankings to the extent that with a COV of 20% V_w became the second ranked parameter after p ; increasing the COV of the critical span distributions, thereby decreasing the percentiles. The effects on the ruling criterion were negligible.

V_{wsig} The results regarding this parameter were very similar to those for V_w except that the changes were less pronounced and less significant.

Of most significance were the results pertaining to changes made in the bending moment factor p and the natural frequency parameter f , in relation to pipelines A and B, respectively.

Table 8 summarises the effects of p on the top six ranking input parameters corresponding with the governing criterion for pipeline A. For the three triangular distributions it is seen that the effect of reducing the mode value was to increase the sensitivity to p ; this occurs with an associated decrease in the rankings of the other parameters. Similar effects were observed in changing from the triangular to the normal distribution with the same mean; the result was, for example, to equalise the rankings of p and V_c .

The statistics of the limiting span length frequency distribution are given in Table 9. For the triangular distributions it may be observed that the reduction in the mode value of p from 16 to 8 had the effect of reducing the mean value, and each of the three percentile values, but increasing the COV. These effects are due to the general increase in the possibility of smaller spans.

However, in contrast, the skewness increased (became less negative) as the mode value decreased; thus, higher values of mode value led to a longer tail over the smaller governing limiting span length than lower values. In comparing the triangular with the normal distribution it can be seen that the only significant changes were a decrease in the coefficient of variation, and increases in the percentiles.

Regarding the proportions of trials dictated by the two criteria, the effect of reducing the mode value in the triangular distributions was to increase the proportion pertaining to the static stress. It is notable that for a mode value of 16 the proportion of trials that were governed by vortex shedding was a half.

For pipeline B the corresponding results for changes in the distribution for f are given in Tables 10 and 11 for top ranking parameters and limiting span length statistics, respectively.

In Table 10 it is seen that a decrease in the COV of f from 13% to 2% (whilst maintaining the mean value) drastically reduced the sensitivity to f , thereby rendering V_c the top-ranking parameter by a very large margin. An increase in the mean from 16.3 to 25.1, resulted in p and V_c becoming the first and second ranked parameters, respectively, with f fairly insignificant.

Table 11 shows that a decrease in the COV of f from 13% to 2% generally led to increases in the 2.5% and 5% percentiles, but most significant were the changes in the skewness of the limiting span distributions: of the order of twenty times. This indicates that the COV changes resulted in the development of a significant tail in the limiting span distribution at the lower end.

In changing the mean of f from 16.3 to 25.1 a doubling of the skewness resulted, but little change in the percentile values occurred. This is surprising given the significant alteration made, but can be explained by the fact that in making the change the pipeline became less dominated by vortex shedding. This is evidenced by the dramatic increase in sensitivity to p (Table 10) and the large increase in the proportion of trials governed by static stress (Table 11).

DISCUSSION

The primary sensitivity analyses revealed that of the 26 input parameters 6 exerted the greatest influence on critical spans. However, pipe wall thickness t was effectively removed from amongst the top six rankings when it was given a more realistic distribution in secondary analyses. The remaining 5 could be classified into two groups pertaining to: modelling of the span response, and hydrodynamic loading. Into the first group fell:

- bending moment factor p
- natural frequency parameter f

and these are, in turn, functions of span end support conditions

and effective axial force in the pipe, not explicitly admitted to the assessment methods.

Into the second group fell:

- current velocity V_c
- maximum wave induced velocity V_w
- significant wave induced velocity V_{wsig}

It was found in the primary analyses that of these two groups the parameters falling into the first were by far the more influential. In considering the second group the current velocity V_c tended to exert the most influence. Of the two pipelines considered, pipeline A was deemed dominated by the static stress criterion and pipeline B by the vortex shedding criterion.

These observations tended to be reflected in some of the secondary sensitivity analyses, wherein changes were made to the distributions of the key parameters on an individual basis.

Alterations made to the distributions of V_w and V_{wsig} in terms of variation of the COV values tended only to result in alteration to their ranking, and had marginal effects on critical span distribution and governing criterion majority. Of the two, the effects of V_w were the more pronounced. The change made to V_c (which was different to the changes made to the distributions of the other two parameters in its group) tended to strengthen its ranking in the top six parameters, with marginal effects on the critical span distribution and majority criterion.

The changes made to the distributions of p and f tended to produce the most significant effects. The results also illustrated the interaction between the two criteria in contributing to the governing limiting span.

Thus, in the case of pipeline A (which from the primary analyses was deemed to be static stress dominated) changes in the mode value and type for the distribution used for p could reduce its influence and increase the ranking of V_c and, to a lesser extent, f . With increases in the mode value the balance between trials governed by static stress or vortex shedding could be radically altered to the extent of half the trials becoming governed by either criterion.

In a similar manner, for pipeline B (which was deemed to be vortex shedding dominated by the primary analyses) a reduction in the COV of the distribution for f (the most important as far as the vortex shedding criterion is concerned) could make its ranking of this parameter quite low and promote V_c to the highest ranked. A simultaneous change in the mean and the COV had the effect of making p and V_c the top two ranking parameters respectively and greatly increased the number of trials governed by the static stress criterion.

Most important for pipeline B, was that, having established the significance of f from the primary analyses, favourable improvements made to the distribution for f did not produce

commensurate increases in allowable span length as determined by, say, the 2.5% or 5% percentile values for the limiting span length distribution. The reason for this is that in making such changes in f individually the result is a reduction in the probability of span length being governed by vortex shedding and an increase in the probability of being governed by static stress, for which no favourable alternations to key parameter distributions were made.

In general, however, for both pipelines the most favourable alterations made to the distributions of p and f individually produced increases in allowable span length of the order of only 10% or less (see Table 12). Thus it is probably necessary to improve all key parameters simultaneously in order that increases in allowable span lengths are more than modest.

Notwithstanding this, increases in allowable span lengths achieved here do not account for the very large, undistressed, free spans observed in the field. This may suggest that of the three sources of conservatism identified in the introduction, the restrictions set by codes of practice and guidelines, and the analytical techniques used in performing the assessment are likely to be the greatest sources of conservatism in pipeline free span assessment.

CONCLUSIONS

- It is evident that there are three possible routes to reducing the conservatism inherent in the span assessment procedure:
 - maintain the usage of the current techniques, and rely on the procurement of 'better' data;
 - adopt more complex analytical span assessment tools that better represent the mechanical behaviour of spans;
 - incorporate less onerous acceptance criteria.
- The analyses highlighted the dangers of classifying a span as being governed by a particular criterion based on a single deterministic calculation. Introduction of variability in the input parameters may influence which criterion governs, which should be based on a balance of probabilities. Changes in the variation assigned to input parameters may result in a parameter assuming an importance greater than that indicated by a deterministic calculation.
- Two groups of parameters pertaining to modelling of the span response, and hydrodynamic loading were found to impose the greatest influence on limiting spans. These groups contained:
 - bending moment factor p and natural

frequency parameter f ;

- current velocity V_c , maximum wave induced velocity V_w and significant wave induced velocity V_{wsig} .

- The parameters in the first group were the most influential and enhanced limiting span lengths may result from improved data on these. However, they will be strongly dependent on span end support conditions and effective axial force in the pipeline, and hence a different structural model would be necessary to determine the relative influences of these.
- It is apparent that for beneficial changes to occur as a result of improved data, improvements may be necessary to all key input parameters as significant enhancement of a single parameter may not necessarily lead to a commensurate enhancement of limiting span length.
- Early indications, however, are that significantly improved limiting span lengths would not accrue from improved data and that the greatest sources of conservatism are most likely the analytical methods and restrictions/criteria imposed by codes and guidelines.

ACKNOWLEDGEMENT

The important contributions of Philip Smedley and Eric Wakley of BOMEL in developing the methodology and performing the analyses from this work is acknowledged.

REFERENCES

- British Standard Institute, 1993, "Code of Practice for Pipelines: Part 3: Pipelines Subsea: Design Construction and Installation", BS 8101.
- Bruschi R. et al, 1989. "Field Tests with Pipeline Free Spans Exposed to Wave Flow and Steady Current", *Proceedings, Offshore Technology Conference*, Houston, Paper No. OTC 6152.
- Bryndum, M.B. et al, 1989, "Long Free Spans Exposed to Current and Waves: Model Tests", *Proceedings, Offshore Technology Conference*, Houston, Paper No OTC 6153.
- Chen, Z.X., Talbot, L. and Morrison, A., 1994, "The Effects of Flow Interference and Vortex Shedding on a Production Riser with a Piggy-back - A Designer's Viewpoint", *Proceedings, 4th International Offshore and Polar Engineering Conference*, Osaka, Vol. 2.
- Det norske Veritas, 1981, "Rules for Submarine Pipeline Systems", (Reprint with corrections, 1982).

Health and Safety Executive, 1993, "Structural Analysis of Pipeline Spans", OTI 93 613, HMSO, London.

Irvine, M., 1993, "On the Mechanics of Spanning in Submarine Pipelines", *Proceedings, 3rd International Offshore and Polar Engineering Conference*, Singapore, Vol. 2, pp.98-105.

Kaye, D et al, 1993, "Pipeline Freespan Evaluation: A New Methodology", *Proceedings, Offshore Europe Conference*, Aberdeen, Paper No SPE 26774.

Murray, B G., 1992, "Pipeline Freespan Vibration Monitoring", Development Engineering International Limited, Report Nos PTIPUB/P3 and PS047/01.

Orgill, G et al, 1992, "Current Practice in Determining Allowable Pipeline Free Spans", *Proceedings, 11th Offshore Mechanics and Arctic Engineering Conference*, Vol. 2-A, pp.139-145.

Raven, RWJ et al, 1985, "Full-scale Dynamical Testing of Submarine Pipeline Spans", *Proceedings, Offshore Technology Conference*, Houston, Paper No. OTC 5005.

Reid, D.L., 1990, "A Generalised in-Line Vortex-Induced Vibration Assessment Method", *Proceedings, Offshore Technology Conference*, Houston, Paper No OTC 6365.

Sarpkaya, T. and Isaacson, M, 1981, "Mechanics of Wave Forces for Offshore Structures", van Nostrand Reinhold Co., New York.

Sheppard, D.M. and Omar, A.F., 1992, "Vortex-induced Loading on Offshore Structures: A Selective Review of Experimental Work", *Proceedings, Offshore Technology Conference*, Houston, Paper No OTC 6817.

Skomedal, E., 1991, "Static Calculation of Pipeline Free Spans", *Proceedings, 1st International Offshore and Polar Engineering Conference*, Edinburgh, Vol. 2, pp.281-289. Tassini, PA., et al, 1989, "The Submarine Vortex Shedding Project: Background, Overview and Future Fall Out on Pipeline Design", *Proceedings, Offshore Technology Conference*, Houston, Paper No OTC 6157.

Tura, F., et al, 1994a, "Guidelines for Free Spanning Pipelines: Outstanding Items and Technological Innovations", ASPECT-94, Society for Underwater Technology, Vol. 33, pp.59-76.

Tura, F., et al, 1994b, "Guidelines for Free Spanning Pipelines: the GUESP Project", *Proceedings, 13th Offshore Mechanics and Arctic Engineering Conference*, Vol V, pp.247-256.

TABLE 1 LIST OF PARAMETERS USED IN SPAN ASSESSMENT

Input parameter		Used in	
		Static stress	Vortex shedding
Pipe outside diameter	D	T	T
Pipe wall thickness	t	T	T
Corrosion coat thickness	t _c	T	T
Weight coat thickness	t _w	T	T
Steel density	D _s	T	T
Corrosion coat density	D _c	T	T
Weight coat density	D _w	T	T
Steel elastic modulus	E	T	T
Steel Poisson's ratio	ν	T	X
Steel SMYS	F _y	T	X
Steel thermal expansion coeff.	α	T	X
Axial restraint factor	κ	T	X
Bending moment factor	μ	T	X
Natural frequency parameter	f	X	T
Max. int. operating pressure	p _i	T	X
Contents density	D _i	T	T
Contents temperature	z	T	X
Min. water depth at LAT	h	T	X
Current speed: top of pipe	V _c	T	T
Max. wave induced velocity	V _w	T	X
Signif. wave induced velocity	V _{wsig}	T	T
Reduced threshold velocity	V _{rn}	X	T
Local seawater density	D _n	T	X
Local seawater temperature	z _c	T	X
Hydrodynamic drag coeff.	C _d	T	X
Hydrodynamic added mass coeff	C _m	X	T

TABLE 2 MAGNITUDES OF PARAMETERS USED IN DETERMINISTIC ANALYSES

Input parameter		Pipeline		Units
		A	B	
Pipe outside diameter	D	762	273	mm
Pipe wall thickness	t	17.5	11.1	mm
Corrosion coat thickness	t _c	5.6	5.0	mm
Weight coat thickness	t _w	33	45	mm
Steel density	D _s	7850	7850	kg/m ³
Corrosion coat density	D _c	1200	1438	kg/m ³
Weight coat density	D _w	3124	2243	kg/m ³
Steel elastic modulus	E	207	207	GPa
Steel Poisson's ratio	<	0.3	0.3	-
Steel SMYS	F _y	358	413	MPa
Steel thermal expansion coeff.	"	0.0000116	0.0000116	/°C
Axial restraint factor	8	1.0	1.0	-
Bending moment factor	p	8.0	8.0	-
Natural frequency parameter	f	16.33	16.33	-
Max internal operating pressure	p _i	9.0	13.9	MPa
Contents density	D _i	585	806	kg/m ³
Contents temperature	T _c	49	49	°C
Min. water depth at LAT	h	29.5	141.0	m
Current speed: top of pipe	V _c	1.07	0.54	m/s
Max. wave induced velocity	V _w	3.22	1.28	m/s
Signif. wave induced velocity	V _{wsig}	1.1	0.29	m/s
Reduced threshold velocity	V _m	3.5	3.5	m/s
Local seawater density	D _w	1025	1025	kg/m ³
Local seawater temperature	T _s	6	4	°C
Hydrodynamic drag coeff.	C _d	1.05	1.05	-
Hydrodynamic added mass coeff.	C _m	1.0	1.0	-

TABLE 3 LIMITING SPANS FROM DETERMINISTIC ANALYSES

Criterion	Limiting span (m) for pipeline	
	A	B
Static stress	29.8	26.3
Vortex shedding	42.9	27.0
Critical	29.8	26.3
Static: Vortex span ratio	69%	97%

TABLE 4 FREQUENCY DISTRIBUTIONS FOR INPUT PARAMETERS USED IN PRIMARY SENSITIVITY ANALYSES

Input parameter		Used in		Distribution used
		Static stress	Vortex shedding	
Pipe outside diameter	D	T	T	Normal: Mean = Nominal, COV = 1.5%
Pipe wall thickness	t	T	T	Normal: Mean = Nominal, COV = 10%
Corrosion coat thickness	t _c	T	T	Normal: Mean = Nominal, COV = 7%
Weight coat thickness	t _w	T	T	Normal: Mean = Nominal, COV = 10%
Steel density	D _s	T	T	Normal: Mean = 7850, COV = 0.5%
Corrosion coat density	D _c	T	T	Normal: Mean = Nominal, COV = 1%
Weight coat density	D _w	T	T	Normal: Mean = Nominal, COV = 5%
Steel elastic modulus	E	T	T	Deterministic value
Steel Poisson's ratio	<	T	X	Deterministic value
Steel SMYS	F _y	T	X	Normal: Mean = calculated COV = 5%
Steel thermal exp. coeff.	"	T	X	Deterministic value
Axial restraint factor	(T	X	Half-normal: Mean 1.0, COV = 33%
Bending moment factor	p	T	X	Triangular: Min=4, mode=12, max=20
Natural frequency parameter	f	X	T	Normal: Mean = 16.33, COV = 13%
Max. int. operating pressure	p _i	T	X	Normal: Mean = Nominal, COV = 10%
Contents density	D _c	T	T	Normal: Mean = Nominal, COV = 3%
Contents temperature	z	T	X	Normal: Mean = Nominal, COV = 6%
Min. water depth at LAT	h	T	X	Normal: Mean = Nominal, COV = 2%
Current speed: top of pipe	V _c	T	T	Uniform: Min, Max from data
Max. wave induced velocity	V _w	T	X	Normal: Mean = Nominal, COV = 10%
Signif. wave induced velocity	V _{wsig}	T	T	Normal: Mean = Nominal, COV = 10%
Reduced threshold velocity	V _m	X	T	Uniform: Min = 3.5, Max = 3.8
Local seawater density	D _w	T	X	Normal: Mean = Nominal, COV = 0.5%
Local seawater temperature	z _t	T	X	Triangular: Min=0, mode=6, Max=9°C
Hydrodynamic drag coeff.	C _d	T	X	Normal: Mean = Nominal, COV = 15%
Hydrodynamic added mass coeff	C _m	X	T	Normal: Mean = Nominal, COV = 15%

TABLE 5 TOP SIX RANKING INPUT PARAMETERS MEASURED BY CONTRIBUTION TO VARIANCE, FROM THE PRIMARY SENSITIVITY ANALYSES

Pipeline A						Pipeline B					
Static		Vortex		Governing		Static		Vortex		Governing	
	%		%		%		%		%		%
p	47.0	f	44.9	p	40.2	p	76.1	f	64.9	f	61.0
V _w	10.9	V _c	34.3	V _c	14.7	t _c	7.3	V _c	16.0	V _c	15.1
t	10.7	V _{wsig}	8.6	t	13.0	t	4.7	V _{wsig}	5.5	t	6.8
C _d	10.3	t	4.5	V _w	8.9	F _y	4.6	t	4.7	V _{wsig}	5.4
C _m	6.0	C _m	2.3	f	6.2	V _w	1.5	C _m	3.1	p	3.8
V _c	5.8	V _m	2.1	C _d	5.5	C _d	1.3	C _d	2.2	C _d	1.5

**TABLE 6 KEY STATISTICS FOR LIMITING SPAN
FREQUENCY DISTRIBUTIONS FROM THE PRIMARY SENSITIVITY ANALYSES**

Limiting span characteristics	Pipeline A			Pipeline B		
	Static	Vortex	Governing	Static	Vortex	Governing
Mean (m)	44.4	46.9	41.7	36.6	28.3	28.0
Coefficient of variation (%)	20.4	9.8	15.3	16.4	8.1	8.4
Skewness	0.31	0.20	-0.28	0.00	0.06	-0.03
Kurtosis	2.96	2.89	2.95	2.72	2.94	3.04
2.5% percentile (m)	28.5	38.6	28.5	24.9	23.9	23.4
5.0% percentile (m)	30.4	39.6	30.3	26.4	24.6	24.1
50.0% percentile (m)	43.9	46.7	42.2	36.6	28.3	28.0
% - age of trials	63	37	static	10	90	vortex
Deterministic span (m)	29.8	42.9	29.8	26.3	27.0	26.3

TABLE 7 INPUT PARAMETER DISTRIBUTIONS USED IN SECONDARY SENSITIVITY ANALYSES

	Used in		Pipeline test case	
	Static stress	Vortex shedding	A	B
p	T	X	Triangular min = 4, max = 20, mode = 8 & 16 Normal: Mean = 12, COV = 22%	N/A
f	X	T	N/A	Normal: Mean = 16.33, COV = 2%; Mean = 25.14, COV = 4%
t	T	T	Normal: Mean = nominal, COV = 2%	
V _c	T	T	Distribution derived from directional data	
V _w	T	X	Normal: Mean = nominal COV = 5% COV = 20%	N/A
V _{wsig}	X	T	N/A	Normal: Mean = nominal COV = 5% COV = 20%

**TABLE 8 EFFECT OF CHANGING DISTRIBUTION OF P ON TOP RANKING INPUT
PARAMETERS CORRESPONDING WITH GOVERNING CRITERION FOR PIPELINE A**

	Triangular distribution, mode value			Normal : = 12 COV = 22.25%
	8	12	16	
p	50.8	40.2	31.7	20.7
V _c	9.1	14.7	20.8	20.0
t	11.7	13.0	15.2	16.6
V _w	6.9	8.9	4.5	14.4
f	2.9*	6.2	13.1	4.6*
C _D	5.5	5.5	2.3*	5.7

* Dropped out of top six

**TABLE 9 EFFECT OF CHANGING DISTRIBUTION OF P
ON GOVERNING LIMITING SPAN DISTRIBUTION KEY STATISTICS FOR PIPELINE A**

Limiting span statistic	Triangular distribution, mode value			Normal : = 12 COV = 22.25%
	8	12	16	
Mean (m)	39.9	41.7	43.0	41.8
Coefficient of variation (%)	17.2	15.3	14.5	14.2
Skewness	-0.11	-0.28	-0.35	-0.33
Kurtosis	2.73	2.95	3.31	3.21
2.5% percentile (m)	26.5	28.5	29.5	29.3
5.0% percentile (m)	28.1	30.3	31.8	31.7
50% percentile (m)	40.2	42.2	43.4	42.0
Static stress (%)	73	63	50	62
Vortex shedding (%)	27	37	50	38

**TABLE 10 EFFECT OF CHANGING DISTRIBUTION OF F ON TOP RANKING INPUT
PARAMETERS CORRESPONDING WITH GOVERNING LIMITING CRITERION FOR PIPELINE B**

	Normal distribution for f		
	16.33	16.32	25.14
Mean	16.33	16.32	25.14
COV (%)	13.0	2.0	3.8
f	61.0	3.0	4.3
V _c	15.1	59.5	23.0
t	6.8	0.7*	0.0*
V _{avg}	5.4	14.8	5.5
p	3.8	3.6	51.9
C _d	1.5	1.4*	0.1*

* Dropped out of top six

**TABLE 11 EFFECT OF CHANGING DISTRIBUTION OF F ON GOVERNING LIMITING
SPAN DISTRIBUTION KEY STATISTICS FOR PIPELINE B**

	Normal distribution for f		
	16.33	16.32	25.14
Mean	16.33	16.32	25.14
COV (%)	13.0	2.0	3.8
Mean (m)	28.0	28.2	33.5
Coefficient of variation (%)	8.4	5.1	9.2
Skewness	-0.03	-0.66	-1.26
Kurtosis	3.04	5.01	4.75
2.5% percentile (m)	23.4	25.2	25.5
5.0% percentile (m)	24.1	26.0	27.0
50% percentile (m)	28.0	28.2	34.2
Static stress (%)	10	8	39
Vortex shedding (%)	90	92	61

TABLE 12 COMPARISON BETWEEN DETERMINISTIC, PRIMARY AND SECONDARY ANALYSES RESULTS

	Pipeline A		Pipeline B	
	Primary	Secondary p only	Primary	Secondary f only
	Table 6	Table 9	Table 6	Table 11
Mean (m)	41.7	41.8	28.0	33.5
Coefficient of variation (%)	15.3	14.2	8.4	9.2
2.5% percentile (m)	28.5	29.3	23.4	25.5
5.0% percentile (m)	30.3	31.7	24.1	27.0
Deterministic (m)*	29.8	29.8	26.3	26.3
* Results from Table 3				